Department of Architecture and Built Environment

Faculty of Science and Engineering

INVESTIGATION OF A COMPACT UNGLAZED SOLAR THERMAL FACADE FOR BUILDING INTEGRATION

Jingchun Shen *BEng, MSc*

Thesis submitted to the University of Nottingham

for the degree of Doctor of Philosophy

December 2016

ABSTRACT

In order to achieve the global carbon emission reduction target, it is expected to become essential for higher fraction of locally available renewable energy sources in energy mix, other than significant reduction of fossil energy consumption. Solar energy is one of the most promising renewable sources locally with various building applications. In addition, the Solar Thermal Facade (STF) system demonstrates a real sense of building integration that can be a potential solution towards energy efficiency improvement and operational cost reduction in contemporary built environment.

This thesis presents a comprehensive investigation into a novel compact unglazed STF system that possesses the advantages of compact structure, economical cost and high feasibility in architectural design. The entire study follows in the basic methodology of combined theoretical and experimental analysis, including procedures of critical literature reviews, optimal concept design, theoretical study, analytical model development, prototype system construction, laboratory-controlled evaluation, techno-economic feasibility analysis and a design strategy for its application. Under the baseline testing condition, the collector efficiency factor F', heat removal factor F_R and channel flow factor F'' were respectively high up to 0.993, 0.992, and 0.985, leading to a relatively high thermal efficiency at about 63.21%, exhibiting a better thermal performance. And the maximum theoretical possible useful heat gain capacity (intercept $F_R a_p$) of such STF at the given operating conditions was about 96.20%. And the mean slope ($F_R U_L$) was as much as about -13.06, representing a sharp decreasing trend of this SFT's thermal efficiency against the $(T_{in}-T_a)/I$ complying with the feature of no glazing cover attached in the front. So in case of current design, such STF could match the applications of heating load for pool heating, domestic hot water and radiant space heating

in those areas with warm air temperature and sufficient solar radiation. Moreover, the techno-economic feasibility study identified that the overall contributions of the STF application in a reference residential building consist of direct solar thermal generation, indirect HVAC load reduction and savings in operation cost. Additionally, the financial outputs from the dedicated business model in Shanghai stated that: the proposed STF system was a profitable investment project with positive overall revenue and acceptable payback period within 6 years; and three different investment schemes have individual advantages in terms of investment risk, payback period and financial output. Lastly, the BIM associated STF design strategy was raised for building performance research in architectural practice. It is ultimately about the evaluation of multiple STF alternatives against different design priorities and the associated STF design information sharing with others to reduce duplication, minimize errors, streamline processes and facilitate collaboration towards sustainable STF integration.

The entire research is expected to configure a technical breakthrough in the subject for the widespread market penetration of the STF technology, a feasible solution for solar thermal technology in future building application, as well as an advanced multifunctional STF development. The research outcomes of this study will conduce to the promotion of such a building integrated solar thermal technology, enrich low-carbon building design strategy, and thus contribute to achieving the domestic and international targets for energy saving, renewable energy utilization, and carbon emission reduction in the building sector.

LIST OF PUBLICATION

Book Chapter

1. Xingxing. Zhang, **Jingchun. Shen**, Tong. Yang, Llewellyn. Tang, Yupeng. Wu, 2016. An initial concept design of an innovative flat-plate Solar Thermal Facade for building integration (Chapter 14), Sustainable Buildings and Structures, Taylor & Francis Group, London, ISBN: 978-1-138-02898-2. (same contents in Chapter 4)

Journal Publications

1. **Jingchun Shen**, Xingxing Zhang, Tong Yang, Llewellyn Tang, et al., 2016. Characteristic study of a novel compact solar thermal facade (STF) with internally extruded pin-fin flow channel for building integration, Applied Energy, 168, pp. 48-64. (5-year IF: 6.330, partly from Chapter 5 and 6)

2. Xingxing Zhang, **Jingchun Shen**, Deborah Adkins, Tong Yang, Llewellyn Tang, et al., 2015. The early design stage for building renovation with a novel loop-heat-pipe based solar thermal facade (LHP-STF) heat pump water heating system: Techno-economic analysis in three European climates, Energy Conversion and Management, 106, pp.964-986. (5-year IF: 4.512, same research methodology in Chapter 7)

3. Xingxing Zhang, **Jingchun Shen**, Llewellyn Tang, Tong Yang et al., 2015. Building integrated solar thermal (BIST) technologies and their applications: A review of structural design and architectural integration, Journal of Fundamentals of Renewable Energy and Applications 215 (5): 182 (5-year IF: 0.31, partly from Chapter 3)

4. Xingxing Zhang, **Jingchun Shen** et al., 2015. Active solar thermal facades (ASTF): From concept, application to research questions, Renewable & Sustainable Energy Reviews, 50, pp. 32-63. (5-year IF: 7.445, partly from Chapter 2)

Conference proceedings

1. **Jingchun Shen**, Xingxing Zhang, Tong Yang, Llewellyn Tang, Yupeng Wu et al., 2016. Experimental study of a Compact Unglazed Solar Thermal Facade (STF) for Energy-efficient Buildings, CUE 2016-Applied Energy Symposium and Forum: Low carbon cities & urban energy systems,13-16 June 2016, Jinan, China (partly from Chapter 6)

2. **Jingchun Shen**, Xingxing Zhang, Tong Yang, Llewellyn Tang, Yupeng Wu et al., 2016. Optimizing the Configuration of a Compact Thermal Facade Module for Solar Renovation Concept in Buildings, CUE2016-Applied Energy Symposium and Forum: Low carbon cities & urban energy systems,13-16 June 2016, Jinan, China (partly from Chapter 4 and 5)

3. **Jingchun Shen**, Xingxing Zhang, Tong Yang, Llewellyn Tang, Yupeng Wu et al., 2016. Conceptual Development of a Compact Unglazed Solar Thermal Facade (STF) For Building Integration. SBE16 Tallinn and Helsinki Conference; Build Green and Renovate Deep, 5-7 October 2016, Tallinn and Helsinki (partly from Chapter 4 and 5)

4. **Jingchun Shen**, Xingxing Zhang, Tong Yang, Llewellyn Tang, Yupeng Wu et al., 2016. The Early Design Stage of a Novel Solar Thermal Façade (STF) for Building Integration: Energy Performance Simulation and Socio-economic Analysis. SBE16 Tallinn and Helsinki Conference; Build Green and Renovate Deep, 5-7 October 2016, Tallinn and Helsinki (partly from Chapter 7)

5. **Jingchun Shen**, Xingxing Zhang, Tong Yang, Llewellyn Tang, Yupeng Wu et al., 2016. Design Strategy of a Compact Unglazed Solar Thermal Facade (STF) for Building Integration Based on BIM Concept, The 8th International Conference on Applied Energy – ICAE2016, 8-11 October 2016, Beijing China. (partly from Chapter 5)

6. **Jingchun Shen**, Xingxing Zhang, Tong Yang, Llewellyn Tang, Yupeng Wu, 2016, Parametric study of a novel compact solar thermal facade (STF), The 8th International Conference on Applied Energy – ICAE2016, 8-11 October 2016, Beijing China. (partly from Chapter 5)

7. **Jingchun Shen**, Xingxing Zhang, Tong Yang, Llewellyn Tang, Yupeng Wu, 2016, Design strategy of a novel compact solar thermal facade (STF) for building integration based on BIM concept, EuroSun 2016, Palma de Mallorca, Spain on 12-14 October 2016.(partly from Chapter 8)

8. **Jingchun Shen**, Xingxing Zhang, Tong Yang, Llewellyn Tang, Yupeng Wu, 2015, An Initial Concept Design of an Innovative Flat-Plate Solar Thermal Facade for Building Integration, The 1st international Conference on Sustainable Buildings and Structures & The 2nd Low Carbon Construction Industrialization Forum 30-31 October 2015, Suzhou, China. (partly from Chapter 4)

Patents

1. Xingxing Zhang, **Jingchun Shen**, Tong Yang, Llewellyn Tang, A novel compact flat-plate heat pipe by sheet metal pressing approach, China patent, under application.

ACKNOWLEGEMENT

LIST of CONTENTS

LIST of FIGURES

LIST of TABLES

LIST of ABBREVIATIONS

AH	Auxiliary Heating	HVAC	Heating Ventilation and Air Conditioning
AIA	American Institute of Architects		
BI	Buying by Instalment	IM	Iterative Method
BIM	Building Information Modelling	IRR	Internal Rate of Return
BO	Buying Outright	LCA	Life Cycle Assessment
BSC	Building Shape Coefficient	LOD	Level of Development
CAAD	Computer Aided Architectural Design	LCI	Life cycle inventory
CEN	European Committee for Standardization	MPCS	Microencapsulated Phase Change Slurry
		NPV	Net Present Value
CFC	Chlorofluorocarbon	O&M	Operation and Maintenance
CFD	Computational Fluid Dynamics	ODP	Ozone Depletion Potential
CHS	Semi-Clathrate Hydrate Slurry	PCEs	Phase Change Material Emulsions
COP	Coefficient of Performance		
CPBT	Cost Payback Time	PCM	Phase Change Material
CPC	Compound Parabolic Concentrator	PCS	Phase Change Slurry
		PPA	Power Purchase Agreement
CPD	Construction Products Directive	PPM	Payback Period Method
CPI	Consumer Price Index	PV	Photovoltaic
CPR	Construction Products Regulation	PV/T	Photovoltaic/Thermal
CPT	Cost Payback Time	PVD	Physical Vapour Deposited
CR	Correlation Coefficient	RIBA	Royal Institute of British Architects
DHW	Domestic Hot Water		
DPP	Dynamic Payback Period	SPCS	Shape-stabilized PCM Slurries
DSF	Double Skin Facade	SPF	Sun Protection Factor
EC	Embodied Carbon / European Conformity	SPP	Static Payback Period
		STC	Solar Thermal Collector
EE	Embodied Energy	ST	Solar Thermal
EFA	Economic and Financial Analysis	STC	Solar Thermal Collector
EPBD	Energy Performance of Buildings Directive	STF	Solar Thermal Facade
		SWHS	Solar Water Heating System
EPBT	Energy Payback Time	TISS	Thickness Insensitive Spectrally Selective
EPT	Energy Payback Time		
ER	Root Mean Square Percentage deviation	TSSS	Thickness Sensitive Spectrally Selective
ESCO	Energy Service Company	TSTC	Transparent Solar Thermal Collector
ETAG	European Technical Approval Guidelines		
		VAT	Value Added Tax
ETC	Evacuated Tube Collector	VTC	Vacuum Tube Collector
gbXML	Green Building XML		
GWP	Global Warming Potential		
HCFC	Hydro Chlorofluorocarbons		

NOMENCLATURES

ΔT	Temperature difference (K);	P	Building potential;
A	Collecting area (m²);	p	Degree of feasibility;
A_{fin}	Total surface area of all fins on the STF surface (m²);	Pr	Prandtl number;
		Q	Energy rate (W);
A_{unfin}	Total surface area of un-finned portion on the STF surface (m²);	$Q_{aux,t}$	Overall auxiliary heat (W);
		Q_E	Electrical output(W);
C	Temperature coefficient of based on power (K⁻¹);	Q_T	Overall thermal load (W);
		Q_u	Useful solar energy (W);
C_P	Specific heat capacity of water (J/kg-°C);	Q_W	Solar energy gained by water (W);
D	Diameter (m);	Re	Renault number;
D_h	Hydraulic diameter (m);	S	Pitch distance (m);
E_{ao}	Annual electricity saving of HVAC system (W);	S_d	Standard deviation;
		SE	System efficiency (%);
E_{th}	Annual useful heat gain (equivalent) (W);	S_h	Absorbed heat rate (W);
		T	Temperature (K);
e_e	Electrical exergy (J/kg);	T_{cm}	Mean PV temperature (K);
e_{th}	Thermal exergy (J/kg);	T_i	Temperature of the fluid entering collector (K);
f	Solar fraction factor;		
F	Correction factor/efficiency;	T_{ref}	Reference temperature for cell efficiency (K);
F'	Absorber efficiency factor;		
F_{fin}	Fin efficiency (%);	T_{wm}	Ending-up temperature of working fluid (K);
F''	STF flow factor, defined as the ratio of F_R to F';		
		U_o	Uncertainty ratio;
F_R	Heat removal factor;	U_{od}	Thermal transmittance (W/m²·K);
h	Heat transfer coefficient (W/m²·K);		
		U_L	Overall heat loss coefficient (W/m²·K);
h_o	Heat convection coefficient (W/m²·K);		
		U_o	Heat transfer resistance from fluid to air (W/m²·K);
h_{PVref}	Photovoltaic efficiency at T_{ref};		
h_r	Radiation heat transfer coefficient (W/m²·K);	V	Velocity (m/s);
		w	Width (m);
I	Solar radiation intensity (W/m²);	X	Variable value;
k	Thermal conductivity (W/m²·K);	r	Correlation coefficient;
L	Length (m);	e	Root mean square percentage deviation;
L_P	Characteristic length of collector (m);		
m	Fin variable;		**Subscripts**
m_w	Mass flow rate of water (kg/s);		
n,N	Number;	a	Air/Ambient;
n_r	Row number in staggered pin-fin bank of STF module;	ac	Annual electricity savings of HVAC system;
		aux,t	Auxiliary heat;
Nu	Nusselt number;	bos	Balance of system;
Nu'	Corrected Nusselt number;	c	Convection;
P	Pressure (pa);	cd	Conductive heat transfer;
pF	PV packing factor;		

cv   Convective heat transfer;

D   Diagonal pitch;

E   Electrical energy consumption

e   Electricity-to-heat;

eq.   Equivalent;

e/exp Experiment result;

fin   finned area;

h   Hydraulic; heater;

i/in   Inlet;

L   Longitudinal pitch; loss;

Load,t Total thermal load;

m   Mean;

max   Maximum;

mtl   Replaced building material;

nofin Surface on STF without fins;

o   Outlet; optimal;

p   Absorber plate;
     Pin fin;

prim   Primary energy;

PV   Photovoltaic;

r   Radiation;
     Discount rate;

rd   Irradiative heat transfer;

s   Sky; surface;

s/sim Simulation result;

T   Total

Tr   Transverse pitch;

th   Thermal;

u   Useful;

unfin Un-finned surface on STF;
     Water; water tank;

w   ending-up temperature of
     working fluid;

Greek Symbols

a Thermal diffusivity (m²/s);
     Absorption coefficient of surface;

η Efficiency (%);

n Kinetic viscosity (m²/s);

ρ Density (kg/m³);

χ Correction factor;

η_c Ideal Carnot efficiency (%);

η_{ex} Overall exergy efficiency (%);

η_o Optical efficiency (%);

η_{PV} Efficiency of photovoltaic (%);

η_{tha} Solar thermal efficiency (%);

ξ_e Electrical exergy efficiency (%);

ξ_{th} Thermal exergy efficiency (%);

σ Stefan–Boltzmann constant;

Σ_{bos} Embodied energy of balance
     of system (W);

Σ_{mtl} Embodied energy of replacing
     building materials (W);

Σ_{STF} Embodied energy of STF
     system (W);

τ Transmittance coefficient of surface;

ε_{fin} Fin effectiveness;

ε_p Infrared emissivity coefficient of
     plate, being 0.10 for polished
     stainless steel plate;

σ Stefan-Boltzmann constant, being
     5.67×10^{-8} W/m²-K⁴;

μ Dynamic viscosity of working fluid
     (N·s/m²).

INTRODUCTION

1.1 Research background

Energy demand in present world is growing continuously, and buildings are responsible for the use of large amount of energy, which accounts for more than a third of the total energy supply (Wall et al., 2012; ESTTP, 2009; Pinel et al., 2011). Buildings are thus one of our potential opportunities for energy conservation and environment protection. Future energy projections, stating the growing gap between energy supply and consumption, have motivated the development of environmentally benign energy technologies. With regards to building application, the utilisation of renewable energy is, without a doubt, one of the most encouraging ecological avenues especially towards the sustainable and resilient city development.

1.1.1   Prospect of solar thermal technology

Solar energy, as a major renewable and eco-friendly energy source with the most prominent characteristic of inexhaustibility, is promising currently to offer potential solutions for sustainable development (Buker & Riffat, 2015). The most common solar technologies nowadays are solar photovoltaic (PV) and solar thermal, which together contribute to a large share of energy supply worldwide (shown in Figure 1-1).

Solar thermal as a mature and reliable technology, has been proven with relatively higher solar conversion efficiency than that of PV systems (Faninger, 2010; Pinel et al., 2011). In addition, solar thermal technology is highly cost effective with much shorter payback period than PV owing to the wide spread of application and massive production globally (Aste et al., 2015; Probst, 2008). As a result, solar

thermal technology exhibits great advantages and potential in large scale building application. With further launch of relevant solar thermal policies worldwide, the development in solar thermal technologies is forecasted to experience a boom similar to the photovoltaic application with a growing solar fraction demand in buildings (Hendriksen et al., 2000; Probst, 2008; MacLeay et al., 2012).

1.1.2   Holistic development of solar thermal technology in both UK and China

Till 2011, solar thermal provides only around 0.5% of estimated global water and space heating demand in the buildings sector in European area (Faninger, 2010; Pinel et al., 2011). In 2005, Europe operated about 10 GW_{th} capacity of solar thermal systems, and this capacity was expected to expand to 200 GW_{th} by 2030, of which up to 50% would be used for delivery of the low and medium temperature water (Compagno, 2002; ESTTP, 2009). In the UK, around 131 GWh of domestic hot water has already been provided by solar thermal systems, which partly replaced the conventional gas and electrical heating appliances in 2011 (Hendriksen et al., 2000; MacLeay et al., 2012). It was indicated that 148.2 million tonnes of oil equivalent was consumed with 66% for space heating, and another 17% for water heating with a total estimation cost of around £33 billion across UK economy in 2013 (Faninger, 2010; DECC, 2014). Meanwhile, the solar driven water heating system has been identified with a potential of around 70% to 90% of total energy required for water heating, thus enabling achieving significant saving in household fossil fuel energy use (Aste et al., 2015; Koene & ECN, 2010; Probst, 2008; DOEC, 2013; Shukla et al., 2013). Along with the issue of the Government's Renewable Heat Premium Payment scheme, solar thermal is expected to offer a great potential in both heat source diversity and both developing cities and towns towards sustainable and affordable ways.

Total capacity in operation [GW_th], [GW_el] and energy supplied [TWh_th], [TWh_el], 2014
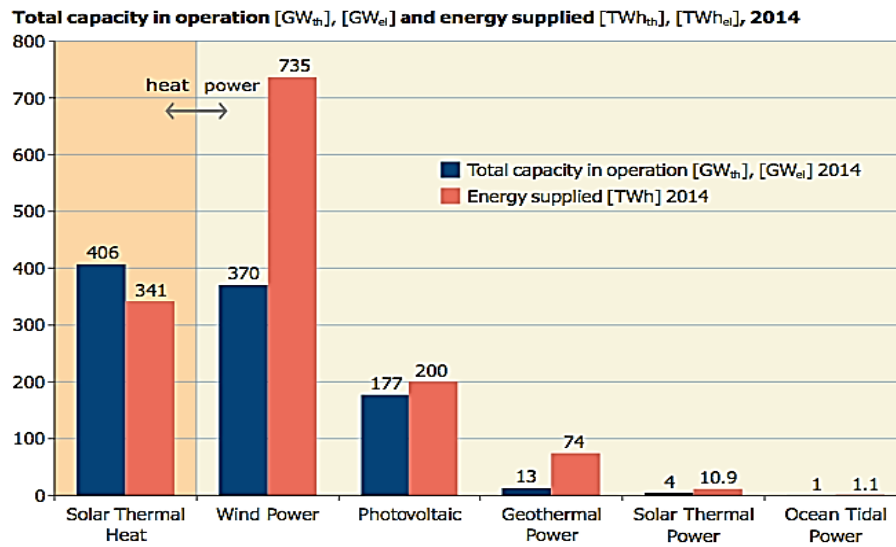
Figure 1-1 Global capacity in operation and annual energy yields in 2014
(Mauthner et al., 2013).

Sub-Sahara Africa: Mauritius, Mozambique, Namibia, South Africa, Zimbabwe
Asia excluding China: India, Japan, Korea South, Taiwan, Thailand
Latin America: Barbados, Brazil, Chile, Mexico, Uruguay
Europe: EU 28, Albania, Macedonia, Norway, Russia, Switzerland, Turkey
MENA Region: Israel, Jordan, Lebanon, Morocco, Palestinian Territories, Tunisia
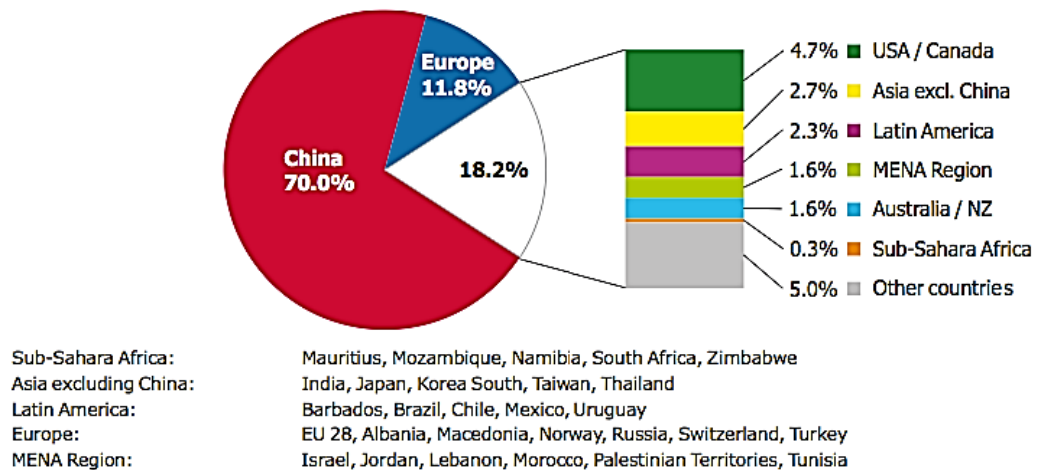
Figure 1-2 Share of the total installed capacity in operation (glazed, unglazed water /air collectors) by economic region at the end of 2013 (Mauthner et al., 2013)

As for China, the installed capacity of solar thermal in operation was 262.3 GW_{th} in 2013 (Mertin et al., 2013; Aste et al., 2015), which was far beyond the installed capacity in any other countries as shown in Figure 1-2 (Mauthner et al., 2013). At the beginning of 2015, Chinese authority released "*Renewable Energy Development Roadmap 2050*" as a long-and-medium-term plan for the development of solar technologies, showing a huge growing space for low-median temperature solar thermal application in supporting a stronger Chinese economy with a low carbon future (Compagno, 2002; Kalogirou, 2004; ESTTP, 2009; Fraas &Partain, 2010).

1.1.3   Necessity for development of new solar thermal technology

In order to achieve the global carbon emission reduction target, higher fraction of locally available renewable energy sources in energy mix is expected to become essential in addition to significant reduction of energy demand. Solar thermal energy would become one of the most significant renewable sources locally available for use in applications of building heating, cooling, hot water supply, or even power production.

However, most solar thermal systems are predominantly applied in small-scale plants. The current demand contribution of overall domestic hot water and space heating worldwide was about 1.2% of the global solar thermal energy in building sector in 2013. Inside, 84% was used for heating domestic hot water by small-scale systems in single family houses and only 10% was used for larger applications attached to multi-family houses, hotels, schools etc. (Mauthner et al. 2013). Moreover, when solar thermal systems come to application in large-scale space heating plants in urban networks, the insufficient suitable-and-oriented roof of most buildings may dictate the solar thermal implementation. It is therefore necessary to develop new solar thermal technologies with feasibility to be truly integrated with different building envelope components. Such requirement is expected to open up a large-and-new market segment of the solar thermal system for both new and existing buildings in need of energy efficient retrofitting and facade renovation. This will be especially considered as a future design solution at district or/and city levels.

1.2 Research objectives

Solar Thermal Facade (STF) systems address a real sense of building integration that can be potential solutions for the enhanced energy effi-

ciency and the reduced operational cost in contemporary built environment. This research aims to develop an innovative unglazed STF modular for facilitating domestic hot water production, plus a package of simulation model and design strategy at early design stage for either a new or existing building. To achieve this aim, the research sets out six interlinked objectives indicated in Figure 1-3:

1) To carry out an extensive literature study into existing building integrated solar thermal technologies, identifying existing technical challenges and to suggest potential solutions;

2) To design a conceptual building integrated solar thermal system incorporating potential initiatives concluded from literature review;

3) To conduct theoretical analysis and develop a computer model through the parametric approach to optimize the configurations of the proposed STF concept so as to predict the corresponding operational performance;

4) To construct and test a prototype system under laboratory-controlled conditions, and validate the simulation model using experimental data;

5) To evaluate annual energy performance of the proposed STF system by integrating it with a reference building in a simulation software, and establish a business model to provide a close-to-life socio-economic feasibility analysis.

6) To tackle design strategy of the proposed STF for building performance design and analysis at the early stage in architectural practice.

The whole works presented in this research plan to exhibit that simple structure, economical cost, versatile modularity, and easy installation can make this active solar facade an innovative and promising technology for the building stock transformation, despite of lower quality of the produced energy due to the low outcome temperature of the unglazed design.
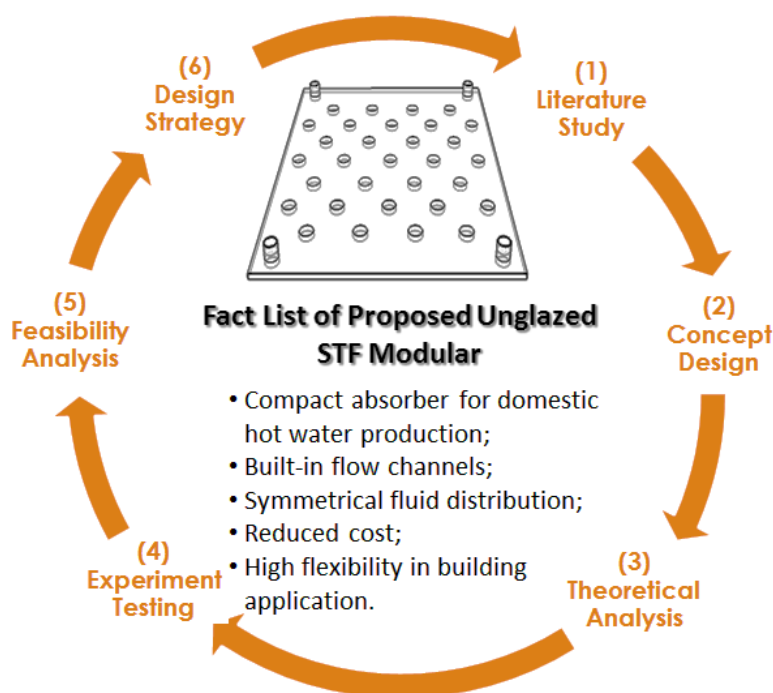
Figure 1-3 Six interlinked research objectives and fact list of the proposed unglazed STF modular for facilitating domestic hot water production

1.3 Research scope

STF is defined as the "multifunctional energy facade" that differs from conventional solar modules as it offers a wide range of solutions in architectural design (i.e., colour, texture, and shape), exceptional applicability, and safety in construction, as well as additional energy production. It also has feasible functions in heating/cooling the building, providing hot water, comfort building environment and overall architectural appearance, shown in Figure 1-4. Commonly, a typical STF system for building service normally comprises a group of modular STFs that receive solar irradiation and convert it into heat energy for the DHW circuit, whereas the heating/cooling circuits further operate based on the integration of an auxiliary heat source, a package of absorption chiller, hot/cold water storages, and a system controller. However, in this research, the proposed SFT concept would only focused on basic hot water generation due to the limited project

budget, while other functions and the integration with real buildings could be explored during future investigation.
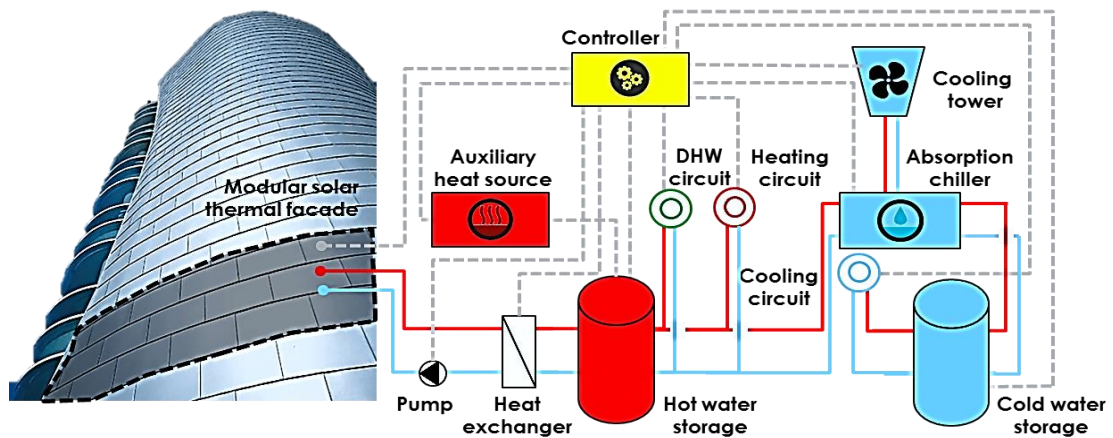
Figure 1-4 Schematic HVAC applications of the modular STF system

1.4 Research methodology

This project abides by the basic principle of the applied scientific research, which follows the procedure of concept formation, the validation/optimisation as well as application. The approaches to processing scientific and technological works are as follows:
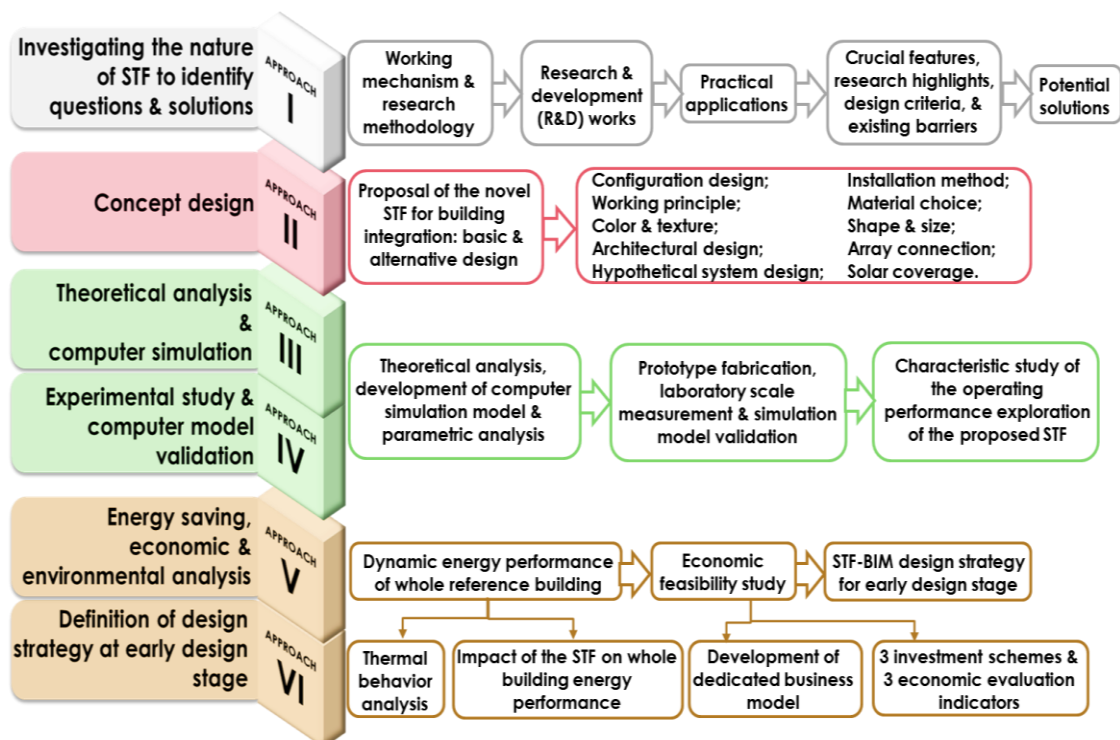
Figure 1-5 Research methodology summary

1) Identification of the nature of STF technology to bring forward questions and potential solutions in Objective (1);

2) Concept design in Objective (2);

3) Theoretical analysis and computer modelling in Objective (3);

4) Experimental testing and simulation validation in Objective (4)

5) Investigations of energy saving, economic, and environmental revenue in Objective (5);

6) Design strategy definition of the STF for high-performance building integration at early design stage in Objective (6).

Approaches (I) and (II) tackle concept formation; Approaches (III) and (IV) are to prove and optimize the proposed concept; Approach (V) and (VI) involve potential application of such STF concept. All these approaches, correlated to the relevant objectives, are given briefly in Figure 1-5.

1.4.1   Approach I

This approach would: 1) identify the fundamental STF working mechanism and research methodology; 2) involve a series of quantitative and qualitative reviews into research and development (R&D) works and the practical applications of the existing STF technology; 3) identify crucial features, research highlights, design criteria, and architectural/technical barriers of the existing STF technology; and 4) propose potential solutions for resolving challenges.

This approach would enable recognition of current STF research status and build the foundation for the other objectives.

1.4.2   Approach II

This approach would 1) develop new STF concept based on the literature review outcomes; 2) complete the sketch drawings of a new STF and its integration with building as various kinds of facade compo-

nent; 3) describe the basic working principle of the proposed concept; and 4) deliver alternative design in terms of material, colour, texture, shape, geometric size, architectural design, installation method, array connection, and hypothetical system application. This approach would generate the concept for building application and lay the foundation for Objectives (3), (4), (5) and (6).

1.4.3   Approach III

This approach would 1) carry out the fundamental mathematical analysis of energy balance and heat transfer processes occurring in the STF module; 2) develop an analytical computer simulation model on the basis of iterative method (IM) to investigate thermal performance of the STF module; 3) validate the simulation model by the published experimental work and 4) operate the model for parametric analysis.

These would enable 1) determination of the STF performance against different variables, 2) clarification of the optimum module configuration, and 3) recommendation of appropriate design and operational parameters for the STF. This approach would lead to the refined concept design addressed in Objective (2), data validation as well as socio-economic feasibility analysis and definition of design rules of thumb to be undertaken in the following objectives.

1.4.4   Approach IV

This approach would 1) propose the fabrication methods for the STF prototype system and construct it according to recommendations; 2) characterise the operational performance exploration of the prototype system under laboratory conditions and verify the simulation model; and 3) conduct error and uncertainty analysis between simulation and testing results. This approach would enable 1) devel-

opment of an experimental prototype using a feasible fabrication method in practice; 2) verification of the simulation models derived from Objective (3); and 3) outputting characteristic performance curves of the STF.

1.4.5   Approach V

This approach would operate a dynamic simulation model in software to explore the operating performance of the proposed STF integraed into a reference residential building. The socio-economic impacts would assess based on a decicated business model at early design stage for both the designer and the investor in the perspective of solar thermal building integration design. This approach would enable the evaluation of potential benefits and impacts of the proposed STF, including energy savings, payback period, life-cycle cost saving, and carbon emission reduction.

1.4.6   Approach VI

This approach would 1) identify the role of STF in building performance design and analysis; 2) demonstrate the importance of building performance simulation and analysis; 3) develop dedicated design strategy based on Building Information Modelling (BIM) concept for the proposed STF application. This approach with necessary steps would ensure economic/environmental factors and energy efficiency strategies integrated with the design process at early stage.

1.5 Research novelty

In brief, this research has the following identifiable novel aspects:

Concept design: two parallel thin flat-plate metal sheets form up the built-in flow channels that eliminate the utilization of tubes and enable a high flexibility in colour, texture, size, and shape according to vari-

ous architectural and aesthetic requirements. Thus, such STF concept is simple, economical, and aesthetically appealing with easy installation (plug & play) similar to metal claddings in building application.

STF flow channel structure: the laser-welding technique is applied to join both the extruded metal sheet with arrays of mini pin-fin corrugations and the smooth metal sheet together, forming up the built-in turbulent flow channels. Besides, two fluid inlets (at the bottom) and two fluid outlets (on the top) are respectively with standard piping joints for a symmetrical fluid distribution. Such unique and compact structure engenders not only high heat transfer performance caused by the finned absorbing surface and the crossflow over pin fins, but also great feasibility in assembly of either parallel or series flow pattern.
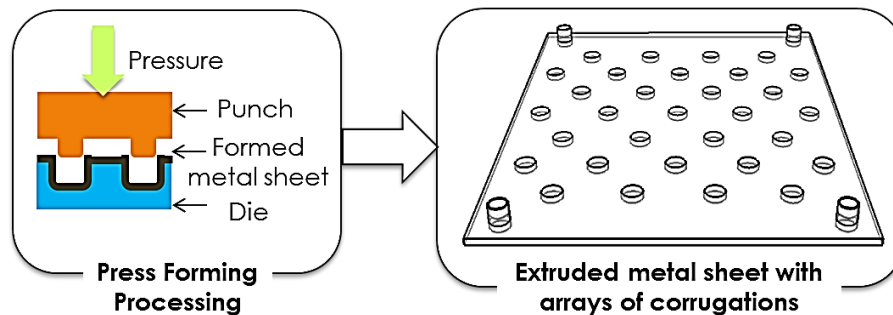
Figure 1-6 Schematic of press forming technology producing the extruded metal sheet in the proposed STF

Fabrication and budget: the fabrication prerequisite is based on the press forming technology of metal sheet (illustrated in Figure 1-6), which is a well-established in large-scale industrial processing and is mainly applied for the heating radiator manufacture. It enables significant cost reduction. In addition, different arrangement and combination of extruded pin-fin banks can form up different channels arrangement. As a result, diverse channel structures allow high feasibility and complexity in generating channel structure at boundary area in cases of various shape or size without any additional cost. Subsequently, the combination of both extruded pin-fin banks and the press

forming process is expected to result in the possibility of developing a high-efficiency, economical STF for more flexible architectural design.

Methodology: a comprehensive package of simulation model and BIM associated design strategy is developed for the proposed STF investigation with full considerations of architectural requirements, system working performance, economic/environmental behaviours and energy efficiency strategies at early design stage.

1.6 Thesis structure

The thesis has 9 chapters in total and its structure is as follows:

Chapter 1, Introduction: it briefly describes the research background, objectives, scope, methodology, and novelty.

Chapter 2, State of the art - theoretical and technical development: it provides a comprehensive review towards recently emerging STF technologies, in terms of concept, classification, structural configuration, indicative performance, economic and environment evaluation, current research and development progress, theoretical analysis as well as economic and environmental performance assessment.

Chapter 3, State of the art - research prototypes and pilot applications: it describes the relevant design criteria for STF design in terms of technical, constructive and safety issues, supplemented with architectural integration methods. Besides, it underlines the applicability of existing STF technologies and the integrity between STF and building component. A large number of research studies, prototypes, commercial products, and pilot engineering projects have been summarized to offer references for future work.

Chapter 4, Concept design of the compact unglazed STF: a novel compact STF design is proposed in terms of configurations, material, colour, texture, shape, geometric size, architectural design, installation

method, array connection, and hypothetical system application for future facade application.

Chapter 5, Theoretical analysis and simulation model development: it develops the computer simulation models by analysing the fundamental equations of the energy balances, solar transmittance, heat transfer, and fluid flow. Through operating simulation model, appropriate STF design/operational parameters are recommended. These results are subsequently applied to the prototype construction and experiment testing.

Chapter 6, Prototype fabrication, experimental evaluation, and simulation model validation: it describes the detailed process and method for the prototype fabrication. A series of laboratory-based experiments are set up to evaluate the prototype system and validate the simulation modelling. The results are applied to identify normal external factors impacting upon system performance. In addition, the verified simulation model can generate characteristics performance curves for following the proposed STF building integration simulation.

Chapter 7, Early design stage of the STF for building integration - energy performance simulation and socio-economic analysis: it explores the annual energy performance of the STF for integration with a reference residential building in Shanghai as well as its impact on the overall building energy loads and the related environmental benefits. It also states the economic feasibility of such STF by a dedicated business model.

Chapter 8, Design strategy of the STF for high-performance building integration: it identifies the role of STF in the building performance design and analysis. And it also demonstrates the importance of building performance simulation and analysis. Furthermore, it establishes dedicated design strategy based on the BIM concept. This approach in-

volves necessary steps in ensuring economic/environmental factors. And energy efficiency strategies are able to get involved with the design process at early stage.

Chapter 9, Conclusions and further work: it concludes the main conclusions from this research. A field testing of this system is described with the initial measurement results within a summer week in Shanghai. Opportunities and challenges are discussed for further development of this technology.

All the above chapters are systematically linked in order to achieve both the project aim and objectives. The overall research results shall be beneficial for further design, optimisation, and application of such a STF within various solar driven systems for building application. Generally, such a STF technology is expected to possess the potential to boost building energy efficiency and literally turn envelopes into independent energy plant. It is possible to deploy the solar-thermal technology in building facades and consequently cut down fossil fuel consumption and CO_2 emission significantly in the coming futu

STATE OF THE ART–THEORETICAL AND TECHNICAL DEVELOPMENT

2

2.1 Chapter abstract

This chapter provides a comprehensive review towards recently emerging STF technologies. It covers the aspects of concept, classification, structural configuration, indicative performance, economic and environmental evaluation, current research and development progress, theoretical analysis as well as economic and environmental performance assessment. And the major tasks in Chapter 2 are:

1) Present both concept and theory of the STF technology;

2) Illustrate a comprehensive literature review into the R&D works of STF from integrated structure and individual components layout, sizing and optimisation; theoretical simulation and economic and environmental prediction;

3) Analyse the review in the categories of STF type and research methodology;

4) Identify the major features, current R&D status, research highlights, and existing technical barriers of various STF technologies.

This part of the work is expected to lay the solid foundation for the entire investigation with additional assists in:

1) Understand the concept and classification of STF;

2) Clarify technical development of current STF;

3) Identify theoretical methods for subsequent chapters.
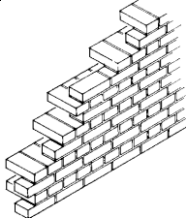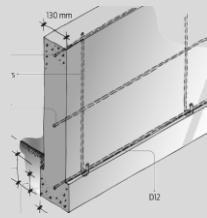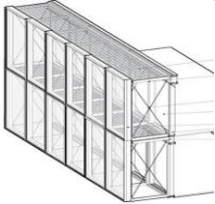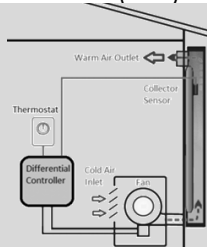
2.2 Concept and fundamentals of STF

In building sector, the term 'facade' stands for the outer envelope of a building, including the transparent/ translucent part, opaque part and shading part. The essential function of transparent part is the supply of vision and daylight, while the translucent part taking privacy into consideration. And the opaque part usually consists of solid walls with the purposes of external/sound insulation and load bearing.

2.2.1   The appearance of STF

Generally, there are 4 principal types of facade in the aspect of construction, briefly illustrated in Table 2-1.

Table 2-1 Classification of common building facade

Types of Building Facade	Definition
Masonry Wall	It has modular nature and has good thermal properties, classifying into natural stone, man-made clay bricks and concrete masonry units. It is commonly used in low or medium rise buildings for flexible construction, and passive architecture design purposes.
Precast Concrete Wall	The prevailing prefabrication and 3D printing technology make the modern production of precast slabs and facade modules possible with additional control properties, such as strength, dimension, workability, pollution and time etc. And it has more frequently applications in medium or high-rise building for a flexible element and curtain wall construction.
Double Skin Facade (DSF)	Compared to conventional walls, two skins/facades are placed into a wall system. DSF brings an extra buffer zone and attracts an architectural trend in new buildings for a modern outlook with additional solar gain. The ventilation of the intermediate cavity can be natural, fan supported or mechanical to assist the HVAC strategy indoor. More cases are found in commercial buildings, such as office.
Multifunctional Wall	Driven by the aesthetic architecture desire, practical demand for improved indoor thermal performance, and the aspiration for on-site energy/thermal generation in a building, the multifunction facade provides a wide range of energy-saving implementations, such as natural ventilation, night-time cooling, natural lighting, the creation of heating, cooling etc. when assisted with additional mechanical system.

Note: resources from: Hendriksen et al. 2000; Reijenga 2012; Compagno 2002.

Recently, the prevalent implementation of multifunction facades has been paid more attentions. In addition to the rising publics' consciousness about energy conservation in building sector, the implementation of renewable energy has been gradually accepted. When

the solar thermal collector is endowed with the other function as a building fabric component at same time, the STF has arisen. And its building functions can be as versatile functions as possible relying on the integrated approach to building design, such windows, walls, roof and floors etc.

2.2.2   The concept of STF

A STF is a special building facade that incorporates a solar thermal absorber into its structure and circulates the cooling medium using a circulation pump. For a typical STF, energy absorption, conversion / transfer processes are shown in Figure 2-1, covering 1) solar absorption and heat gain by thermal absorber; 2) conductive and convective heat transfer caused by temperature difference between thermal absorber and surrounding air or working medium; and 3) thermal radiation exchange between facade and its surroundings. The fundamental equations for the above energy conversion/transfer processes are given below:

Solar absorbing $\qquad$ $Q_f = A \times \alpha \times I$ $\qquad$ [2-1]

Conductive heat transfer $\qquad$ $Q_{cd} = A \times U_{cd} \times \Delta T$ $\qquad$ [2-2]

Convective heat transfer $\qquad$ $Q_{cv} = A \times h_{cv} \times \Delta T$ $\qquad$ [2-3]

Irradiative heat transfer $\qquad$ $Q_{rd} = A \times \sigma \times (T_1{}^4 - T_2{}^4)$ $\qquad$ [2-4]

,where, A is the collecting area, m²; a is the absorption coefficient of absorbing surface layer; I is the solar radiation intensity, W/m²; U_{cd} is the thermal transmittance, W/m²K; ΔT is the temperature difference, K; T_1 and T_2 generally refer to absolute temperature (K) between two irradiative associated surfaces; h_{cv} is the convection coefficient, W/m²K; σ is the Stefan–Boltzmann constant (Szokolay 2008).
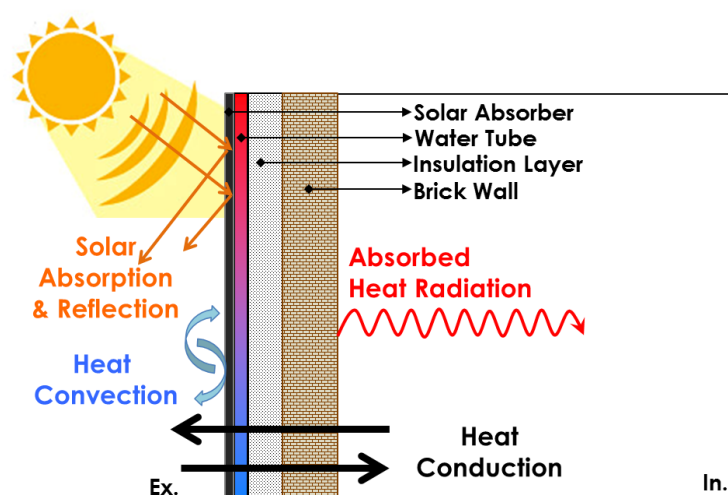
Figure 2-1 Schematics of the heat transfer mechanisms in a typical unglazed STF

A STF could not only increase the thermal insulation of a building but also collect a certain amount of heat from the solar radiation striking onto its surface. Due to the prevailing prefabrication of building construction, the industrialized production of precast slabs and precast functional facade modules make possible to manufacture such STF modules. STF based on different working mechanisms can have several additional functions, e.g. heating, ventilation, and shading for active purpose, thus enabling both energy capture and distribution.

Recently, the STF has become an increasingly attractive building component to replace the separately installed solar thermal collector, with several identified merits as: 1) adequate capacity to collect, and transfer solar thermal energy for various purposes in buildings; 2) dissipation of solar gains away from building envelopes leading reduced cooling load in summer; 3) integrated design taking into account shielding, thermal collection, piping connection, load bearing and withstanding of extreme weather condition et al.; 4) saving in building services occupation space by integrating them into building facades, thereby creating larger available interior space; and 5) acting as the weather proof skin to improve building's thermal insulation.

2.3 Classification of STF

Classification of STFs can be made by building part, thermal collection typologies, transparency, application, as well as heat-transfer medium, which is illustrated in Table 2-2.

Table 2-2 Overall classification of STF

Types	Classification
Building part	• Wall; • Window; • Balcony; • Sunshield; • Roof;
Facade Transparency	• Transparent solar collector for window integration; • Translucent-air heating vacuum tubes collector; • Opaque-angle selective & glare protection building integrated photovoltaic; • Opaque to human eye but highly transparent to solar energy;
Collecting Typology	• Evacuated tube collector (direct-flow/heat-pipe); • Glazed flat plate collector (liquid/air based); • Unglazed flat plate collector (liquid/air based/ perforated plate/transpired air); • Hybrid photovoltaic/thermal;
Heat Transfer Medium	• Air; • Hydraulic (water, refrigerant) ; • Phase Change Material (PCM); • Heat pipe ;
Building service function	• Ventilation or heat recovery; • Hot water production; • Heating/cooling-dual use; • Electricity/heat-dual use.

2.3.1   In terms of building part

STF panels can be classified as wall-, window-, balcony-, sunshield and roof-based types. These STF components can work as traditional building components, and meanwhile remain functions as a solar absorber. Within a typical STF, there is a thermal insulation layer that is also used to retain solar heat outside, an absorbing plate or a top glazing that also have waterproof and anti-corrosion function.

2.3.2   In terms of facade transparency

STF panels can be classified as transparent, translucent, and opaque, types. The transparent and translucent types offer the dual functions of solar heat absorption and daylight transmission. The semi-transparent type selectively transmits parts of solar light within a certain spectrum range, while collecting the remaining part of solar radiation in form of heat. The selective see-trough type is opaque to the human eye but highly transparent to solar energy (Mertin et al. 2013).

2.3.3   In terms of solar collecting typology

STF panels can be briefly classified as the evacuated tube, glazed and unglazed flat-plate. The typical operating temperatures and the degree of efficiency are listed in Table 2-3.

Table 2-3 Main characteristics of typical collectors

Collector Typology	Operating temperature	Efficiency	Energy production (kWh/m² p.a.) [1]	Price range (€/m²) [2]
Evacuated tube	70-130℃	80-85%	480-650	500-1100
Glazed flat plate	60-90℃	65-70%	400-600	320-480
Unglazed flat plate	30-40℃	40%	300-350	200-260

Note: (1) Switzerland -field surface: 6m², and the same regional price data in 2010.
(2) resources from: (Shukla et al. 2013; Probst 2008; Probst & Roecker, 2007; Probst & Roecker, 2012)

2.3.4   In terms of heat transfer medium

STF panels can be classified into air-, hydraulic- (water/heat pipe/refrigerant) and PCM-based types. Air based type is characterized by lower cost, but lower efficiency due to the air's relatively lower thermal mass. This system usually uses the collected solar heat to pre-heat the intake air for purpose of building ventilation or space heating. Hydraulic-based STFs are most commonly used in building integrated solar thermal devices that enable the effective collection of the striking solar radiation and conversion of it into the heat for purpose of hot water production and space heating.

The PCM-based type is usually operated in combination with air, water or other hydraulic measures that enable storing part of the collected heat during the solar-radiation-rich period, and releasing it to the passing fluids (air, water, or others) during the low solar radiation period, thus achieving a longer operation period (Zhang et al., 2015a).

To study each heat transfer medium category further into each sub-category, Table 2-4 illustrates and summarizes the comprehensive features of each heat transfer medium (Zhang et al., 2015a).

Table 2-4 The characteristics of heat transfer mediums

Heat transfer medium	Advantages	Disadvantages
Air	• Anti-freezing or boiling; • Non-corrosive; • Low cost; • Simple structure;	• Low heat capacity & thermal mass; • Potential leakage & noise; • Lower efficiency; • Large volume;
Water	• Nontoxic; • High in specific heat; • Cost effective; • Almost constant energy collected; • Smaller storage volume;	• Potential mineral deposits; • Possible leakage, freezing; • Corrosion and overheating; • Unstable heat removal effectiveness;
Refrigerant	• Small fluid volume; • Quick response to solar heat; • Stable performance; • High efficiency;	• High cost; • Unbalanced liquid distribution; • Requirement of recharging refrigerant;
Heat pipe	• Compact & high heat exchange ability; • Low in hydraulic & thermal resistances; • Versatility, scalability, & adaptability	• High cost; • High degree in vacuum processing;
PCM	• Improvement in thermal comfort & building envelope; • Diversity in building integration.	• Difficult to operate; • Complex behavior; • Diverse affection factors; • Sensitive heat injection.

1) Air-based solar thermal facade system

Air-based solar thermal systems use air as the working fluid for absorbing and transferring solar energy. It can directly heat a room or pre-heat the air passing through a heat recovery ventilator or an air coil of an air-source heat pump.

Single Air Channel

Ex.   In.   OR   Ex.   In.

From left to right:
- Glass Pane
- Glass Tube With Air Inside
- Insulation
- Wall / Glass Pane

From left to right:
- glazing,
- Absorber
- Insulation
- Wall

Ex.   In.

From left to right:
- Glazing
- PV Panel
- Insulation
- Wall

Ex.   In.

From left to right:
- Double Glazing
- Air Cavity
- Venetian Blind
- Internal Glazing

Ex.   In.

From left to right:
- PV Panel
- Air Cavity
- Insulation
- Wall

Ex.   In.

From left to right:
- PV Panel
- Air Cavity
- Double Glazing

Ex.   In.

From left to right:
- Transpired Plate
- Air Cavity
- Insulation
- Wall

Ex.   In.

From left to right:
- External Sheet
- Air Cavity
- Insulation
- Facade

Double Air Channel

Ex.   In.

From left to right:
- Glazing
- Outer Air Duct
- PV Panel
- Glaze
- Inner Air Duct
- Insulation

Ex.   In.

From left to right:
- Double Glazing
- 1st Air Cavity
- Venetian Blind
- 2rd Air Cavity
- Internal Glazing

Ex.   In.

From left to right:
- Glazing
- Cooled PV Panel
- Insulation
- Wall

Fan   Fan
Hot air   Cold air
Ex.   In.
Water Pump

From left to right:
- Transpired Plate
- Plenum 1
- High Porosity Sand Tile
- Plenum 2
- Insulation
- Wall

Figure 2-2 Schematics of main air flow channel layouts in STFs

It is a promising solar thermal technology with the main advantages of: anti-freezing and anti-boiling operation, non-corrosive medium property, and low cost and simple structure. Therefore no damage caused by leakage, stagnation condition and frost problems needs to be dealt with, offering a possibility of reliable and cost-effective solutions even at a low irradiation levels. But air has a very low thermal capacity of only 0.32 Wh/Km^2, resulting in higher mass or volumetric flow and poor thermal removal effectiveness for STF system. In other words, more occupancy space is necessary in building facade components to contain air-handling equipment (ducts and fans) compared to piping and pumps in the hydraulic-based system. In addition, higher required pumping power and acoustic problem associated with the air-based operation are worthy of attention.

In general, air-based STF system could be simply delivered from the single channel and the double channels, as shown in Figure 2-2. The air-based solar thermal facade could be formulated by incorporating an air gap between the back surface of glazing cover, PV panel, external sheet, construction mass, and the building fabric (facade, glazing or roof). In practical application, the air based STF in space heating systems are usually operated with fixed airflow rates, thus the outlet temperature varies along with the varying solar irradiation in a day. Whereas, it runs at a fixed outlet temperature with a varying flow rate. Both heat removal factor and collector performance would be low when flow rates are low (Kalogirou 2004). When air circulation is combined within PV/T modules, effectiveness for PV cooling would be very low, if the air temperature is above 20 ℃ (Kalogirou 2006).

2)   Water-based solar thermal facade system

Water owning to its high thermal capacity, thermal conductivity, low viscosity and cost, is the suitable heat transfer medium for solar thermal technology. Besides, it allows easy storage of solar gains, and is suitable for direct domestic hot water production and indirect space heating. However, different from other heat transfer mediums, water is corrosive in nature (especially at high temperature) as well as freezing and scaling risks, which pose challenges in the design of tubing and plumbing (Delgado et al. 2012; Shukla et al. 2013; Zhang et al. 2011; Tian & Zhao 2011). Though glycol/water mixture has been widely adapted to lower freezing risk, it is still worthy of attention with water pressure difference at different facade levels (heights). And more measures should be taken into considerations regarding envelope structure, accessibility and protection of water leakage (Probst & Roecker, 2012).
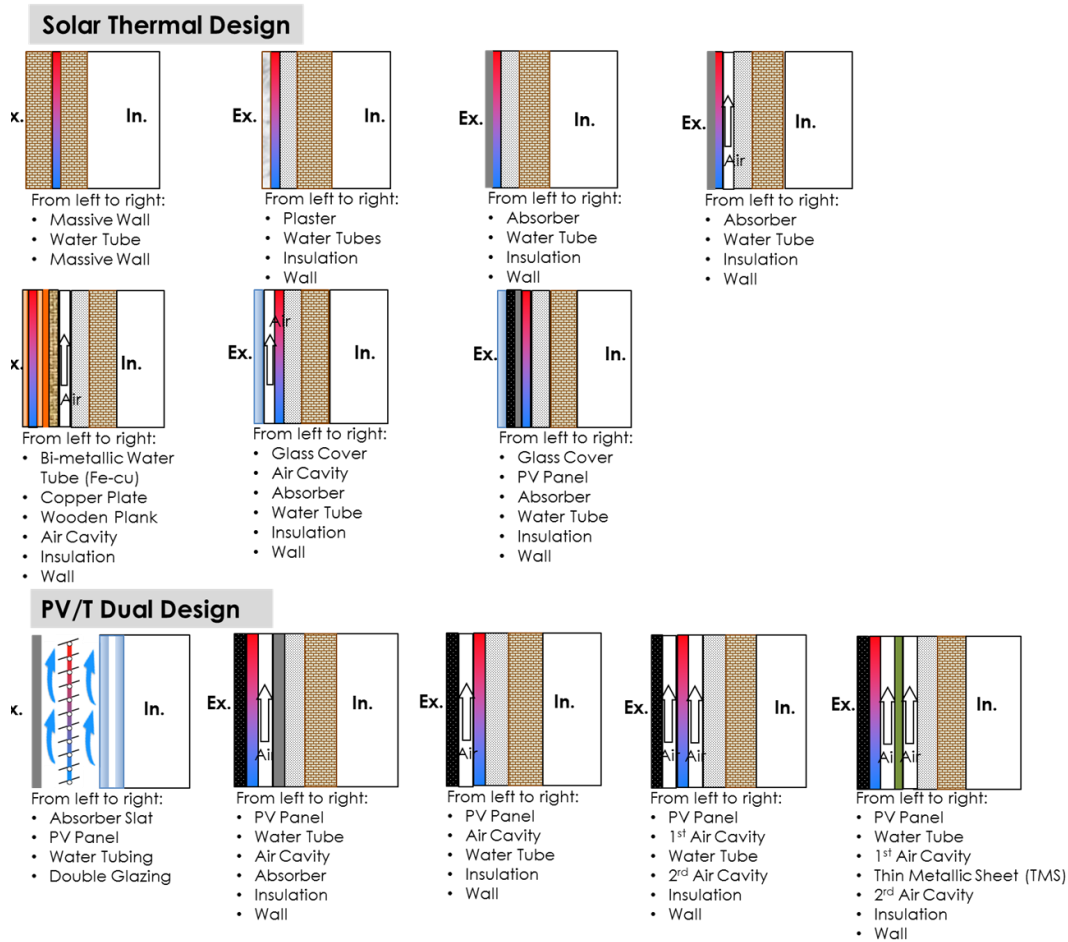
Figure 2-3 Schematics of main water flow channel layouts in STFs

Figure 2-3 demonstrates different kinds of water based solar thermal facades. It can be mainly divided into two modes of arrangement: the single water channel and the multiple flow channels (integrated air and water flow). The former structural arrangements are evolved from the mechanism of the passive solar heating, which often provide the solutions to hot water purpose. The latter structural arrangements are normally formulated by incorporating additional air gap between the PV module (absorber, water flow tubes) and the building fabric. As a result, air could be delivered from above, below or on both sides of the water tubes. By means of additional electrical or mechanical equipment, these designs can provide the solutions to the inversed thermo-siphon phenomena and the uncertainty of heat transfer. In some cases, the PV module acts as the thermal absorber (named PV/thermal design) and the water flow channels could be round, rec-

tangle and other irregular geometries. The water-based PV/thermal designs take advantages of both electricity production and heat extraction. At present, the technical drawback of the traditional PV panels lies in the relatively low electrical efficiency in the range 6% to 18%. PVs' electrical efficiency varies in an inversely linear trend with the PV cells' surface temperature, leading to around 0.5% efficiency declining per degree rise in cells' temperature. The water-based PV/Thermal designs are therefore developed to control the temperature of the PV cells, to increase the corresponding electrical efficiency during practical operation, and meanwhile make advanced utilization of the waste PV heat. Usually, the multiple water flow channels structure is designed for the end-users who have multiple demands in hot air, space heating, agriculture/herb drying or increased ventilation, and electricity generation.

3)   Refrigerant-based solar thermal facade system

Compared to water, refrigerant has properties of lower boiling/freezing, lower viscosity, and higher thermal capacity. Therefore even a small amount enables a larger amount of heat transfer. In the indirect heat-pump based STF system, the thermal collector also works as a heat-pump evaporator, which could respond more quickly to the absorbed solar heat even in poor weather conditions compared to other STF systems. In terms of the refrigerant types, Chlorofluorocarbons (CFC) are the most commonly-applied heat-transfer fluids due to the properties of stability, non-inflammability and non-corrosively. But CFC has high Ozone Depletion Potential (ODP) and Global Warming Potential (GWP). As a result, the hydrochlorofluorocarbons (HCFC) took place. Recently, natural fluids, such as propane (R-290), butane (R-600), isobutane (R-600a), propylene (R-600), ammonia (R-717) and carbon dioxide (R-744) have been considered as long-term heat

transfer fluid with great environmentally behavior at a very low or near zero ODP and GWP (Shukla et al., 2013).

Refrigerant as the working fluid is more prevalent in the application of PV/thermal system coupled with the heat pump (Punjabi & Miranda, 2005). From the simulation results, it can be found that a lower evapo-ration temperature was associated with higher system efficiency. Be-cause a lower evaporation temperature leads to a lower surface temperature of absorbers for solar cells to override the limitation of electricity generating efficiency, meanwhile the heated refrigerant can be further re-utilized for thermal production with increasing the coefficient of performance (COP) of heat pumps (Tripanagnostopou-los, 2002).

4) Heat pipe-based solar thermal facade system

The solar collector incorporating with the core heat transfer compo-nent of the heat pipe ensures advantages as one-directional, two-phase thermosyphons, very low hydraulic resistance, constant liquid flow and isothermal heat absorbing surface. The heat pipe technolo-gy has significant development in the evacuated tube collector (ETC) with two basic types of single-tube and double-tube. Because of the major drawback of fragile glass cover, the sole utilization of heat pipe has been introduced to alleviate this problem (Chen et al. 2010). And it has been currently brought forward as an individual heat transfer component into the design of STF system. Because of the special characteristics of heat pipe technology, it has been identified that heat pipe based system presents a great potential acting as the fa-cade integrated system, which requires of small weight, versatility, scalability, and adaptability of the design (Rassamakin et al. 2013). From the literature reviewed, there are three main types of heat pipes used in heat pipe based system, including conventional heat pipe,

loop heat pipe, and micro-channel heat pipe, shown in Figure 2-4. As a potential heat transfer medium applied in STF system subsequent to the water-based STF system, the heat pipe based STF system has to overcome the limitations in on-site assembly requiring higher vacuum degree, higher manufacture costs caused by intensive labour processing, and difficulties in maintenance and replacement.
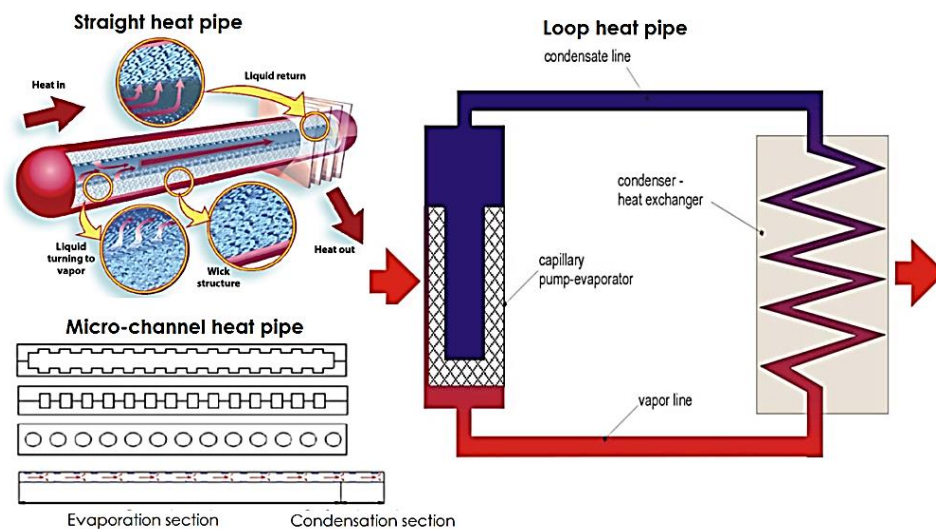
Figure 2-4 Schematics of main heat pipe structures applied in STFs (Wang et al. 2012; Deng et al. 2013)

5) PCM-based solar thermal facade system

Phase Change Material (PCM), with higher energy storage density and thermostatic fusion, is particularly attractive for the latent heat transfer (Tian & Zhao 2011). In recent years, a new technique has been proposed to use the Phase Change Material Slurry (PCS) as a kind of pumpable heat transfer fluid and heat storage systems (Delgado et al. 2012; Zhang et al. 2011; Tian & Zhao 2011). As for the application in STF system, more potentials of a heat transfer fluid exist for PCS in the building integrated solar thermal system application. It allows the increase of system energy efficiency, reduces the size of pipes and collector area, and saves pumping power consumption due to less amount of heat transfer fluids (Youssef et al. 2013; Zhang et al. 2011). But till now, more applications of PCM (Tyagi & Buddhi 2007;

Alvárez et al. 2013; Koschenz & Lehmann 2004; de Gracia et al. 2013; Zhao et al. 2010; Haillot et al. 2012; Gracia et al. 2012; Saman et al. 2005; Diarce et al. 2013; Rodriguez-Ubinas et al. 2012) have been found in the STF system with the function of thermal storage that characterized by a great thermal energy storage capacity, high heat transfer property and positive phase change temperatures. Because the heat transfer process of PCS evolves with complicated phase change, PCS still needs more intensive investigation for its function as heat transfer fluid.

2.4 Structural configuration of STFs

The basic structure of STF is originally derived from the conventional solar thermal collector (Figure 2-5), which includes three fundamental configurations as glazed, unglazed flat-plate and evacuate tube shapes.
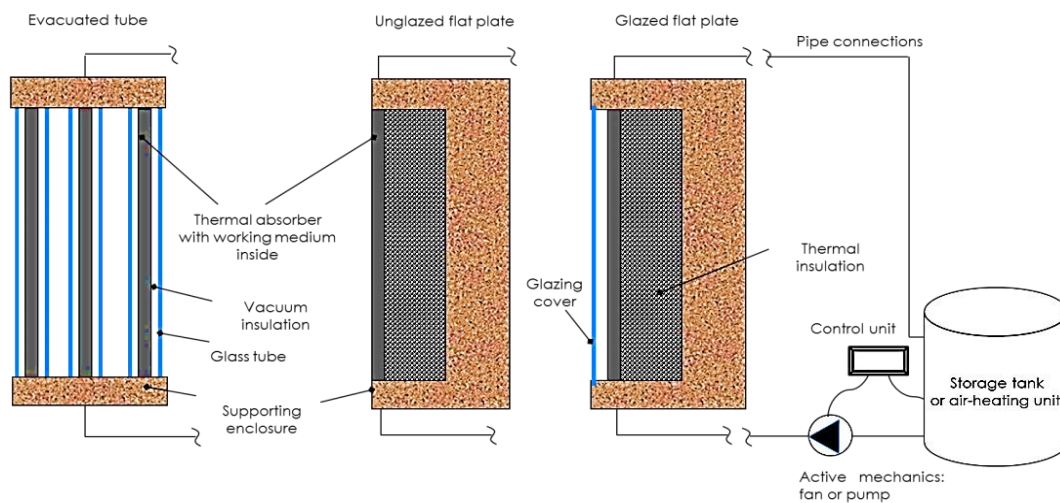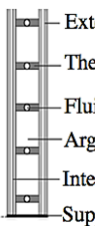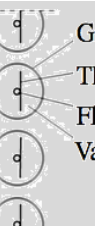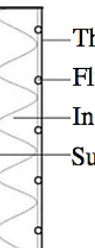
Figure 2-5 Fundamental structures of STFs

The flat-plate STF usually compromises a glazing cover (optional), a fluid-cooling thermal absorber, an insulation layer (optional), and supporting enclosure, whilst the cylinder STF normally consists of evac-uated tubes with fluid-cooling thermal absorbers inside. The overall STF system has a storage tank and additional mechanical devices, such as fans, pumps, complex controllers, or other auxiliary devices to redis-

tribute solar energy. However, the specific structures of the STF systems are various when they serve as different building elements in practice as summarized in Table 2-5.

Table 2-5 Summary of STF structures in terms of building components

Schematic structure	Note
Glazing / Thermal absorber / Fluid-cooling circuit / Insulation / Supporting enclosur — Typical wall based STF	Flat-plate structures have wide applications in the wall-based STFs which consist of modular rectangular boxes with several layers as: 1) a glazing cover (optional); 2) a metal plate with a selective treatment as solar absorber; 3) a fluid-cooling circuit adhere to the absorber; 4) a back insulation layer; 5) the supporting enclosure; The wall-based STFs could either be glazed or unglazed structure, but are usually opaque to buildings with heat transfer medium of air/ hydraulic/ PCM slurry.
External glazing / Thermal absorber / Fluid-cooling circuit / Argon or vacuum insulation / Internal glazing / Supporting enclosure — Typical window based STF	Flat-plate structures are also commonest in the window-based STFs which consist of several layers in the module: 1) an external glazing cover; 2) a metal plate with a selective treatment as solar absorber; 3) a fluid-cooling circuit adhere to the absorber; 4) an argon gap or vacuum insulation space; 5) an internal glazing cover (optional); 6) the supporting enclosure; The window-based STFs could be with multiple glazing units fixed in the frames for insulation, natural lighting and building service, which are usually translucent to buildings with heat transfer medium of air /hydraulic/PCM.
Glass tube / Thermal absorber / Fluid-cooling circuit / Vacuum insulation — Typical baclony based STF	Evacuated tubes are especially recommended for integration of balcony. They are composed of several individual glass tubes, each containing: 1) a glass tube; 2) a black or black-tube thermal absorber; 3) a fluid-cooling unit bond to a heat pipe; 4) a vacuum insulation; The balcony-based STFs are usually translucent with the heat transfer medium of air / heat pipe.
Thermal absorber / Fluid-cooling circuit / Insulation / Supporting enclosure — Typical roof based STF	Flat-plate structures are the most promising in the roof-based STFs with either modular rectangular or tile geometry. They normally consist of several layers: 1) a glazing coverer (optional); 2) a selective treatment as solar absorber plate (optional); 3) a fluid-cooling circuit adhere to the absorber/ glazing; 4) a back insulation layer 5) the supporting enclosure; The roof-based STFs can either be glazed or unglazed structure. And they are usually opaque or transparent to buildings with the heat transfer medium of air or hydraulic.

2.5 Indicative performance, economic and environmental evaluation

Up to date, few published legal standards are available to specifically address performance parametrical figures of STF. In this situation, the methods used for evaluating the solar thermal collector were recommended to determine the performance of STF systems. To summarize, the technical performance of the STF systems is usually evaluated by using following indicative parameters:

2.5.1   Solar thermal efficiency

The thermal performance is a factor determined under a heat balance evolving convection, conduction and radiation. Under steady-state conditions, the useful heat delivered by a Solar Thermal Collector (STC) is equal to the energy absorbed by the heat transfer fluid minus the direct or indirect heat losses from the surface to the surroundings, therefore the equation of the thermal efficiency can be written as followed:

$$\eta_{th} = \frac{Q_u}{Q_T} = \frac{Q_u}{I \times A_P} = F_R \tau \alpha - F_R U_L \frac{T_i - T_a}{I} \qquad [2\text{-}5]$$

,where A_c is the aperture area of collector, m^2; F_R is the heat removal factor due to the fact that the fluid entering the collector is heated in the direction of the flow affected only by STC characteristics, fluid type, and fluid flow rate through the collector; Q_u is the useful solar energy, W; I is the total solar energy incident on the collector aperture, W/m^2; U_L stands for the overall heat loss coefficient respectively; T_i is the temperature of the fluid entering collector, K and T_a is the ambient temperature, K.

2.5.2   Solar fraction

Solar fraction is defined as the fractional ratio of the primary energy saving that a STC can obtain to the overall energy demand, and could be expressed as:

$f= (Q_{load,t} - Q_{aux,t}) / Q_{load,t}$ [2-6]

,where $Q_{load,t}$ and $Q_{aux,t}$ is the overall thermal load and auxiliary heat required, W. The higher the solar fraction in solar thermal system, the lower amount of fossil energy required for auxiliary heating, but in the extreme case 100% is none at all.

2.5.3   System efficiency

The system efficiency gives the ratio of solar heat yield to the global solar irradiance on the absorber surface with respect to a given period of time, e.g., one year. It could be written as:

$SE= (Q_{load,t} - Q_{aux,t}) / (I \times A_p)$ [2-7]

The system efficiency is strongly dependent on the solar fraction. If solar fraction upsurges due to the increased collector area, the system efficiency will decrease. This means that the cost for obtaining additional unit energy is getting higher.

2.5.4   Economic and environmental evaluation

In terms of the economical evaluation, the simplified approach for assessing the economical measure of the STFs is using Cost Payback Time (CPBT). Such a measure is based on the predicted annual energy savings of an STF and its initial cost, representing cost difference between STF and conventional facade of same area. The drawback of this measure is that it only provides an approximate index without counting the time related factors and maintenance cost.

Technically innovative STF is generally more expensive than a 'business as usual' product, Cappel et al. found that STFs have between a 150% and 333% higher initial investment cost when compared with standard walls. They also noted that the area of an STF would need to be increased by a factor of between 1.5 and 2.0 when compared with tilted solar thermal collectors (Cappel et al., 2014). As a result, the

whole life cycle cost is principal in application of the STF systems. Therefore, the basic cost information of the components of an STF is critical to the comparative study between technical renovation and financial value of an STF. Based on the referenced price list given in Table 2-6 and a study made by Koene et al., following conclusions could be drawn up: 1) in terms of economic benefits, the STF providing a low temperature heat source for heat pump seemed to be a cost effective approach; 2) the concepts using conventional PV-panels or PV sun shading were more cost effective than the sole-functional STCs, due to the relatively high yield of PV panels in terms of primary energy and the relatively lower cost of investment compared to a solar heating and cooling system.

Table 2-6 Cost range for novel components used in a renovation project

Component	Price Range	Unit
Active Solar Facade System With Individual Heat Pump And Local Thermal Storage Tanks	450-550	€/m² facade
KF Vacuum Tube Solar Collector	300-500	€/m² facade
Transparent Solar Thermal Single Skin Facade	250-350	€/m² absorber
Transparent Solar Thermal Double Skin Facade	150-250	€/m² absorber
PV-Sun Shading	500	€/m²

Note: All cost data are from Switzerland including 20% VAT and include cost of labor for installation (Koene, 2012)

In terms of the environmental impact assessment, the Energy Payback Time (EPBT) and the Life Cycle Assessment (LCA) are the commonly used parameters. EPBT is the ratio of the embodied energy of the STF and its annual energy output; while the embodied energy refers to the quantity of required energy during the STF production period. Chow suggested a mathematic expression of EPBT (Chow, 2010):

$$EPBT = \frac{\sum STF + \sum bos + \sum mtl}{E_{PV} + E_{th} + E_{ac}}$$

[2-8]

whereby Σ_{STF}, Σ_{bos} and Σ_{mtl} are the embodied energy of the STF system, the balance of system and the replacing building materials; E_{pv} is the annual useful electricity output; E_{th} is the annual useful heat gain

(equivalent), and E_{ac} is the annual electricity saving of HVAC system due to thermal load reduction.

According to ISO 14040/14044, LCA method takes into account the inputs and outputs of the manufacturing, system installation and associated operational and maintenance costs over the system's life cycle (Karlessi, 2013). For each step, a list of input and output data for the used materials, consumed energy and associated emissions are quantified. Connecting the process input and output data to the impact categories by means of characterization model can carry out an impact assessment. Results for such an impact assessment provide information regarding the potential environmental impacts that a product might have, e.g. the potential contribution to climate change or the consumption of resources (Löwe et al., 2011).

Till now, Lamantou et al. organized the system covering life-cycle inventory, life-cycle impact assessment and interpretation. It consists of 30 solar collectors for the configuration with flat-plate collectors, and additional functional units (such as storage tank, pump, external tubes with their insulation, glycol). In the system, the boundaries refer to the whole system in terms of the phases of: material manufacture (collectors and system additional components), manufacture of the collectors, system installation, use/maintenance, transportation and disposal. (Lamantou, 2016).

2.6 Research and development progress of STF

In the beginning of a state of art review into STFs, first comes the abundant research works based on solar collector development since collector is the core component in STF system with working performance, specific shape, materials and cost etc. The more flexibility lies in solar collector, the more chances can be offered for successful

building integration design. Therefore a comprehensive review is addressed at first to provide a solid and fundamental technic support in the application of a reliable and efficient STF proposal.

2.6.1   Components design

From the sequence of layers in a solar collector, **glass** has been widely used as the cover of glazed solar collectors owing to its high transmittance in shortwave irradiation while transmitting virtually none of the long-wave radiation out. Traditionally, glass cover accounts for around half weight in the glazed flat-plate collector between 15 and 20kg/m², which posed a weight problem for STF application (Sonnenenergie, 2010; O'Hegarty et al, 2016). But the existence of glass cover(s) has directly relations with the values of convective and radiative heat transfer coefficients and the absorption of solar radiation on inner/outer surface temperatures for a flat plate solar thermal collector. Compared to a single glazed collector, the increase in glass cover temperature due to absorption of solar radiation could be as high as 6K, while the increase of first and second glass covers of a double glazed collector could be as high as 14K and 11K, respectively (Maurer & Kuhn, 2012). In a consequence, the difference of including and neglecting the convective heat transfer coefficient between the absorber plate and the first glass cover was as substantial as 49% (Akhtar & Mullick, 2012). Nowadays, the conventional clear glass is being replaced by the low iron glass owning to its relatively high absorption coefficient for solar radiation (approximately 0.85–0.87) and an essentially zero transmittance coefficient for the long-wave thermal radiation (5.0μm–50μm) (Tian & Zhao, 2013; Kalogirou, 2004). Khoukhi et al. (Kalogirou, 2005; Kalogirou, 2007) studied the glass cover of flat solar thermal collector taking both the absorption and emission effects into account. The profiles of resulted efficiencies curves implied to be not linear in shape for both systems with clear and low-

iron glasses accordingly, and the instantaneous efficiency was higher in case of low-iron glass cover.

As for the evacuated tube collector, since glass cylinders are positioned outside of internal absorbers to reduce thermal losses, the different level of vacuum degree has the direct relevance with the thermal losses through convection and conduction (shown in Figure 2-6), whereas selective coating can reduce the radiation losses in the same way as the glass panel.
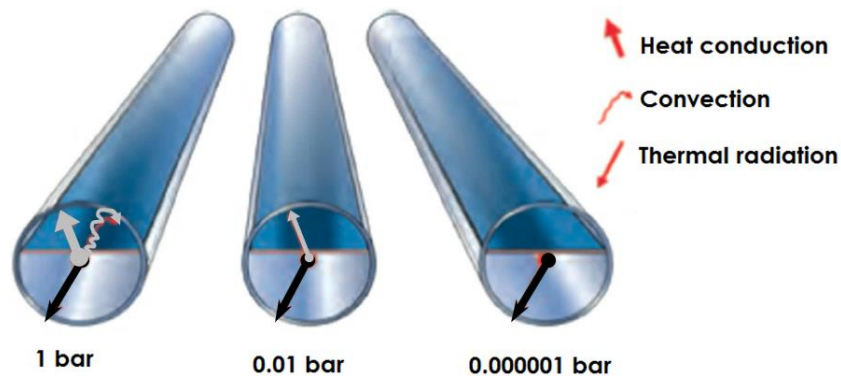
Figure 2-6 Heat transfers in relation to vacuum degree (Sonnenenergie, 2010)

Instead of glass material, **more cover choices** are feasible for the unglazed solar collector, which can be briefly categorized into asphalt, polymeric materials, massive materials and metals. The variety choices of front cover provide feasibility for STF application. The metal one offers good heat transfer performance and flexible ability in moulding, they are expensive and require special treatment for anti-corrosion. In comparison, the economic competitive polyolefin materials are of high relevance and interest for absorbers with supplemental overheating protection. The polypropylene grades were of high potential for black absorbers of collectors with overheating control (Khoukhi et al., 2007). The massive materials were good thermo-physical properties with a high workability and stability to thermal stresses with low cost and offer a great freedom and harmony as construction component, but time-lag between solar availability and building demand

would be a problem (D'Antoni & Saro, 2012). The concrete solar collectors offer a cheaper alternative to other expensive STFs primarily because of their bulk mono-material makeup, while complex framing is not necessary (O'Hegarty et al, 2016). All-ceramic solar collector with the thermal efficiency about 47.1% on-site as balcony railings and 50% as pitched building roof, is characterized by low cost, long lifetime, no attenuation of absorbance, and building integration (Yang et al., 2013). In spite of having a lower thermal conductivity and heat storage capacity than massive collector, the black colour and asphalt mixtures ensure asphalt solar collectors perform better than the massive ones. However special attention should be paid during the construction process with hot mix asphalt, since the high temperature of asphalt mixture can damage the tube system (Bobes-Jesus et al., 2013).

Furthermore, the **additional film and coating** can guarantee a solar collector with a high light-absorption capacity and lowest possible thermal emissivity. For example, plastic films and sheets possess high shortwave transmittance as well as generally limited the temperatures without deteriorating or undergoing dimensional changes. But only a few types of plastics can withstand the sun's ultraviolet radiation for long periods (Kalogirou, 2004). Through the addition of a Teflon film or a Teflon honeycomb, antireflection treatment of the cover glazing and combinations of these improvements, the experimental results showed that a combined increase in the absorption coefficient from 0.95 to 0.97 and a decrease in the emissivity coefficient from 0.10 to 0.05 can be obtained with the annual performance enhancement of 6.7% at 50 ℃ operating temperature, while the augment in the performance by installing a Teflon film and the antireflection treatment of cover glazing as second glazing were estimated to increases the an-

nual output 5.6% at 50 ℃ and 6.5% at 50 ℃ respectively (Hellstrom et al., 2003).

Except of the optimisation of heat collection function, **colour, texture and finish of cover surface** are the special characteristics for building integrated STF. A mixture of special matching degree between flat plate collector appearance and building external layer is necessary to be compatible with other building skin materials. It includes surface geometries, such as corrugated embossed, perforated, regular/irregular, etc. (shown in Figure 2-7) and surface finishing, such as matt, glossy, structured, etc.
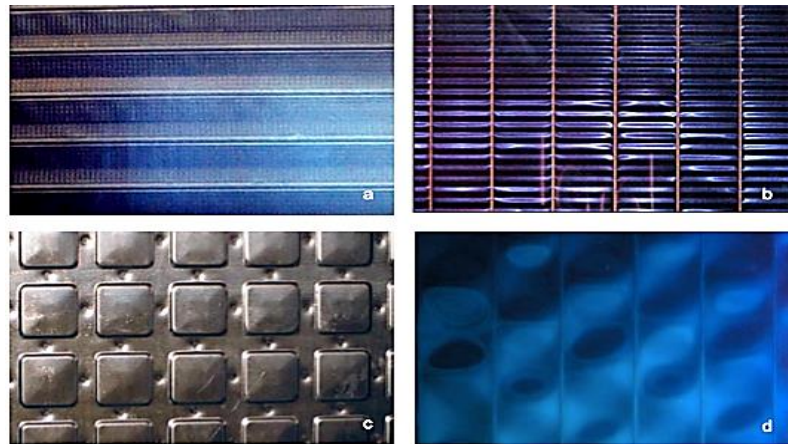
Figure 2-7 Four types of absorber surface geometries (Probst, 2008)

The absorber plate absorbs the incident solar radiation, and transfers the retained thermal energy to working fluid with minimum thermal loss. The enhancements in the values of solar radiation absorbance and heat transfer rate, and the decreased emissivity coefficient are the dominating approaches for conventional solar collector optimal design and additional aesthetical appealing design for the STF system.

First of all, **paint and coatings** possess a clear advantage to alter the optical and radiation properties from a surface, regarding cost, ease of application and simplicity (Wijewardane & Goswami, 2012). The absorbance depends on the nature of coating colour and incident angle. Typically, a absorber plate is with black coating to absorb as

much heat as possible, however the monotonous colour has been re-placed by various colour coatings for a dramatic outlook (Maurer & Kuhn, 2012; Tripanagnostopoulos, 2007). Via the simulating results from TRNSYS, the coloured solar absorbers decreased the amount of col-lected energy slightly with the medium coefficient of absorbance value (a=0.85) in the three locations (about 7–18%) compared to col-lectors with black absorbers (a=0.95). Additionally, the LCA implied that the economics of the systems employing colour collectors were attractive for fabrication and application on buildings (Kalogirou et al., 2005). Later, the theoretical and experimental investigation into the relation between thermal performances and a series of colours of ab-sorber's plate showed that different coloured absorbers keep heating loads within a reasonable fraction range, as shown in Figure 2-8.
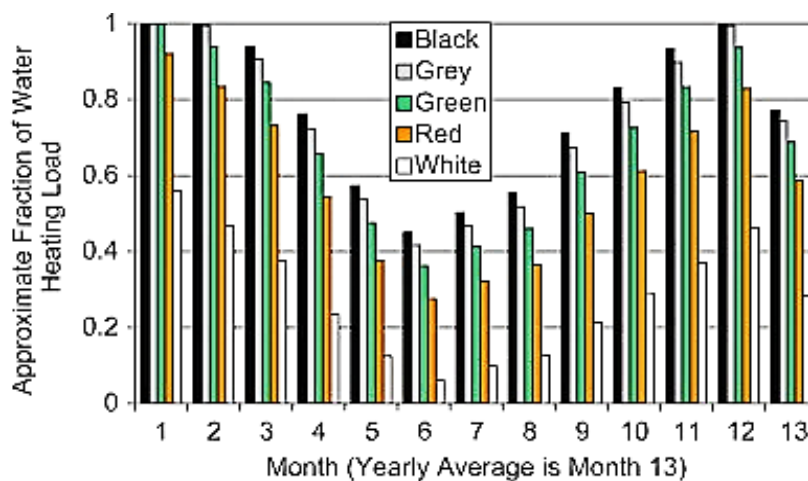
Figure 2-8 Fractions of water heating loads for coloured glazed solar collectors (An-derson et al., 2010)

As long as the collector surface temperature is much higher than the ambient air temperature, the emission control of thermal radiation from a surface is particularly important to the solar selectivity of any surface, which evaluates the spectral property of **solar selective ab-sorbing coatings** (Kalogirou et al., 2005). Therefore other than the paint technology, coating technology has been exploited with a va-riety of materials and composites for mid- to high-temperature appli-cations (Zhang K. et al., 2017). Some inorganic compounds and met-

al/dielectric composites can be used as selective coatings in various solar thermal applications (Tesfamichael et al., 2001; AlShamaileh, 2010; Kurzböck et al., 2012).

The metal/dielectric composites coating have attracted many attentions of researchers because of its high reflectance in the infrared region and semi-transparency in the visible region, as well as excellent solar absorption and low thermal emittance (Oelhafen P. et al., 2005; Wijewardane & Goswami, 2012). For instance, the free electron metals as Cu, Ag have emissivity values down to 0.02-0.04, showing the desirable selective properties. Mo–Al_2O_3, W-AlN , Pt–Al_2O_3 and and Ag–Al_2O_3 etc. have been successfully applied for mid- to high-temperature solar thermal power plants for electricity generation (Du X. et al., 2008; Zhang Q. et al., 1996; Zhang Q. et al., 2001; Nuru Z. et al., 2012; Nuru Z. et al., 2016). The transition metal oxides, nitrides, as well as oxynitrides coatings, such as Ti–Al-N, Zr–C–N, Zr–O–N, Ti–Al–O–N , and Nb–Ti–O–N have also attracted great deal of attentions due to their higher diffusion block ability than the metal–dielectric nanocomposite coatings at high-temperatures (Blickensderfer R. et al., 1977; Selvakumar N. et al.,2012; Liu Y. et al., 2012; Rebouta L. et al., 2012; Barshilia H., 2014). In the market, most commercial absorber coatings are prepared with chromium or titanium as absorbing layer (Zhang et al., 2017). For environmental and physiological reasons the substitution of the chromium by titanium is desirable. And titanium containing amorphous hydrogenated carbon films (a-C:H/Ti) have already been the focus of considerable attention due to their application as hard and wear resistant protective coatings (Schüler et al., 2000). Recently, the high-temperature photonics using self-organization of superalloys has raised attention for solar selective absorbers application (Shimizu M. et al., 2014).

From another prospect, the **improvement in heat transfer capacity** in absorber structure is the other optimized design route, aiming to achieve a good thermal connection between piping system and absorber plates. Firstly, a horizontal comparison in thermal connection approaches between absorber and pipe system is critically exhibited. From Table 2-6, it seems that certain promising solutions are beneficial to provide cost effective cassette modules offering freedom in dimensions. Then a number of design essentials have been summarized to improve the heat transfer performance in absorbers. It can be concluded as (Tripanagnostopoulos et al., 2002; Tripanagnostopoulos, 2007; Ackermann et al., 1995):

1) Roughening channel wall with ribs or fins;

2) Interposition of corrugated sheet or thin metal sheet;

3) Additional tube placement;

4) Using wall surface of high emissivity within different channel walls or even simply placed on the channel wall for the purpose of heat extraction enhancement in collectors;

5) Combination of decreasing fin pitch;

6) Increasing fin thickness;

7) Increasing thermal conductivities of fin materials (in Figure 2-9).
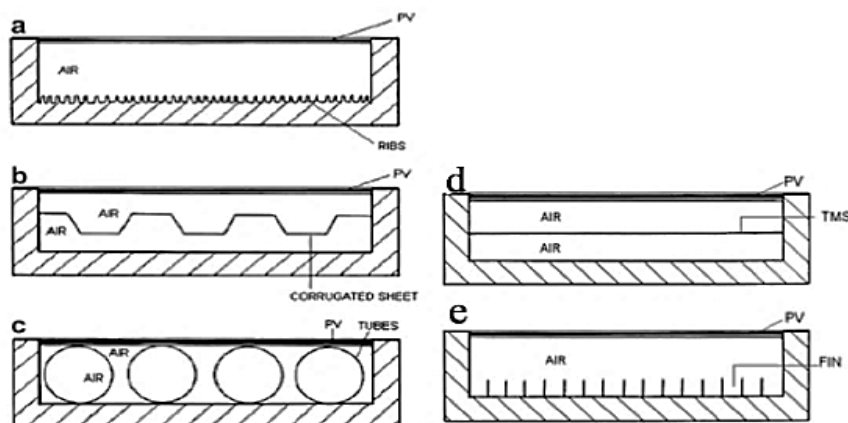
Figure 2-9 Schematic of air heat extraction improvements of the PVT/ air system (Tripanagnostopoulos, 2007)

Other than the hydraulic based solar collector, the air/gas based collector that employed with metallic sheet is especially suitable for the

pre-heating purpose in building integration. The external perforated sheet is around 100-300 mm sealed to create an air channel from the back sheet, which can be an envelope for building integrated implementation or a non-perforated insulated sheet in case of standalone system (Shukla et al., 2013). The principle ensuring a good thermal connection between air/gas and absorber requires a larger contact area as to overcome the heat transfer penalty caused by lower heat transfer coefficients of air/gas absorber, and the recommended value of perforations, also known as porosity, generally covered the fraction between 0.5% and 2% of total area for the single pass thermal collector to achieve a better flow distribution (Kalogirou, 2009; Dymond & Kutscher, 1997).
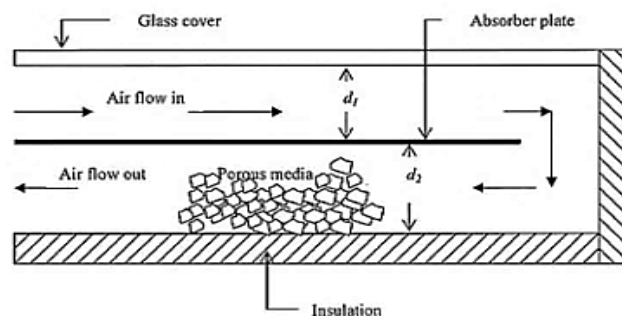
Figure 2-10 Schematic of double channel solar thermal collector with porous media
(Sopian et al., 2009)

In terms of double-pass STC, the presence of porous media in the second channel increases the outlet temperature, shown in Figure 2-10, therefore increased the thermal efficiency of the system around 60-70% but with unavoidable pumping power (Sopian et al., 2009). Nevertheless, passive heat transfer augmentation techniques have been studied through the modification in terms of shape and arrangement of baffles in Figure 2-11(Ucar & Inallı, 2006).
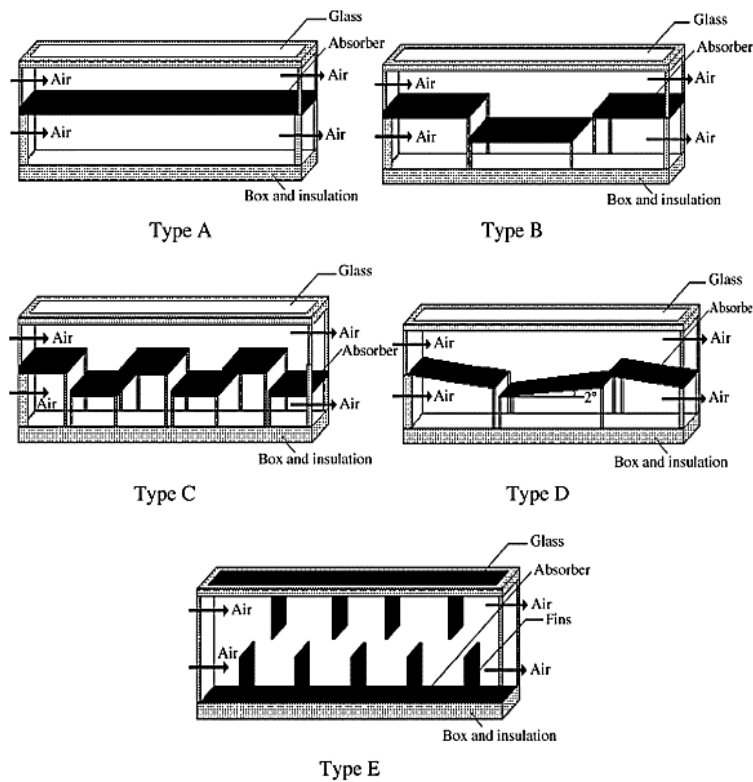
Figure 2-11 Cross-sectional views of the solar air collectors with different shape and arrangement of baffles (Ucar & Inallı, 2006)

By sectional blocking absorber surface, attaching fins on absorber surface and giving a tilt angle to the sectional surfaces, the efficiency of solar collector has been increased approximately 10% to 30%, while the exergy loss has been decreased from 64.38% to 43.91% in comparison with the conventional solar collector (Sopian et al., 2009). Based on baffle design, extending the trajectory of airflow and increase the speed of air within the collector were succeeded in raising the concept of turbulence creation through the utilization of obstacles or baffles (Ucar & Inallı, 2006).

In order to realize the considerable device heat transfer performance improvement, another available prospect route for the air/gas based solar thermal collector is the application of external recycles design to strengthen forced heat convection. Through the investigation of a double-pass structure for solar absorbing plate with recycle, a considerable improvement in heat transfer was obtainable in comparison

with those in single-pass devices or conventional double-pass solar heaters under the same flow rate. It was concluded that the channel thickness ratio and adding recycle at both ends were suitable to increase collector efficiency (Romdhane, 2007). The combined effects from fins attached and external recycle were theoretically investigated in the upward-type double-pass flat plate solar air heaters. It was found that the collector efficiencies increase as growths in air flow rate, number of fins attached and incident solar radiation, and more than 80% improvement in collector efficiency was obtainable with external recycle (Ho et al., 2011).

Despite the thermal connection between absorber plate and pipe system, the proper mechanical joining is another link to guarantee a good thermal bond from processing aspect (Kalogirou, 2004). The joining should fulfil the requirements, including conductivity, mechanical strength, deformation, reliability, and durability. Up to now, the common mechanical connection process is welding or soldering (Duerr, 2006). Because of soldering has the limitation in operating temperature and corrosion risk, modern manufacturing techniques of ultrasonic welding, laser beam welding and robotic automation have been gradually introduced into the industry. Unfortunately, less literature has covered these manufacturing techniques in the field of STF till now. However it is important to consider which manufacturing technique and kinematics are best for a particular solar application task and where vision fits, as well as where there are the greatest return opportunities.

2.6.2   Dimension and position

There are several major factors relevant to the position and dimension of STF, such as available area on building facade, seasonal solar radi-

ation on accessible surface, Inclination, orientation and insolation
(Probst & Roecker, 2012).
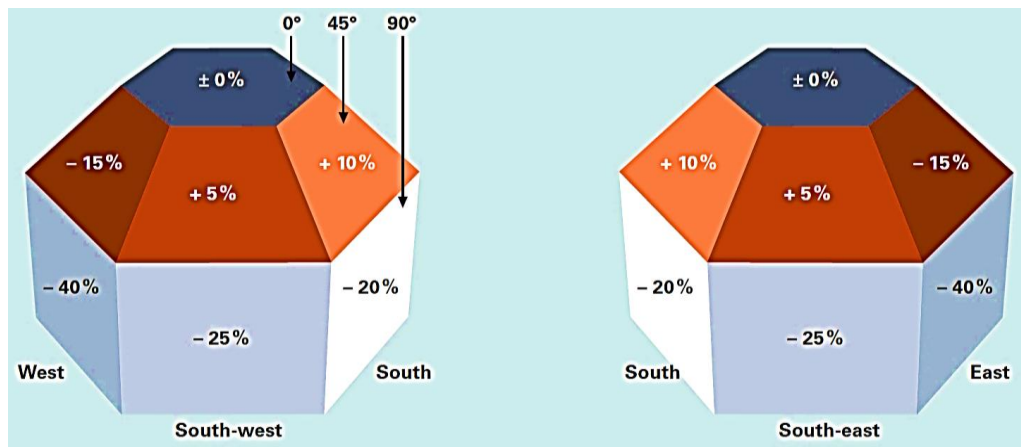
Figure 2-12 Deviation schematic of global radiation in Germany (Werke, 2015)

Figure 2-12 reveals the general interaction relations of **inclination, orientation, and insolation** in a case study in Germany. The values of global radiation energy are influenced by the inclination of the receiver surface. The amount of energy is greatest when the radiation hits the receiver surface at the right angle.

Table 2-7 Comparisons of common connection approaches between absorber and pipes（GSES, 2010）

Type	Advantage	Disadvantage
Roll-bonded absorber	• Numerous branches can be produced in single materials; • Good heat transfer with working fluid;	• Subject to corrosion of aluminum in connection with copper tube; • Only function on high purity aluminum;
Absorber strips with pressed-in copper tube	• High flexibility in form and shape for composed collector; • Beneficial to mass production;	• Many solder points;
Absorber sheets with pressed-in tube system	• No mixed materials; • Simplifies subsequent recycling;	• Heat transfer not optimal;
Absorber with all-around contact with tube system	• Same materials between tube and absorber; • Optimal heat transfer;	• High in manufacture cost;
Absorber with soldered-on tube system	• Flexible in design;	• Asymmetrical heat transfer;
Full flow-through absorber	• Good heat transfer to liquid; • Easy processing;	• High weight, thermal inertia;
Serpentine absorber	• Only two solder points in tube system; • Easy in piping connection;	• High pressure loss and temperature difference; • Cannot work effectively in thermosiphon mode;
Full-surface register tube & Vane register tube	• Lower pressure loss than serpentine absorber;	• Many solder points in tube system; expensive;

In the northern hemisphere, an orientation towards the south is ideal. Subject to the angle and orientation of a surface, the level of insolation – relative to a horizontal area would reduce or increase. A range can be defined between south-east and south-west at angles between 25° and 70°, where the yields achieved by a solar thermal system are ideal. Greater deviations for systems on vertical walls can be potentially compensated for by correspondingly larger collector area. So the vertical STF can possibly produce more solar heat than that on the other building position due to the potential availability of larger solar collecting area. Moreover, the vertical STFs are less sensitive to the weather conditions, such as dust, rain and snow (Werke, 2015). As a result, the optimum installation position for the STF, if from the energy yield point of view, should be depending on different building scenarios or limitations, rather than particular one.

From the "thermal system" point of view, a series of comparative studies in the aspect of collector tilt-angle from 22° to 46° indicated that the collector tilt-angle has significant influences on the daily collectible radiation and daily solar heat gain but less on both heat removal capacity from collector to storage tank and the daily solar thermal conversion efficiency (Tang et al., 2011). Chandel et al. (Yadav & Chandel, 2013) compressively reviewed the topic of tilt angle optimization and listed a number of optimization techniques. He mentioned that for urban areas, the obstacles affecting the solar radiation should also be considered for computing optimum tilt angles.

Apart from direct influence on the efficiency of energy production, the theoretical simulation in Figure 2-13 provided the comparison between the monthly sun radiations available on the optimal south exposed tilted surface and a vertical south exposed surface in three Eu-

ropean locations from the standpoint of the aesthetical building integration (Giovanardi, 2012).
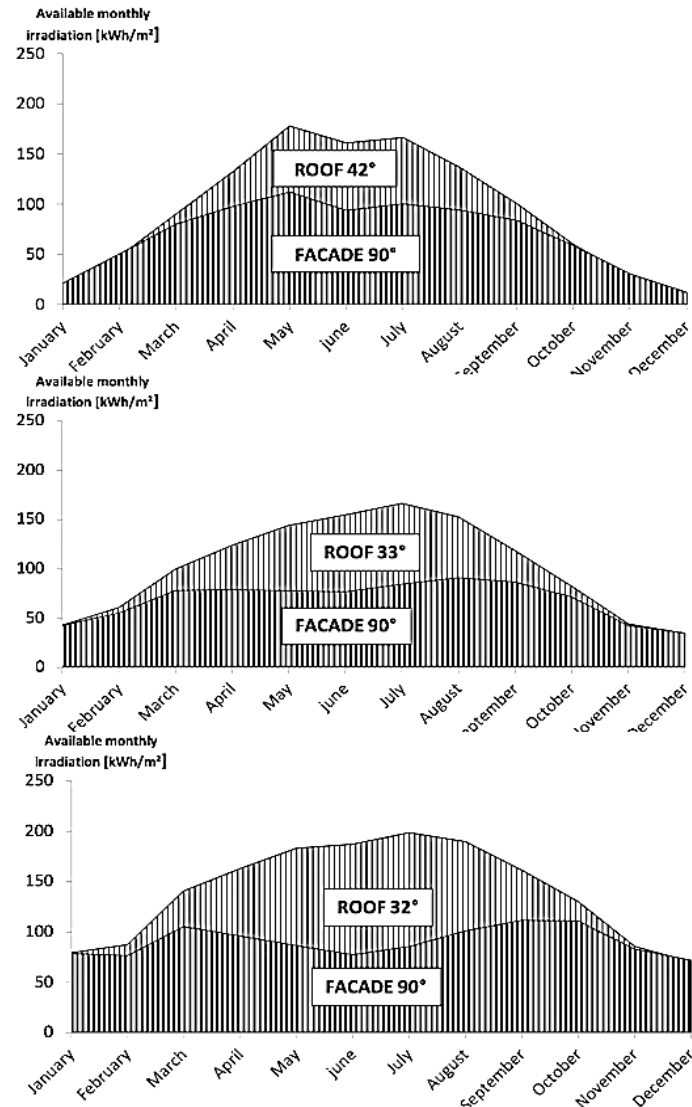
Figure 2-13 Comparison of available monthly irradiation on a south exposed tilted surface vs. a vertical south exposed surface in Stockholm, Sweden/Zurich, Switzerland/Rome, Italy respectively (Giovanardi, 2012)

The energy production profiles of the STC showed that annual solar energy production profiles had almost constant lower performances in three locations, and the great variations occurred during summer time, when thermal heat was at lowest demand (Giovanardi, 2012)). Accordingly, facade integrated collector could achieve the solar fractions up to 90% without common overheating problem with less influence to weather conditions and the external powers (Son-

nenenergie D., 2010; Giovanardi, 2012; Probst & Roecker, 2012; Weiss, 2003; Matuska & Sourek, 2006).

Matuska & Sourek further revealed the relation between **collecting area** and **slope tilt angle**. It was found that a vertical area increased by approximately 30% is able to achieve the usual 60% solar fraction compared with the conventional roof STCs with a 45° slope, and further increases in the solar fraction above 70% lead to a required area comparable with roof collectors but with less stagnation periods (Matuska & Sourek, 2006). Sensitivity study of the potential yielded energy quantity towards the sizing parameters implied that the steel-made coloured unglazed absorbers could reach appreciable efficiency for domestic water preheating in wind-sheltered environment than for space heating, and the acceptable sizing parameters were advisable with high absorbance, less sensitive emissivity and tilt angle between −50° and +50°(Bonhôte et al., 2009).

Lobaccaro et al. discussed the energy generation of solar envelopes from a more building oriented aspect through a preliminary set of dynamic annual simulations in urban contexts. The shape modification of building, selection of claddings and solar access of surrounding buildings have been all identified to impact on the sizing of STF system because of the variation in solar radiation and superficial temperature (Lobaccaro et al., 2012). Golic et al. defined a general model of STF system with several basic phases in order to facilitate problem-solving and to enable the individual optimization processes for variant design of residential building refurbishment (Golić et al., 2011).

Thermal energy storage and release is another essential measure for STF application with less occupancy space and higher efficiency. The inner configurations of both tank and immersed heat exchanger were regarded have significantly effects on the stores performance (Spur et

al., 2006). The materials used for solar thermal energy storage can be classified into three main categories according to different storage mechanisms, as sensible heat storage, latent heat storage and chemical heat storage (Tian & Zhao, 2013). Sensible heat storage using thermal mass or water tank is the most common-used technology with a large number of available materials of both solid status and liquid status in a more cost-effective way. But this type of storage depends on the material mass and specific heat, which can make the storage unit unsatisfactory large. PCMs, instead of directly used as the working fluid, provides a nearly isothermal way when storing/releasing thermal energy with a reasonable storage size due to much higher storage density (Zhan et al., 2011). But it's also worth pointing out that effective, reliable and practical application of PCMs were still the restriction for application. In order to overcome the low thermal conductivities of PCMs, the embedded metal foam or graphite-PCM composite was specially explored by many researchers to significantly enhance heat transfer for phase change materials, resulting from both high thermal conductivities and large specific surface area (Zhao et al., 2010; Tian & Zhao, 2011). In comparison with the storage densities of latent heat storage in the order of MJ/m^3, chemical heat storage has much higher storage densities in the order of GJ/m^3. However, chemical storage has not yet been extensively researched. The application of chemical storage is limited due to the following problems: 1) complicated reactors needed for specific chemical reactions; 2) weak long-term durability (reversibility); and 3) chemical stability (Tian & Zhao, 2011).

In an indirect STF system, **a heat exchanger** is unavoidable component to transfer absorbed solar heat from the working fluid to the storage. The prevailing configurations of heat exchange are the immersed coil-in-tank, the shell-and-tube, and the mantle heat exchanger (showed in Figure 2-14). Because of simply system construc-

tion with few components and less occupied space, stores with im-mersed heat exchangers are often installed in solar systems for one- and two-family houses. These internal heat exchangers are wound with (Cu-) plain, finned tube or plain steel or stainless steel tube (Spur et al., 2006).
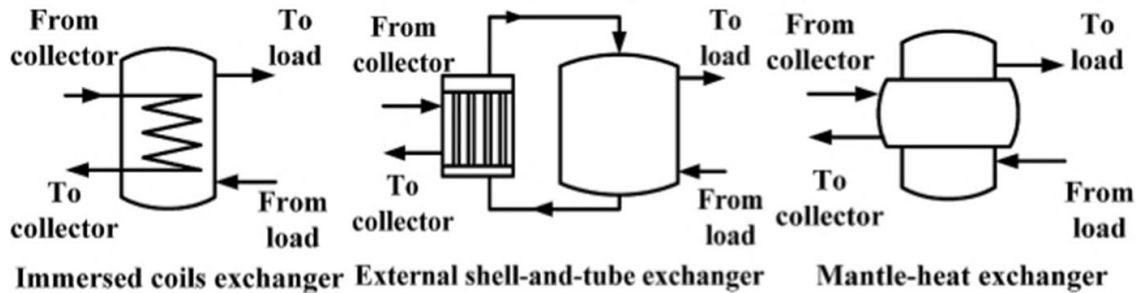
Figure 2-14 Most prevailing configurations of heat exchange (Han et al., 2009)
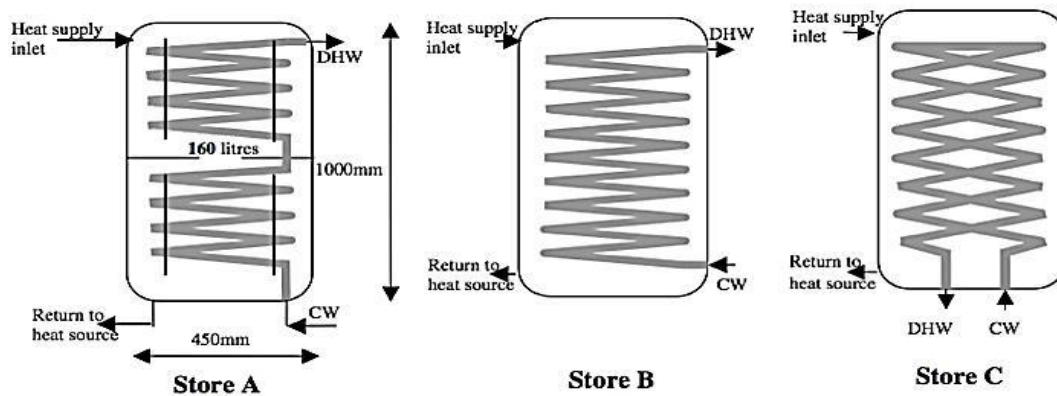
Figure 2-15 Schematic design of Tanks (Store A is the novel stratified-store, while Stores B and C are commonly used) (Spur et al., 2006)

Figure 2-15 demonstrates three basic schematic designs of **water tank**. By means of a daily course of discharging a store with a realistic domestic hot water withdrawal-profile, the novel store can reached 20% over when considering domestic hot water delivery temperature and 32% over when considering the hot-water equivalent volumes delivered, compared to the common ones. And because of heat-extraction, both coiled upwards and located in the upper part of the tank enable the immersed heat exchanger to achieve a high rate of heat-extraction (Spur et al., 2006).

2.6.3   Operation conditions

In the prospect of operation, the proper control of operational environment, such as temperature and flow rates, is common important factor for the performance enhancement of STF (Badescu, 2007). But solar radiation is not the significant affecting factor for the efficiency of air based solar collector (Pesaran et al., 1994; Leon & Kumar, 2007), whilst the **airflow distribution and upward heat loss** caused by ambient wind and the approach velocity have considered closely affecting the operation performance of the air based STF system. Gunnewiek et al. (Gunnewiek et al., 2002) studied the airflow distribution on the face of an unglazed solar thermal collector in a computational fluid dynamics (CFD) model at a constant wind speed of 5 m/s. The wind was found to reinforce the factors producing outflow, and the recommended minimum average suction velocity required to avoid such outflow were given for four operating conditions. Fleck et al. experimentally expanded the **effects of ambient wind** on working performance in regard of wind direction, speed and fluctuation intensity on an unglazed solar collector. The measurements indicated that a high magnitude of turbulence dominated near wall, and the maximum collector efficiency occurred at the wind speeds between 1 and 2 m/s instead of non-wind speeds (Fleck et al., 2002). Kumar et al. conducted a two-year field study focusing the influence between wind induced convective heat transfer and upward heat losses in unglazed collectors. The estimated wind heat transfer coefficient correlates against wind speed by a linear regression and a power regression (Kumar & Rosen, 2011). Shukla et al. reported that the increase in approach velocity increased collector efficiency, but as the approach velocities reached certain level, the effect on efficiency became negligible (Shukla et al., 2012).

As for the hydraulic-based solar collector, **mass-flow rate** has been considered as a variable for the extraction of maximum exergy, which can lead to identification of inefficient parts and optimum operating conditions. Although the present control method that regulate the outlet temperature of the collector field by suitable adjusting the working fluid flow may ensure a smooth operation (Meaburn & Hughes, 1996), but the reported experimental results were usually around 3% for the maximum exergetic efficiency. Badescu et al. implemented a direct optimal control method in a detailed collector model with realistic meteorological data. The proposed operation at a properly defined constant mass-flow rate may be necessarily associated to maximum exergy extraction, but it required a priori knowledge of meteorological data time series (Badescu, 2007). Variation optimisation were presented in a general simulation model for the optimal design and operating of solar collectors (Farahat et al., 2009). Apart from aforementioned assumptions either assuming a constant overall heat loss coefficient or considering the fluid inlet temperature equal to the ambient temperature, Jafarkazemi et al. both compared and evaluated the energetic and exergetic performance of a flat plate solar collector. Based on the theoretical results, it was obvious that energy and exergy efficiencies had conflicting behaviours in many cases. Designing the system with inlet water temperature approximately 40℃ more than the ambient temperature as well as a lower flow rate can enhance the maximum energy and exergy efficiency close to 80% and 8%, whereas thickening back insulation over 5 cm had little effect on both energy and exergy performance (Jafarkazemi & Ahmadifard, 2013).

As for the hydraulic-based solar collector, **high temperature** is detrimental to the reliability, durability and safety during operation. Normally, the maximum stagnation temperatures are 160–200℃ for the

well-insulated glazed flat-plate collector and 200–300℃ for the evacuated tube collector (Jafarkazemi & Ahmadifard, 2013). Overheating problems usually occur when no hot water is used or the circulation of working fluid fails to transfer enough thermal heat (Akhtar & Mullick, 1999; Mahdjuri, 1999). Fan et al. elucidated operating conditions, such as flow rate, properties of working fluid and heat transfer condition in a glazed solar collector. The decreased flow rate and decreased content of glycol in the glycol/water mixture were discovered to lead a growing risk of overheating in the upper part of the collector panel (Fan et al., 2007). The magnitude of the stagnation temperature for a solar collector depends on solar insolation level and the ambient air temperature (Harrison & Cruickshank, 2012). Therefore many approaches have been tried to avoid the overheating of both solar absorbers and the STF system. Except for the simply approaches like utilizing high temperature tolerant components, venting or shading absorbers, a more intelligent method is to purposely degrade the optical performance. The relevant techniques are optical switches based on scattering layers, thermotropic layers and temperature varied particle solubility fluid (Stephens, 1981). In order to block initially light to the collector, incorporating a prismatic structure in a solar collector was proposed as an optical solution. It was based on the principle of switchable total reflection using a prismatic structure. And the experimental study indicated that the maximum temperature inside the collector can be regulated by thermal evaporation or manual regulation of the switching fluid level near the prisms, and there was a strong light reducing effect around noon with less sensitivity for seasonal changes (Slaman & Griessen, 2009). On the other side, the enhancement of heat transfer using oscillatory flows to prevent the overheating phenomenon is another way to degrade thermal performance from a solar thermal system aspect (Lambert et al., 2006). The preliminary estimations showed a dramatic heat transfer enhancement using oscilla-

tory flows compared with the forced convection using standard unidirectional flows. Furthermore, Harrison et al. proposed a summary and overview of **stagnation control** from both the collector level and system level approaches as listed in Table 2-8 (Harrison & Cruickshank, 2012). To optimise the performance of the **latent heat storage** in solar air heating system, Arkar et al. studied the relations among PCM melting temperatures, air flow-rate through the thermal storage and the overall performance of solar air heating system. Based on the transient conduction-dominated numerical model, the optimal air flow-rate of 40m^3/h-m^{-2} was suggested (Ucar & Inallı, 2006; Arkar & Medved, 2015).

2.6.4   Theoretical simulation and prediction

Overall, there are plenty of research methodologies applied to theoretical studies of solar thermal systems, depending on the contents and objectives of the researches. Generally, the research works can be classified as the theoretical and numerical study, and the computer simulation.

1) Theoretical and numerical study

A large number of theoretical works have been carried out focusing on the performance of solar collector. These studies were dedicated to 1) reveal the relations between thermal performance and the cover of a STC from layers, surface condition and colour; 2) optimise the structural/geometrical parameters of a STC including constitution, connection, geometrical shape and sizes; and 3) recommend the favourite operational conditions e.g. flow rate, inlet temperature, etc. , to enhance performance.

Table 2-8 Summary and overview of some collector and system level approaches to stagnation control (Harrison & Cruickshank, 2012)

Control Scheme	Protects Collectors?	Protects System Components?	Fail-safe Operation?	Cost Impact?	Performance/durability Impact?
Drain-back or drain-down	No	Yes	Yes (must be installed to drain completely if also used for freeze protection);	Pumping power consumption may be increased	Collector loop open to atmosphere may increase corrosion or fouling;
Control based	Yes	Yes	No. (requires active control and pumping);	Not for hardware. (additional pump use & potential energy loss)	May result in available energy being dumped at night;
Steam Back	Not always	Not always	Yes (careful design and placement of system components required);	Expansion tank may have to be oversized	Potential thermal shock/scalding on restart;
Collector Venting (Integral to collector)	Yes (if carefully designed)	Yes (if carefully designed)	Yes (for thermally activated versions);	Modest hardware cost	May experience small performance penalty if not carefully implemented;
Heat waster on Collector loop	Yes	Yes	Some designs operate passively - others require power or pumps, fans etc.;	Significant hardware cost	If powered may require auxiliary generators or PV;
Heat pipe control (Evacuated-tube collector)	No	Yes	Yes (for thermally activated versions).	Modest Hardware cost	System may be inoperable for remainder of day.

Basically, theoretical analyses can be divided into **the analytical model and the numerical model**.

The analytical models done so far referred to study the effect of absorption or/and emission with surface temperature distribution in glass cover(s) (Akhtar & Mullick, 2012; Khoukhi & Maruyama, 2005; Khoukhi et al., 2007); address optical, thermo-analytical, mechanical and morphological properties and structures of the solar absorbers using black pigmented polypropylene materials (Kurzböck et al., 2012); examine the fully developed laminar flow and heat transfer characteristics in solar collector panels with internal, longitudinal, corrugated fins(Ackermann et al., 1995); comparatively study the tilt angle and direct influence on the efficiency of energy production for the STC from different aspects (Tang et al., 2011; Yadav & Chandel, 2013; Giovanardi, 2012); pinpoint parameters that have direct effect on entropy generation rate for the STC(Saha & Mahanta, 2001); investigate the collected energy with different coloured absorber in different places(Kalogirou et al., 2005); develop the relation between the energy yields and operational parameters (e.g., absorbance, emissivity, orientation, wind, surface, radiator outlet temperature) in different European climate conditions (Bonhôte et al., 2009); and understand the influence on the sizing of STF system with building shape, claddings structure and solar access of surrounding buildings(Lobaccaro et al., 2012).

The numerical models included the one-dimensional and multi-dimensional ones. The one dimensional model was used to determine the physical parameters of a flat-plate solar collector using a special water-alumina or the Al_2O_3 nanofluid (Nasrin et al., 2012) and understand the heat transfers occurring in different parts of a solar thermal collector (D'Antoni & Saro, 2012), while the multi-dimensional numeri-

cal model was used to understand the heat transfers in solid matrix in the massive solar thermal collectors(D'Antoni & Saro, 2012); analyse the heat transfer enhancement using PCMs metal foams(Zhao et al., 2010); study the airflow distribution across the face of an unglazed solar collector with the presence of wind to avoid outflow in the air based STF system (Gunnewiek et al., 2002); provide the best operational strategies for the open loop flat-plate solar collector system with a detailed simulation model and real meteorological data (Badescu, 2007); develop the energy and exergy analyses to evaluate the thermal and optical performance, exergy flows and losses, as well as exergetic efficiency for a typical flat plate solar collector under dedicated operational conditions (Farahat et al., 2009).

2)   Computer simulation study

Different from common solar thermal devices, the STF also acts as the critical part of the building envelope. For this regard, development of the dedicated design simulation is important for building design. From the previous studies, the digital design tool seems to be cost-effective and informative in determining the system size, optimizing system configuration and predicting its solar yield and associated energy saving in the building. Up to date, there are some architecture-related digital tools available for architect, engineer and researcher, which can be mainly classified into: **the computer-aided architectural design (CAAD) tool, the visualization tools and the simulation tools** (Witzig et al., 2009.; Dubois & Horvat, 2010; Sonnenenergie, 2010).

In terms of building design, the CAAD tools, as part of building information modelling (BIM) programme, were mainly used to simulate and refine the geometry of STFs and the whole building. Till now, the direct and explicit feedbacks from building parameter modification on passive solar gains basically relied on plug-ins from connected

third-party software to realize energy simulation prediction(Griffith & Ellis, 2004). The visualization tools mainly study the direct and diffuse light penetration patterns and shading effects on building facades and internal luminous environment. Overall, the simulation tools can be classified as the static calculation program, dynamic time-dependant program and comprehensive program. Till now, the available simulation tools for solar thermal design are Ecotect, IES (VE), TRNSYS, DK-INTEGRAL, IDA ICE, LESOSAI, Polysun, SOLTOP and TSol (Witzig et al., 2009.; Griffith & Ellis, 2004.; Sonnenenergie, 2010).

Based on the multiple functions of the computer programs, the prediction and interpretation of the performance of multi-functional building facades could be easily accomplished. And the results of the modelling could form the supplementary part of the whole building simulation and carry out the whole building performance assessments.

2.6.5   Economic and environmental performance assessment

Some literatures address the energy saving and environmental beneficial potentials for using the STF systems in real buildings. In terms of economic concern, simple payback time and life cycle analysis were addressed, taking into account of the primary fossil fuel energy conservation, increasing in manufacturing and maintenance costs during the operational phase, while the approaches of enhancing system energy and exergy efficiencies, and reducing the greenhouse-gas emissions, were also presented in order to assess the environmental impact of STFs.

1)   Economic performance assessment

Generally, the overall STF performance was simply evaluated by the outputs of heat in different ways. One way is to determine the cost saving from heating energy tariffs, which was a market-based ap-

proach to assess the energy cost savings and associated benefit to energy management. However, this method has a drawback of ignoring the impact of policy factor that is therefore not universally valid (Bosanac et al., 2003). As the implementation of the STF system is much different from a 'business as usual' component, it is worth to treat the business related problems as an investment project to make it financially attractive.

Koene et al. assessed the cost effectiveness for a financially attractive STF in the building renovation using a more practical method (Koene, 2010). In terms of economic issue, the present discounted value was used to represent a future amount of money discounted to reflect its current value. A business model was brought into consideration and this included a few critical factors: 1) instalments + interest to return the investment over a 15 year duration; 2) operational & maintenance costs (O&M); 3) fixed energy service charge in case that a third party provides the energy services; 4) energy costs minus revenues from renewable electricity generation, and 5) rent. A list of costs of all the elements in all renovations was entered into the business model, for instant, the costs for the novel STFs were in the range 450 to 550 €/m^2 per facade including 20% VAT and labour cost for installation (from Table 2-6). A sensitivity analysis using the Monte Carlo model was then undertaken by considering the variation of a number of parameters, including the investment cost and discount rate. From this study, it was found that the main parameters that determine a positive outcome of the business cases were the rent and the investment cost, nevertheless, the effect of the energy bill (and its annual increase) had a much smaller effect on the outcome of the business cases (Koene, 2012). Apart from the basic functional structure investment, auxiliary facilities as the temperature control measures are also essential. Harrison et al. (Harrison & Cruickshank, 2012) summarised

and compared some collector and system level approaches of stagnation temperature control. It was noticed that the temperature control measures were indispensable with considerable potential benefits. The stagnation temperature control is necessary to prevent losses such as replacement or collateral damage, inefficient thermal performance, wastes of operational time and energy due to increased maintenance or shut down periods, the reduction of component life, increased service and maintenance costs etc. Expenses vary depending on the approach used and level of temperature stagnation protection desired. Further, most of the mentioned costs and gains should be evaluated using the time value of money as well, including inflation, tax and/or company discount rates.

2) Environmental performance and social acceptance analyses

Based on the studies, there were very few literatures addressing the LCA works relating to the STF systems and their real building integration (Lamnatou et al., 2015).

Katrin Löwe et al. (Löwe et al., 2011) carried out an EU funded project "Cost-Effective" which focused on the existing European high-rise building stock for non-residential use with an approach for assessing the environmental influence of energy generating components by means of parameterized LCA models within the GaBis software. On the basis of the modular approach for environmental impacts calculation, the LCA assessment was divided into "multifunctional component" and "technical concept composed of the component integration and modernization activities". It followed a "Cradle to Grave" approach for the both parts, considering the various stages of the product life-cycle process including construction, in-use, and end-of-life, according to the regulation of European Standard prEN15978.

K. Golic´ et al. (Golić et al., 2011) defined a general model of solar water heating system (SWHS) integration in the residential building to explore its potential energy saving and associated environmental impact. The model was divided into five basic phases including 1) calculation of integration; 2) type selection; 3) generation and optimization of the integration design variants; 4) evaluation of the SWHS integration design variants; and 5) selection of optimal SWHS integration design variants to solve problems related to the functional and aesthetic, energy performance, economic and ecological conflicting classes of requirements. The measures for 'Building Potential', P_B, and 'Degree of Feasibility', p_B, were first introduced to assess the adaptability of the SWHS integration. Finally, a decision on SWHS integration in the building is made by the Decision-Maker (i.e., Investor) on the basis of p_B value. Till now, the proposed general model has been successfully applied to a real problem in the suburb of "Konjarnik" in Belgrade, Serbia.

Currently, the case for the life-cycle impact assessment by Lamnatou et al. additionally studied the environmental performance and social acceptance analyses in another direction, presented in Table 2-9 (Lamnatou et al., 2015). They investigated a patented building-integrated solar thermal collector with three configurations based on both methodologies of embodied energy (EE) and embodied carbon (EC). Two databases, as inventory of carbon & energy and Alcorn, and multiple scenarios (related to material recycling, electricity mix, etc.), were considered. The results showed that the EPBT of the reference system fell to less than 2 years by means of the parallel connection and even to 0.5 years by using the material recycling. The EE of the systems was around 3 GJ_{prim}/m^2 and around 0.4–0.5 GJ_{prim}/m^2 by recycling. And the EC of the configurations was approximately 0.16 t $CO_{2.eq}/m^2$ without recycling and around 0.02–0.03 t $CO_{2.eq}/m^2$ with

recycling, which were strongly related to the electricity mix. This study also exhibited a promising potential for further development, e.g., by improving heat transfer processes (Lamnatou et al., 2015).

Table 2-9 Life cycle inventory (LCI) of the studied BI solar thermal systems (Lamnatou et al., 2015)

One collector materials/components	Mass(kg)
Black absorber (aluminum)	0.196
Cover (glass)	1.417
Tube for cold water (copper)	0.253
Tube for hot water (copper)	0.253
Thermal insulation (Rockwool)	0.231
External casing (aluminum)	0.615
Two blades (polycarbonate)	0.048
Polyester (at the case)	0.007
Gutter: external casing (aluminum)	0.728
Polyester (at the gutter)	0.010
System additional materials/components	--
Storage tank (stainless steel)	12.479
Storage tank (Rockwool insulation)	4.081
Tubes (copper)	5.637
Tubes (polyurethane insulation)	1.804
Propylene glycol	1.400
Pump (stainless steel)	3.000

Although the STFs could achieve a better environmental benefit in the climatic regions of high solar radiation, cold places with low solar radiation were also studied. Several studies also indicated that STFs could harvest certain environmental benefit in these areas.

An integrated solar water heater incorporating a reflector and a heat storage unit was studied for its application in Northern Europe, i.e., Ireland, indicating that the primary embodied energy of the materials was 2.94 GJ while the total embodied energy for the unit was 3.81 GJ. In general, the total energy used in the manufacture of the collector was recovered in less than 2 years (Smyth et al., 2000).

Meanwhile, it was found that the solar energy use in the UK was steadily growing over the past years owing to the implementation of a number of low carbon legislations (Burnett et al., 2014). To study this impact, Burnett et al. carried out a series of assessments of the solar

irradiation resources at the present and future climatic conditions across the UK, using the UKCP09 probabilistic climate change projections. This specified that the current average UK annual solar radiation intensity is 101.2 Wm^{-2}, with the maximum of 128.4 Wm^{-2} in the south of England and the minimum of 71.8 Wm^{-2} in the northwest of Scotland. This suggested that the southern regions of the UK would be most suitable for the application of solar thermal technologies (Burnett et al., 2014).

In the residential building context, according to statistics, a solar thermal system incorporating a 4 m^2 of solar collector could provide up to 50–60% of a typical household's annual hot water demand, or space heating demand in summer time. In the commercial building context, a well-designed solar system may be able to meet 30–40% of the annual hot water load. In order to fully replace the traditional gas-fired domestic heating systems, a large area of solar collectors should be installed on the building facades or integrated into the building construction; these should also be in combined use with a heat pump (DECC, 2013).

In summary, solar water heating could annually provide 9.5% of domestic heat consumption in a typical UK house (Rogers et al., 2013). Rogers et al. further studied the potentials in solar thermal water heaters to meet household hot water demand during the summer period in a high solar intensive area, i.e., the latitude between 50° to 60° north, giving a positive solution of the technology. It was seen that laying down a solar panel in an inclined angle was not necessary in summer; instead, a vertically mounted solar panel could provide a very high solar fraction (Rogers et al., 2013).

2.7 Chapter executive summary

Although both the conventional flat plate and the evacuated tube solar collector are mature technologies, they still face challenges such as fragile, heavy weight for installation and shipment, and unlikely breakthrough in cost reduction. Therefore a critical review towards the recently emerging STF technologies has been carried out in this chapter.

Main issues addressed in Chapter 2 are:

1) Introducing the technical concept and heat transfer mechanisms relating to STFs;

2) Classifying STFs in terms of building part, thermal collection typologies, transparency, application, as well as heat-transfer medium;

3) Listing indicative parametric/factor/coefficient of STFs relevant to the evaluations in performance, economic and environment;

4) Outlining current research and development progress of STF from the aspects of components design, dimension and position and its operation conditions;

5) Presenting existing theoretical and numerical research methods as well as the associated computer simulation tools;

6) Reviewing the economic and environmental performance assessments.

Eventually, such a technical review helped to:

1) Understand the concept and classification of STFs;

2) Clarify the technical developments in current STFs;

3) Identify theoretical foundation for the subsequent chapters.

STATE OF THE ART–RESEARCH PROTOTYPES AND PILOT APPLICATIONS

3

3.1   Chapter abstract

This chapter specially underlines the applicability of the existing STF technology and the integrity between STF and building components. A large number of research studies, prototypes, commercial products, and pilot engineering projects have been summarized to offer suggestion for future work. Following the theoretical accomplishments in the R&D, this chapter mainly focuses on:

1) Identification of STF design and integration criteria/standards;
2) General review on experimental work done so far;
3) Review the market available STF products;
4) Describe the integrity in the existing STF pilot projects;
5) Discuss the opportunities for further development of STF.

This part of the work continues to establish the foundation for the entire investigation and helps to:

1) Complete sound scientific methods for STF experimental testing;
2) Investigate common fabrication process and installation standards/approaches of STF;
3) Propose research concepts for next chapters;
4) Find possible ways to promote STF application.

3.2 Design criteria for STF system

Generally, STFs as the building facade replacements should be guaranteed with the basic protection from external conditions (as solar irradiation, temperature, humidity, precipitation and wind) in order to maintain an acceptable indoor thermal comfort. Consequently, it is vital to take consideration of technical issues, in terms of the efficien-

cy, effectiveness, safety, durability and flexibility, together with constructive and formal issues at early design stage of a STF system application (GSWH, 2012).

3.2.1 Relevant standards for STF design

Although no specific guidelines or standards have been found especially applicable to the STF at the moment, some European requirements could be adaptable to the STF in Table 3-1.

Table 3-1 Compliance of STF with construction sector requirements (Koene, 2010)

Requirement	Component Type	Source of the requirement & classification
CE marking based on CPR & relevant directives	TSTC/PV/VTC	From 2014 onwards
Deutsches Institutfür Bautechnik/ EOTA member	TSTC/PV/VTC	From 2013 onwards
Energy labeling	TSTC/ VTC	From 2013 onwards
Solar Keymark	TSTC/VTC	From 2014 onwards
EN 61646-2008	PV	PV type approval
IEN 61730-1 & -2	PV	PV safety qualification
EN 13501-1-2007	PV	Fire classification

Regarding as the construction component, there are statutory instruments, directives and standards for the facade application. In European, currently available standards cover:

1) Regulation 305/2011 defines the essential requirements of building construction product placed on the market for an economically reasonable life cycle;

2) European Technical Approval Guidelines seriously address the technical requirements for building components;

3) Construction Products Directive (CPD) and Construction Products Regulation (CPR) that gave the upper and lower limit figures relating to the construction products;

4) Directive on the Energy Performance of Buildings (EPBD) that specifies the detailed requirements for building, with extensive impacts to selection and application of a range of construction products.

Table 3-2 outlines the currently available standards in relation to solar thermal systems. Some of them are mainly testing standards that provide guidelines for testing procedures of solar thermal products. Meanwhile the other part, such as the European Standards EN 12975-1, EN 12977-1 and EN12978-1 specify the requirements related to the product itself. In general, the compulsories addressed cover the items of high temperature resistance, exposure, external thermal shock, internal thermal shock, rain penetration, impact resistance and mechanical load (GSWH, 2012). Although most standards and regulations are limited to certain regions or countries, efforts have been made when updating the EN 12975 standard to address the global concerns in evaluating the conventional and advanced solar thermal products. Additionally, other efforts have also been made to create the multi-parts standards for various solar collectors including their components and materials; these include Vienna Agreement Part 1: Evacuated tube durability and performance; Part 2: Heat pipes for evacuated tubes - Durability and performance lead by ISO; Part 3: Absorber surface durability; and some more parts to address glazing and insulation materials lead by CEN/TR and CEN/TS (Serra et al., 2010).

On the whole, STF is fundamental to possess the construction, hydraulic and hygiene characteristics (listed in Figure 3-1).
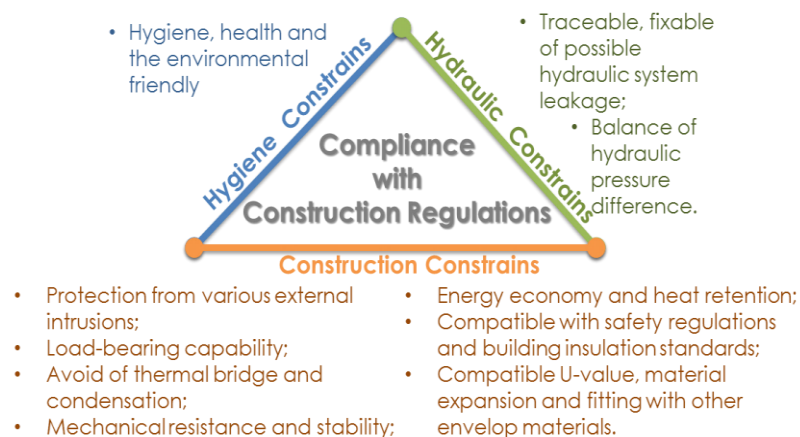
Figure 3-1 Integration constrains associated with STF (non-exhaustive)

Table 3-2 List of standards related to solar thermal system in main countries (GSWH, 2012; Sonnenenergie, 2010)

Country(ies)	Standard	Description	Focal point
Australia/New Zealand	AS/NZS 2712:2007	Solar and heat pump water heaters - Design and construction	Collector & System
Brazil	ABNT/NBR 10184/1988; EN 12975; ANSI/ASHRAE 93-2003; ANSI/ASHRAE 96-1980; RA 1989; ASTM E 823-81; FSEC-GP-5-80	Flat plate solar collectors for liquids	Collector
Canada	CSA F378-87 (R2004)	Solar collectors	Collector
	CSA F379-09	Packaged Solar Domestic Hot Water Systems	Collector& System
China	GB/T 17049-2005	All glass evacuated solar collector tube;	Collector
	GB/T 6424-1997	Evacuated tube solar collector;	Collector
	GB/T 17581-1998	Specification for flat plate solar collectors;	Collector
	GB/T 19141-2003	Specification of domestic solar water heating system	System
EU	EN 12975:2006	Thermal solar systems and components - Solar collectors - Part 1: General Requirements; Part 2: Test methods;	Collector
	EN 12976:2006	Thermal solar systems and components - Factory made systems - Part 1: General Requirements; Part 2: Test methods;	System
	EN 12977:2008	Thermal solar systems and components - Custom built systems ;- Part 2: Test methods for solar water heaters and combi-system; Part 3: Performance test methods for solar water heater stores;	System
	prEN12975-3-1	Qualification of solar absorber surface durability.	Collector
India	IS 12933:2003	Solar Flat plate Collector Part 1-5	Collector
International	ISO 9459-5	Solar heating -- Domestic water heating systems - Part 5: System performance characterization by means of whole-system	System

		tests and computer simulation	
	ISO 9806	Test methods for solar collectors - Part 1: Thermal performance of glazed liquid heating collectors including pressure drop; Part 2: Qualification test procedures; Part 3: Thermal performance of unglazed liquid heating collectors (sensible heat transfer only) including pressure drop	Collector
South Africa	SANS 1307:2009	Domestic solar water heaters	Collector
	SANS 6211	Domestic solar water heaters Part 1: Thermal performance using an outdoor test method; Part 2: Thermal performance using an indoor test method	Collector
	SANS 9459-2	Solar heating - Domestic water heating systems Part 2: Outdoor test methods for system performance characterization and yearly performance prediction of solar-only systems	System
U.S.A	ASHRAE 93-2010	Methods of Testing to Determine the Thermal Performance of Solar Collectors (ANSI approved)	Collector
	ASTM E905-87 (2007)	Standard Test Method for Determining Thermal Performance of Tracking Concentrating Solar Collectors	Collector
UK	BS EN 12975 2001	Thermal solar systems and components	Collector
	BE EN 12976 2001	Thermal solar systems and components	System

1)   In terms of the function, shielding, comfort maintaining and com-
     munication availability are the items to be addressed;

2)   In terms of the construction concern, protections from external in-
     trusions, load-bearing capability, prevention of thermal bridge and
     moisture condensation, mechanical stress, stability, energy effi-
     ciency, thermal reservation, safety in use, provision to material vol-
     ume expansion, as well as fitting with other envelope materials are
     the factors to be considered;

3)   In terms of hydraulic concern, prevention from the water leakage,
     and balance to the hydraulic pressure difference should be con-
     sidered; in terms of hygienic concern, health, environmental
     adaptability should be the issues to be addressed (Probst, 2008;
     Chambrier *et al.*, 2009).

4)   Additional safety attentions should pay to STF, including the *Micro-
     generation Installation Standard MIS 3001(Issue 1.5); EST CE131, So-
     lar water heating systems – guidance for professionals – conven-
     tional models* (Chambers *et al.*, 2010).

5)   Because the common STF components are relatively heavier than
     the conventional facade component, risk assessment and man-
     agement should be particularly addressed for achieving a safe in-
     stallation.

3.2.2 Architectural integration methods of STF design

A great deal of work has been thoroughly conducted in the technical
assessment of STF systems, such as configuration design, absorber ma-
terial, coatings, and connection methods etc. It can be found that
the solar thermal collector does not lack of technical advanced and
cost effective devices. However, the general application of the exist-
ing building based solar thermal collector pinpoints the lack of con-
siderations as a kind of building facade replacement. Therefore, Table
3-3 summaries the possible characteristics of STF integration with build-
ing (Zhang et al., 2015a).

1)   The wall-based application provides the greatest collecting area
     compared to others being an economic choice. From constructive
     point of view, the opaque facade is usually composed of multi-

layers with functions of external protection and insulation. Such features exactly offset the limitations of flat-plate STF, which is less flexible in translucency and module thickness. In addition, it not only provides homogenous covering but also facilitates smooth hydraulic connection with less pipe runs and fittings.

2) The transparent and translucent window-based application concerns more on daylight transmission, outdoor visual relation and partial sun shading. In such cases, the light-weighted glazed/unglazed collector or evacuated tubes are recommended to integrate with glazing in an alternating or interlaced pattern to have partial sun shading, or create a dummy effect.

3) The evacuated tube shows more promising applications in the balcony-based integration for its lightweight, higher efficiency and convenience in assembly and pipe connections.

4) The roof is the conventional place for the installation of solar systems. However, as a STF system, more considerations should be taken in terms of additional imposed static, wind, snow load, and possible occasions, such as water leakage, thermal breakage and expansion under high temperature.

3.3 Experimental works

As a high grade of practical technology, experimental study is not negligible for the STF development. Running from the individual component to the whole system scheme, the experimental works can be briefly classified with the following objectives:

1) Understand the real performance of components and whole system under particular operating conditions;

2) Determine the optimal operation parameters for energetic and exergetic evaluation;

3) Examine the reliability and accuracy between theoretical analysis and practical application, and establish their further correlations;

4) Provide evidences for amendment and modification to theoretical model for future use.

Experimental and combined modelling/experimental works done so far include:

1) System efficiency and its relevance to various design parameters, surface treatment and structure improvements (Hellstrom et al., 2003; Sopian et al., 2009; Ho et al., 2005; Martinopoulos et al., 2010; Ho et al., 2011; Matuska and Sourek, 2006; Mintsa Do Ango et al., 2013);

2) Impactions of operational parameters on system's working performance (Fleck et al., 2002; Jafarkazemi & Ahmadifard, 2013);

3) Thermal performances variation through different colours on absorber's plate (Anderson et al., 2010; Orel et al., 2007b);

4) Overheating protection and its relevance with material composition, surface treatment, structure modification, control method and ambient environment (Stephens et al., 1981a; Stephens et al., 1981b; Lambert et al., 2006; Wallner et al., 2008; Slaman & Griessen, 2009; Weber & Resch, 2012; Harrison & Cruickshank, 2012);

5) Comparison and validation between the modelling results and the experimental results (Motte et al., 2013a; Anderson et al., 2010; Martinopoulos et al., 2010).

Jie Ji et al. conducted the outdoor experiment of a dual- functional solar facade to validate the dynamic numerical model based on practical air-conditioned room design conditions in Figure 3-2. The water heat gain in the tank was found to be 3.41 MJ/m^2 and 6.57 MJ/m^2, based on the water temperature rise from the initial 26.8/18.2℃ at 8:00 to the final temperature of 41.8/47.6 ℃ at 16:00 with the overall thermal efficiency of 50.8%/ 48.4% in Figure 3-3. The operational performance of the solar facade in a typical autumn day seemed to be better than in a typical summer day(Ji et al., 2011).

Table 3-3 Characteristics of STF integration with building

Envelope	Advantages	Disadvantages
Wall-based	• Economical and high efficient solution to embed a solar collector in finishing layer of external insulation; • Lessen climate disturbance of original facade unit; • Improving building's thermal insulation; • Offset against the cost of conventional façade; • Most solar collecting area; • Simplify in piping arrangement; • High grade of pre-fabrication possible.	• Renewable energy component requires high demands in self quality, material expansions compatible and installation due to totally external exposure; • More costs for outdoors cleaning and maintenance; • Risk of condensation and thermal frost within insulation; • Cold bridge and acoustic problem at penetration hole; • Additional imposed static, wind that requires additional fixed structure.
Window-based	• No reduced life expectancy if placed within glazing unit; • Regulating visual relations between inside/outside and the supply of fresh air / daylight and passive solar gains; • High grade of pre-fabrication possible.	• Low light transmission through renewable energy component; • Additional moveable shading in clear vision area is necessary; • Risks in reducing life expectancy caused by water leakage, or thermal breakage and expansion under high temperature.
Balcony/ Sunshield-based	• Optimum overall shading with full room height vision allowing adequate daylight distribution; • Energy output independent for orientation and solar angle for the vacuum tube collector; • Easy cleaning and maintenance; • Making solar energy visible; • Well suited for superimpose in existing building; • High grade of pre-fabrication.	• Renewable energy component requires high demands in both quality and installation due to totally external exposure (for both overall performance and safety aspect; • Additional moveable shading in clear vision area necessary; • Additional support structure is needed.
Roof-based	• Simplify in piping arrangement; • Lessen climate disturbance of original roof structure; • Improving the roof's thermal insulation; • Less costs for installation, cleaning and maintenance.	• Additional imposed static, wind, snow load that requires additional fixed structure and load assessment; • Risks in reducing life expectancy caused by water leakage, thermal breakage and expansion under high temperature.
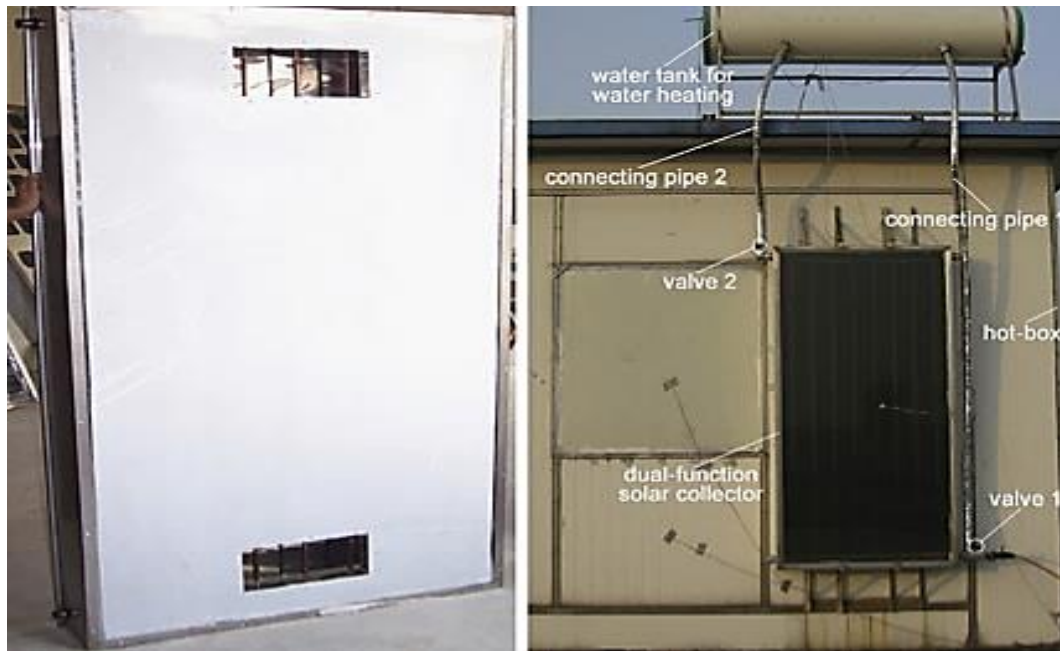
Figure 3-2 Test rig of the building-integrated dual-function solar system (Ji et al., 2011)

a. Comparison of the total cooling/heating loads of the room with and without the modified collector system during a typical summer(left)/ autumn (right) day

b. Variation of water temperature in storage tank during a typical summer(left)/ autumn (right) day
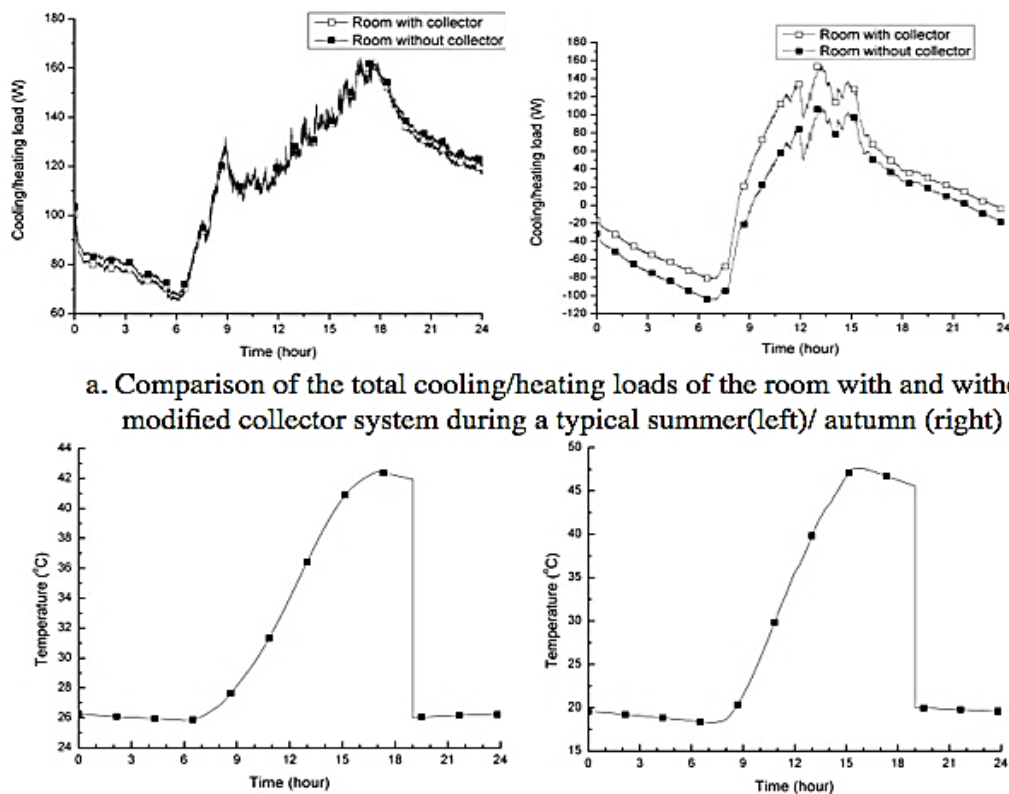
Figure 3-3 Comparison of both numerical simulation and experimental measurements during a typical summer/autumn day (Ji et al., 2011)

Figure 3-4 Structure of solar water collector of H2OSS (Motte et al., 2013b)
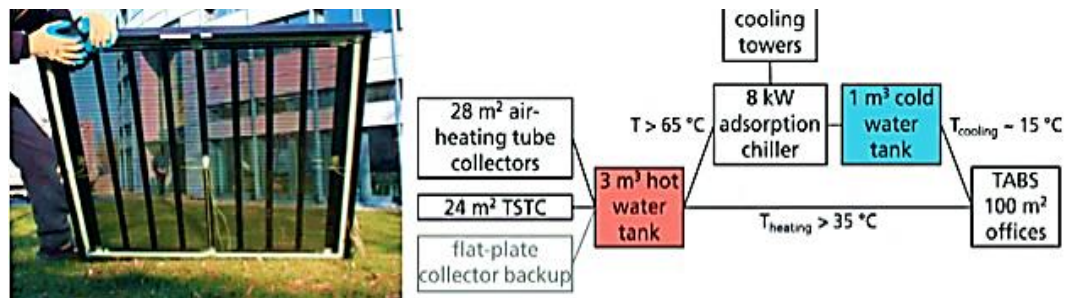
Figure 3-5 Transparent solar thermal collector with its HVAC system (Maurer & Kuhn, 2012; Maurer et al., 2012)
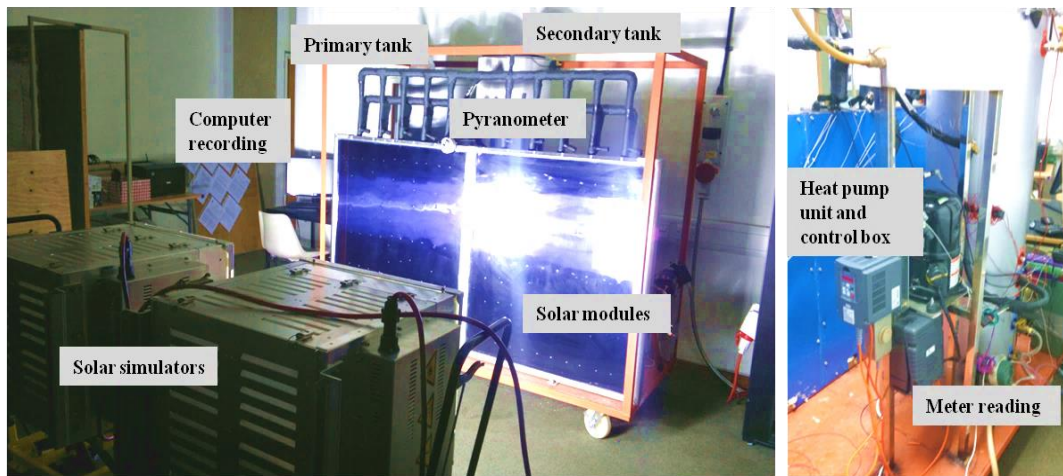
Figure 3-6 Photograph of the loop heat pipe solar facade prototype (He et al., 2015)

Motte et al. (Motte et al., 2013b) presented a new conceptual STF component with a remarkable rainwater gutter application. The experimental duration was about a whole year under various meteorological situations. A good accuracy between modelled and experimental temperatures was achieved by computing the absolute and relative Root Mean Square Errors for the outlet water temperature over four seasons (about 90 days). The thermal efficiency was around 60%, which was similar to conventional solar collectors when operat-

ing at low temperature. Future improvements, such as influence of material change, structure modification or possible improvements would follow on with the proper validation in Figure 3-4 (Motte et al., 2013b).

Anderson et al. looked into the thermal performance of different colour absorber plate. By using the combined experimental and numerical techniques, the performance of coloured solar collectors could be accurately presented, as shown in Figure 2-8 (Anderson et al., 2010). Although the conventional black-coloured collector had the highest thermal efficiency, the least performed white-coloured collector yet provided approximately 25% of the heating load. Therefore, there would be large scope of variation in terms of solar collector colour and solar heat output (Anderson et al., 2010).

Christoph Maurer et al. (Maurer & Kuhn, 2012; Maurer et al., 2012) experimentally studied a transparent solar thermal system specifically for high-rise buildings integration with a detailed physical model based on the laboratory measurements. The showcase installation in Ljubljana not only delivered extensive real-time operational data, but also provided a comparison between the modelling and on-site testing results, as shown in Figure 3-5. The dedicated modelling indicated that the primary energy savings of around 30% could be achieved if replacing the opaque walls with transparent collectors, while the solar factor proved to depend not only on the irradiation, but also on the operation of the solar collectors.

He et al. designed a novel heat pump assisted solar facade loop-heat-pipe (LHP) water heating system. The proposed system aimed to provide a solution to a building-integrated, cost-effective, high efficiency and visually pleasant solar water heating system (He et al., 2015). The experimental prototype was constructed and tested under

the laboratory condition shown in Figure 3-6. Under the controlled operation condition, the average thermal efficiency was 71%, and the coefficient of system performance was nearly 1.5–2 times over the conventional air-source and solar-assisted heat pump water-heating system. Through comparing between the modelling and the experimental results, the model could achieve the acceptable accuracy in predicting the system's operational performance, with the error scale in the range of 1–11%.

In summary, the above experimental studies keep the consistency of technical investigation. Majority of them focused on the working performance of the sole solar thermal device.

3.4 Review of commercial STF products

Although the STF technology is still at start-up stage, a large number of commercial products and engineering projects can be found in real world. A state of art review is conducive to a better understanding in the STF development. Table 3-4 outlines several kinds of innovative STF products incorporating distinct features. Table 3-5 displays the technical performance comparisons of commercial STFs depending on facade components. The reviewed commercial STF products have presented a considerable energy saving prospective and innovative solar thermal approaches for building integration. In general, the endeavors of these STF devices can be summarized into three points:

1) Enhanced heat transfer capacity with efficient and durable approach;

2) Innovative design in solar technical components with variable choice of colors and textures;

3) Employment of advanced processing and installation techniques.

However, these collectors in essence still have been identified with several inherent problems (Spur et al., 2006), mainly concluded as: 1) bulky size; 2) lower level of flexibility in solar thermal technology; 3) complex structures placement; 4) less choice of different surface treatments, such as texture and colour; 5) ignored effect of dirt; 6) overheating risks; 7) relative low optical efficiencies; 8) fewer multi-functional construction elements choice; 9) higher overall cost; and 10) almost similarity in block and rigid size among most STF products, which definitely require extra more effort for architects to combine as construction materials.

Although the evacuated tube collector has a satisfactory overall efficiency and gets rid of greater thickness, the monotonous structure and appearance somehow constrains the implementation as envelope except for balcony railings or sun shading element. And since this kind of absorber occupies multiple heat absorbing pipes and heat-exchanging units, and each component is closely connected, components are not easily replaced in case of damage or problems. Especially, overheating is delicate for most plastic and silicone parts and cause unsatisfactory stagnation phenomenon. Finally another limitation is lack of relevant dummy parts as standard options.

Therefore these reasons restrict current STF system in positioning to the exposed areas, and leads to abundant sizing in geometric/architectural dimensioning (Probst, 2008). Moreover, the lower optical efficiencies are attributed to the intended harmony with building design, while the solar efficiencies of available products are mostly limited from low heat absorption of water pipes (or air ducts) and low heat transfer within the heat exchange units. Even though several special advanced technologies in regards to enhance physical thermal connection and solar absorbance resulting relatively higher solar

efficiencies in some products. Fewer emphases yet have been dedicated on optimal product design from collector size, material and multi-function. From another aspect, the limitation in heat transfer performance is also inherently linked with working fluid. Water and glycol mixture is the most common working fluid as reviewed. Nevertheless, because of the antifreeze working fluid loses its chemical characteristics and goes from the liquid to the irreversible gaseous state, which would generates some problems, including an increased pressure drop and a reduced heat transfer (Giovanardi, 2012).

3.5 Overview of STF Prototypes and pilot project applications
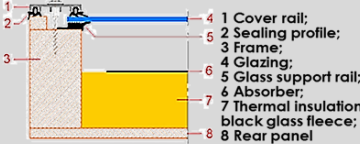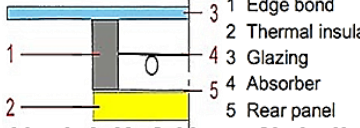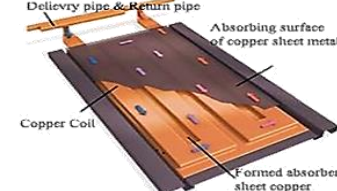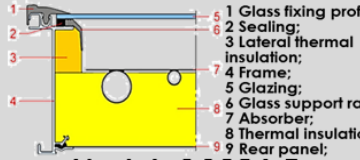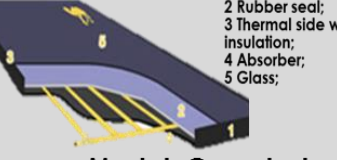
Apart from a list of commercial STF products, there are a wealth of ongoing research prototype and STF pilot applications presenting successfully innovative combinations between solar thermal energy systems and building facades.

3.5.1   Prototypes of innovative STF prototype application

1)   A facade based air heating vacuum tube collector

This prototype consists with a Sydney tube with one closed end, air ducts and headers distributing air into tubes in Figure 3-7 (left). Besides, a new tube with two-side openings can also be utilized to connecting each other in series over a longer distance. This kind of tube with a new micro porous thermal insulation has advantages in improving pressure drops and decrease volume of air ducts, and the thermal conductivity at a temperature of 200 ℃ is 0.020 W/(m-K). The glass tube connection is realized through a new method of laser welding. It assists in the elongation compensation units of the inner absorber tube, which offers a faster and precisely controlled treatment of the glass tubes.

Table 3-4 Overview of commercial STF systems

System schematic structure	Distinct features	System schematic structure	Distinct features
 1 Cover rail; 2 Sealing profile; 3 Frame; 4 Glazing; 5 Glass support rail; 6 Absorber; 7 Thermal insulation, black glass fleece; 8 Rear panel **Model: AKS Doma Flex** www.waf-solarfassade.at/en/	• Efficiency up to 86.7% • Aluminum absorbers with a highly selective coating *Mirotherm®*; • Laser-welded copper pipes guarantee optimum performance; • Wood or aluminum frame provides a very high level of freedom in both size and shape.	 **Model: HelioPower A/S** heliopower.com	• The world's first 100% invisible collector with two innovative materials of natural slate and bitumen; • Its efficiency is 20- 30%, while the asphalt roof system has the efficiency of 25% with a measured temperature up to 70 ℃ on upper side of roofing felt.
 3 Edge bond 2 Thermal insulation 4 Glazing 1 5 Absorber 2 5 Rear panel **Model: H+S MegaSlate II:** www.ch-solar.ch	• Thickness is only 38mm; • Same gluing technique as in double-glazing, helping to ease the integration into building skin and provide a new level of freedom for glazed collector; • Argon gas filled in-between gap to reduce heat losses.	 **Model: TECU Solar System** www.kme.com	• The heats transfer fluid in the rectangular copper path, capturing solar heat to produce thermal energy; • The whole collector is positioned integrally with roof system, therefore it is fully protected from external intrusions and completely invisible.
 1 Glass fixing profile; 2 Sealing; 3 Lateral thermal insulation; 4 Frame; 5 Glazing; 6 Glass support rail; 7 Absorber; 8 Thermal insulation; 9 Rear panel; **Model: COBRA Evo** www.solarhome.org	• The consistently lasered copper serpentine coil, making both arches and manifolds thermally active; • There are a large range of mounting accessories for roof-mounted, stand on flat roof and building facade.	 1 Aluminum manifold; 2 Rubber seal; 3 Thermal side wall insulation; 4 Absorber; 5 Glass; **Model: Camelsolar** www.camel-solar.com	• Seamless connected facade; • Inside absorber has no welding lines allowing for 6-8% increase in its efficiency; • Low-soiling coating on glass is anti-dust and anti-corrosive, keeping glass clear with same optical characteristics.

1 Glass fixing profile;
2 Glass support rail;
3 Casing;
4 Double-sided adhesive tape;
5 Glazing;
6 Glass support rail;
7 Absorber;
8 Aluminum foil;
9 Thermal insulation
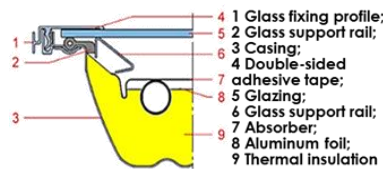
Model: Genersys
www.genersys-solar.com

- Consisting of a one-piece forged metal casing through a frame made from non-corrosive aluminum profile;
- Stamped al-mg sheet absorber fins with high-selective conversion layer span the copper pipe meander;
- The series connected collectors ensure good options for building integration elements.

1 Thermal insulation;
2 Protective cassettes;
3 RHEINZINK surface;
4 System batten/fastener;
5 Fluid carriers;
6 Collector tube with plug-in connector;
7 Flexible metal hose;
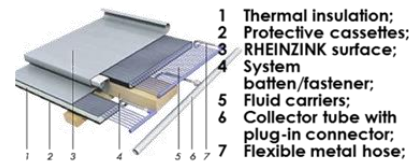
Model: QUICKSTEP Solar Thermie
http://www.rheinzink.hu

- An innovative, low efficiency, unglazed roof system is credible both visually and economically;
- The system can be integrated into the *RHEINZINK* roof covering system;
- The module looks exactly like traditional non-active ones without any field positioning and dimensioning issues.

SolTech Sigma kan installeras på tak som lutar minst 22°

300 mm   375 mm
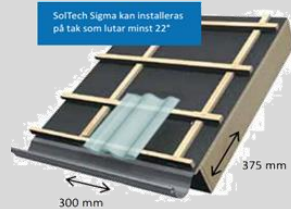
Model: SolTech Sigma
www.soltechenergy.com/

- A specially developed tile for more transparent active energy roofs;
- Glass roof panel with the specially developed liquid based absorber modules harvests solar energy.

Model: Atmova roof title
www.atmova.ch

- It can collect thermal energy from the ambient air, wind, and rain as well as any available solar radiation;
- The high-energy yield together with the long lifetime of the system guarantee the above- average economic benefit of the system.

1 – Outer pane: Extra white glass, thermally tempered
2 – Argon filling
3 – Inner pane: Float glass tempered with a low-e soft coating (pos.3)
4 – Aluminium strips with PVD silver coating (one side) reflectors: 98% visible light – 95% total reflection
5 – Extra white glass, thermally tempered or float 44.2, UV glued over the reflectors (4) with the inner pane (3)
6- One piece copper serpentine with warm transfer fluid
7 – Aluminium ∩-shape profiles with a solar selective absorber coating

Ext.   Int.

Model: RobinSun solar thermal glass
www.robinsun.com/en

- It includes two layers of glass panes, a certain volume of argon filling, a group of ∩-shape profiled thermal absorbers, and a copper serpentine pipe with working fluid and aluminum strips.
- A semi-transparent appearance, working as similar thermal properties to a highly insulated glazing all year round;
- Employment of mirror strips creating comfort natural light and relatively even daylight distribution at the back of rooms.
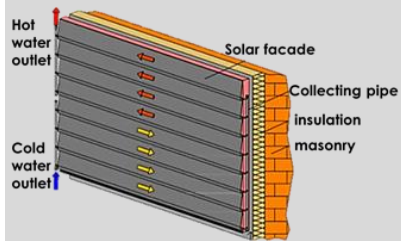
**Model: WAF solar facade
www.waf.at/solar-systems**

- Suitable for both new constructions and refurbishment of existing structures;
- Adaptable thickness of thermal insulation;
- Light weight for easy assembly;
- Architecturally attractive design;
- All the weatherboarding pieces are assembled via the mounting clicks, enabling an easy self-assembly approach.
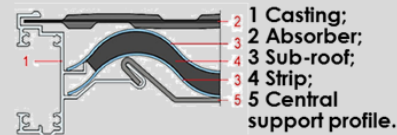
**Model: Energie Solaire Roof
www.energie-solaire.com**

1 Casting;
2 Absorber;
3 Sub-roof;
4 Strip;
5 Central support profile.

- 2 corrugated stainless steel sheets are welded together to form a thermal absorber with the cushion structure upon rubber roof insulation;
- The peculiar structure enables various types of integration on all types of roof profiles, even curved ones;
- It has a perfect waterproof quality due to self-draining aluminum profiles under solar absorber.
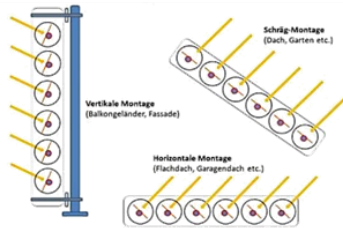
**Model: Swisspipe
www.schweizer-energie.ch**

- Peculiar evacuated tube collector in a parallel module;
- Each tube is composed of individual glass tube, a black or black-tube thermal absorber with fluid-cooling system, surrounded by a vacuum interior space;
- The tubes are standardized products with easy joining while the number of paralleled tubes can be flexible according to heat demand or construction size.

**Model: VarioSol A/E collector
www.winklersolar.com**

1 Wooden frame, open to diffusion insulation (55mm);
2 SKYTECH absorber;
3 Special solar glass with antireflective coating;
4 Profile system;
5 Tube connections;

- *Skytech* absorber technology is made by roll-folding technology connecting absorber sheet and tube over its entire circumference with an optimized heat transfer to the fluid inside;
- It is made on a one-off wood basis, while *VARIOSOL A* is a unit from aluminum with no screw at surface providing tightness for longer run;
- The thin collectors can be simply mounted onto flat roof rather than modified original building structure, providing an optimum solution for building renovation.

Table 3-5 Technical performance comparisons of STFs by facade components

Position	Model name	Type	Conversion factor η_0[1]	Stagnation temperature (℃)	Typical solar yields (kWh/m²)[2]		
					DHW	Water pre-heating	Space heating
Wall	AKS Doma	Glazed flat plate	0.82	194	500	727	331
	H+S MegaSlate II	Glazed flat plate	0.83	182	541	791	374
	WAF solar wall	Unglazed flat plate	0.67-0.79	N/A	N/A	N/A	N/A
	PCM STF	Unglazed flat plate	0.11-0.40	N/A	N/A	N/A	N/A
	Heliopan	Glazed flat plate	N/A	N/A	N/A	N/A	62.5
Window	RobinSun	Glazed flat plate	0.53-0.54	127.81	400	N/A	N/A
	Transparent STF	Glazed flat plate	0.58-0.61	N/A	N/A	N/A	N/A
	Vacuum-tube STF	Evacuated Tube	0.70-0.90	N/A	N/A	N/A	
Balcony	Swiss Pipe	Evacuated Tube	0.88	N/A	669	860	
	WAF solar balcony	Glazed flat plate	0.67-0.79	N/A	N/A	N/A	N/A
Sun shield	S-Solar	Glazed flat plate	N/A	N/A	450	N/A	N/A
	Ritter XL	Glazed flat plate	0.68	N/A	N/A	N/A	N/A
Roof	VarioSol E	Glazed flat plate	0.79	N/A	502	720	341
	Genersys	Glazed flat plate	0.83	164	504	749	336
	Energie Solaire	Glazed flat plate	0.84	175	497	776	320
	COBRA Evo	Glazed flat plate	0.88	187	549	813	372
	Quickstep Solarthermie	Unglazed flat plate	0.54	90	N/A	N/A	N/A
	Atmova roof title	Unglazed flat plate	015	73		800	
	TECU Solar System	Unglazed flat plate	N/A	N/A	N/A	N/A	N/A
	Heliopower Slate	Unglazed flat plate	0.20-0.30	N/A		250	
	Heliopower Roof	Unglazed flat plate	0.25-0.40	N/A		250-400	
	SolTech Sigma	Glazed flat plate	N/A	N/A	255	N/A	N/A

Note: 1)The technical data of both the Conversion factor η_0 and the Typical solar yields are evaluated from SPF Testing;
2) Climate: Central Switzerland, orientation of the collectors: South, Cold water 10℃, Hot water 50℃, Irradiance Gs=1000 W/m², Ambient temperature ta=30℃

The absorber can be clipped onto a stainless steel central tube, while the air carrying central tube is connected to the outer glass tube by a longitudinal compensator to provide the vacuum tightness of the tube. Figure 3-7 (right) shows the application example of a glazing door (Kollektorfabrik, 2011).

2) Unglazed facade collector

The cost effective active solar facade system is a low temperature unglazed solar collector, shown in Figure 3-8, coupling with a reversible heat pump. It works as a low temperature solar collector, an atmospheric heat exchanger as well as a nighttime heat-dissipater in order to boost the heating/cooling efficiency of the whole system. The internal capillary mat was embedded in the finishing layer of the external insulation of building. This cost effective solution enables one-step installation of both external insulation and active facade. And a glycol solution circulates in the capillary tubes to transfer heat to the heated room via the storage and the heat pump (ESTTP, 2009).

Figure 3-7 Prototype of air collector mounted at the windows of Kollektorfabrik store-house (Kollektorfabrik, 2011)

Figure 3-8 Collector installation for Long-term laboratory tests of the integrated concept (ESTTP, 2009)

3) A transparent thermal collector for window integration

The innovation displayed in Figure 3-9 was achieved with the integration of the angular selective apertures, which was realized by a specifically developed punching tool. After a magnetron sputtering coater, the angular selective apertures were tightening with flat plate absorber, in which the aluminium pipe system was welded to a blank aluminium sheet at first. The manufacturing process was finalized with the integration of the close-up collector in a triple glazing unit (PG, 2011).

Figure 3-9 The complete collector ready for the testing, external (left) and internal (right) view (PG, 2011)

4)   A solar thermal tube inside facade

This prototype in Figure 3-10 is made predominantly from glass (tubes, glass panes), aluminium (frame profiles, heat conductor profiles) and stainless steel (collector pipe-work), consisting in vacuum tubes fitted with Compound Parabolic Concentrator (CPC) mirrors. Owing to the vacuum tube employed, its working temperature is around 60-90℃, along with the perforation of CPC reflector, it can collect sunlight and protect rooms from direct solar radiation as well as introduce part of sun penetrate to provide low-glare natural light and visual transparency. It is primarily available in the form of flat plate collectors with a thermally insulated opaque rear wall (Giovanardi, 2012).
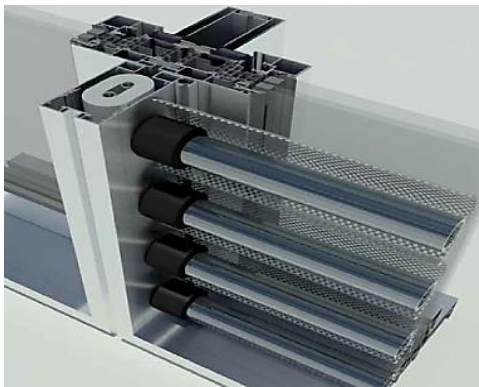
Figure 3-10 Visualisation of connection details of the solar thermal tube (Giovanardi, 2012)

Figure 3-11 Close-up of BIONICOL prototype collector (Hermann, M., 2012)

5)   Bionic facade collector

The distinguished feature of this light-weight solar collector lies in the advanced aluminium roll-bond absorber with a Bionic Fracterm© channel. From Figure 3-11, it can found that there are multiply branched in a fractal way to obtain a uniform flow distribution, a low pressure drop as well as a high thermal efficiency. This collector aims to have maximum efficiency and minimum costs in the meanwhile being flexible in size and dimension, as parallelogram, triangle or arcs. Therefore it is proposed to integrate on roofs and in facades (Fraunhofer ISE, 2009; Hermann, 2012).

6)   Solabs facade collector

This product is a novel performing unglazed metal collector based on coated steel sheet, shown in Figure 3-12.

Figure 3-12 SOLABS plank hydraulic system (left) and the resulting demo site proto-type (right) (Probst & Roecker, 2007)

Special focuses have been put on facilitating the architectural integration, such as materials and constrains, cladding modules and jointing, surface texture and finish, surface colour were discussed in detail by authors. Similarly, the hydraulic system is designed attached at the back of the collector ensuring both an optimal heat transfer and a perfectly smooth front surface. And its horizontal piping system is proposed to be compatible with the cut to length dimension of the modules (Probst & Roecker, 2007).

3.5.2   Overview of STF pilot project application

In addition to prototype application, Table 3-6 presents a list of representative STF incorporated projects. Detailed descriptions are given in each project (Probst, 2008; Giovanardi, 2012; Maurer and Kuhn, 2012; Zhang et al., 2015a). In summary, both the prototypes of innovative solar thermal collectors and pilot STF projects display how synergic a collaboration between manufacturers and researchers can be.

Diverse directions with miscellaneous motives have led to a lot of different STF building integration variations. Typical strategies can be as-

signed to dissimulation into building envelope, special placement, and modular building component design. Furthermore, it can be found that majority of new building project belongs to the solar house, the passive house or even the net zero energy building design, while renovation projects provided a new direction of functional transformation instead of sole repairing. More focuses have been put on threatening resource shortage, comfort living environment, as well as position architectures themselves in the niche market. It is worthy mention that as an innovative choice of multifunctional building envelope, STF has superiority in good insulation, use of solar heat gains and high compactness, fully satisfying the current booming branch of "high performance buildings", "green buildings" and even "zero energy buildings" (Musall et al., 2013)

Table 3-6 Overview of demonstration projects with STF application

Category 1: Family house & apartment cases

VKR Holding A/S	**"Home for life" concept house, Aarhus, Denmark** STF dissimulates within roof to form an active house with a living area of 190 m². The total 6.7m² solar collecting area is integrated in the lowest part of roof surface with auxiliary heat pump system, which directly supply 50-60% of the annual household hot water heating demand and a supplement for the downwards room heating.
AEE INTEC	**Petersbergenstrasse, Austria** It exhibits a case of prefabricated STF system to streamline installation. The 50 m² wall based glazed solar collector has been erected 10° southwest oriented for DHW preparation and space heating. These pre-manufactured fields are made by frames with only about 10 steel angles for fixation, which fixing wooden back wall of collector to timber almost without any effect on thermal bridges.
SIKO SOLAR GmbH	**KOMBISOL® house, Tyrol, Austria** This shows a perfect example of cladding facade by 70m² solar collectors and the thermal mass storage by concrete. The whole STF can provide needed energy for hot water preparation and space heating with an additional geothermal heat pump. When there is excess energy from solar thermal collectors, it can be not only stored in ground but also in the concrete core of the house. It enables a comfortable and warm climate in winter and also a cooling function in summer.
Solaripedia	**Sunny woods, apartment house, Zürich-Höngg, Switzerland** The whole STF application is natural and plain in the integration design with simple accessible external connections. The solar-tube collectors act as a transparent baluster for the balcony, while the valuable sunshine can be stored through window into stone flooring.
Domasolar	**House J, single family house, Nenzing, Austria** It exhibits building integration between dummy elements and glazed collectors. A dark blue cladding was chosen as finishing to cope with the imposed dark blue solar collectors mounted on south facade. As the use of similar collector size fitting with modular rhythm of standard cladding, the same types of jointing, homogeneity of color, size and jointing make two parts of facade component acceptable.
Energie Solaire SA	**The centre d'exploitation des Routes Nationales, Bursins, Switzerland** A large area of stainless steel unglazed metal collectors is utilized as multifunctional facade claddings in south-facing façade for floor heating, DHW and an excellent corrosion-resistant building envelope. STF harmonized entire active and non-active panels with stainless steel elements of same dimension and appearance, so they fit modular demands of building. The active solar panels weigh about 10 kg/m², an important consideration for easy assembly.

Picture source:Jadarhus AS

Jadarhus AS

Jadarhus ISOBO Aktiv, Sandnes, Norway

The STF looks like mosaic titles inserted in timber roof of the traditional rafter construction with a total living area of 178 m^2 and an annual heat demand of 44kWh/m^2. The solar collectors make up an area of 8 m^2 as the roof surface for 90% of hot water preparation and 95% of space heating.

Viessmann

2-flat penthouse in Vienna, Austria

As a project of sustainable renovation, this ingenious STF application with two direct flow vacuum tube collectors with 2.88 m^2 are installed at the roof terrace area as an innovative, modern, solar pergola. They have multi-functions as hot water production, sun shading and pergola. This project exhibits a special case of building integration from overall architectural concept.

SIKO SOLAR GmbH

Sun house, Tyrol, Austria

There are two groups of inclination installations: 1) the roof with 45° inclination for a maximum yield in the summer; and 2) the facade with 70° inclination for a maximum yield in winter. Therefore it shows a good exhibition for both the solar thermal collectors and the photovoltaic modules perfect adaption into the house.

Aventa AS

Passive house Rudshagen, Oslo, Norway

This project utilizes the high performance polymer collectors (19.5m^2) in the south facing facade of the "solar house" to satisfy both space heating and domestic hot water preparation, which is 61 kWh/m^2/year in total heat demand. This STF application was benefit from lightweight collector for easy domestic installation.

Viessmann

Row dwelling I-Box concept building, Tromsoe, Norway

The whole design paid considerable attention to various building materials, forms, and colors of the architectural composition of envelope without abrupt STF appearance. Each 5 m^2 STF system was whole integrated with each residential units.

Category 2: Commercial & public building cases

Schweizer-metallbau

School building in Geis, Switzerland

This is a successful prefabricated STF application. At early design phase intervention, designers paid considerable attention to facade design, layout, size and fixed modular dimensions of the solar. The total 63m^2 collector field fully respects the rhythm of window, the color of both window frame and concrete bricks, showing a convincing result.

AEE INTEC

HQ, AKS DOMA Solartechnik

This project realizes the neutral CO_2 energy supply for the 470m^2 offices and the 1,380 m^2 production hall through the STF application. The total 80m^2 STF provides whole heating through a wall heating system and a floor heating operated with very low flow temperatures, which offer ideal conditions for the operation of solar thermal plant.

Hotel Jezerka, Czech Republic

This STF application pays special consideration to the horizontal installation with 236m² solar collectors in the south facing balconies for heating tap water and swimming pools. These collectors were designed as handrails of balconies or as flat roofs. The price of each collector was € 364.8 with total solar gain of 120 000 kWh/year.

Thermosolar

Environmental Research Station Schneefernerhaus - UFS, Germany

This retrofitting project with STF system is located at Germany's highest mountain. With adding additional thermal insulation, 100m² solar collectors were integrated as building facade for both DHW and space heating. The related water based heat distribution consists with floor heating and radiators, while heat pump and electricity are set for auxiliary heating.

Fraunhofer ISE
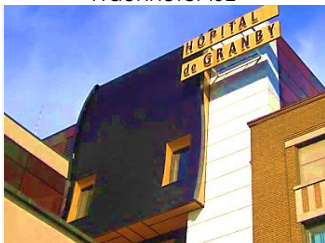
Granby Hospital, Granby (Quebec) / Canada

The transpired solar fresh air heating system is specially designed to satisfy the demand of large amounts of fresh air. The solar system is aesthetically presented with 82 m²-curved facades to provide 8160 m³/h to the space below. The perforated metal absorber draws in heated fresh air of the surface of south-facing walls, where it is then distributed throughout the building as pre-heated ventilation air.

Matrix Energy

Social housing in Paris, France

The new multifunctional semi-transparent collector is encapsulated into a double skin façade of the social house, which weights 45kg, offers privacy from the passengers commuting nearby, ensuring light penetrate into the back area of room, and restricts noise flow. And the solar panel captures solar energy to produce enough power to meet 40% of the domestic hot water.

ROBIN SUN

The Bellona Building, Oslo, Norway

This is constructed of in-situ concrete with facades in plaster and glass. The installation shapes of solar collectors serve as self-shading facade and cover large parts of south-facing wall. There are windows on the inward-facing part and 240 solar collectors on the outward-facing part. Due to good insulation, excellent window, minimized thermal bridge and low air leakage factor, solar collectors and geothermal heat pump can cover all the heating demand.

Finn Staale Feldberg

Retrofitted Office Building in Ljubljana, Slovenia

This is a detail designed retrofitting project with STF application. The air heating vacuum tube collectors were replaced the balustrade on the 5th floor, while the transparent solar thermal collectors were attached to the stairwell. Both collector areas face almost south, the solar collectors 15° towards east and the air-heating tubes 15° towards west. Both components were developed to be a substitute for the building skin as well as the thermally activated building system of 100m² office space with fluid at temperatures above 35 ℃ during heating season.

(Maurer and Kuhn, 2012)

3.6 Opportunities for future development

3.6.1   Development of new absorber structure for STF

The majority of currently available STF solutions mainly emphasize on the maximisation of energy production yet match neither the multi-functionality nor the integration possibility in facade designs, such as module thickness, size, colour, texture, shape, jointing typology, and collector field dimension. There do exist some commercial applications of solar thermal collector in the refurbishment market but are mainly conceived for implementation in new buildings. It is therefore required to conceive new thermal absorber structures for STF technologies for both new and existing buildings that can meet the required criteria, such as aesthetic feature, economical cost, modularity, good flexibility in the building integrated design, and easiness of installation and maintenance.

3.6.2   Real-time experimental measurement for a long-term scheme

This real-time experimental measurement shall involve the field-testing of the integrated STF-based building service system in real buildings. The operational system performance and the impacts in the whole building shall be tested, monitored, and recorded for the long-term duration (more than 12 months). The test results shall be further contributed to explore the operational features of the STF-based system in real buildings, which shall then be compared with the operational performance predicted from the simulation models. The difference between the test and predicted data shall then be analysed and if a gap is found, a potential solution for further improving the operational performance of the STF-based system or enhancing the accuracy of simulation models shall be investigated. A measurement standard especially for the long-term dynamic test method shall also be further developed as well.

3.6.3   Economic and environmental performance assessment and social acceptance analysis

The economic assessment shall further involve into the new facade modules with the associated building service system in terms of capital cost, life cycle, energy/bill saving, as well as payback time. Furthermore, the environmental benefits of utilizing such systems in buildings shall be assessed by analysing the potential annual and life-cycle fossil fuel energy saving and carbon reduction volumes. Social acceptance or feasibility level of the new modular STF and associated building service systems shall also be analysed taking account of the survey results from the public and the views of the consortium members. The potential impact of the new STF technology shall be assessed under both the environmental certification programs and building simulation platforms. Based on above works, there is necessary to establish an integrated simulation model to predict the social-economic performance goals, including building energy saving, facade costs, life cycle fossil fuels and billing savings and carbon reduction, as well as payback time etc.

3.6.4   Development of an integrated database/software/platform across design process

One of the major impediments to promote the STF technology is the lack of formal feedback among architectures, policy makers, and engineers during the building integration design. An interactive interface or platform, such as BIM concept, for discussion among different stakeholders can be open for development by integrating knowledge, information, and experience from relevant building energy projects of STF design cases, architecture initiatives, and requirements of structural and building energy performance. The designer-engineer-orientated relational database/platform will give practitioners access to design cases, knowledge, insights and cost that are relevant to

their current STF technologies in an integrated way. The platform shall enable continuous expansion of the STF design cases thus maximising the updates of its scope, frequency, and quality. In addition, the impact of utilizing a STF system on the whole building energy load is especially necessary to examine using simulation.

3.6.5   Dissemination, marketing and exploitation strategies

In order to motivate the use of STF technology, more dissemination activities should be presented to the public using various approaches, including the publication of roadmaps, showcases, workshops, on-site visits, open days, newsletter, conferences, and exhibition presences. Such kinds of professional events should invite both local and national media (television, newspapers, etc.) to conduct live reports throughout the regions, nations and all over the world.

Analysis of the market potential is crucial for the development of STF products. It is well known that solar technology is expected to provide nearly 50% of the low-and-medium temperature heat within the EU. A market investigation of STF products is suggested in terms of conducting the following:

1) Case studies of existing STF products to identify the applicability for the user, climatic regions, market positions, and recommendations;

2) Feasibility study of STF application in various locations, building types and energy systems;

3) Market survey of customers/designers' preferences;

4) Establishment of a generic extrapolating methodology for the market analysis of STF systems.

The exploitation strategies shall further involve collection and identification of the important technical breakthroughs or findings, and exploitation of the results through appropriate routes to help achieving

the successful replication and deployment of the dedicated STF technology throughout regional and worldwide, including:

1) Identifying sensitivity of the publishing items;

2) Dealing with intellectual property related issues;

3) Completing license agreement;

4) Identifying the potential business opportunities and setting up business ventures;

5) Completing technology implementation plans;

6) Developing a commercial plan;

7) Developing a financial plan for commercialisation.

3.7 Proposal for novel STF system in the PhD project

In summary, in accordance with the existing research results and future potential opportunities in the development of STF technology, this PhD project would address the following aspects:

1) Propose an innovative and compact STF proposal;

2) Develop the computer simulation models for the purposes of initial concept design, configuration/operation optimisation, evaluation of energy performance and socio-economic analysis of the STF proposal;

3) Characterise the STF technology under laboratory controlled conditions;

4) Operate the simulation model to explore the impacts of such STF for whole building integration throughout a whole year;

5) Develop an integrated strategy for different stakeholders to promote the application of such STF technology at the early design stage.

These are intended to achieve the systematic development of a new STF technology and cover some of the missing points in previous researches. The results will contribute a certain added value to the development of STF technology.

3.8 Chapter executive summary

This chapter summarized the standards and regulations related to STF design and installation, and then reviewed the existing STF implementations from commercial STF products, innovative prototypes, to pilot projects.

The in-depth overview of existing STF implementations exhibited technical attractive design and harmony with existing building components. However, several inherent limitations of:

1) Bulky size;

2) Lower level of flexibility in solar thermal technology;

3) Complex structures placement;

4) Less choice of different surface treatments, such as texture and colour;

5) Ignored effect of dirt;

6) Overheating risks;

7) Relative low optical efficiencies;

8) Fewer multifunctional construction elements choice;

9) Higher overall cost;

10) Almost similarity in block and rigid size among most STF products, which definitely require extra more effort for architects to combine as construction materials.

In line with these findings, more innovative scientific efforts are needed from the aspects of structure design, operating parameter, and research methodology. For the future development, progressive steps are recommended as:

1) Developing a new feasible, economic and energy efficient STF system;

2) Optimising structural/geometrical configurations and operating parameters of the new STF for greater overall performance;

3) Studying dynamic performance and feasibility assessment of the STF linking system's performance with building's comfort and

energy consumption for a long-term scheme under real climate condition;

4) Carrying an economic feasibility study and environmental analysis with consideration of climatic conditions;

5) Developing an integrated platform (i.e. BIM) for different stakeholders providing information exchange, integrated architectural design and engineering performance simulation;

6) Implementing dissemination, marketing and exploitation strategies to boost the use of STF technology in a wider range.

This part of study helps in:

1) Illustrating of the current status of STF application in the real life;

2) Completing the sound research methods for new STF concept including experimental testing;

3) Investigating common fabrication and installation approaches of STFs;

4) Proposing research concept for next chapters;

Together with the conclusions from Chapter 2, it has been found that developing an economical, thermal-efficient, simply-structured, and aesthetically-attractive STF for building application is in urgent need to create a technical combination in this subject for the widespread market penetration. As a result, this PhD project would develop such a new STF concept by the mentioned progressive steps.

4

CONCEPT DESIGN OF THE COMPACT UNGLAZED STF

4.1 Chapter abstract

This chapter proposes an innovative unglazed STF modular for facilitating domestic hot water production with:

1) Develop the sketch drawings of the STF and its integration with building as various facade components;

2) Describe basic working principle of the proposed concept;

3) Deliver alternative designs in terms of material, colour, texture, shape, geometric size, architectural design, installation method, array connection, hypothetical system application function, and solar coverage.

The concept design hereby illustrates precedence for the hypothetical function through creating new ideas, and forming up the physical structure investigations in the following chapters.

4.2 Concept design of a novel compact STF

The design concept of the new STF starts with a fundamental solar thermal system that should be lower in overall cost for greater facade area application, and convenient for daily operation and maintenance (O&M). In addition, a flexible building integration solution should be simultaneously covered with regard to architecture expression freedom and worksite installation.

4.2.1   STF module configuration and its integration with building

The basic configuration of the STF module is presented in Figure 4-1. The single-side-embossed absorber panel is made up with two stainless steel sheets. One sheet is physically extruded by machinery metal roller which has concave pattern surface finish to formulate arrays of pin-fin corrugations, while the another

sheet working as the absorbing surface remains smooth, and can be coated into optional colour or texture treatment according to different requests. The two metal sheets welded together around the perimeter forming an absorber unity and built-in channels.
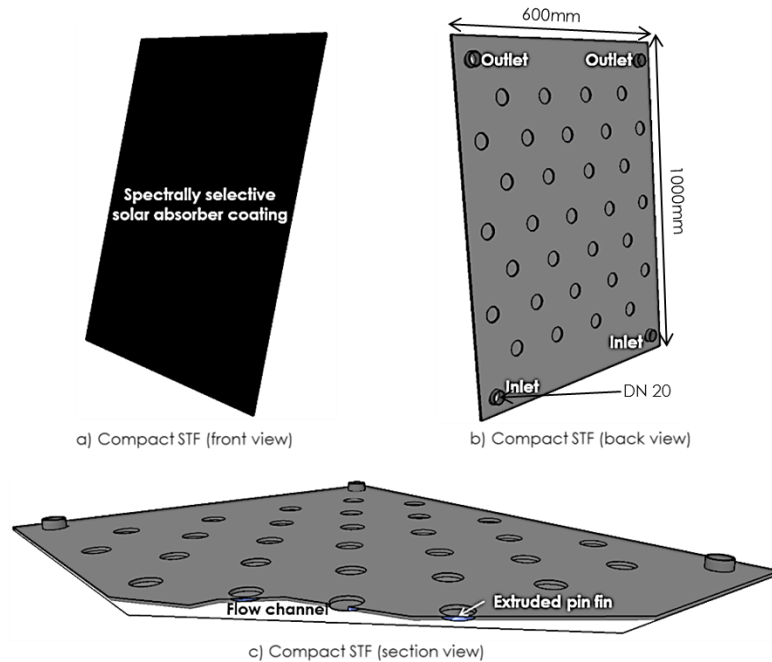
Figure 4-1 Concept design of the compact STF panel with internally extruded pin-fin channel

In contrast to the traditional tubes attached absorber, such built-in channel structure is designed to eliminate the utilization of redundant tubes and further enables a high flexibility in size or shape. Because the general machining equipment, for examples, the roll forming machine, the embossing machine and the stamping machine can fully realize the fabrication. And these are well-established large-scale industrial machines for metal sheet processing and are popular in the productions of metal roof, decorated metal sheet and heating radiators in China. So that it is expected that significant cost reductions and various architectural and aesthetic requirements could be achieved with the increased flexibility in industrial mass production. In addition, different arrangement and combination of the extruded pin-fin banks can also form up different channel structures with a high

complexity yet without any additional costs via the roll forming technology. This enables high feasibility in channel structure design at the boundary area in cases of various shape or size.

In general, such a unique compact STF design engenders not only high heat transfer performance and economical overall cost, but also great feasibility in assembly of either parallel or series flow pattern for architectural design.
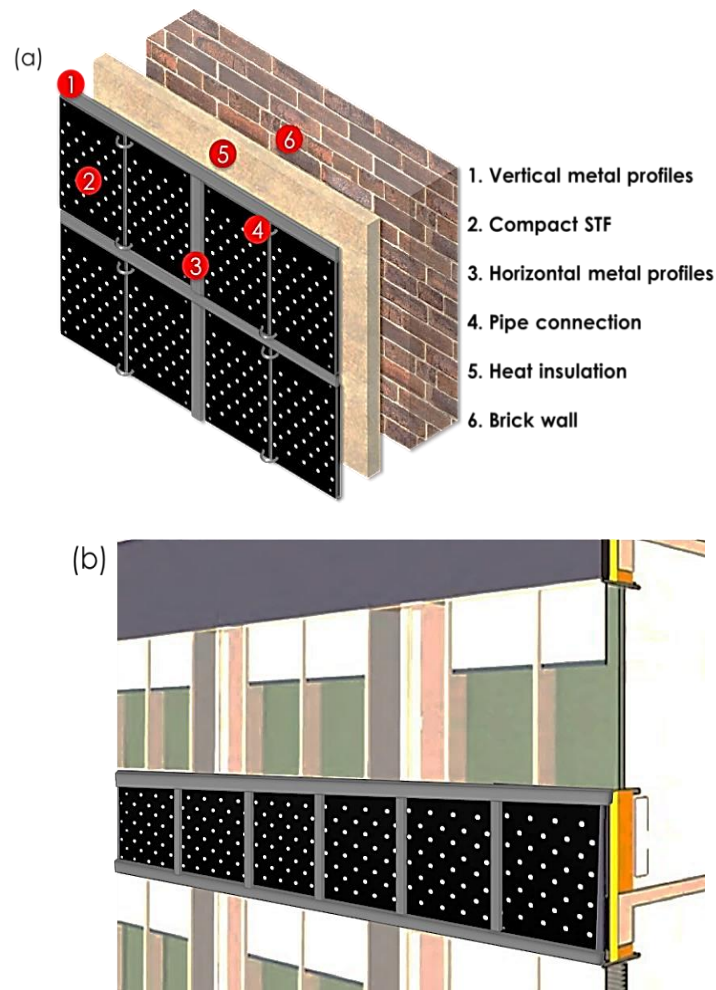
Figure 4-2 Schematic of compact STF integration with (a) wall; (b) sill

In practice, the proposed STF could be applied as either wall/roof or balcony external cover/claddings, which can be attained via the integration with supporting enclosure and insulation layer, as illustrated in Figure 4-2(a) and (b). The novel STF could be in the form of a standard modular size to take shape of

the building external decorator for both horizontal and vertical installation, which is also beneficial to the architectural aesthetic of buildings. Each STF module is fitted with two sets of tubular fluid inlets at the bottom/on the top that allow connection from module to module using the ease-off flexible couplers and pipes in either serial or parallel flow pattern. This creates a heating network to heat up the water gradually to the required temperature level. After completing the fixing-up and piping connection, the gaps between the adjacent STF modules could be sealed with a high standard sealant (e.g. stick rubber). All the connectors, fixing-up points and sealants are hidden behind side wings of the enclosures to avoid affecting the aesthetical appearance.

4.2.2   Building installation method

Compared to conventional solar thermal technology, installation is a more vital step that transfers STF into real multifunctional facade component and ensures the safety and durability for its long term operating. Currently, there are four available methods for installation of such a STF with buildings, as given schematically in Figure 4-3:

1) Anchor bracket and hang rail;
2) Tongue and groove;
3) Integral hanging rail;
4) Screw fixing.

Both the anchor bracket & hanging rail and the tongue & groove belong to the bracket method, which are suitable for the STF application in the form of cassette for large-scale envelope area. Vertical forces (caused by dead loads) together with horizontal forces (caused by live loads) would be transferred to the building supporting structure. On the other hand, the integral hanging rail and the screw fixing can be categorized as me-

chanical fixing methods, which are usually applied in the form of panel for small envelope area.

a) Anchor bracket and hang rail   b) Tongue and groove

c) Integral hanging rail   d) Screw fixing
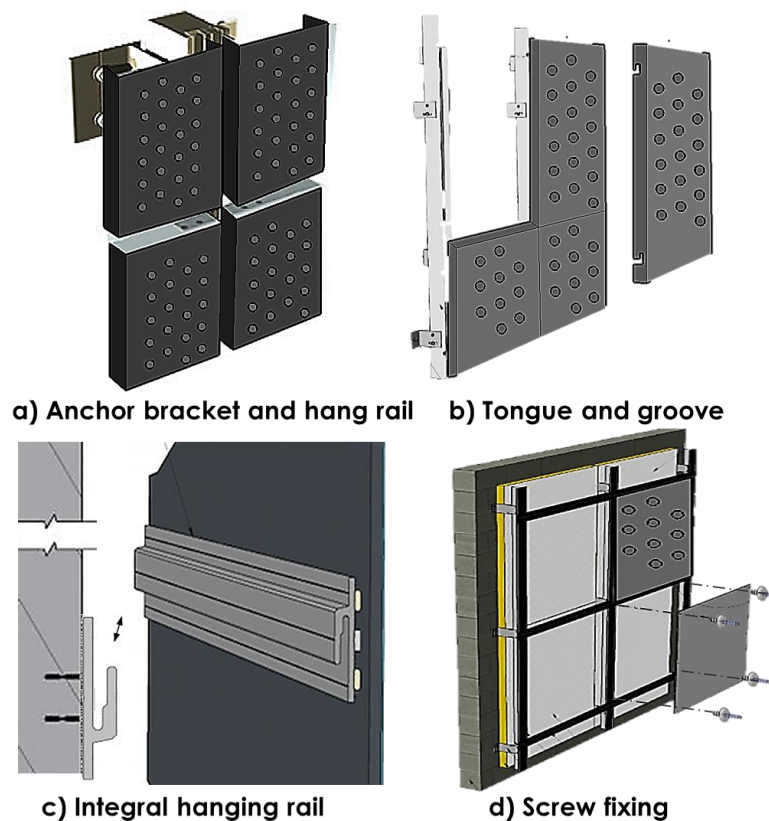
Figure 4-3 Several STF installation options using different jointing methods

4.2.3   Working principle of STF module

In operation, the STF works on the same principle as conventional unglazed solar thermal collectors, consisting of a series processes:

1) Solar absorption and heat gain via STF smooth surface;

2) Conductive and convective heat transfer caused by temperature difference between the STF smooth surface and the surrounding air or the working medium;

3) Thermal radiation exchange between STF and its surroundings.

Thanks to a selective solar coating, part of the solar energy is optimally converted into thermal energy once it strikes onto the STF's surface. A working medium, in general a water-glycol mixture, passes through the built-in channels from the bottom inlets

and attains the solar heat from the pin-fin banks and the STF's sur-
face directly (as indicated in Figure 4-4). Afterwards, the gener-
ated thermal energy is output from the top outlets and further
transferred as the useful energy to the heat circuit by a heat ex-
changer for storage or utilization. Finally, the returned water en-
ters into the STF bottom inlets again to complete the circulation.
In the meanwhile, the rest of solar energy is dissipated to the sur-
roundings as the form of heat loss.
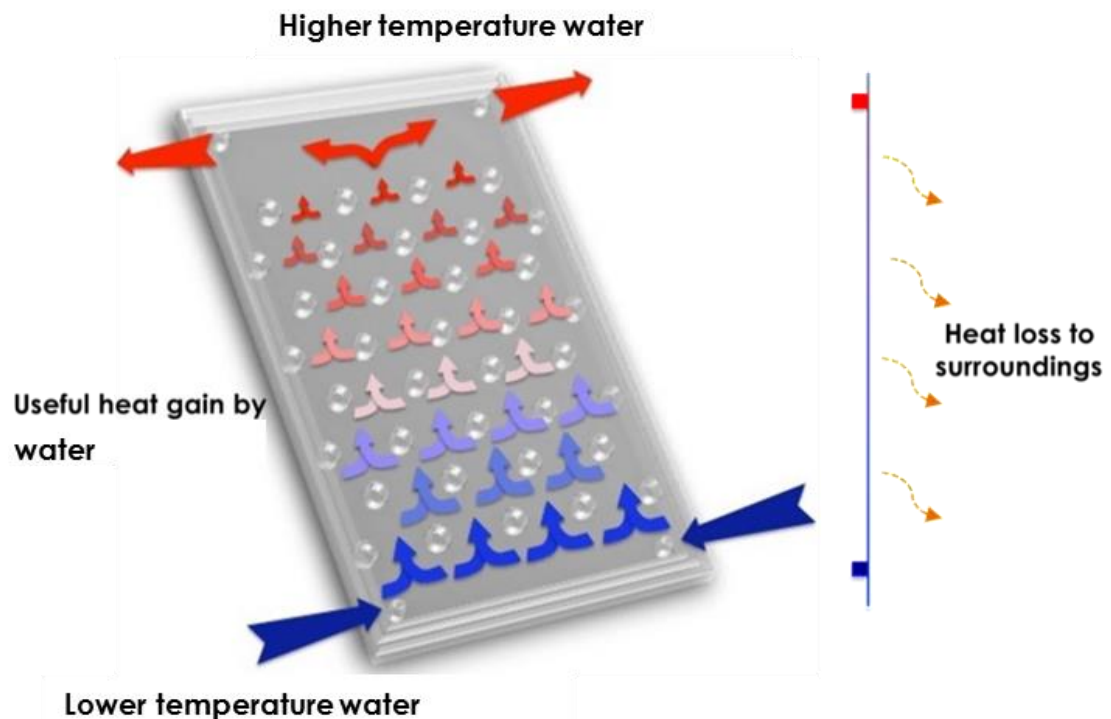
Figure 4-4 Schematic fluid flow of the STF

4.2.4   STF's material choice

In the view of solar technology, metal panels have already been
developed for optimal heat exchangers. The initial design needs
to additionally spotlight on the possibility of compact dimension,
fabrication, durability and cost. Currently, the popular metals for
piping and construction are stainless steel, aluminium, copper,
and bronze as shown in Figure 4-5.
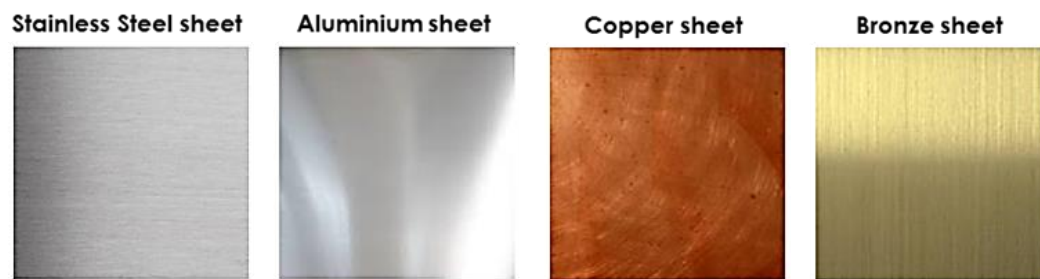
Figure 4-5 Potential metal materials of the STF

Proper STF materials should avoid much additional weight increase, thermal dilation and galvanic corrosion and with the superiorities in heat transfer performance and advanced manufactory technologies through processes like cutting, folding, pressing, and welding. According to such selection criteria, the detailed evaluation of these materials and the ultimate determination will be conducted in the following theoretical analysis part.

4.2.5   Colour and texture

Figure 4-6 illustrates several colourful palettes for STF smooth surface developed in the comparative study between typical selective black-chrome coating and the TISS paints. Different absorbance (a) and emissivity (ε) values characterize the various colours of the palette. It comprises both high and low efficiency shades, leaving to the architect and engineers with the choice of using a more or less efficient colour according to building and context specificities (Probst, 2008). The selection should be balanced in terms of the aesthetics and the energy efficiency criteria in order to maximize solar absorption rate and minimize the infrared heat loss from the STF.

Selective black-chrome *a 0.97* *ε 0.09*		
S-RAL-5002-2 *a 0.78* *ε 0.37*	**S10204-7** *a 0.799* *ε 0.274*	**S-R-130-1** *a 0.88* *ε 0.64*
S-5056-7 *a 0.820* *ε 0.369*	**S-4044-7** *a 0.841* *ε 0.384*	**S-R-130-13-60%** *a 0.89* *ε 0.40*
S-4047-7 *a 0.839* *ε 0.395*	**SPK-1055-5** *a 0.763* *ε 0.318*	**SCG-167-50%** *a 0.84* *ε 0.38*

Figure 4-6 Colourful palettes for the STF smooth surface (Probst, 2008)

According to such selection criteria, the detailed evaluation of these colours and the ultimate recommendation will be conducted in the theoretical analysis in Chapter 5. In addition to the high flexibility in colour options, the STF surface could be dressed with different surface expression, such as mirror, embossed, etched, sandblast and vibration etc., to meet various architectural requirements. Figure 4-7 demonstrates the available stainless steel surface textures in the market of China.
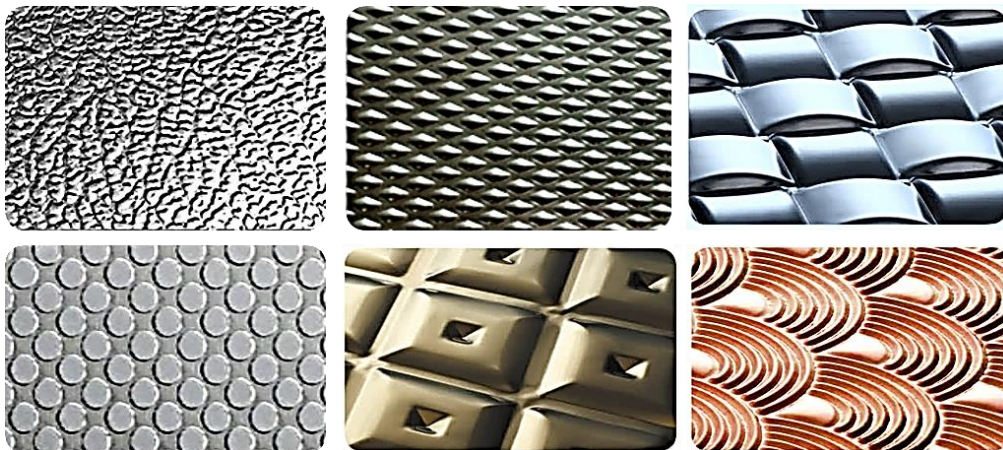
Figure 4-7 Texture options for the stainless steel STF surface

4.2.6   Shape and size

Apart from the flat-plate and rectangle shapes, the STF could be made into curved or polygon ones, as shown in Figure 4-8. Potentially, such STF can be tailored depending on various architectural and aesthetic geometric requirements by cutting the metal sheets into different sizes. These variations greatly enhance the aesthetical appealing and the utilization of overall wall area, thus further improving a diverse range of architectural and aesthetical needs.
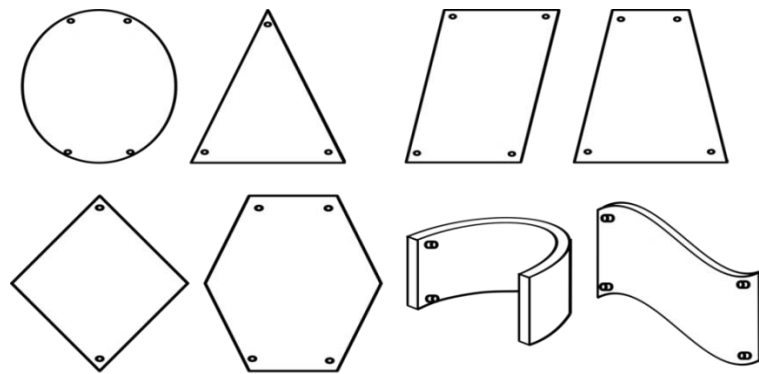
Figure 4-8 STF cladding designs with different shape changes

4.2.7   Architectural design of STF for building integration

1) Two STF design variants

Figure 4-9 presents two design variants of the proposed STF respectively for existing and new low-rise building typologies, i.e. (a) the cladding system and (b) the prefabricated STF wall system.

The STF cladding system aims to act as the rain screen cladding system, which is particularly developed for the low-rise building or facade renovation. This STF variant can be mounted onto the original wall system for purposes i.e., preventing rain, improving heat preservation, reducing excessive air leakage, and carrying wind load. The prefabricated STF wall system is recommended for the new building for the multifunction of the active solar absorber and the insulated wall.

(1) Stainless steel sheet;
(2) Water fluid channel;
(3) Stainless steel sheet;
(4) Insulation board;
(5) Waterproofing membrane;

Variant a-Cladding system

(1) Stainless steel sheet;
(2) Water fluid channel;
(3) Stainless steel sheet;
(4) Insulation board;
(5) Plaster;
(6) Concrete block;
(7) Plaster.

Variant b-Prefabricated wall system
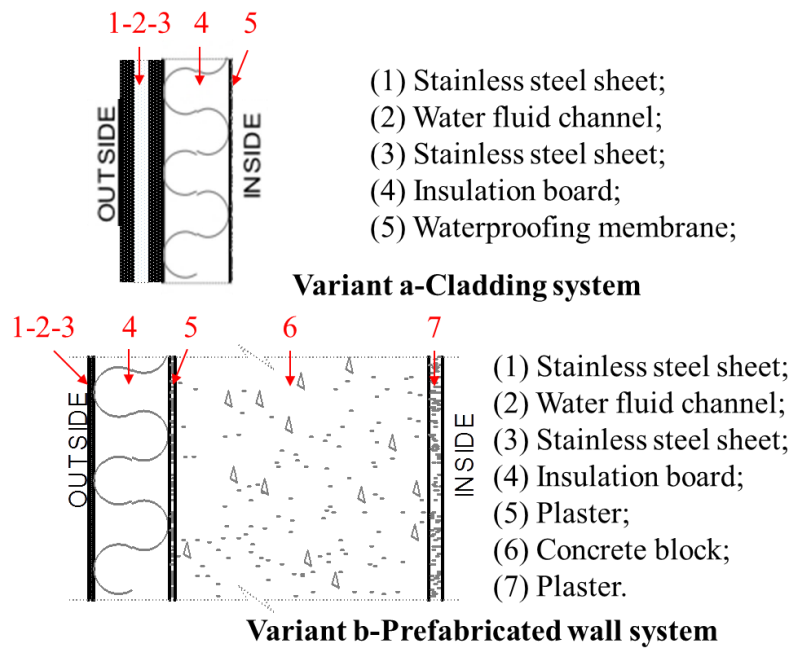
Figure 4-9 Schematic designs of STF for low-rise building typologies

2) Integration design for mid/high-rise building typologies

Figure 4-10 generally illustrates 8 types of the proposed STF integration with different building typologies. **Type (1)** is integrated on the opaque solid wall, while **Type (2)** is applied in an alternating pattern with the curtain walling system. **Type (3)** and **Type (4)** are similar to **Type (1)** integrating around a punched/strip window. **Type (5)** is installed as the balcony component. The proposed STF can also be used as local shading due to its compact structure. In such a case, **Type (6)**, **Type (7)**, and **Type (8)** present examples of self, horizontal, and vertical shading respectively.

Type (1)- Integration of STF within opaque solid wall
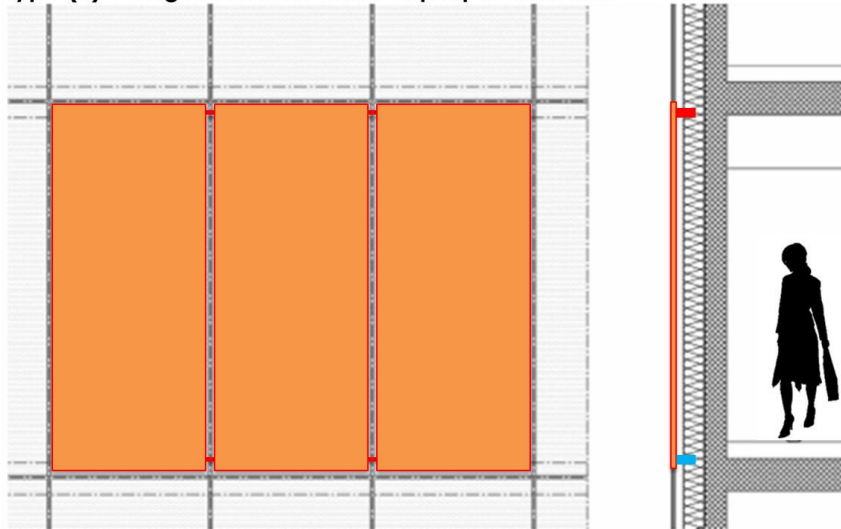
Type (2)- Integration of STF with curtain wall in an alternating pattern
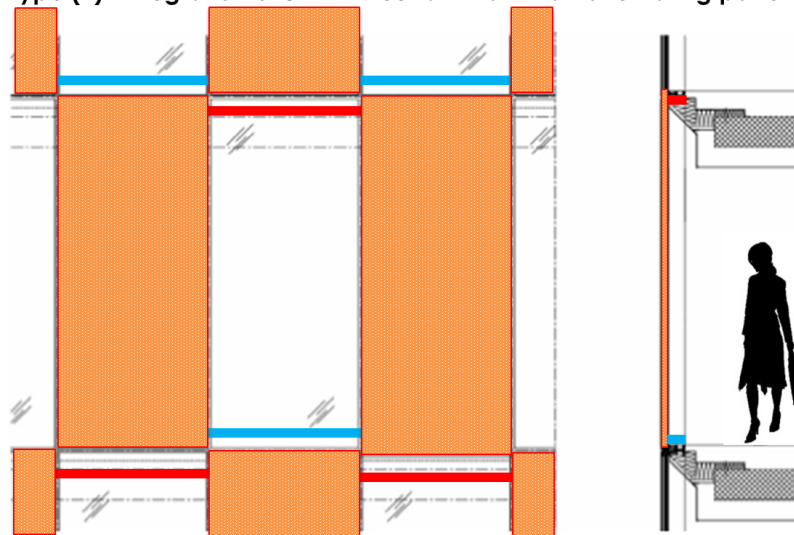
Type (3) – Integration of STF with punched window
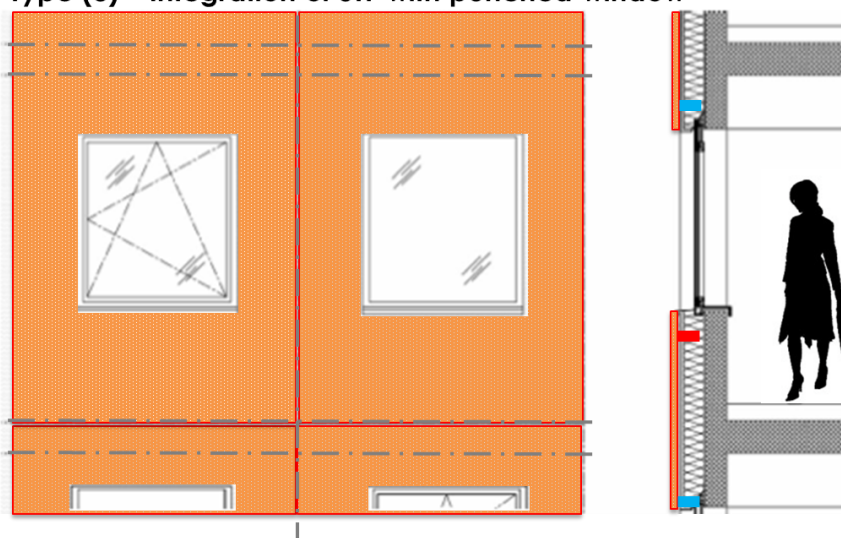
Type (4) – Integration of STF with strip window
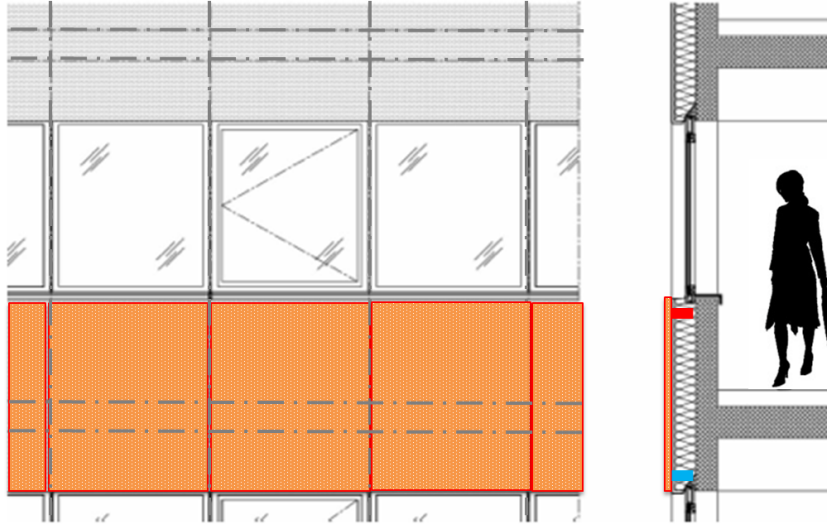
Type (5) - Room height windows with STF balcony
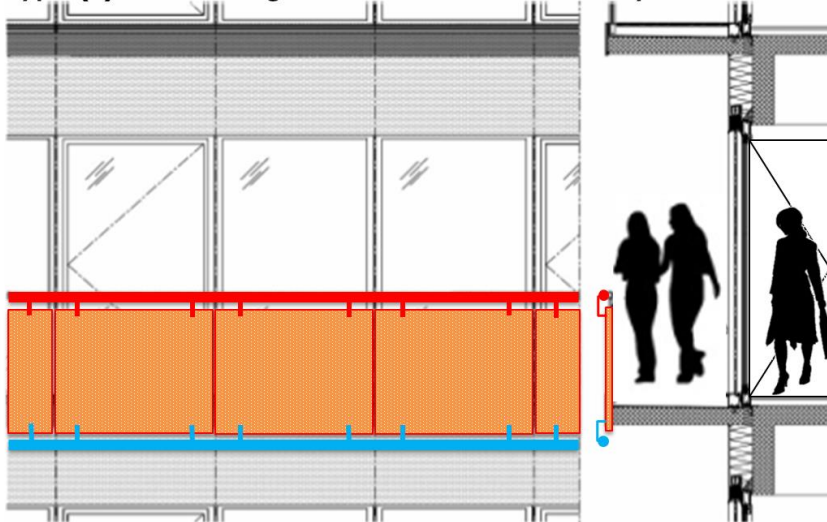
Type (6)- Single skin STF self shading
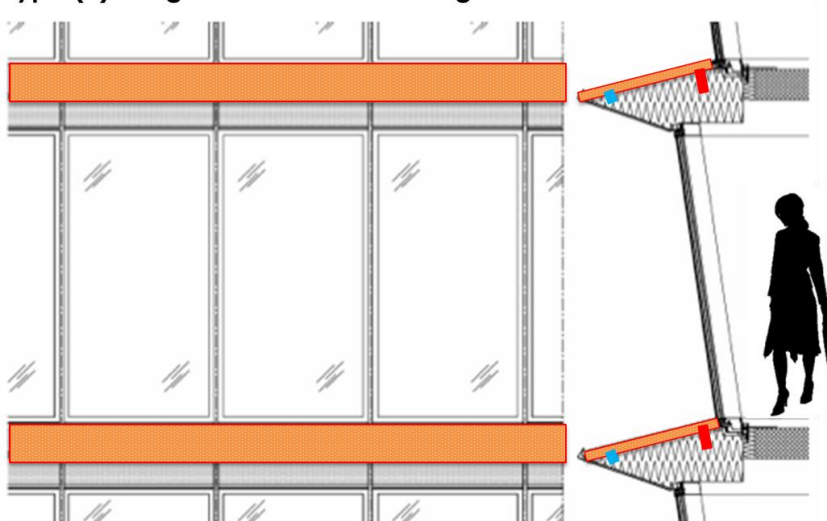
Type (7) - Single skin with horizontal STF shading
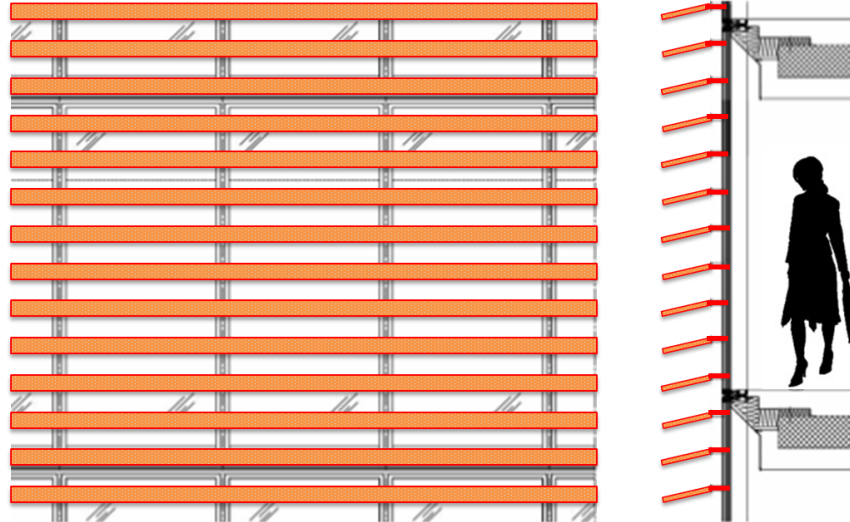
Type (8)- Single skin with vertical STF shading
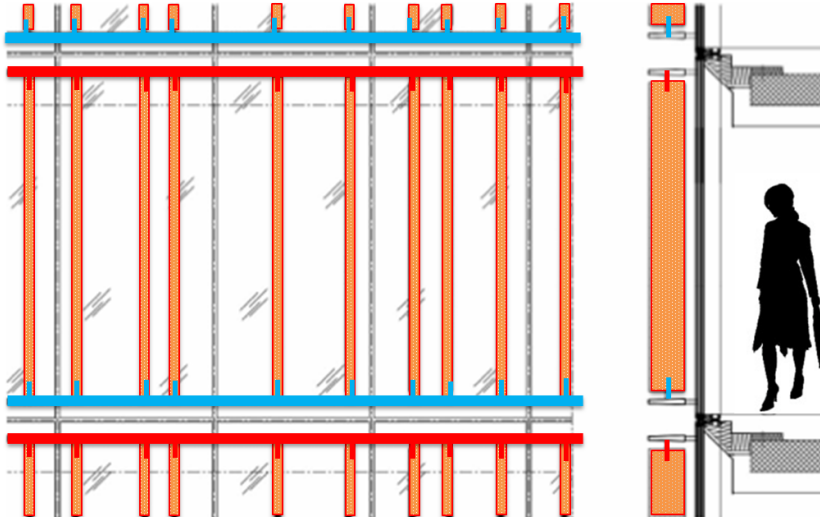
Figure 4-10 Schematic designs of STF for the mid/high-rise building (Drawings revised on pictures from (Emmer Pfenninger Partner AG, 2012))

4.2.8   STF array connection

Owing to the lower outputting temperature of the unglazed STC, a large collection area of STF arrays is necessary for satisfactory solar yield. There are three typically hydraulic array connection methods, as series, parallel, and combined.
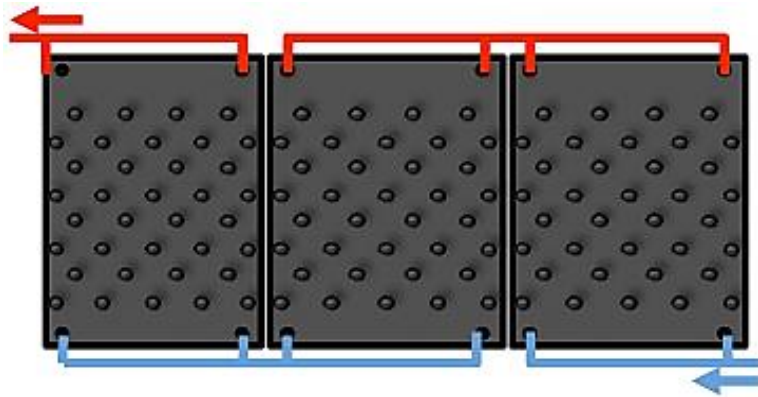
Figure 4-11 Series connection in the STF array (Sonnenenergie, 2010)

In case of the series connection, all the STF modules are connected successively as illustrated in Figure 4-11. The type of connection ensures a uniform flow for a higher solar yield; however it should be in proportion to the number of modules so as to take away all the arising solar heat. Another feature of this type connection is that the flow resistance increases with the number of modules, therefore the number of connected modules are limited by the pumping power (Sonnenenergie, 2010). In contrast, the parallel connection is well designed with merits of inherently balance, lower pressure drop, and easy drainage.

(a) External manifolding type

(b) External manifolding type

(c) Internal manifolding type

(d) Internal manifolding type
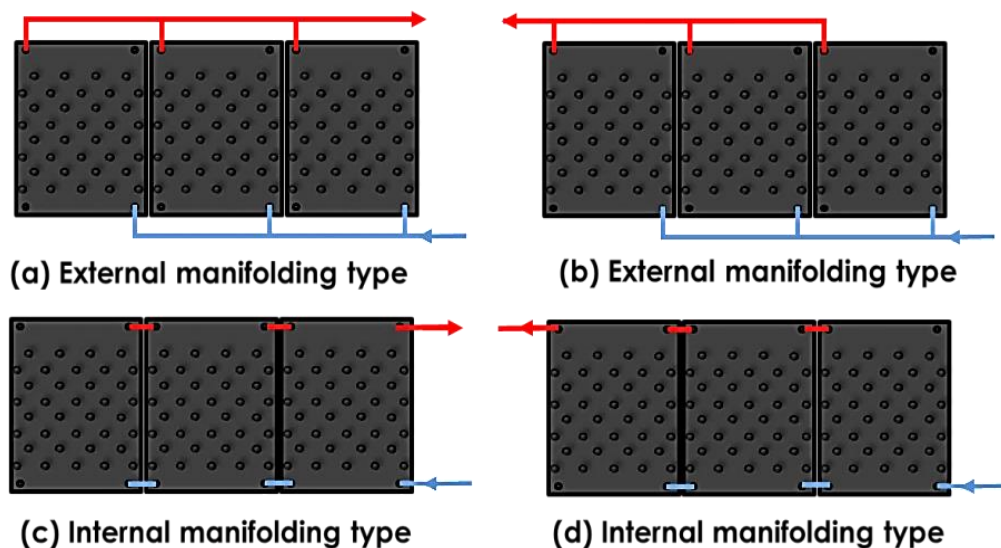
Figure 4-12 Parallel connection in the STF array (Kalogirou, 2009)

Figure 4-12 illustrates four different parallel arrangements, i.e. the external types of (a) and (b), and the internal types of (c) and

(d). The external type is connected individually to the manifold. As a result, each module is independent that provides high flexibility in maintenance. Such parallel connection is frequently used in small projects (Kalogirou, 2009). And the internal type is connected side by side of each module forming a continuous supply and return manifold respectively. Because of the integral manifold piping method, it requires less fittings, insulation and support accessories. Accordingly, it is more accessibility for worksite installation and more economical for a large number of STFs installation. Such connection type also eliminates external manifold that is associated with extra heat loss and exposure damages.

For large-scale STF application, a combination of series and parallel connection should be considered, as illustrated in Figure 4-13, since both array hydraulics and installation quality are equally important (Sonnenenergie, 2010). In order to achieve uniform flow through the module arrays with lower flow resistance (less pumping power), the empirical design recommends either (a) installation of balancing valves in the return manifold or (b) application of long reversed return manifold.

(a) Direct return array piping   (b) Reverse-return array piping
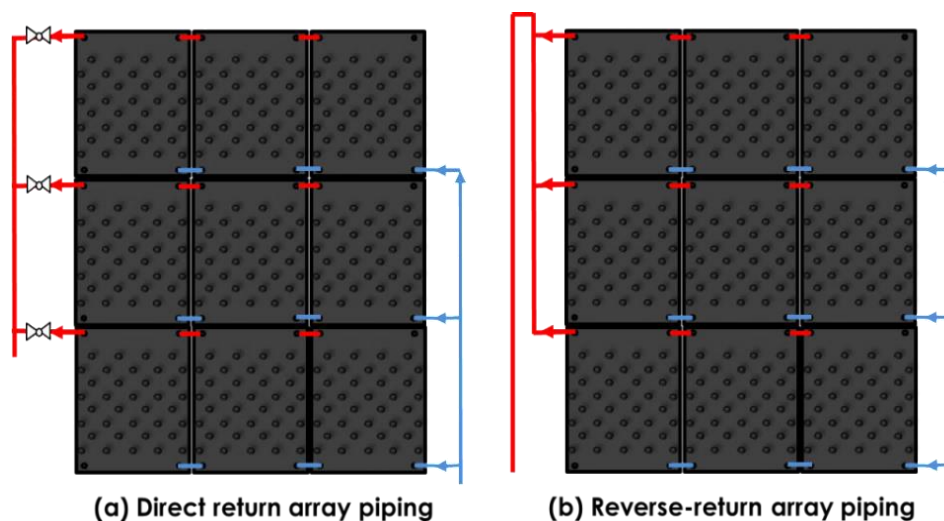
Figure 4-13 Combined connection in the STF multi-array system (Sonnenenergie, 2010)

4.2.9   Decentralized connection design

In the case of a multifamily household or mid/high-rise applica-
tion, it is suggested to install the proposed STF system close to the
end user as the decentralized connection rather than the cen-
tralized connection. As a result, the system loop does not need to
run though the entire building that would save considerable pip-
ing and reduce large amount of flow resistance/heat loss than
that in the conventional centralized system.

1. Vertical metal profile
2. Proposed STF panels
3. Horizontal metal profile
4. Heat insulation layer
5. Brick wall
6. Tee joint valve
7. Heat exchanger (buffer tank)
8. Auxiliary heater (heat pump)
9. Floor heating
10. Domestic hot water supply
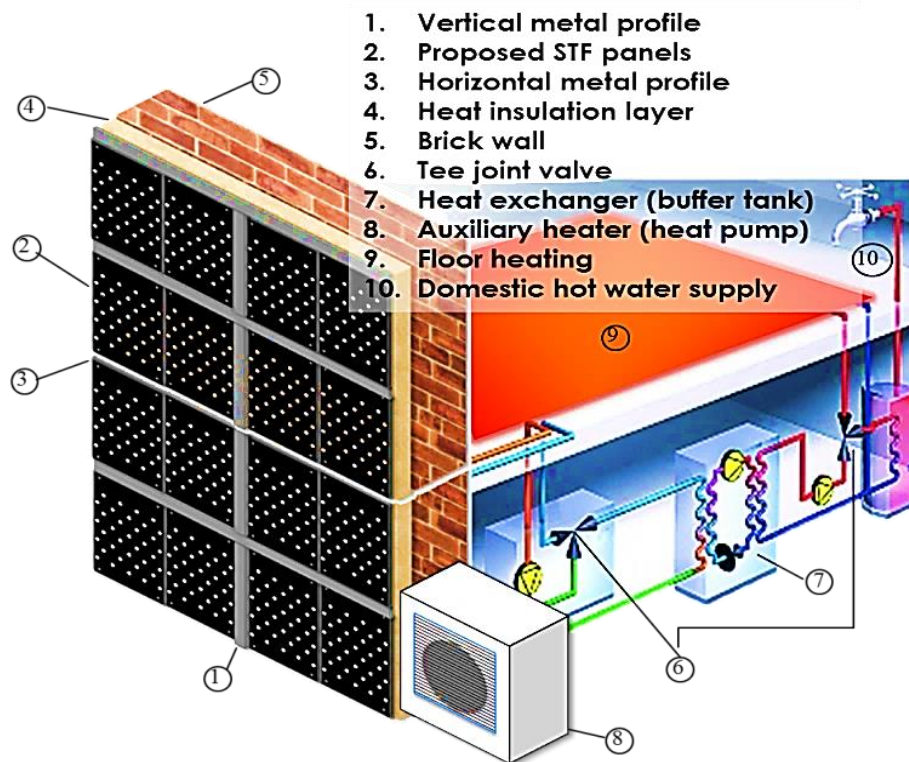
**Figure 4-14 Conceptual design of the facade application with the proposed
STF**

Figure 4-14 presents a typical concept design of the STF system
application in a multifamily household for the purposes of hot
water and space heating delivery. The STF modules are con-
nected in the decentralized arrangement for each household
unit, which allows the low-and-medium-temperature solar gain to
be effectively delivered into the end user and so maximally re-
duces the sensitive transportation losses.

4.2.10 Hypothetical system design for hot water generation

Figure 4-15 illustrates different types of STF modules for hot water generation. All these types are featured of the internal solar heat exchanger arranged at the bottom position inside the water tank.
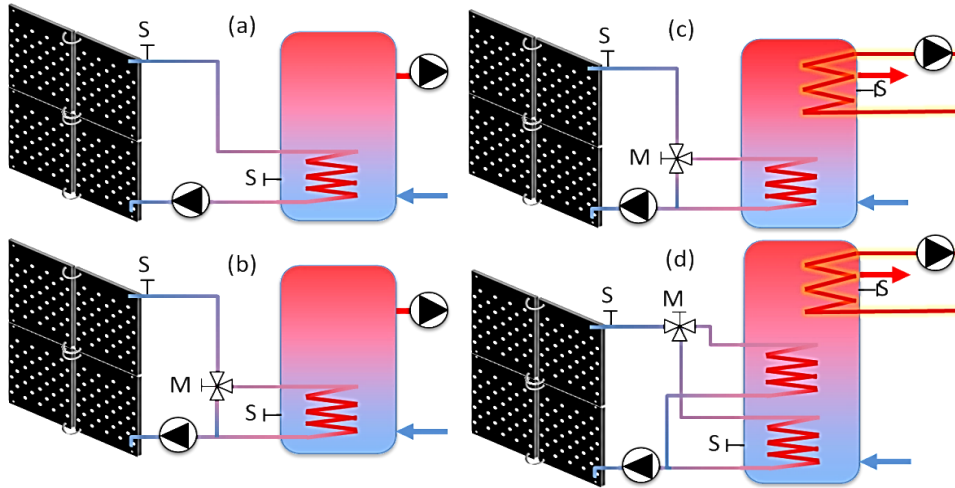
Figure 4-15 Possible variants of the compact STF system connections

Type (a) is the most cost-effective design with least components and lowest system pressure loss, which is usually applied in areas with abundant annual solar radiance resource, or in a dual-mode operation for preheating purposes.

Type (b) improves the overall system performance by a bypass circuit design that helps to prevent the reversible heat transfer form water tank to the unglazed STF modules.

In **Type (c)**, an auxiliary heating circuit is supplemented in condition of insufficient solar radiation.

Similarly, **Type (d)** has two internal heat exchangers and feeds water tank with a tee joint at two different heights. It has advantage in rapid reaching of useful temperatures in the standby area with increased system efficiency.

For auxiliary heating devices, for instance the conventional gas/electric boiler and heat pump, can achieve relatively high

overall efficiency, while the electric heater is good in small heat storage loss, quick heating response and compatible system occupancy volume. Therefore, the appropriate choice of auxiliary heater depends on specific scenarios.

4.2.11 Solar coverage

Solar coverage is an essential variable required for designing a solar thermal system, which states the ratio of the energy supplied by the solar thermal system to the overall energy load. Solar coverage takes into account of the heat losses from system components like water tank, pipe, valve, heat exchanger etc. The higher the solar coverage results in greater the savings in conventional energy, shown in Figure 4-16.
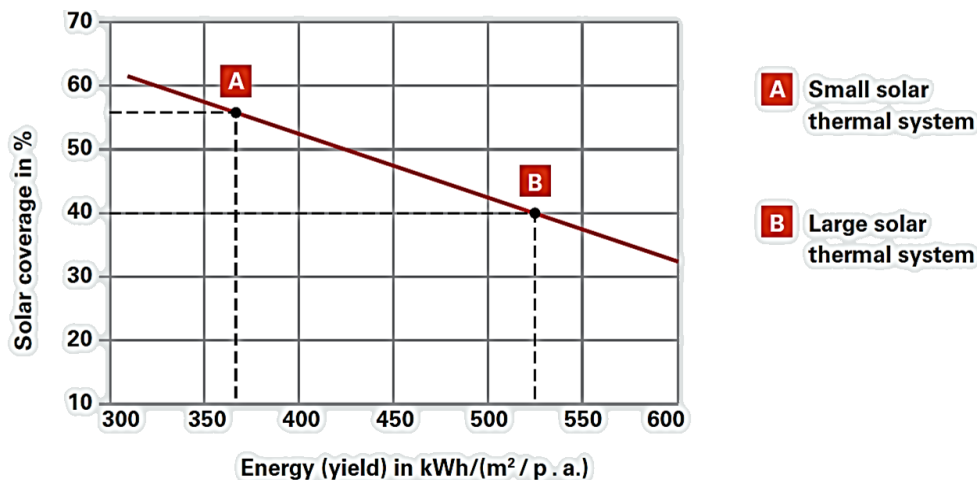
Figure 4-16 Solar coverage for hot water generation (Werke, 2015)

But when STFs are further applied for large-scale projects, the thermal efficiency may drop depending on the scalability due to the unavoidable rising temperature differential between STF and ambient temperature during the system circulation. As a result, the higher the solar coverage (scalability) means the lower specific yield (efficiency). So a good compromise between solar coverage (scalability) and solar yield (efficiency) must be found for each system during the facade integration design.

It is customary to design for a solar coverage of 50 to 60 percentages for water heating in detached houses due to more occupancy with higher DHW demands, meanwhile 30 to 40 percentages in apartment buildings on accounts of less exposed building facade area and lower DHW demands (Werke, 2015).

4.3 Chapter executive summary

This chapter described the novel unglazed STF modular concept for facilitating domestic hot water production and its working principle. The proposed STF concept is expected to engender simple structure, economical cost, aesthetically appealing, and easy installation (plug & play) with a relatively greater thermal efficiency in relative to the conventional unglazed solar collector. Moreover, more considerations have been taken in terms of:

1) Building installation of STF using different jointing methods;
2) Material choice of panel in STFs;
3) Colour and texture choice of STF's surface;
4) Optional shape and size of STF module;
5) Architectural design of STF module towards building integration, in terms of design variants and integrated building design types;
6) Inclination, orientation and insolation of STF's placement;
7) Array connection methods of whole STF system;
8) Comparison between the centralized connection and the decentralized connection of whole STF system design;
9) Recommended solar coverage for whole STF system performance optimization.

The concept design hereby illustrates the precedence for the hypothetical function by the creation of new idea and also forms up the physical object for investigations in the following chapters.

THEORETICAL ANALYSIS AND
SIMULATION MODEL DEVELOPMENT

5

5.1 Chapter abstract

Based on the established concept design, this chapter discusses the theoretical analysis, the development of computer model and the parametric analysis for STF design optimization. The main works achieved in this chapter are:

1) State the modelling objectives for STF performance;

2) Outline the assumptions in the mathematical analysis;

3) List all the relevant technical expressions;

4) Summarize the analysis method and algorithm for the steady-state model development and operation;

5) Conduct design parametric analysis for the STF optimization.

This part of the work facilitates the foundation of the prototype fabrication and experimental testing, as well as the socio-economic assessment, which will be addressed in Chapter 6 and Chapter 7.

5.2 Thermal analysis and simulation model

5.2.1   Modelling objectives

The purpose of developing a mathematical model is to characterise the operation performance of the novel compact STF module. It would enable：

1) Determination of STF performance against design variables;

2) Recommendation for the optimum operational parameters.

All the analytical results will be useful for further system prototype fabrication, experimental testing, and socio-economic assessment.

5.2.2   Thermal fluid theory and the associated mathematical equations of the steady-state model

According to thermal performance investigations associated with the similar fin-theory approach, both Stojanovic et al. and Colombo et al. preferred the simplified one-dimensional model of the unglazed solar collector flat panel as a valuable tool due to good agreements with other complicated models for fast and reliable collector simulation at the steady-state condition (Stojanović, 2010; Colombo et al., 2014). Therefore the one-dimensional matrix was considered here.

In the steady state, the performance of the STF module can be described as an energy balance in [5-1] that indicates the useful solar heat gain Q_u equals to the difference between the absorbed solar energy and the thermal losses. The thermal losses from the STF to the surroundings are convention and infrared radiation that can be represented as the value of a heat transfer coefficient (U_L) times the difference between the mean absorber plate temperature (T_p) and the ambient temperature (T_a).

$$Q_u = A_P[I\alpha_P - U_L(T_p - T_a)] \qquad\qquad\qquad [5\text{-}1]$$
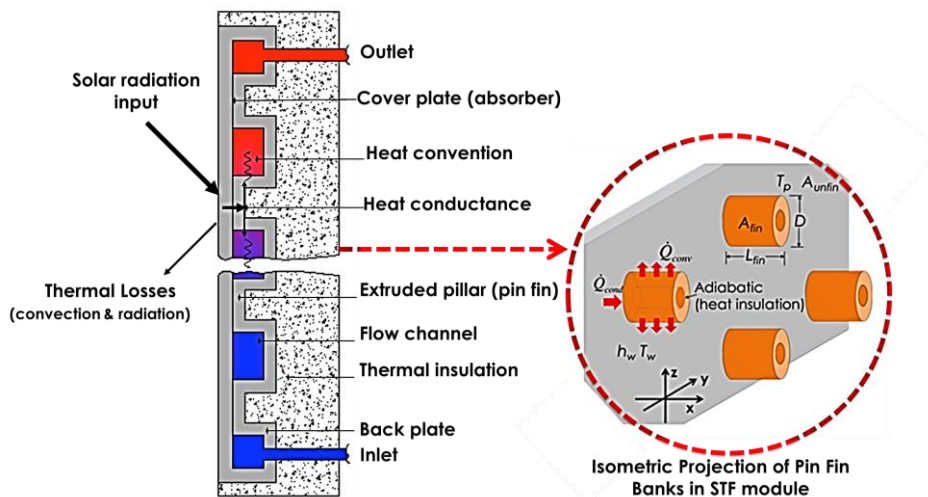
Figure 5-1 Schematic of solar heat transfer of the compact STF module

In the proposed STF module, the solar energy conversion and transfer involves two processes as revealed in Figure 5-1:

1) Absorbing most solar radiation while the remaining being dissipated into the surroundings in the form of heat;

2) Converting the absorbed energy into heat and transferring it to the passing working fluid via the circular cooling fins.
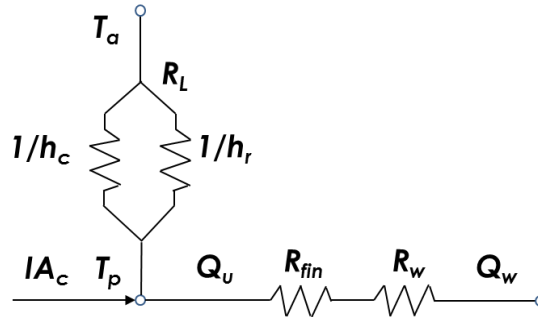
Figure 5-2 Thermal network for the compact STF module

The associated thermal network is given in Figure 5-2. These processes are inter-linked and finally can achieve a balance under the steady state operation. A number of simplifying assumptions are made to lay the foundations without obscuring the basic physical situation. These assumptions are as follows:

1) The system operates under quasi-steady state condition;

2) There is one-directional heat flow through the fin base to the fin tip and the temperature gradients along other directions (well insulated) can be negligible;

3) Heat losses from the fin tip are negligible (adiabatic fin tip);

4) Heat losses across the module insulation layers (back and edge) are negligible;

5) The temperature gradient across cover thickness is ignored;

6) Heat transfer coefficient is constant and uniform over the entire fin surface.

1) Heat loss to the surroundings

The energy loss through the top is the combined result of convection and radiation. The overall heat loss coefficient U_L is the joint efforts of convection and radiation, which is expressed as:

$$U_L = h_c + h_r \qquad\qquad\qquad [5\text{-}2]$$

For a surface exposed to the outside wind, the convective coefficient, h_c in Equation [5-2] from the absorber plate to the ambient air could be calculated using the Klein equation, addressed below

$$h_c = max[5, \frac{8.6V_a^{0.6}}{L_p}] \qquad\qquad [5\text{-}3]$$

,where, V_a is the wind speed (m/s); L_p is the characteristic length of the absorber (m). The minimum convective coefficient for a wind-exposed surface is considered to be 5 W/m²-k; if the above calculation gives a lower value, this should be replaced by the minimum value of 5 (Duffie & Beckman, 2006; Kalogirou, 2009).

The heat transfer process from the plate also accounts for radiation exchange with the sky. The radiative heat transfer coefficient, h_r between two grey, diffuse surfaces in Equation [5-2] can be written as (Bergman, T.L. et al., 2011; Kalogirou, 2009):

$$h_r = \varepsilon_p\sigma(T_p + T_s)(T_p^2 + T_s^2) \qquad\qquad [5\text{-}4]$$

,where, ε_p is the infrared emissivity of the absorber plate, being 0.10 for the polished stainless steel plate; σ is the Stefan-Boltzmann constant, being 5.67×10⁻⁸ W/m²-K⁴. And the sky temperature, T_s in Equation [5-4] could be expressed as (Kalogirou, 2009):

$$T_s = 0.055T_a^{1.5} \qquad\qquad [5\text{-}5]$$

2) Heat transfer from the finned surfaces

The heat transfer process of the absorber case involves the primary heat transfer by the conduction from the absorber plate surface to the cylindrical pin fins, which are featured with adiabatic end, length of L_{fin} and diameter of D, and the perpendicular heat transfer by the convention from the cylindrical pin fins at temperature T_p to the surrounding working fluid with the uniform heat transfer coefficient h_w at a mean temperature T_w. Therefore the heat transfer process here can

be depicted as the heat transfer from an extended surface, as indicated in Figure 5-1.

A common approximation used in the analysis of such a kind of fin is to assume the fin temperature to only vary in one direction along the fin height. Because the cross-sectional area of such a fin is small, the temperature variation at any cross section can be considered negligible (Cengel & Ghajar, 2014). Accordingly, under the steady condition, the useful heat gain, Q_u transferred from the absorber plate is equal to the heat transfers, $Q_{fin,total}$ to the finned areas, Q_{fin} and the remaining surface, Q_{unfin}, written as:

$$Q_u = Q_{fin,total} = Q_{unfin} + Q_{fin} = h_w(A_{unfin} + F_{fin}A_{fin})(T_p - T_w) \qquad [5\text{-}6]$$

The pin tip fin efficiency. F_{fin} in Equation [5-6] is used to account for the effect of temperature decrease between the actual heat transfer and the ideal heat transfer from a fin (if the entire pin fin was at the same temperature). Taking reference from (Cengel & Ghajar, 2014), it can be expressed as:

$$F_{fin} = \frac{Q_{fin}}{Q_{fin,max}} = \frac{tanh(mL_{fin})}{mL_{fin}} \qquad [5\text{-}7]$$

In Equation [5-7], the fin variable, m of a pin fin with rectangular profile can expressed as (Cengel & Ghajar, 2014):

$$m = \sqrt{\frac{4h_w}{k_{fin}D}} \qquad [5\text{-}8]$$

The mean working fluid temperature, T_w in Equation [5-6] is difficult to calculate or measure, therefore simply given as:

$T_w = (T_{in} - T_o)/2$ $\qquad\qquad$ [5-9]

$A_{fin} = n\pi D L_{fin}$ $\qquad\qquad$ [5-10]

$A_{unfin} = A_p - A_{fin} = A_p - n\,\pi D^2/4$ $\qquad\qquad$ [5-11]

,where A_{fin} is the total surface area of all the pin fins on the absorber, A_{unfin} is the area of the un-finned portion of the absorber (Bergman *et al.*, 2011; Cengel & Ghajar, 2014).

As known, the pin fins are used to increase the heat transfer from a bare surface, yet with a conduction resistance addition to heat transfer from the original surface. For this reason, the fin effectiveness, ε_{fin} is used for the assessment of the overall enhancement in heat transfer relative to the no-fin case. If $\varepsilon_{fin} = 1$, it indicates that the addition of pin fins to the bare absorber plate does not affect heat transfer at all; If $\varepsilon_{fin} < 1$, it indicates that the application of fins actually acts as insulation, slowing down the heat transfer from the original plate; If $\varepsilon_{fin} > 1$, it indicates that the use of fins are enhancing heat transfer from the original plate. And it is expressed as (Cengel & Ghajar, 2014):

$$\varepsilon_{fin} = \frac{Q_{fin}}{Q_{nofin}} = \frac{Q_{fin}}{h_{w,nofin}A_p(T_p - T_{wm})} = \frac{h_w(A_{unfin} + F_{fin}A_{fin})}{h_{w,nofin}A_p} \qquad [5\text{-}12]$$

$$h_{w,nofin} = \frac{k_w Nu_{w,nofin}}{D_h} \qquad [5\text{-}13]$$

Both h_w and $h_{w,nofin}$ in Equation [5-12] stand for the heat transfer coefficient of the fined surface and of the surface without fin respectively. For a rectangular flow channel without pin fins, the hydraulic diameter, D_h, in Equation [5-13] is defined by its height, L and width, W, as:

$$D_h = 2\frac{L \times W}{L + W} \qquad [5\text{-}14]$$

When assuming the turbulent flow is fully developed in the channel without pin fins, the *Nusselt* number can be determined by Dittus-Boelter equation, as below: (Cengel & Ghajar, 2014):

$$Nu_{w.nofin} = 0.023 Re_{w,nofin}{}^{0.8} Pr_{w,nofin}{}^{0.3} \qquad [5\text{-}15]$$

The *Prandtl* number is written as:

$$Pr_{w,nofin} = \frac{\nu}{\alpha} = \frac{\mu c_p}{k} \qquad [5\text{-}16]$$

,where υ stands for kinetic viscosity of the working fluid (m²/s), a is thermal diffusivity expressed as thermal conductivity divided by density and specific heat capacity at constant pressure (J/kg-K), and μ is the dynamic viscosity of the working fluid (N·s/m²). And the Reynolds number for the channel without pin fins is in Equation [5-15]:

$$Re_{w,nofin} = \frac{V_w D_h}{\nu} \qquad [5\text{-}17]$$

3) Heat convection across the pin-fin bank

As the pin-fin arrays affect the flow pattern and the turbulence level downstream, then affects the heat transfer coefficient h_w accordingly. The working fluid across the pin fins is then regarded as the cross-flow over the staggered pin-fin banks. And the heat transfer analysis here can treat all the pin-fins in the bundle at once. The arrangement of the pin-fin bank is characterized by the transverse pitch S_T, longitudinal pitch S_L, and the diagonal pitch S_D between pin-fin centres. The outer fin diameter D is taken as the characteristic length for the cross-flow. And the diagonal pitch is deterred from (Cengel & Ghajar, 2014):

$$S_D = \sqrt{S_L{}^2 + (S_T/2)^2} \qquad [5\text{-}18]$$

When the fluid enters the pin-fin bank, the flow area decreases from A_{in} to A_T between the fins. Consequently, the fluid velocity increases, and the velocity in the diagonal region would be increased further in the staggered pin-fin bank. In the pin-fin bank, the flow characteristics are dominated by the maximum velocity $V_{w,max}$ that occurs within this area. Subsequently, the Reynolds number is defined by $V_{w,max}$ in Equation [5-18] as (Cengel & Ghajar, 2014):

$$Re_w = \frac{V_{w,max} D}{\nu} \qquad [5\text{-}19]$$

The maximum velocity of the working fluid, $V_{w,max}$ is determined from the conservation of mass requirement for steady incompressible flow. According to the staggered arrangement showed in Figure 5-3, the

fluid approaches to area A_{in} firstly, then passes through A_T and goes into two A_D areas when it wraps around the pin fine in the next row. Therefore the maximum velocity is expressed as (Cengel & Ghajar, 2014):

$$If\ 2A_D > A_T, V_{w,max} = S_T V_w/(S_T - D) \qquad [5\text{-}20]$$

$$If\ 2A_D \leq A_T, V_{w,max} = S_T V_w/2(S_D - D) \qquad [5\text{-}21]$$
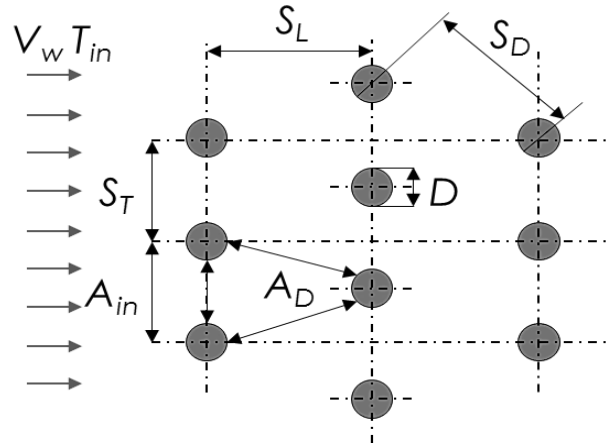
Figure 5-3 Cross section arrangement of the staggered pin-fin banks

The maximum velocity in Equation [5-20] occurs at A_T between two fin pins, while the one in Equation [5-21] occurs at the diagonal cross section of A_D. Meanwhile, the flow areas indicated in Figure 5-3 are given by (Cengel & Ghajar, 2014):

$$A_{in} = S_T L_{fin} \qquad [5\text{-}22]$$

$$A_T = (S_T - D)L_{fin} \qquad [5\text{-}23]$$

$$A_D = (S_D - D)L_{fin} \qquad [5\text{-}24]$$

Because the heat transfer analysis in the pin-fin bank is too complex, it is used experimentally based correlations for the *Nusselt* number. The average heat transfer coefficient for the entire pin-fin bank depends on the number of fin rows along the flow as well as the arrangement and the size of pin-fins. Cengel et al. has proposed a correlation for flow over the entire pin-fin bank when number of rows in flow direction is larger than 16, and 0.7<Pr_w<500 (Cengel & Ghajar, 2014):

If $0 \leq Re_w \leq 500$,

$$Nu_w = 1.04 Re_w{}^{0.4} Pr_w{}^{0.36} (\frac{Pr_w}{Pr_{fin}})^{0.25}$$ [5-25]

If $500 \leq Re_w \leq 1000$,

$$Nu_w = 0.71 Re_w{}^{0.5} Pr_w{}^{0.36} (\frac{Pr_w}{Pr_{fin}})^{0.25}$$ [5-26]

If $1000 \leq Re_w \leq 2 \times 10^5$,

$$Nu_w = 0.35(\frac{S_T}{S_L})^{0.2} Re_w{}^{0.6} Pr_w{}^{0.36} (\frac{Pr_w}{Pr_{fin}})^{0.25}$$ [5-27]

If $2 \times 10^5 \leq Re_w \leq 2 \times 10^6$,

$$Nu_w = 0.031(\frac{S_T}{S_L})^{0.2} Re_w{}^{0.8} Pr_w{}^{0.36} (\frac{Pr_w}{Pr_{fin}})^{0.25}$$ [5-28]

It should be addressed that all properties except Pr_{fin} need to be evaluated at the arithmetic mean temperature of the working fluid T_w. If the total row number of the pin-fin banks is less than 16 rows, it is corrected by a correction factor F whose values are given in Table 5-1 (Cengel & Ghajar, 2014):

$$Nu_w{}' = F \times Nu_w$$ [5-29]

Table 5-1 Correction factor F for the pin-fin banks less than 16 rows and Re_D greater than 1000

Pin-fin rows n_r	1	2	3	4	5	7	10	13	16
Correction F	0.64	0.76	0.84	0.89	0.93	0.96	0.98	0.99	1

As a result, the overall heat transfer coefficient of working fluid is:

$$h_w = k_w Nu_w / D$$ [5-30]

Under the steady condition, the heat gained by working fluid should be also equal to the useful heat gain, expressed as:

$$Q_W = Q_U = m_w C_p (T_o - T_{in})$$ [5-31]

Therefore the mass flow rate of working fluid, m_w in the staggered pin-fin banks becomes (Cengel & Ghajar, 2014):

$$m_w = \rho_w V_w (n_r S_T L_{fin})$$ [5-32]

,where ρ_w stands for the density of working fluid; n_r stands for number of rows in the staggered pin-fin banks of the STF module. And accordingly, the irreversible pressure loss between the inlet and the outlet is defined as (Cengel & Ghajar, 2014):

$$\Delta P = n_r f \chi \frac{\rho_w V_{w,max}^{\;2}}{2} \qquad\qquad [5\text{-}33]$$

,where f is the friction factor and *χ* is the correction factor, which can be determined using below Figure 5-4.
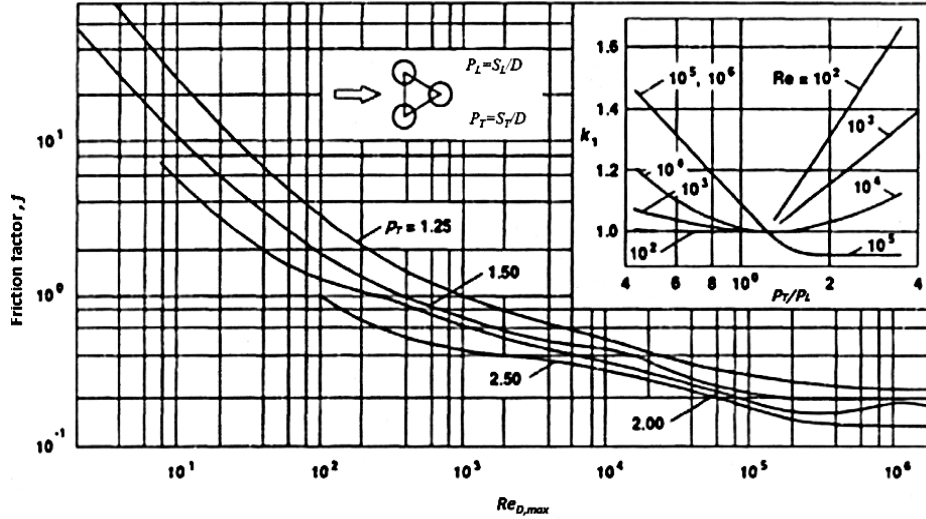
Figure 5-4 The friction factor and the correction factor against the Reynolds number
(Cengel & Ghajar, 2014)

In general, the equations presented in this section are integrated mainly for the calculation of overall heat transfer coefficient of the working fluid inside of the STF structure (Equations from [5-18] to [5-30]) as well as the corresponding useful heat gain by working fluid (Equations from [5-31] to [5-32]) and the irreversible pressure loss between inlet and outlet (Equation [5-33]).

5.2.3   STF efficiency factor, heat removal factor, flow factor and thermal efficiency

The STF efficiency factor, *F'* represents the ratio of the actual useful energy gain to the absorbed heat gain at the local working fluid temperature, so that the interpretation of *F'* is:

$$F' = \frac{Q_u}{Q_{abs}} = \frac{I\alpha_P - U_L \times (T_p - T_a)}{I\alpha_P - U_O \times (T_w - T_a)} \qquad\qquad [5\text{-}34]$$

It should be noted that the U_O at the denominator of Equation [5-34] is the heat transfer resistance from the working fluid to the ambient air. The STF's efficiency factor is essentially a constant factor under the

fixed physical and operating condition. However, this factor's value may: 1) decrease with the increasing fin numbers; 2) increase with increasing STF thermal conductivity; 3) decrease with increasing the overall heat loss coefficient, and 4) increase with decreasing the overall STF heat transfer resistance.

Heat removal factor, F_R represents the ratio of the actual useful energy gain to the absorbed energy gain at a certain working fluid inlet temperature. This is equivalent to the effectiveness of a conventional heat exchanger, expressed as (Duffie & Beckman, 2006; Kalogirou, 2009)

$$F_R = \frac{m_w c_p}{A_p U_L} [1 - exp\left(-\frac{A_p U_L F'}{m_w c_p}\right)]$$

[5-35]

The STF flow factor, F'' is defined as the ratio of F_R to F'. As shown in Equation [5-35]. It is a function of only a single variable factor, the dimensionless collector capacitance rate of $\frac{m_w C_p}{A_p U_L F'}$ (Kalogirou, 2009).

$$F'' = \frac{F_R}{F'} = \frac{m_w c_p}{A_p U_L F'} [1 - exp\left(-\frac{A_p U_L F'}{m_w c_p}\right)]$$

[5-36]

Hereby, the useful heat gain can be rewritten by F_R and the inlet working fluid temperature, T_{in} (Kalogirou, 2009)

$$Q_u = A_p F_R [I\alpha_P - U_L(T_{in} - T_a)]$$

[5-37]

And the STF thermal efficiency, η_{th} is then

$$\eta_{th} = \frac{Q_u}{IA_p} = F_R[\alpha_P - U_L(T_{in} - T_a)]/I$$

[5-38]

And the mean absorber temperature of STF thermal is then

$$T_p = T_{in} + \frac{Q_u}{F_R U_L A_p}\left(1 - F_R\right)$$

[5-39]

5.3 Algorithm for steady-state model development and operation

The heat transfer processes in the STF module will eventually achieve through the energy balance at the steady state condition and each part of the STF will establish a certain temperature in operation. The algorithm used for modelling is shown schematically in Figure 5-5 and illustrates as follow:
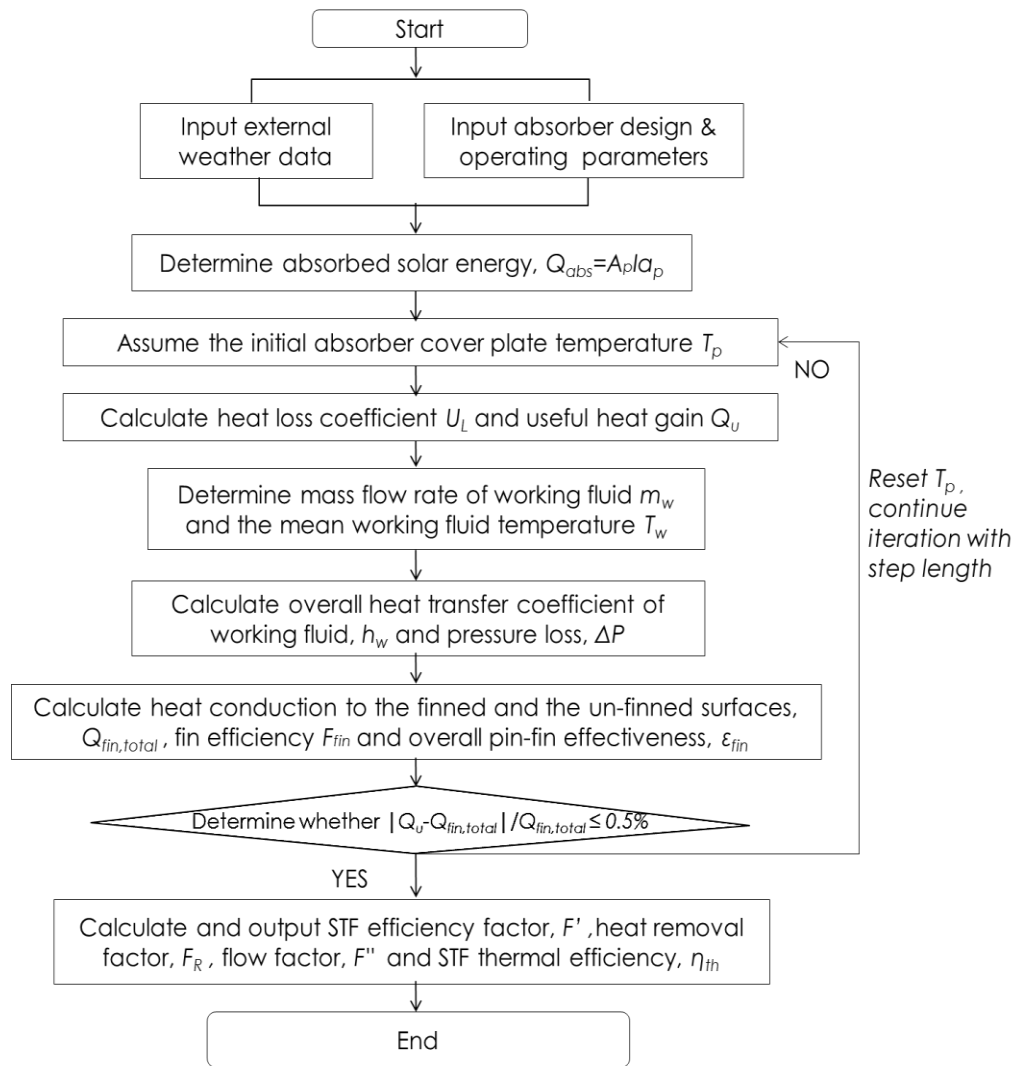
Figure 5-5 Flow chart for the computation process of the steady-state STF module performance

1)   Inputting the external weather conditions, STF module design and operating parameters;

2)   Assuming the absorber plate temperature, T_p, and taking into below heat transfer analyses:

 (1) Heat balance of the absorber plate could be analysed using

equations from [5-1] to [5-5], which results in determination of the heat loss coefficient, U_L and the useful heat gain, Q_U;

(2) Heat balance of the working fluid heat gain could be analysed using Equation [5-31] and Equation [5-32], which results in determination of the mass flow rate of working fluid in the STF, m_w and the mean working fluid temperature, T_w;

(3) Heat convection process across the staggered pin-fin banks could be analysed using Equations [5-18] to [5-30] and Equation [5-33], which results in determination of the overall heat transfer coefficient of working fluid, h_w and pressure loss, ΔP;

(4) Heat conductance process though the surface containing cylindrical pin-fin banks could be analysed using Equations [5-6] to [5-17], which results in determination of the total heat conduction (to both the finned pin and the un-finned surfaces), $Q_{fin,total}$, the fin efficiency, F_{fin} and the overall pin-fin effectiveness, ε_{fin};

(5) If $(Q_{fin,total}-Q_U)/Q_{fin,total} > 0.5\%$ (error allowance), then increasing T_p by 0.1K and return to step (ii) for re-calculation;

(6) If $(Q_{fin,total}-Q_U)/Q_{fin,total} < -0.5\%$ (error allowance), then decreasing T_p by 0.1K and return to step (ii) for re-calculation;

(7) If $-0.5\% \leq (Q_{fin,total}-Q_U)/Q_{fin,total} \leq 0.5\%$, the STF is considered to achieve the heat balance;

3) Calculating STF efficiency factor, F', heat removal factor, F_R, STF flow factor, F'' and STF thermal efficiency, η_{th} using Equations [5-34] to [5-38];

4) Finally determine the absorber plate temperature, T_p using Equation [5-39], and stop the program with results outputs.

5) Results output and program stops.

5.4 Validation of the simulation model by the published data

The steady-state STF model is validated for its suitability and accuracy by comparing modelling results with the published experimental data. Because there is a similarity between the fin-and-flat plate of the solar air heater (as displayed in Figure 5-6) and the built-in finned channel structure in the proposed STF module. The published experimental re-

sults of the solar air heater are utilized in the validation of the developed analytical computer simulation model in previous section.

1: Air inlet; 2: Air outlet; 3: Insulation layer; 4: Absorber plate; 5: Glazaing cover; 6: Fins
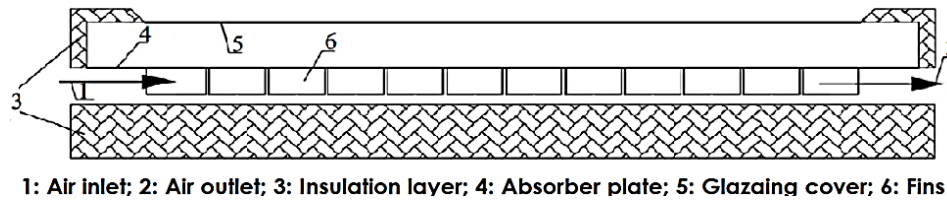
Figure 5-6 Schematic structure of the reference solar air heater (Chang et al., 2015)

The low-temperature air, delivered from left inlet by a mechanical blower, abstracts heat through the top absorber plate and the fins directly, which finally exists from the right outlet at relatively high temperature (Chang et al., 2015). Figure 5-7 schematically shows the testing design and its onsite rig with dimensional details as follows:

1: Temperature sensors; 2: Bracket; 3: The fin-flat plate collector;

4: Total irradiance meter; 5: Hot wire anemometer; 6: Air blower
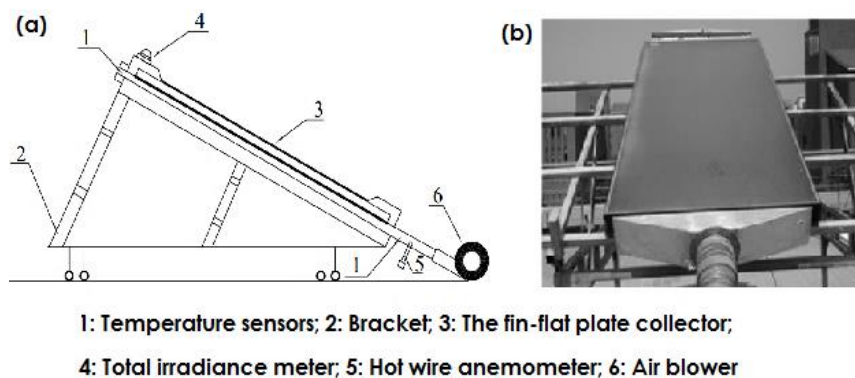
Figure 5-7 Schematic testing design and onsite testing rig of the referenced solar air heater (Chang et al., 2015)

1) The total useful collecting area is 1.90m² with the framework of 2000 mm×1000 mm×120 mm;

2) The thermal insulation layer is made of polyurethane at 50mm thickness;

3) Glass cover is tempered glass with about 95% of absorption rate and 5% of emission rate;

4) The experimental conditions were maintained in a (quasi) steady-state;

5) The irradiance was at 800 ± 50 W/m²;

6) The mass flow of air was in the range of 0.01kg/s-0.09kg/s;

7) The float of inlet temperature is within 1°C.

By inputting these parameters and the related air thermal attributes

into the developed analytical computer simulation model, the dedi-cated comparison between the simulation results and the published experimental data can be carried out to verify the model's accuracy.

It need to be stated that the typical thermal resistances of the glazing cover and air layers in a solar thermal collector was particularly add-ed into the simulation model in order to keep consistent with the phys-ical structure of the referenced solar air heater (Kalogirou, 2009). The performance indicator of thermal efficiency is defined congruously according to the mathematical descriptions in previous section. The correlation coefficient (*CR*) and the root mean square percentage deviation (*ER*) defined from Equation [5-40] to Equation [5-42] were applied to analyse the difference between the theoretical and the published experimental results

$$CR = \frac{N \times \sum(X_{exp}X_{sim}) - \left(\sum X_{exp}\right) \times \left(\sum X_{sim}\right)}{\sqrt{N \sum(X_{exp}{}^2) - \left(\sum X_{exp}\right)^2} \sqrt{N \sum(X_{sim}{}^2) - \left(\sum X_{sim}\right)^2}} \qquad [5\text{-}40]$$

$$ER = \sqrt{\frac{1}{N}\sum[100 \times (\overline{X_{exp}} - X_{sim})/\overline{X_{exp}}]^2} \qquad [5\text{-}41]$$

$$\overline{X_{exp}} = \frac{1}{N}\sum_{1}^{N}X_{exp,i} \qquad [5\text{-}42]$$

,*where*, *N* is the number of experiments implemented; and X_{exp} and X_{sim} represent experimental results from the reference and simulation results from the developed analytical computer simulation model, re-spectively (Chang et al., 2015).

Figure 5-8 presents simulation results of the module thermal efficiency against external air mass flow rates by inputting design, operating, and weather conditions from the referenced solar air heater experi-mental study. As a result, the correlation coefficient (*CR*) and the root mean square percentage deviation (*ER*) of the module thermal effi-ciency were 0.9975 and 1.71%, respectively.

Because there was similarity between the fin-and-flat plate of the so-lar air heater and the built-in finned channel structure in the proposed STF module, the corresponding heat transfer processes in the published model were similar to those described in the algorithm. A good agreement between the experimental and simulation data was therefore observed. Meanwhile the discrepancy between the experimental and simulation data might be caused through potential reasons: 1) the utilisation of the simplified assumptions/empirical formulas, and 2) an inaccurate estimation of the heat loss coefficient caused by wind data shortage.
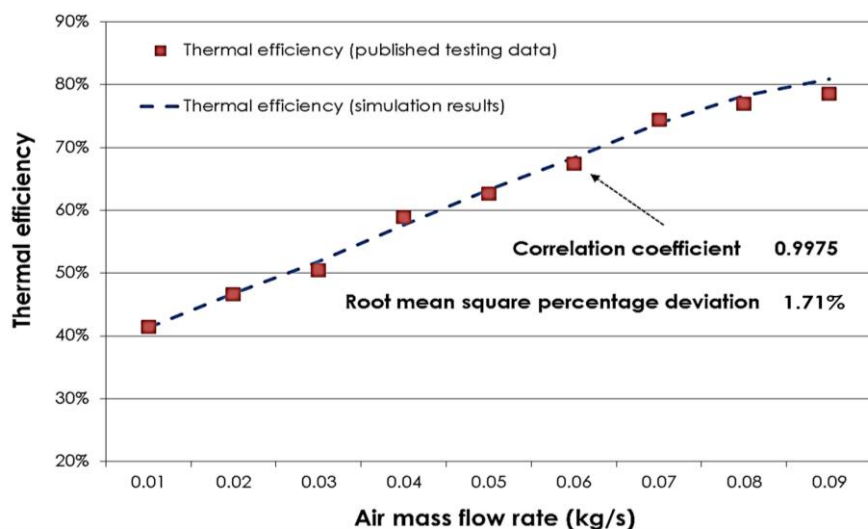
Figure 5-8 Comparison of simulation results with the published testing data based on reference experimental results (Chang et al., 2015)

In general, the accuracy achieved by this model was acceptable from the engineering point of view, and could be therefore applied to characterise the STF performance and recommend appropriate parameters for further fabrication, operation, and assessment. In addition, this model would be further verified for accuracy by the dedicated experiments described in the next chapter.

5.5 Parametric analysis by the simulation model

The STF's thermal performance is a factor that depends upon several design parameters, i.e., fabrication materials, colourful paint types,

pin-fin diameter, pin-fin length, number of pin-fin rows, longitudinal and transverse distance between fin rows. The impacts of these parameters on STF's thermal performance are presented in the following sections and the results are then discussed to address important recommendations for the follow-on prototype fabrication and testing. The STF is assumed with the working medium as water under the lab-controlled environment (basic conditions given in the laboratory): weather conditions, i.e. solar radiation of 500 W/m², air temperature of 20°C; air velocity of 1m/s, and the constant operational conditions, i.e. inlet water temperature of 30°C, water mass flow rate of 1 l/min.

5.5.1   Impact of STF fabrication materials

While keeping all other design and operating parameters constant, changing the material types led to a variation in the STF thermal performance as indicated in Figure 5-9.
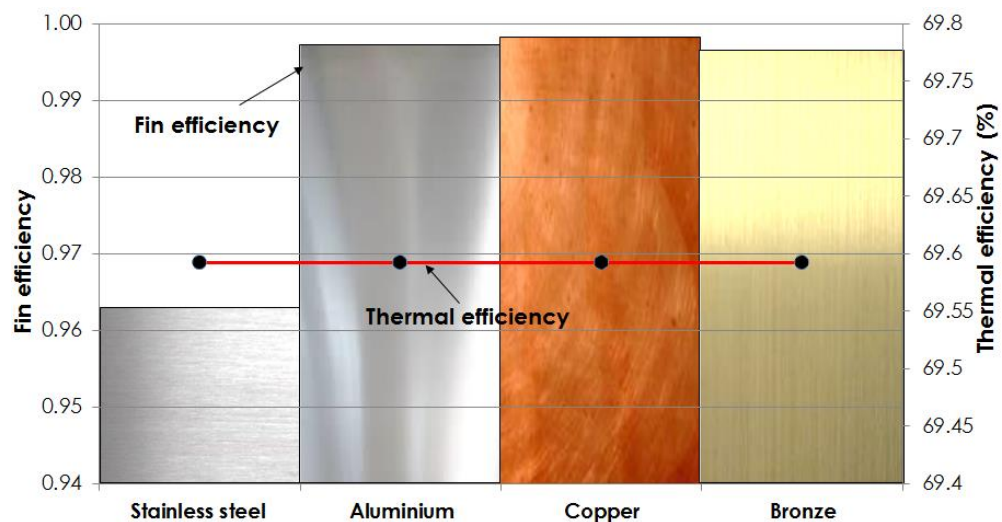
Figure 5-9 Impact of fabrication materials on STF thermal performance

As addressed in Chapter 4, stainless steel, aluminium, copper and bronze were selected for analysis by inputting their respective thermal conductivities into the simulation model. It is seen that the material types didn't affect the STF's thermal performance too much. For instance, although the stainless steel made STF has the lowest thermal conductivity, its corresponding fin efficiency and the overall thermal

efficiency were nearly the same as those STFs made by the other materials. Despite on the equivalent thermal impact, the proper STF materials should additionally take consideration of weight, cost and galvanic corrosion. According to such selection criteria, the stainless steel material seems the best option for the initial STF design since the aluminium is too soft and it also requires special treatment to avoid corrosion while copper/bonze are too heavy and expensive in large scale building integration.

5.5.2   Impact of colourful coatings/paints

The correlation between colourful coatings/paints and STF thermal performance is given in Figure 5-10, while remaining the other design and operating parameters the same. Ten different coatings/paints discussed in Chapter 4 were considered as the STF's front colours.
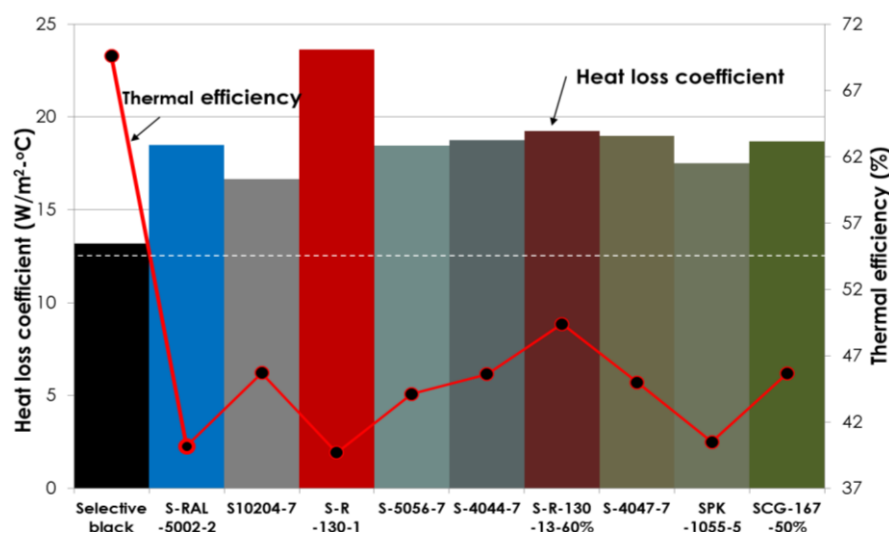
Figure 5-10 Impact of colourful coatings/paints on STF thermal performance

By inputting their characteristic values, like absorbance and emissivity, into the established simulation model, their respective impacts on the STF thermal performance could be then observed. The selective black chrome reached the best performance with the highest thermal efficiency (nearly 70%) and the lowest heat loss coefficient (about 13.17W/m²-°C) due to its high absorbance and low emissivity. In contrast, the red paint (S-R-130-1) based STF achieved the worst thermal

efficiency of less than 40% due to its highest emissivity at 0.64. The rest paints have the equivalent impact to the STF's thermal efficiency in a reasonable range of 40%-60% with absorbance $a \geq 0.76$ and emissivity $\varepsilon \leq 0.4$. So it could recommend that the best colour choice in these cases should be the selective black chrome while the other alternatives need to remain their absorbance and emissivity values in the acceptable range as indicated as above.

5.5.3   Impact of pin fin diameter

The correlation between the pin fin diameter and the STF thermal performance is illustrated from Figure 5-11 to Figure 5-13 by remaining the other design and operating parameters constant. The thermal efficiency, fin effectiveness, Reynolds number, flow pressure loss and heat removal factor all increased with the diameter of pin fins varying from 25 to 55 mm.
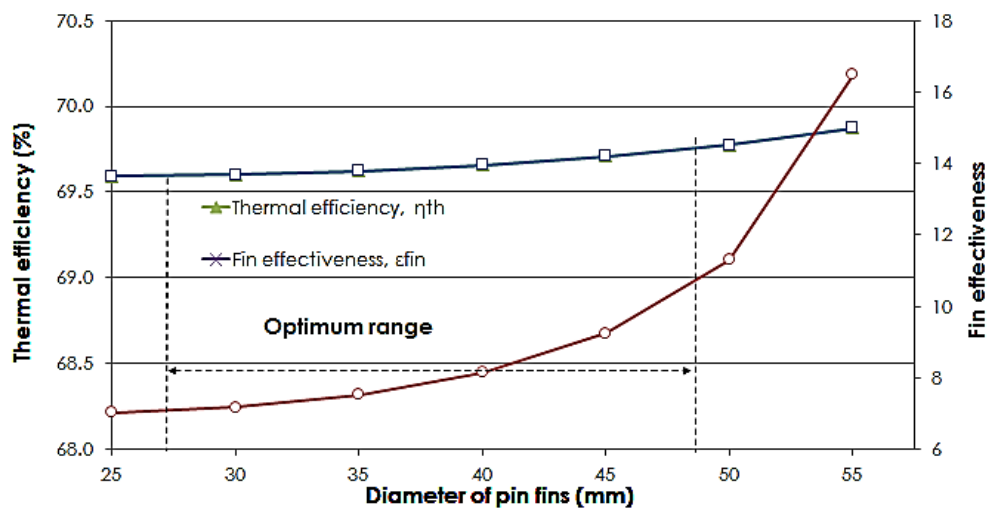
Figure 5-11 Impact of pin fin diameter on STF thermal performance: thermal efficiency and fin effectiveness

This phenomenon could be explained as larger pin fins led to more turbulent flow across the fin bank with higher Reynolds numbers, which subsequently increased the heat transfer coefficient and the heat removal factor of the working fluid as well as the fin efficiency (before the diameter variation of 48 mm). These impacts further raised

up the overall thermal efficiency of the STF module. In addition, the stronger turbulent flow resulted in the higher pressure drop when crossing the pin fin bank.
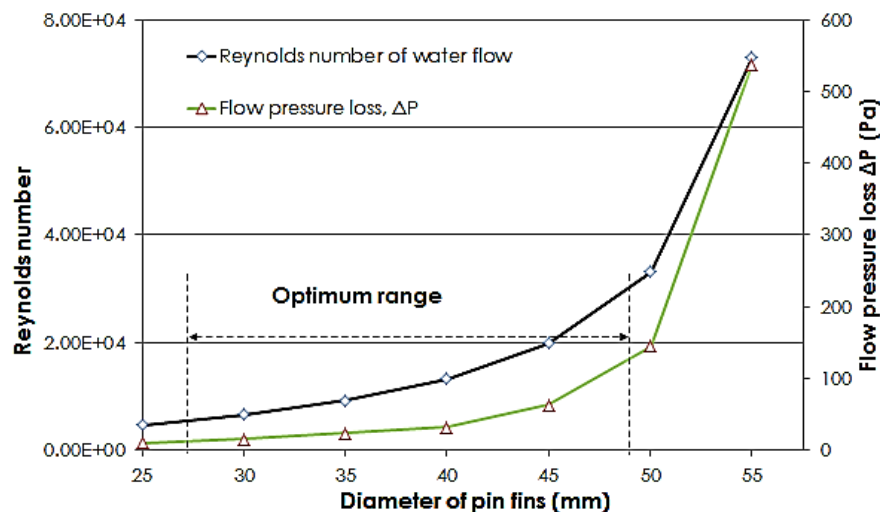
Figure 5-12 Impact of pin fin diameter on STF thermal performance: Reynolds number and fluid pressure loss
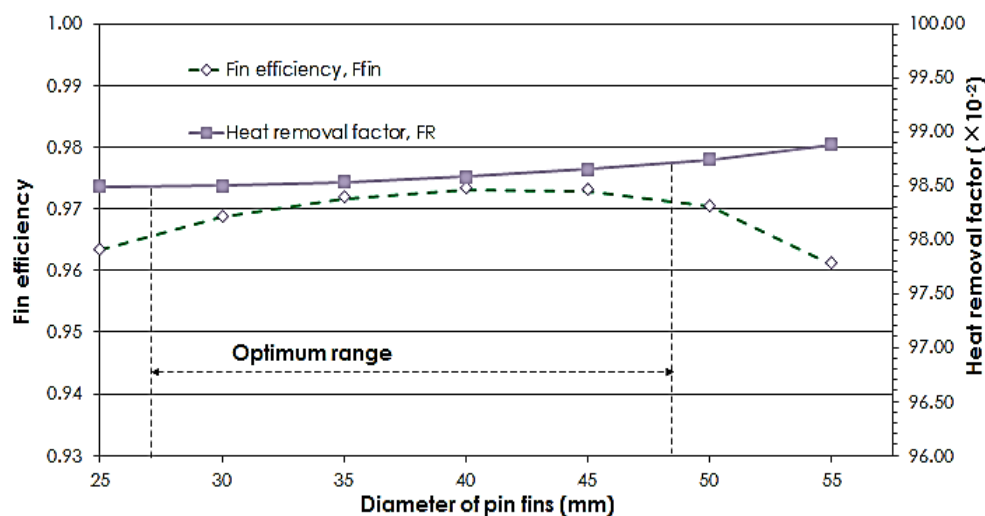
Figure 5-13 Impact of pin fin diameter on STF thermal performance: fin efficiency and heat removal factor

On the other hand, the larger pin fin means the greater finned surface which thus enhanced the overall fin effectiveness but weakened the independent fin efficiency after the diameter was more than 40 mm (the dominant factor for the fin efficiency afterwards). In order to balance the overall thermal efficiency and the pressure loss of the fluid, an optimum/equilibrium range should be recommended. The pres-

sure loss increased significantly after the diameter of pin fins was over 48 mm while the thermal efficiency varied slightly all the time. Meanwhile, the suggested STF module dimension is around 600-1000mm taking reference to the practical installation and placement of cladding system. As a result, the optimum range was determined from 25 to 48 mm in terms of the pin fin diameter.

5.5.4   Impact of pin fin length

While remaining the other design and operating parameters the same, the correlation between the pin fin length and the STF thermal performance is presented in Figure 5-14 and Figure 5-15. It is found that thermal efficiency, fluid flow factor, and heat removal factor all increased with the length of pin fins varying from 0.5 to 5 mm.
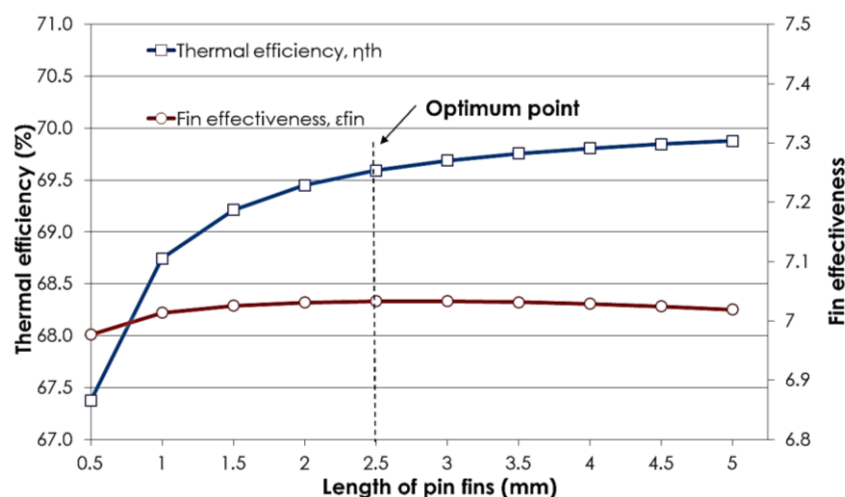
Figure 5-14 Impact of pin fin length on STF thermal performance: thermal efficiency and fin effectiveness

This phenomenon could be explained as longer pin fins enabled more surface area for the fluid flow to remove heat and therefore increased the total amount of heat transfer to the working fluid. These positive impacts also dominated before the pin fin length of 2.5 mm but dropped down after reaching 2.5 mm, showing a longer fin was much less effective. In the meanwhile, the variation of the pin fin length didn't have too much effect on the other parameters, like Reynolds number and pressure loss. In order to balance the fin effi-

ciency and the fluid flow factor as well as the fluid heat removal factor, an optimum/equilibrium range was recommended from 2.4 to 2.7 mm in terms of the pin fin length, and the optimum length of 2.5 mm was found from the aspect of the fin effectiveness.
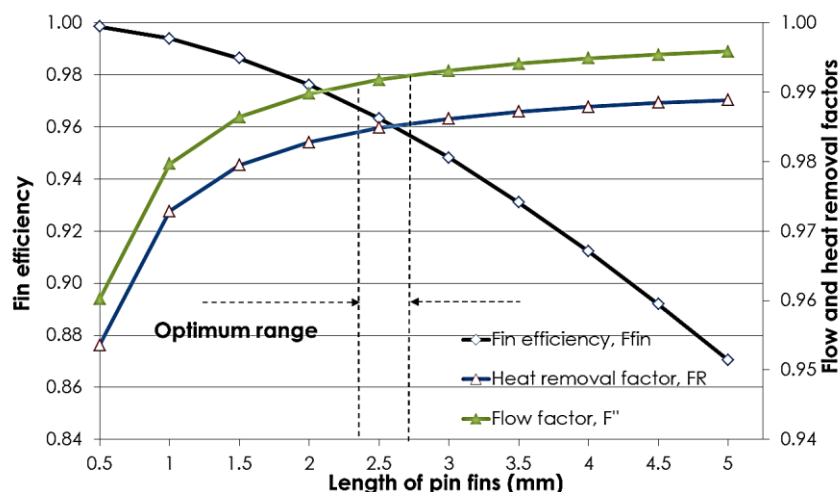
Figure 5-15 Impact of pin fin length on STF thermal performance: fin efficiency, flow factor and heat removal factor

5.5.5   Impact of number of pin fin rows

While remaining the other design and operating parameters the same, the correlation between the number of pin-fin row and STF thermal performance is presented in Figure 5-16 and Figure 5-17. It is found that all the main performance indicators, like thermal efficiency, fin effectiveness, fluid flow factor, heat removal factor, and pressure loss, increased with the number of pin-rows varying from 2 to 10.

This phenomenon could be explained as more rows of pin fins enlarged heat exchanging surface area between the fluid flow and the fins. The heat exchange process therefore increased the total amount of heat transfer from the fins to the fluid shown in the form of the increasing thermal efficiency. These positive impacts also applied to fin effectiveness, fluid flow factor, and heat removal factor. On the other hand, the increased pin fin rows resulted in higher pressure drop. In the meanwhile, the increasing number of pin fin rows only strength-

ened on other parameters slightly, like fin efficiency, Reynolds number and heat transfer coefficient of fluid. In order to balance pressure loss and other thermal performance indicators, an optimal pin fin row number was recommended from 4 to 7 based on the suggested STF module dimension around 600-1000mm in length for building application.
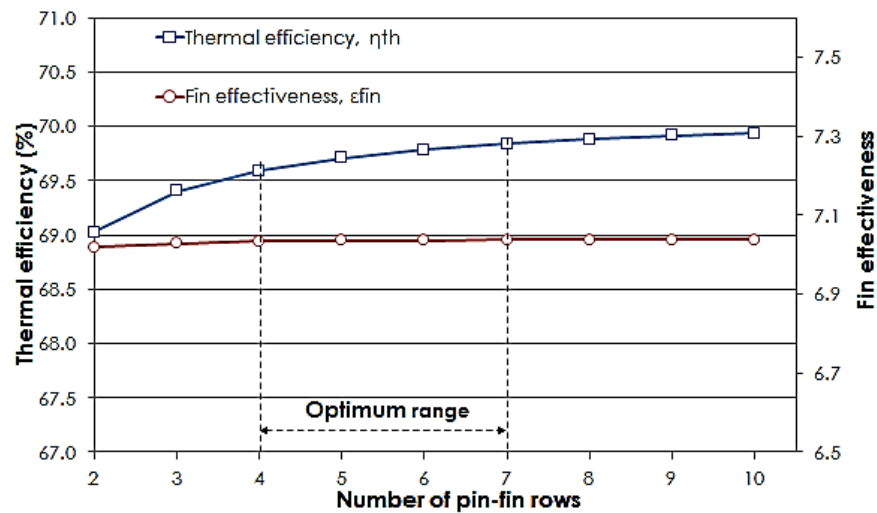
Figure 5-16 Impact of number of pin fin rows on STF thermal performance: thermal efficiency and fin effectiveness
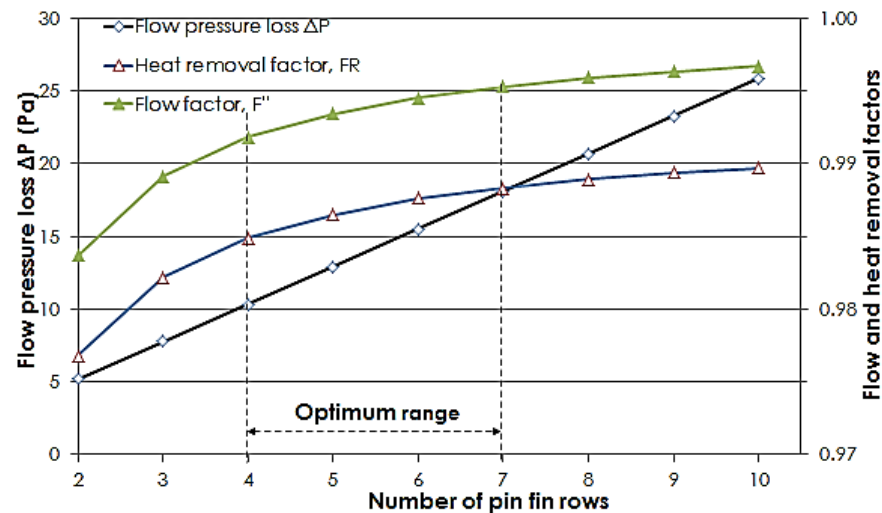
Figure 5-17 Impact of number of pin fin rows on STF thermal performance: fin efficiency, flow factor and heat removal factor

5.5.6   Impact of longitudinal distance between fin rows

While remaining the other design and operating parameters the same, the correlation between the longitudinal distances of pin fin rows and

the STF thermal performance is displayed from Figure 5-18 to Figure 5-20. It is found that thermal efficiency, fin efficiency, flow factor, and heat removal factor of fluid increased with the longitudinal distance between fin rows varying from 30 to 100 mm. In contrast, fin effectiveness, Reynolds number, and pressure loss of fluid varied in the opposite tend.
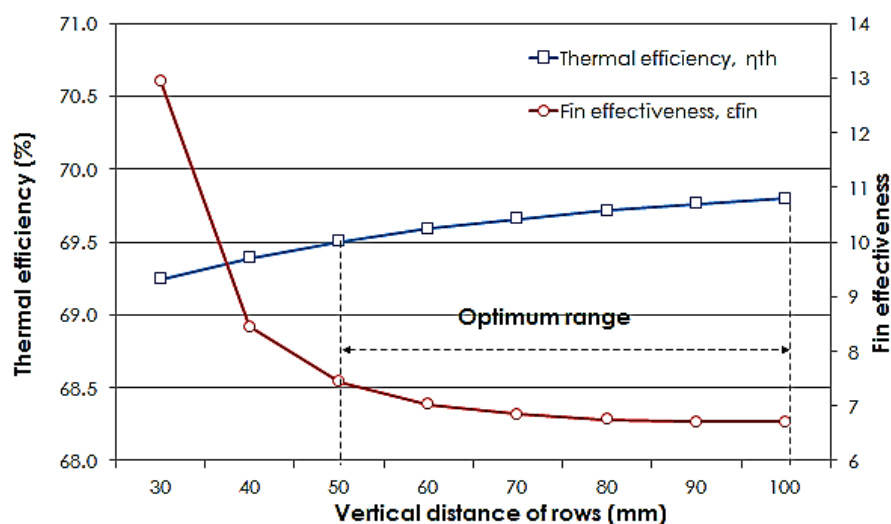
Figure 5-18 Impact of longitudinal distance between fin rows on STF thermal performance: thermal efficiency and fin effectiveness
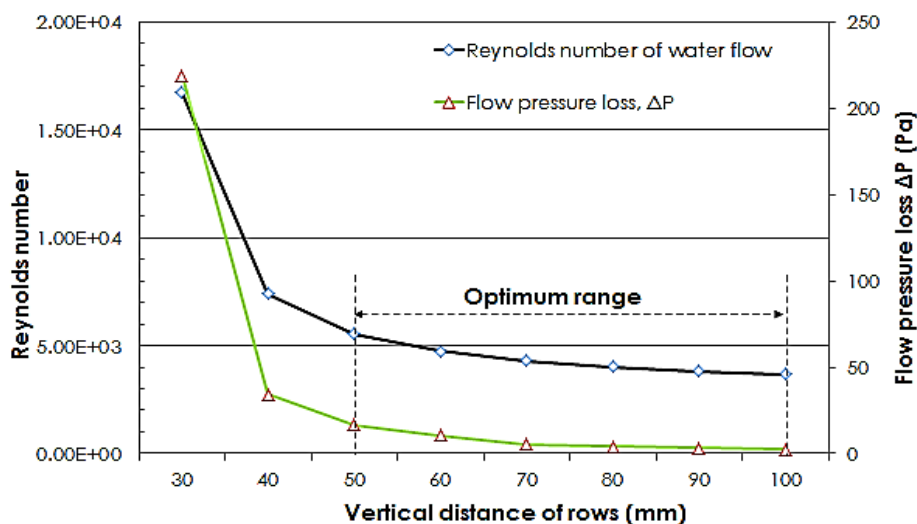
Figure 5-19 Impact of longitudinal distance between fin rows on STF thermal performance: Reynolds number and fluid pressure loss

This phenomenon could be explained as larger longitudinal distance between fin rows enlarged the heat exchanging space between the fluid flow and the fins, leading to more fluid passing through the fin bank. Such heat exchange process therefore increased the total

amount of heat transfer from the fins to the fluid shown as the rising thermal efficiency. These positive impacts also applied to the fin effectiveness, the fluid flow factor, and the heat removal factor. On the other hand, the larger longitudinal distance between fin rows caused less turbulence of the fluid flow (lower Reynold number) and resulted in the lower pressure drop for the fluid. By considering the variation trends of both pressure loss and other thermal performance indicators, an optimum range was recommended from 50 to 100 mm in terms of the longitudinal distance between fin rows.
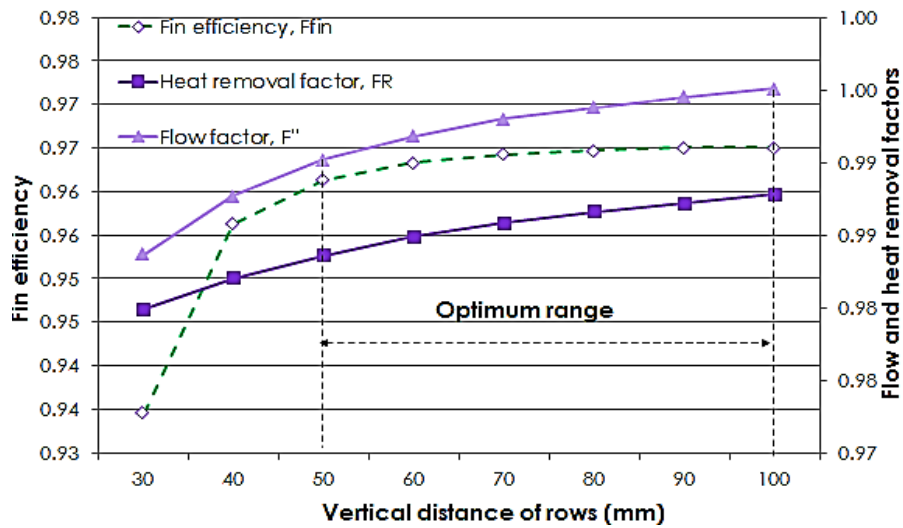
Figure 5-20 Impact of longitudinal distance between fin rows on STF thermal performance: fin efficiency, flow factor and heat removal factor

5.5.7   Impact of transverse distance between fin rows

While remaining other design and operating parameters the same, the relations between the transverse distances of pin fin rows and the STF thermal performance are from Figure 5-21 to Figure 5-23.

It is found that thermal efficiency, fin effectiveness, Reynolds number, pressure loss and heat removal factor decreased with the transverse distance between fin rows varying from 30 to 100 mm. In contrast, fin efficiency and flow factor varied in the opposite tend.
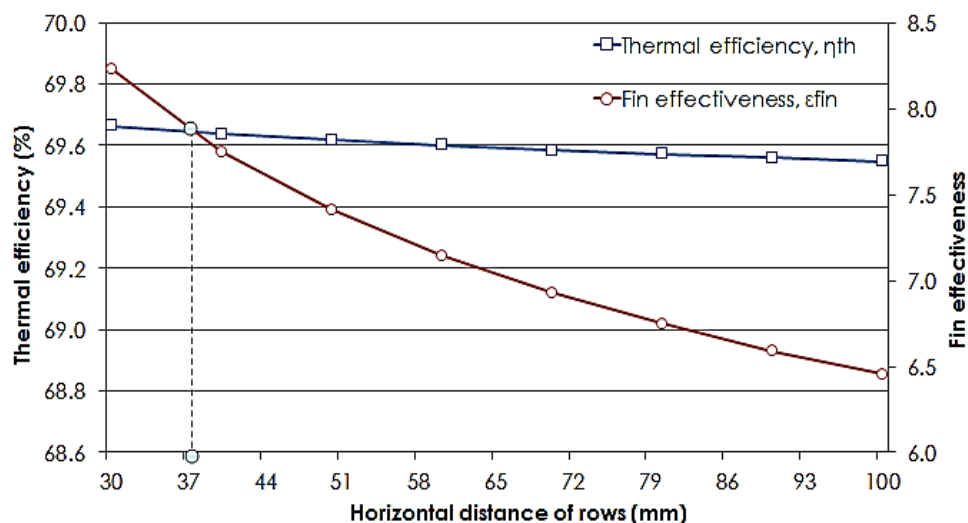
Figure 5-21 Impact of transverse distance between fin rows on STF thermal performance: thermal efficiency and fin effectiveness
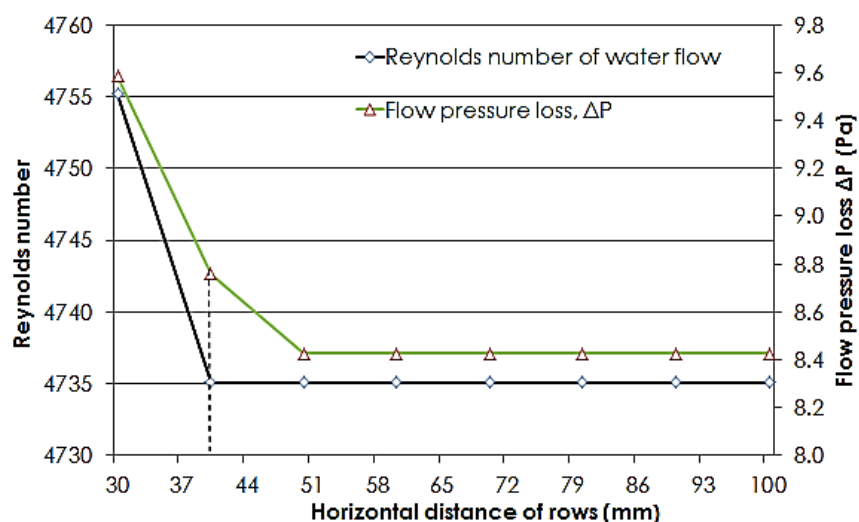
Figure 5-22 Impact of transverse distance between fin rows on STF thermal performance: Reynolds number and fluid pressure loss
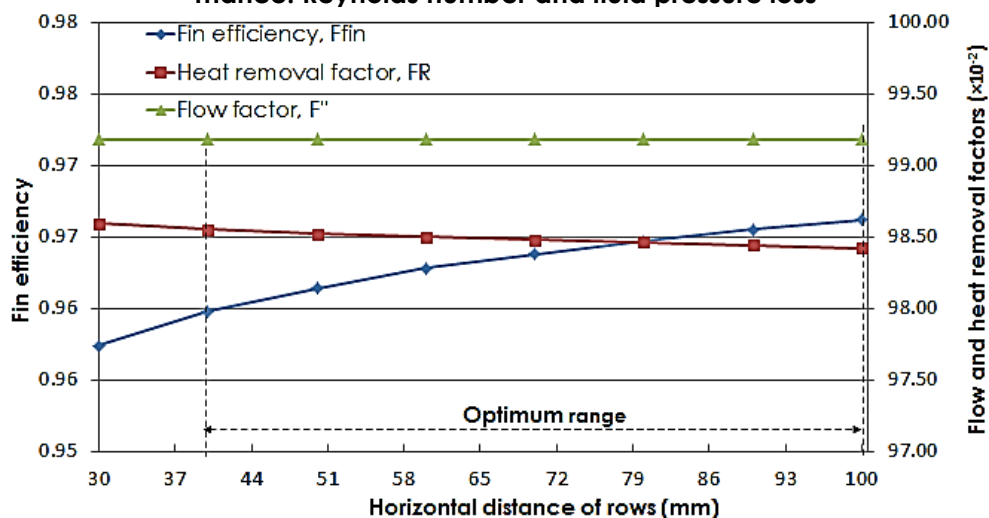
Figure 5-23 Impact of transverse distance between fin rows on STF thermal performance: fin efficiency, flow factor and heat removal factor

Although the larger transverse distance between fin rows enabled more fluid across the fin bank for heat exchange, the reduced fluid flow turbulence became the primary restrictive factor that pulled the thermal efficiency and fin effectiveness downwards. However, all these variations seemed very slight in terms of the magnitude margin. The transverse distance between fin rows had very limited impact. As a result, the optimum range was recommended in the range of 40 to 100 mm.

5.6 Chapter executive summary

This chapter investigated the theory behind the proposed STF module and developed a computer simulation model for thermal performance evaluation. The simulation model was preliminarily validated by the published test results with a reasonable accuracy in predicting the STF thermal performance.

In the established analytical model, seven impact factors were considered in the parametric studies with results in Table 5-2. Through these recommendations, the follow-on prototype fabrication as well as the parallel comparison between the computer simulation and the laboratory-controlled test could therefore be conducted in next chapter.

Table 5-2 Design parametric conclusion from STF optimization simulation

No.	Design Variables in STF	Baseline Design Solution
1	Fabrication materials	Stainless steel;
2	Colourful coating/paint	Selective black chrome while the other alternatives need to remain absorbance a ≥0.76 and emissivity ε ≤0.4;
3	Pin fin diameter	25 mm, from the optimum range of 25mm-48 mm;
4	Pin fin length	2.5 mm, from the optimum range of 2.4mm to 2.7mm;
5	Number of pin fin rows	4, from the optimum range of 4-7
6	Longitudinal distance between fin rows	60 mm, from the optimum range of 50mm-100mm
7	Transverse distance between fin rows	60 mm, from the optimum range of 40mm-100mm

6

PROTOTYPE FABRICATION, EXPERIMENTAL EVALUATION AND SIMULATION MODEL VALIDATION

6.1 Chapter abstract

This chapter introduces the specific fabrication process for the proposed compact STF prototype system. The major works completed in this chapter are presented as follows:

1) Detailed descript the fabrication process for the compact STF module and hot-water system connection;

2) Carry out a group of laboratory-controlled experiments for the characterisation of the STF's thermal performance, based on the experimental prototype rig;

3) Investigate a number of operational impacting factors, including solar radiation, air temperature, air velocity, inlet water temperature, and mass flow rate, in terms of their correlation with the STF' thermal efficiency;

4) Conduct an equivalent comparison between the modeling and the experimental results under a series of laboratory-controlled conditions was conducted to enable validation of the steady-state simulation model.

The verified simulation model can produce the characteristic performance curves for later socio-economic assessment addressed in Chapter 7. The established experimental rig was further tested under the real climatic conditions outlined in the Chapter 9.

6.2 Fabrication of the Prototype System

According to the concept design and recommendation in previous chapters, a STF prototype system has been fabricated at Shanghai Pacific Energy Centre, China. The whole fabrication process can be detailed with two main aspects, as the production of STF module and the whole system connection.

6.2.1   Production of the STF module

The novel compact STF exploited the stainless steel sheets as the basic material. Each sheet was only 1.2 mm in thickness so as to limit added load for building integration. Figure 6-1 provides the flow chart of the main production processes of such a STF module.
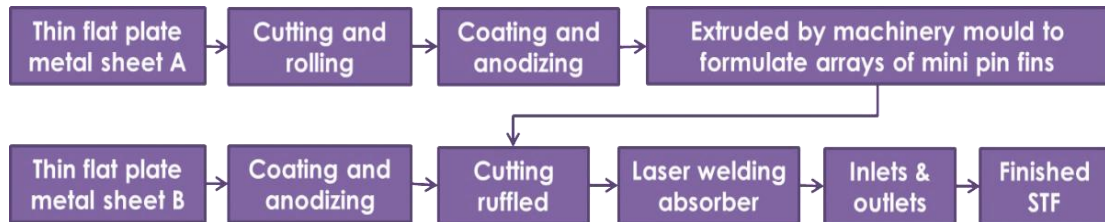
Figure 6-1 Production flow chart of the STF

Figure 6-2 Photograph of the STF prototype

Figure 6-2 displays the complete STF prototype:

1) Initially, two stainless steel sheets were tailored into specific geometry or size by the rolling machines. In this process, module shape and size can be possessed at the high level of freedom to satisfy the requests in building integration design;

2) Both the sheets A and B were then put into the process of anodizing in order to prevent the corrosion;

3) The front smooth sheet B was additionally coated with the black chromium film at 20 μm thick for an improved thermal performance;

4) Afterwards, Sheet A was extruded or pressed using the machinery mould to formulate arrays of mini corrugations in the form of pin fins. Each pin-fin corrugation was fabricated at the dimensions of 25mm in diameter and 2.5 mm in depth;

5) In consequence, two sheets were assembled together by overlapping folded periphery through laser welding;

6) Finally, two sets of headers (D20) were employed as pipe inlets and outlets respectively at four corners of the STF module. Till now, a compact metal absorber with two sets of inlet and outlet is formed.

6.2.2   Whole STF prototype system connection

The polypropylene piping system (named PP-R) was selected for the STF prototype system connection.
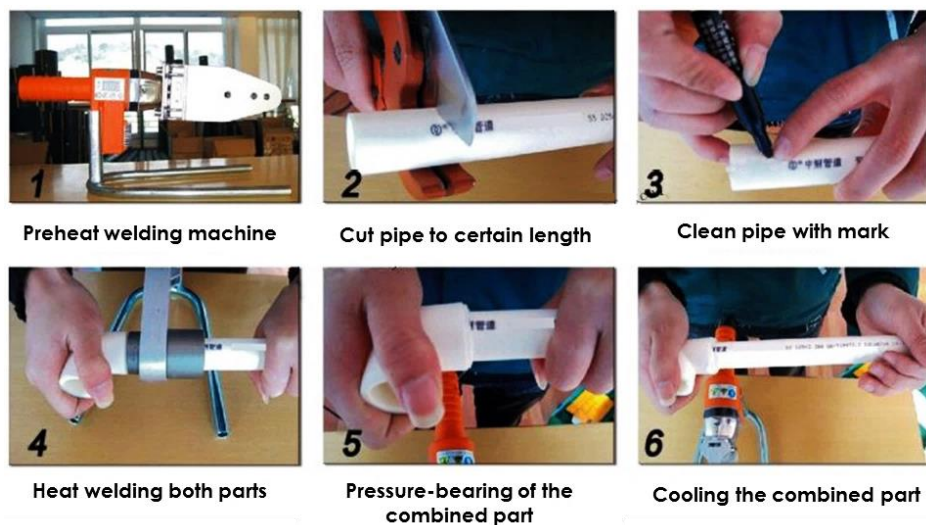
Figure 6-3 Processing flow of PP-R piping system connection

The reasons of selecting PP-R are: 1) the thermal conductivity of PP-R material is only 0.21 W/m-K, therefore it can eliminate the pipe insulation under most situations; 2) the maximum bearing temperature of PP-R pipe is high to 95 ℃ that can meet the hot water requirements in specification of building application; 3) PP-R is stable in property even

under ultra violet exposure to avoid thermal dilation and galvanic cor-
rosion risks; 4) PP-R pipe has high feasibility in joint integrity and long
term cost effectiveness. Figure 6-3 presents each pipe connection
process for the STF hot water prototype system connection.
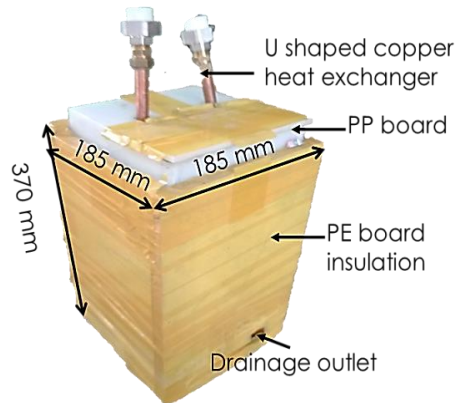
Figure 6-4 Dimensional of the custom made insulated water tank

The STF prototype, with the dimension of 488 mm× 348 mm, was fixed
vertically onto a fixed frame to simply present vertical wall integration.
A magnetic regeneration water pump was installed in the water loop
to power the cooling water cross. A water tank of 35 litres with built-in
heat exchanging coils (as shown in Figure 6-4) was also installed and
connected to the circulation loop to obtain heat and store the heat-
ing water. The polystyrene board was added for the STF module to
minimise the heat loss. An electrical rubber heating plate with the
percentage controller, which acts as the equivalent solar radiation
source, was closely attained to the external surfaces of the STF mod-
ule. The image of the whole experimental rig of the STF hot water pro-
totype system is presented in Figure 6-5.

It needs to be addressed that this prototype system is only used to
prove the concept at the early design stage. When such STFs are fur-
ther connected into arrays for large-scale application, the thermal ef-
ficiency may drop depending on the scalability due to the unavoid-
able rising temperature differential between STF and ambient tem-
perature during the system circulation. As a result, the higher the solar

coverage (scalability) means the lower the specific yield (efficiency). So a good compromise between solar coverage (scalability) and solar yield (efficiency) must be found for each system during the facade integration design.
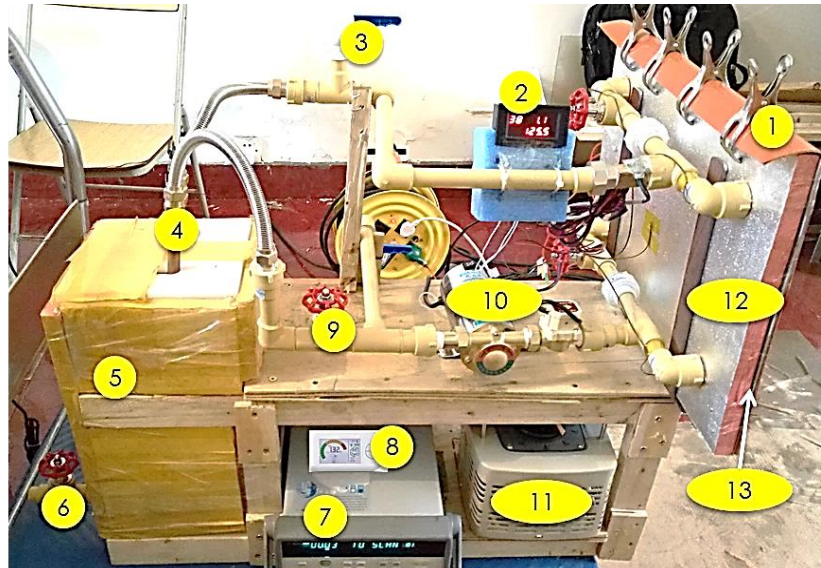
1.	Electrical rubber heating plate	8.	Power meter
2.	Ultrasonic thermal flow meter	9.	Stop valve
3.	Vent valve	10.	Water pump
4.	Copper heat exchanger	11.	Power regulator
5.	Insulated water tank	12.	Thermal insulation
6.	Drainage valve	13.	STF prototype
7.	Data logger		

Figure 6-5 Experiment rig of the proposed STF hot water system

6.3 Experimental set-up under laboratory condition

The whole testing of the STF prototype system was conducted under the controlled indoor conditions in the laboratory of Shanghai Pacific Energy Centre. The whole system components were installed on the experiment bench, which was fixed with a trolley for a mobile movement. Table 6-1 displays the measurement instruments during the testing, while Figure 6-6 provides a schematic illustration of the experimental rig.
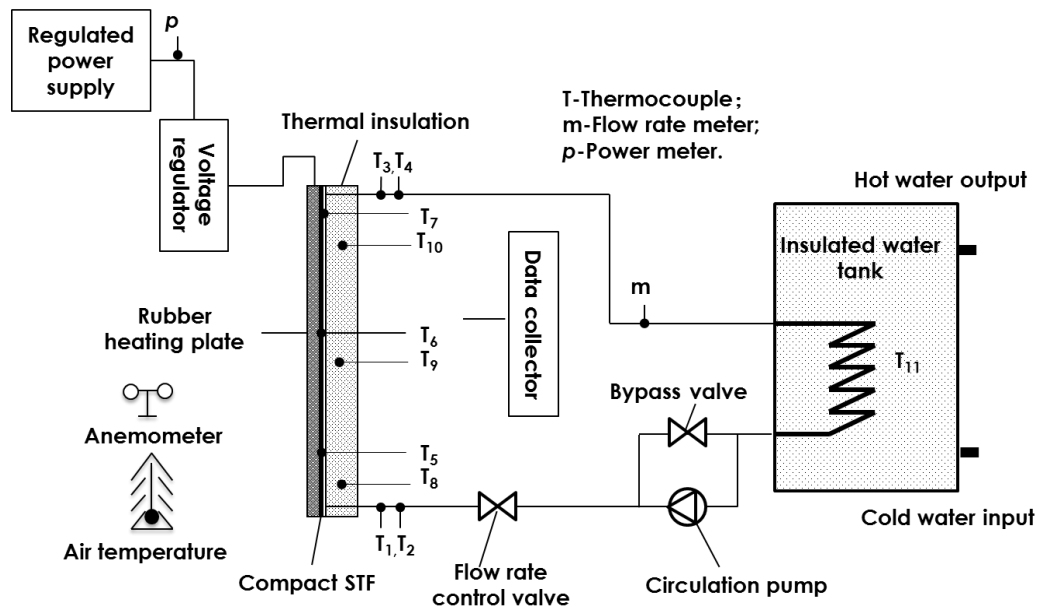
Figure 6-6 Schematic experiment rig of the indoor STF testing rig

The measurement instruments were selected and set up in the appropriate positions in the system to enable laboratory-controlled testing. A number of T-type thermocouples were attained to the external surfaces of the STF, and installed in the inlet/outlet and inside of water loop and water tank: there were totally six thermocouples (NO. 5-10) equidistantly attached along the external surfaces of STF from top to bottom which were used to measure the mean temperature of the STF; another four dedicated thermocouples were respectively placed in the inlet/outlet (NO. 1-4) of water loop and the central of the water tank (NO. 11) to measure their related average temperature. All of them were linked to the Agilent 34970A data logger associated with a computer for data recording. And the ultrasonic thermal flow meter was connected within the system to measure the instantaneous flow rate. In addition, a smart electricity meter was used here to measure the instantaneous electric power consumed by the heating plate. In general, these instruments aim to collect three kinds of parameter as temperature, heating input power, and flow rate.

6.4 Experimental processing

A series of laboratory steady-state tests were implemented, and the results of the tests were used for the thermal performance evaluation of the STF. During operation, the tank water temperature would be gradually growing higher owing to the continuous heating input from the absorber. In order to keep a relatively constant inlet temperature, the water tap would remain open to enable adequate amount of main water to be fed into the loop. As soon as the water tank was fully charged, the drainage valve would be turned on to allow the extra amount of water to be discharged. The steady state would be eventually achieved as long as the thermal properties of the STF stay stable against the operating time under the dedicated testing mode.

All tested operating conditions displayed in Table 6-2 including variations in: 1) the equivalent solar radiation (heater power) in the range of 493 W/m² (90W) to 986W/m² (180W); 2) surrounding air temperature in the range of 20.0℃ to 24.0℃; 3) air velocity in the range of 0 to 2.0m/s; 4) cooling water flow rate in the range of 0.1 to 2.0 l/min; and 5) water inlet temperature in the range of 20.0℃ to 40.0℃. The baseline testing condition applied is: 493 W/m² (90W) of the equivalent solar radiation (heater power), 20.0℃ of surrounding air temperature, 1 m/s of air velocity, 1.0 l/min of water mass flow rate and 30.0℃ of water inlet temperature. Given the defined standard testing condition, one parameter was changed while the others kept constant, thus enabling develop the correlations between the STF heat output and the associated operational parameters.

In general, the measurement data would be recorded at 5-second interval and logged into the computer using the data logger for following analyses. To be mentioned, all the tests were carried out three times at each condition, and their arithmetic mean values were then

regarded as the final value during the whole experiments. Once the steady-state conditions have been achieved, the test period would be continued with a successive 10-hour interval period producing results varied non-monotonically by less than one percent.

Table 6-1 List of fittings and measurement instruments in the testing rig

Component name	Model No.	Description
PP-R water pipe	S3.2 DN20×2.8mm	2.8m in length
PP-R tee joint	DN20×1/2	Internal thread
PP-R bend	DN20×1/2	Internal thread
PP-R connector	DN20×1/2	Internal thread
PP-R loose connector	DN20×1/2	Internal/external/both-end thread
PP-R stop valve	DN20	--
Stainless steel water pump	15WGO.5-8	Power: 100W, Hydraulic head: 8m, Flow rate: up to 16 liters/min
Customized stainless steel STF		488×348×5mm
Customized water tank		185×185×370mm, weld by PP boards, inserted with a U shaped copper tube heat exchanger
Ultrasonic thermal flow meter	YG-RLM(C)	Flow rate range: 0.05-5 m³/h
Customized rubber heating plate		Dimension of 500×400mm with external power regulator
Micro weather station	Misol WS-HP2K-1	Temperature; Humidity; Wind speed/direction; Barometric pressure; Precipitation; Lux.
Smart electricity meter	British gas	To measure heating input load
T-type Thermocouple	RS:621-2164	Min/max temperature sensed: -200 ~350℃;
Data logger and data recording equipment	34970A	10 channels to record data

Table 6-2 List of operational modes for the experimental study of the STF

Test mode	I (W/m²)	T_a (℃)	V_a (m/s)	m_w (l/m)	T_{in} (℃)
1	493/548/603 /712/986	20.0	1.0	1.0	30.0
2	90	20.0/21.0/22.0 /23.0/24.0	1.0	1.0	30.0
3	90	20.0	0/0.5/1.0 /1.5/2.0	1.0	30.0
4	90	20.0	1.0	0.1/0.5/1.0 1.5/2.0	30.0
5	90	20.0	1.0	1.0	20.0/24.0/30.0 /34.0/40.0

6.5 Statistical analysis

During the testing, the heating tap is assumed to transfer electricity to heat at an efficiency of η_e, and therefore the heat released from the heating tap, Q_h can be defined as:

$$Q_h = \eta_e Q_E = A_p I \alpha_p \qquad \qquad [6\text{-}1]$$

Inside, Q_E is the measured electrical energy consumption (W) of the heating tap from the smart meter. So, the STF thermal efficiency due to the experiment is:

$$\eta_{th,exp} = Q_u / Q_h \qquad \qquad [6\text{-}2]$$

The computation model was operated at the identical condition as the experiment did in order to enable a parallel comparison between the simulation and the experimental results. To identify the discrepancy between theoretical and experimental results, the correlation coefficient (CR) and the root mean square percentage deviation (ER) are applied using equations from [5-40] to [5-42].

Because accuracy and precision play important roles in this experimental measurement, the calibrations of the instruments have been done by comparing with a standard power detector and a room temperature instrument prior to the experimental study. However, there were still some uncertainties due to variation in the measurements or normal random error during the testing that should take into consideration. For instance, the electricity-to-heat efficiency of heating tap might become lower once the heating tap attached on the external surface of the STF surface due to an increased contact thermal resistance. There might be also some occasions of fluctuations in the supply voltage, air-temperature, cooling-water-temperature, and supply water pressure, as well as loosened thermocouples from the attached surfaces due to vibration in operation. Furthermore, analyses of

the testing results need to take into account the potential instruments uncertainties, e.g., the tolerance of the input power (±0.5 W) and the temperature measurement discrepancy (±0.1K). In addition, there were still some potential random errors, which may be caused by personal fluctuation, random electronic data logger fluctuation and influences of friction inside water pipes due to metal particles from the absorber etc.

The uncertainties of whole experiments were analysed on basis of the standard deviation method addressed in the guide of the expression of uncertainty in measurement (JCGM, 2008), which is a widely used measurement of variability or diversity in statistics and probability theory. It shows how much variation or "dispersion" there is from the average value. A low standard deviation, S_d indicates that the data points tend to be very close to the mean value, whereas high standard deviation, S_d indicates that the data are spread out over a large range of values.

$$S_d = \sqrt{\frac{1}{N}\sum_{1}^{N}\left(X_{exp,i} - \overline{X_{exp}}\right)^2} \qquad \text{[6-3]}$$

And the uncertainty is expressed by the error bars in graphs to give a general idea of how accurate is the measurement. The uncertainty ratio of the experimental results is given:

$$U_C = S_d\sqrt{X_{exp}} \qquad \text{[6-4]}$$

,*where*, N is the number of experiments implemented; X_{exp} is the experimental value, respectively; $\overline{X}_{exp}$ is the arithmetic mean experimental value.

6.6 Results and discussion

The characteristic studies of the operating performance exploration of the proposed STF were conducted under different operational conditions by virtue of both the established computation model and the experimental testing. The parallel comparison between the modelling and testing results led to verification or modification of the model accuracy in performance prediction. Further, the impacts of the operating conditions (e.g., equivalent solar radiation, surrounding air temperature, surrounding air velocity, water mass flow rate and inlet water temperature) on system performance were investigated individually. Given the baseline testing condition defined in Table 6-2, the physical parameters of the collector under the baseline design parametric are listed in Table 6-3.

Table 6-3 Physical Parameters of the baseline designed STF

Physical Parameters	Value
Efficiency Factor, F'	0.9930
Heat Removal Factor, F_r	0.9918
Channel Flow Factor, F''	0.9849
Nominal Thermal Efficiency, η_{th}	63.21%
Overall Effectiveness, ε_{fin}	7.03

This demonstrates that such a STF, with simpler structure, economical cost and higher feasibility in architectural design, can achieve better or equivalent thermal performance while comparing to the recent reported bionic STF ($F'=0.963$) (Medved et al., 2003)

6.6.1   Impact of equivalent solar radiation

The impact of equivalent solar radiation was studied under the test mode 1 presented in Table 6-2. The rate of equivalent solar radiation (heater power) was varied from 493W/m^2 (90W) to 986W/m^2 (180W), while remaining other parameters constant, i.e., 20.0℃ of surrounding air temperature, 1.0 m/s of air velocity, 1 l/min of water mass flow rate

and 30.0°C of water inlet temperature. The simulation results that were carried out using the established computation model were then compared with the testing results conducted under the same operational condition, which yielded the results in Figure 6-7.
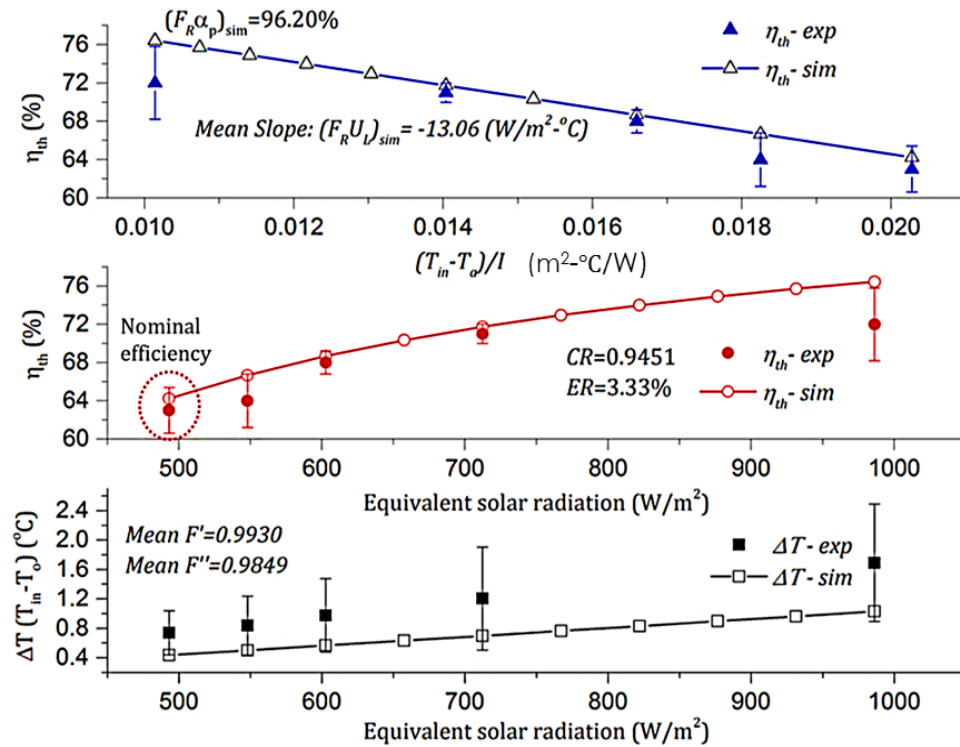
Figure 6-7 Linear regression graph & Performance curves of the proposed STF based on equivalent solar radiation variation

Good agreement between the modelling and experimental results was observed with the CR and the ER of 0.9451 and 3.33% respectively for the thermal efficiency. It is found that increasing the solar radiation led to the raise in the STF surface temperature and therefore the corresponding temperature difference (ΔT) between the inlet water and the outlet temperature increased from 0.74°C to 1.70°C. A higher solar radiation yielded an enhanced solar heat transfer, which helped to improve the solar heat gain and the STF's thermal efficiency from 63.21% to 72.32% during the experiment. The STF thermal efficiency factor F' stayed constant at 0.9930 since the STF design and water flow rate were remained. The STF flow factor F'' was almost the same as 0.985 due to the nearly unchanged heat loss coefficient U_L. It is

mostly contributed by the radiative heat transfer coefficient, which could be ignored against the increase of solar radiation. Similarly, the pressure drop ΔP between the inlet and outlet also remained nearly unchanged at 6.18 Pa when the changes of maximum water flow velocity $V_{w,max}$ and its corresponding Reynold number Re_w could be neglected using the Equations from [5-19] to [5-33]. This also resulted in the stable fin efficiency F_{fin} of 0.963 and its overall effectiveness ε_{fin} over almost 7.02, representing a really high-efficient heat transfer at the finned STF surface.
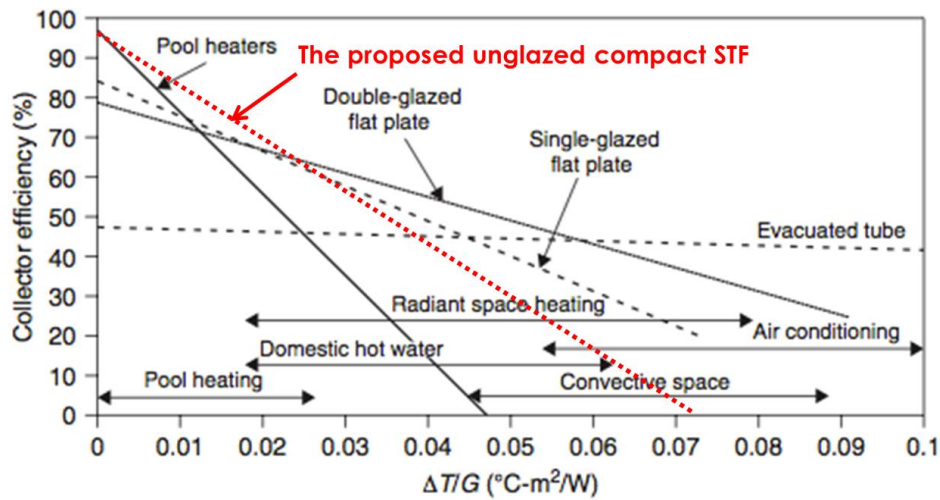
Figure 6-8 Theoretical thermal efficiency of the proposed STF

The thermal efficiency was also plotted as a function of $(T_{in}-T_a)/I$ in Figure 6-8. The maximum possible useful heat gain ability (the intercept $F_R\alpha_p$) of such STF at the given external weather conditions and the inlet water temperature was about 96.20%. The mean slope ($F_R U_L$) was as much as about -13.06, representing a sharp decreasing trend of this SFT's thermal efficiency against the $(T_{in}-T_a)/I$ since its unglazed metal absorber characteristic. So in case of current design, such STF could match the heating purposes of pool heating, domestic hot water preparation and radiant space heating etc. in the preliminary screening of various solar thermal collectors (Kalogirou, 2009). While regarding the variables like ΔT and solar radiation, the current STF de-

sign seems more suitable to be applied in those areas with warm air temperature and sufficient solar radiation.

6.6.2   Impact of surrounding air temperature

Under the test mode 2 presented in Table 6-2, the surrounding air temperature varied from 20°C to 24°C, while remaining other parameters constant, i.e. 493W/m² (90W) of the equivalent solar radiation (heater power), 1 m/s of air velocity, 1 l/min of water mass flow rate and 30°C of water inlet temperature. The simulation was carried out using the established computation programme, and the simulated results were then compared with the testing results in the same operational condition, which yielded the results in Figure 6-9.
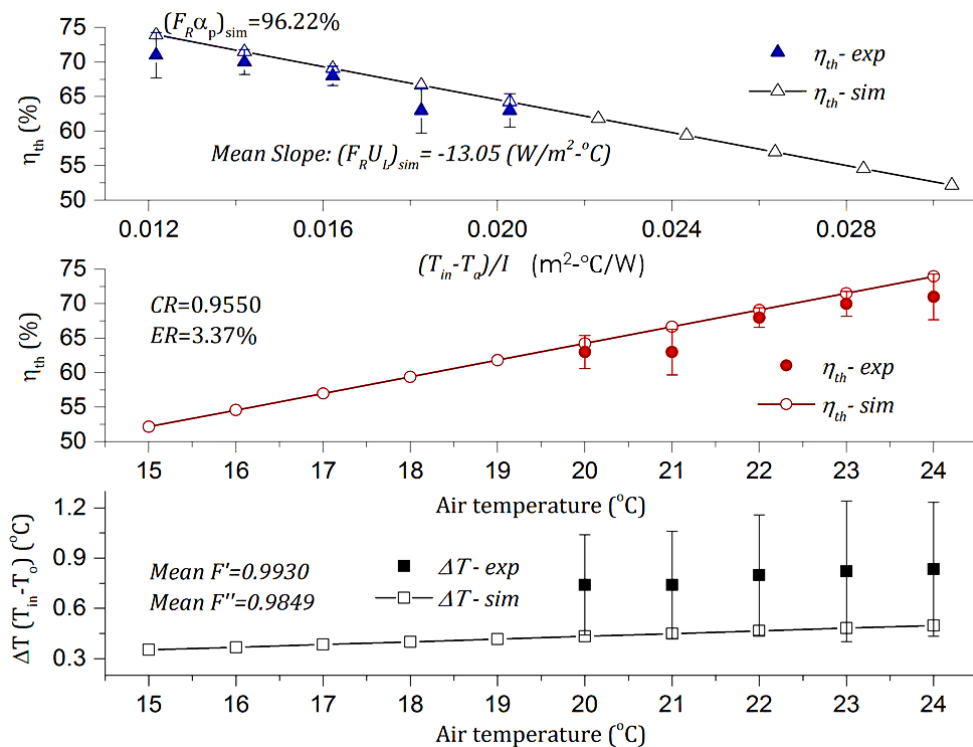
Figure 6-9 Linear regression graph & Performance curves of the proposed STF based on air temperature variation

Good agreement between the modelling and experimental results was observed with the CR and the ER of 0.9550 and 3.37% for the thermal efficiency, respectively. It is found that increasing the surrounding air temperature caused the increased STF surface tempera-

ture and thus the corresponding temperature difference (ΔT) between inlet and outlet increased from 0.74°C to 0.83°C. A higher air temperature led to less heat loss from the STF surface, which assisted in improving the solar heat gain and the STF's thermal efficiency from 63.21% to 71.44% during the experiment. The other physical parameters, such as the STF thermal efficiency factor F', flow factor F'', thermal efficiency intercept $F_R a_P$, mean slope $F_R U_L$, pressure drop ΔP, fin efficiency F_{fin} and its corresponding overall fin-surface effectiveness ε_{fin}, all remained nearly the same as the values addressed in the section 6.6.1. This is because both the STF design and the water flow conditions kept unchanged, and hence the change of heat loss coefficient U_L (contributed by the radiation heat transfer coefficient in this case) could be ignored against the increase of air temperature.

6.6.3   Impact of surrounding air velocity

Under the test mode 3 presented in Table 6-2, the surrounding air velocity varied from 0 to 2 m/s while remaining other parameters constant, i.e., 493W/m² (90W) of the equivalent solar radiation (heater power), 20°C of surrounding air temperature, 1 l/min of water mass flow rate and 30°C of water inlet temperature. The simulation was carried out using the established computation programme, and the simulated results were then compared with the testing results in the same operational condition, which yielded the results in Figure 6-10.
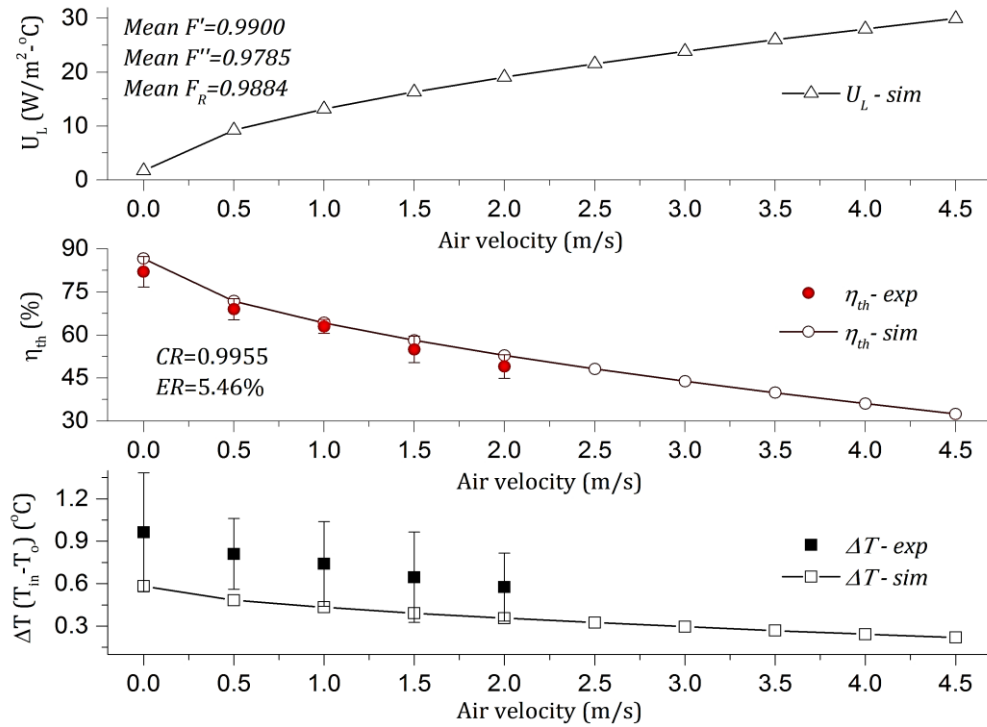
Figure 6-10 Performance curves of the proposed STF based on air velocity variation

Good agreement between the modelling and experimental results was observed with the CR and the ER of 0.9955 and 5.46% for the thermal efficiency respectively. It is found that increasing the surrounding air velocity decreased the STF surface temperature and thus reduced the corresponding temperature difference (ΔT) between inlet and outlet from 0.96°C to 0.58°C. Variation of the air velocity affected largely on the convective heat transfer coefficient and therefore the overall heat loss coefficient U_L. A larger air velocity led to greater heat loss from the STF surface, which weakened the solar heat gain and cut down the STF's thermal efficiency from 82.13% to 49.07% during the experiment. According to the simulation results, the overall heat loss coefficient U_L increased from 1.71 to 29.96 W/m^2-°C while the air velocity varied from 0 to 4.5 m/s. This led to slight changes in STF thermal efficiency factor F', flow factor F'' and heat removal factor F_R when comparing with the values in section 6.6.1. The other physical parameters, such as pressure drop ΔP, fin efficiency F_{fin} and its corre-

sponding overall fin-surface effectiveness ε_{fin}, all remained constant as the values in section 6.6.1 for the unchanged water flow conditions.

6.6.4   Impact of water mass flow rate

Under the test mode 4 presented in Table 6-2, the water mass flow rate varied from 0.I to 2 l/min while remaining other parameters constant, i.e., 493W/m² (90W) of the equivalent solar radiation (heater power), 20°C of surrounding air temperature, 1m/s of air velocity and 30°C of water inlet temperature. The simulation results that were carried out using the established computation model were then compared with the testing results conducted under the same operational condition, which yielded the results in Figure 6-11.
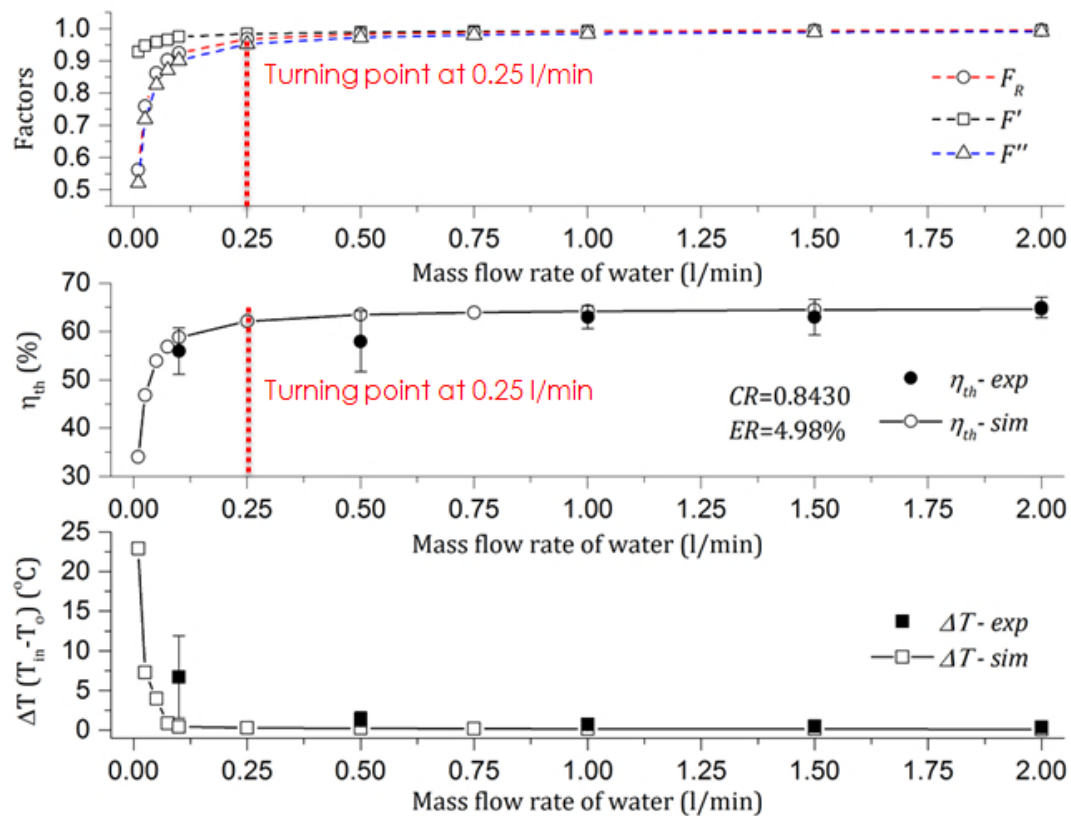
Figure 6-11 Physical factor curve & Performance curves of the proposed STF based on mass flow rate of water variation
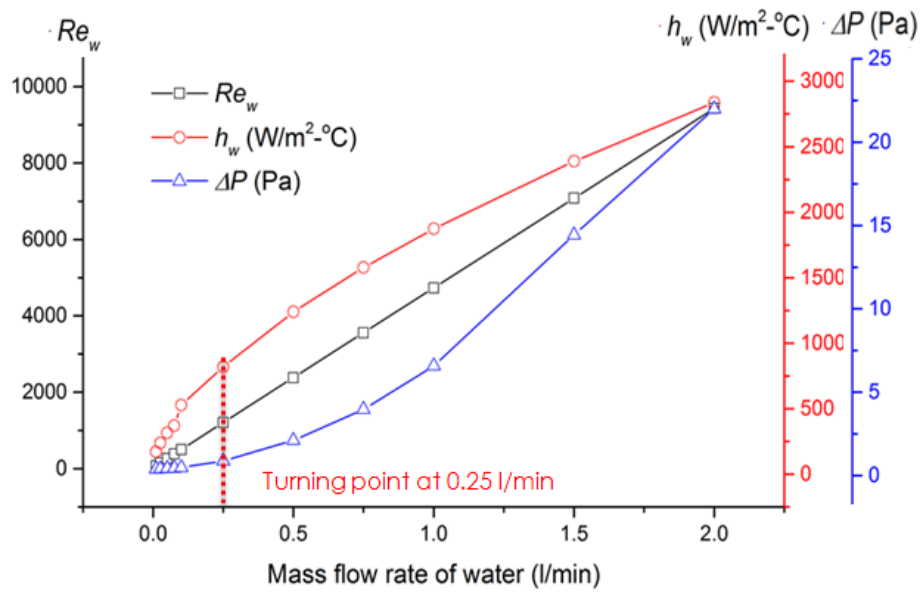
Figure 6-12 Reynold number, water heat transfer coefficient and pressure difference as a function of water mass flow rate

Good agreement between the modelling and experimental results was observed with the CR and the ER of 0.8430 and 4.98% for the thermal efficiency. It is found that increasing the water mass flow rate decreased the STF surface temperature and therefore reduced the corresponding temperature difference (ΔT) between inlet and outlet from 6.71℃ to 0.39℃. Variation of the mass flow rate largely affected on the heat transfer coefficient of water h_w. A larger mass flow rate led to greater heat removal capacity from the STF surface, which strengthened the solar heat gain and increased the STF's thermal efficiency from 56.33% to 65.47% during the experiment. However, the increase extent in the thermal efficiency became very limited upon the water mass flow rate over 0.25 l/min. This variation discipline also applied to the impact of the water mass flow rate on the physical parameters, like thermal efficiency factor F', flow factor F'' and heat removal factor F_R. According the simulation results indicated in Figure 6-12, the overall heat transfer coefficient of water flow h_w increased from 170.96 to 2837.90 W/m²-℃ while the mass flow rate varied from 0.01 to 2.0 l/min. This was because the Reynold number of water flow increased almost linearly against the variation of mass flow rate from

79.78 to 9432.10. The pressure drop ΔP, as a result, was raised up from about 0.002 Pa to 21.60 Pa owing to the increases in both maximum water flow velocity and the Reynold number. It is therefore suggested that the water mass flow rate should be at most 0.25 l/min for the current SFT design in order to achieve a pleasant solar thermal efficiency while consuming the least pumping power.

6.6.5   Impact of inlet water temperature

Under the test mode 5 presented in Table 6-2, the inlet water temperature varied from 20°C to 40°C while remaining other parameters constant, i.e., 493W/m² (90W) of the equivalent solar radiation (heater power), 20°C of surrounding air temperature, 1m/s of air velocity and 1 l/min of water mass flow rate. The simulation results that were carried out using the established computation model were then compared with the testing results conducted under the same operational condition, which yielded the results in Figure 6-13.
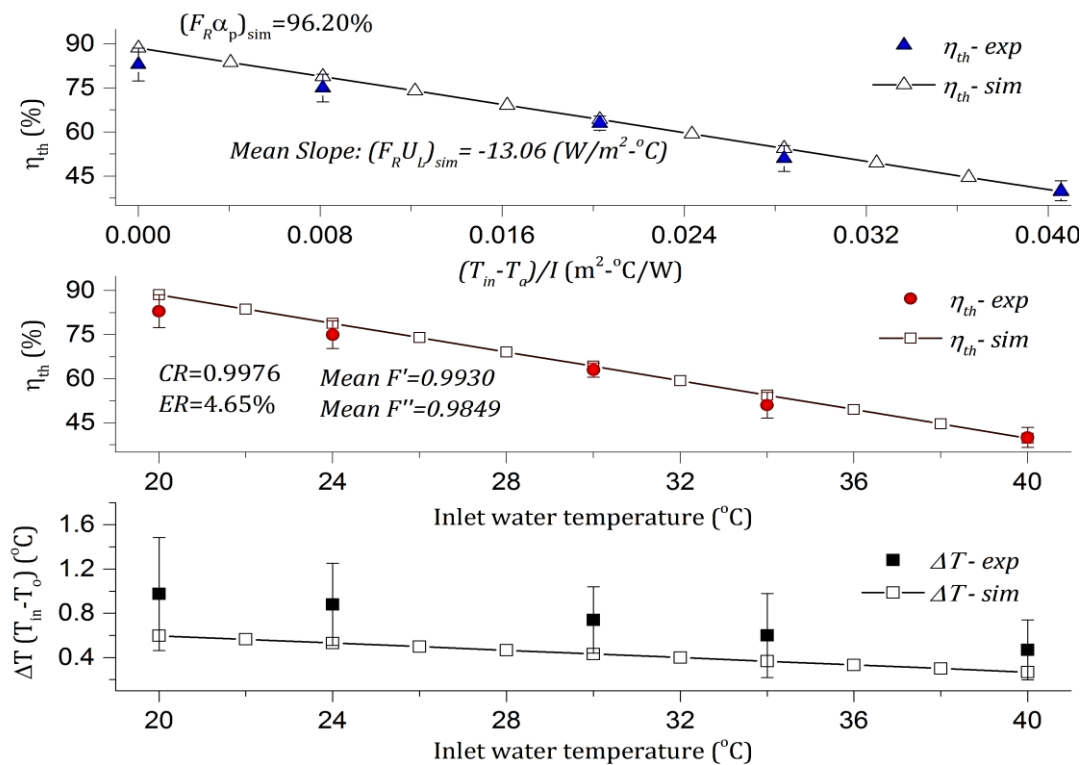
Figure 6-13 Linear regression graph & Performance curves of the proposed STF based on equivalent inlet water temperature variation
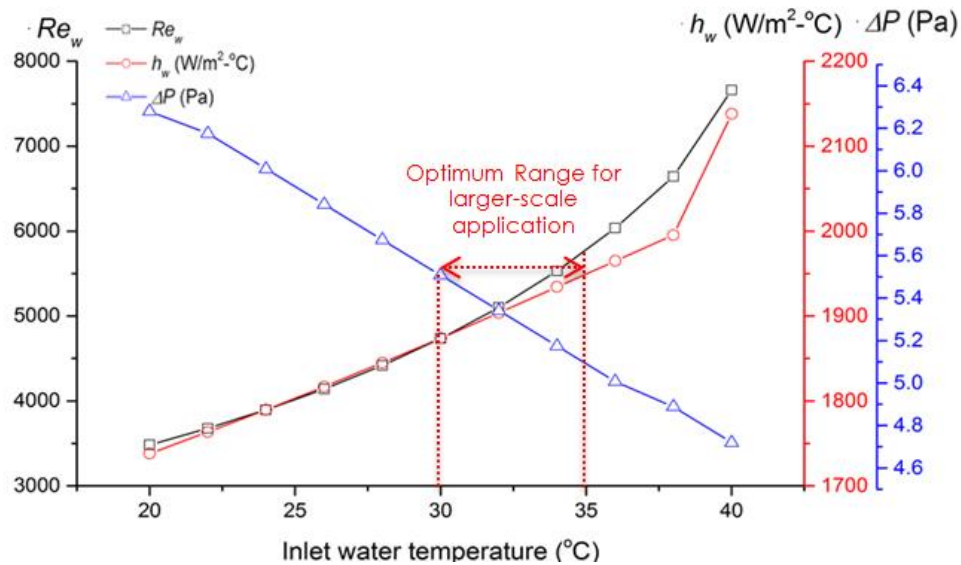
Figure 6-14 Reynold number, water heat transfer coefficient and pressure difference as a function of inlet water temperature

Good agreement between the modelling and experimental results was observed with the CR and the ER 0.9976 and 4.65% for the thermal efficiency. It is found that increasing the inlet water temperature reduced the water temperature difference (ΔT) directly between inlet and outlet from 0.97°C to 0.47°C. A higher inlet water temperature led to a greater temperature at the STF surface, which cut down solar heat gain by dissipating more heat to surroundings. So the STF's thermal efficiency decreased largely from 83.23% to 40.67% during the experiment. Meanwhile, variation of the inlet water temperature affected on the thermal properties of water and then the corresponding heat transfer coefficient h_w. This led to slightly changes in STF thermal efficiency factor F', flow factor F'', thermal efficiency intercept $F_R a_p$, mean slope $F_R U_L$, and fin efficiency F_{fin} when comparing with the values addressed in section 6.6.1. The overall fin-surface effectiveness ε_{fin} slightly decreased from 7.65 to 6.17 owing to the increased thermal properties of water.

According the simulation results indicated in Figure 6-14, the overall heat transfer coefficient of water flow, h_w increased from 1738.02 to

2138.10 W/m^2-°C, when the inlet water temperature varied from 20 °C to 40°C. This was because high water temperature increased the corresponding thermodynamic attributes and thus the Reynolds number varying from 3482.80 to 7660.60. Although the Reynold number and the correction factor χ increased against the inlet water temperature, the pressure drop ΔP reduced from about 6.28 Pa to 4.72 Pa. This was because higher water temperature led to the decreased water dynamic viscosity and therefore the reduced friction factor f, which dominates the overall the pressure drop ΔP oppositely to the inlet water temperature. Higher inlet water temperature brought the lower thermal efficiency but would consume a little bit less pumping power. It is therefore recommended that the appropriate inlet water temperature should be as low as possible when there is no concern about the power consumption from pump. But for a large-scale application, it is preferable to have around 30-35°C of inlet water temperature for current SFT design to achieve a trade-off between the solar thermal efficiency and the pumping power consumption.

6.6.6   Error and uncertainty analysis

Comparisons between the simulation and the experimental results as well as the uncertainty ratios under the five testing modes have been given in Figure 6-7, Figure 6-9, Figure 6-10, Figure 6-11 and Figure 6-13. In addition to the certain impacts from instruments, there are also some possible reasons for the deviations as the fluctuation of surrounding conditions (air temperature and velocity), the fluctuation of inlet water (temperature and flow rate), and the slight fluctuation of equivalent solar radiation due to voltage variation of electrical heating tap in the laboratory. Generally, the CR was found no less than 0.843, and the ER for the thermal efficiency were all below 5.46%. When considering the uncertainties existing in the measurement, the

validation results were acceptable for the general engineering applications. This indicated that the developed simulation model could predict the thermal performance of the proposed STF at a reasonable accuracy.

The above addressed discrepancies could be possibly caused by both (either) theoretical and (or) measurement inaccuracies. From the theoretical side, some simplified assumptions and empirical equations were involved, including ignorance of the heat losses across the insulation layers, neglecting the temperature gradient across the cover plate thickness, assumption of constant and uniform temperature over the fin surface, and adopting the empirical equations for calculating *Nusselt* number, etc. From the experimental side, a few of uncertainties addressed above may be the potential reasons for the deviation. However, the experimental measures were less likely to cause the major errors owing to the effective instrument and the repeated operations. Based on these considerations, the errors may be attributed by the theoretical inaccuracies and it would be better for the simulation model to be refined to further improve its accuracy in prediction based on the experimental results.

6.7 Chapter executive summary

This chapter provided a method for fabricating the STF hot water system and examined its characteristic performance, which provided useful clues for the further development of large-scale system and how to achieve the potential optimal system performance in terms of appropriate configuration parameters and favourable operational conditions.

The characteristics of operating performance are summarized in Table 6-4 according to parallel comparison between the STF's thermal efficiency and operational conditions.

Table 6-4 Characteristics of the operating performance exploration in STF

No.	Variables	Characteristics of operating performance
1	Solar radiation (500-1000W/m^2)	A higher solar radiation yielded an enhanced solar heat transfer, improving the solar heat gain and the STF's thermal efficiency from 63.21% to 72.32%, while its thermal efficiency factor F', flow factor F'' stayed constant at 0.993 and 0.985 respectively. And the stable fin efficiency F_{fin} of 0.963 and its overall effectiveness ε_{fin} over almost 7.02, represented a really high-efficient heat transfer at the finned STF surface;
2	Surrounding air temperature (15-24 ℃)	A higher air temperature led to less heat loss from the STF surface, which helped to improve solar heat gain and the STF's thermal efficiency from 63.21% to 71.44%. And the STF thermal efficiency factor F', flow factor F'', fin efficiency F_{fin} and its corresponding overall fin-surface effectiveness ε_{fin}, all stayed nearly the same as in No. 1;
3	Surrounding air velocity （0-4.5 m/s）	A larger air velocity led to greater heat loss from the STF surface, which weakened the solar heat gain and cut down the STF's thermal efficiency from 82.13% to 49.07%. This also led to the slightly changes in STF thermal efficiency factor F', flow factor F'' and heat removal factor F_R when comparing with the values addressed in No. 1;
4	Water mass flow rate （0-2.0 l/min）	A larger mass flow rate led to increases in heat removal capacity, thermal efficiency factor F', flow factor F'' and heat removal factor F_R, but the increase extent in the thermal efficiency became very limited after the water mass flow rate in excess of 0.25 l/min;
5	Inlet water temperature (20-40 ℃)	Increasing the inlet water temperature reduced the STF's thermal efficiency largely from 83.23% to 40.67%. However, this led to the slightly changes in STF thermal efficiency factor F', flow factor F'', and fin efficiency F_{fin} when comparing with the values addressed in the section 6.6.1. The overall fin-surface effectiveness ε_{fin} slightly decreased from 7.65 to 6.17 owing to the increased thermal properties of water.

In addition, the maximum theoretical possible useful heat gain capacity and the sharp mean slope ($F_R U_L$) match well with the feature of the unglazed STF module, which in no glazing cover attached in the front. So in case of current design, such STF could match the applications of heating load for pool heating, domestic hot water and radiant space heating in those areas with warm air temperature and sufficient solar radiation.

7

EARLY DESIGN STAGE OF THE STF FOR BUILDING INTEGRATION: ENERGY PERFORMANCE SIMULA-TION AND SOCIO-ECONOMIC ANALYSIS

7.1   Chapter abstract

This chapter explores the operating performance of the proposed STF hot water system for whole building application, as well as the related environmental benefits. It also evaluates the socio-economic feasibility of such STF system through a decicated business model for the early design stage assessment. Generally, it is intended to complete the following tasks:

1) Introduce a techno-economic research approach to access the 'cost effective' concept for the proposed STF system;

2) Establish an integrated simulation model of a reference residential building model derived from DOE with the associated inputs;

3) Operate the validated STF simulation model to produce the characteristic performance parameters of the prototype in Shanghai;

4) Analyse the simulation results;

5) Incorporate a dynamic business model to assess the potential investment feasibility of the proposed STF system.

This part research presents a novel multidisciplinary research method that is expected to be beneficial for the strategic decision at the early design stage for the proposed STF integration design. Moreover, it offers a different angle to assess the economic performance of the STF application.

7.2   Strategy of the techno-economic research

In terms of a new concept for building integration, the reliable theoretical analysis and simulation would often an effective and common way to investigate the adaptability and feasibility of the proposed concept in a dedicated climate region, especially at the early stage for building design or renovation.

The simulation can compare the effectiveness of the proposed design in different scenarios affected by weather condition, governmental policy, and energy tariffs etc., which presents the greatest opportunity to achieve the high energy performance building after construction or refurbishment. Since most planning of building services are usually decided at early design stage, it is very useful to provide the pertinent energy performance information for the designer or the decision-maker from multidisciplinary and comparative points of view. This research strategy would be consequently useful in guiding the practical design of the proposed STF system in new building design or building renovation.

Step 1: Acquisition of characteristic performance values of the proposed STF system;

Step 2: Choose of a reliable simulation engine;

Step 3: Operation of the integrated building simulation model to study energy potentials & comfort challenges;

Step 4: Set business model combined with simulated results and basic financial data for the adaptability and feasibility investigation;

Step 5: Recommendations for strategic decisions at the early design stage.

Figure 7-1 Multidisciplinary simulation strategy for the proposed STF proposal

Figure 7-1 illustrates the research paths in providing strategic support in the techno-economic aspect for the designer to make decision on applying the proposed STF proposal at the early design stage.

1) The first step is to input the characteristic performance parameters from the validated STF simulation model into a DoE reference residential building model with all design parameters derived from ASHRAE standards;

2) Then to run a reliable building simulation within the combi-simulation engine that has the reasonable accuracy in predicting overall building energy performance;

3) From the integrated building simulation model, it can estimate energy/carbon emission conservation potential and possible comfort challenge in building environment with the STF proposal in a dedicated climate region;

4) After those, the adaptability and feasibility study under different scenarios can be carried out using the business model involved with basic financial data.

5) Finally, recommendations can be given for building design or renovation with the proposed STF system at early design stage.

7.3   Simulation tool selection and its research process

In practice, various kinds of simulation programs have been found to build the link between theoretical analyses and practical application. Each tool has its own characteristics and possibilities in the field of dimensioning renewable technology size, optimizing renewable technology solution and expecting both solar yield and energy conservation amount in a building (Witzig, 2009).

Table 7-1 Capabilities of simulation software in performance prediction

Software name	Adaptation	Thermal	Optical	Electrical
ESP-r	×	√	√	√
EnergyPlus	×	√	√	√
TRNSYS	√	√	×	√
IES (VE)	√	√	√	√

From the comparison in Table 7-1, IES (VE) software was finally selected for the supplementary prediction and interpretation of the multiply functioned building facade component at the early design stage elevation. The reasons are its prediction capacities covering: 1) adaptive features of building shell; 2) physical interactions between the novel component and the building envelope; 3) a mix of solar resource and thermal performance indicators; and 4) renewable energy assessment (Zhang et al., 2015b).
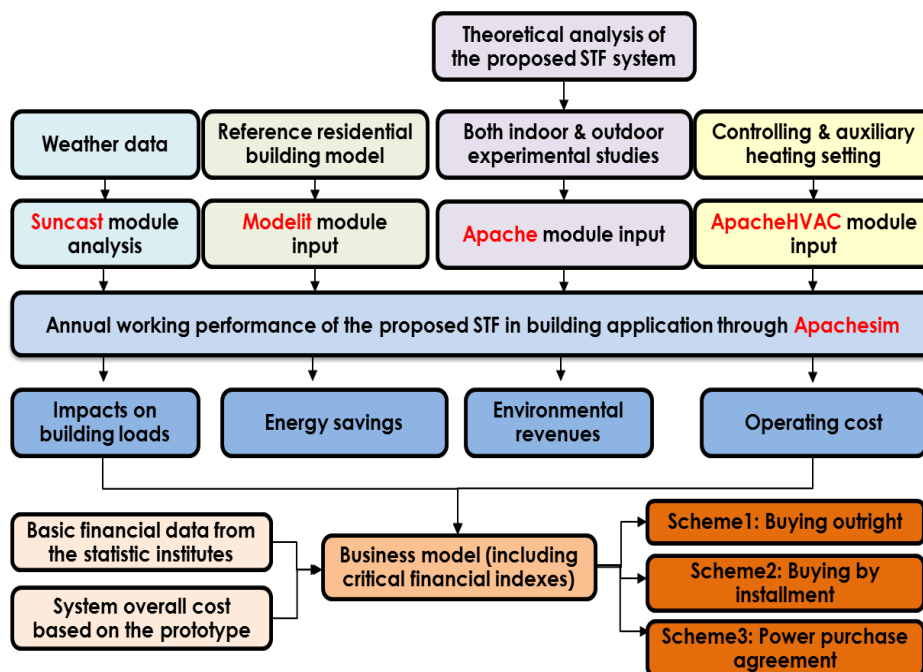
Figure 7-2 Schematic of simulation method for STF system in the reference residential building in IES (VE) software

Figure 7-2 shows a schematic simulation process in IES (VE) software that is used for the indoor thermal environment assessment, the dynamic time-step energy prediction, and the operating cost estimation of the STF proposal implementation in a referenced residential building. The whole simulation involved with a suite of integrated analysis modules, as *Modelit*, *Suncast*, *Apachesim* and *ApachHVAC*.

Firstly, both the building model and the proposed STF component were initially input in *Modelit*. And then, *Suncast* was utilized to pre-process all the exposed facade states for the purposes of annual time-series solar factor values, annual solar exposure hours and the received solar energy. According to the relevant studies (Buker, M. & Riffat, 2014; Schimpf & Span, 2015; Fudholi, *et al.*, 2015), the characteristic performance parameters of STF system derived from previously validated simulation model were input into *Apachesim* for the overall dynamic building environment modelling, while basic controlling and auxiliary heating were roughly realized in *ApachHVAC*.

The whole simulation is targeted to explore the thermal environment assessment, the dynamic time-step energy prediction and the operating cost estimation at whole building level, thereby assessing how the integrated renewable technology physical interacts with building construction, and to understand the associated operational performance in a larger-scale application.

7.4   Reference building model

The reference building model is a south-facing high-rise residential building, derived from the U.S. Department of Energy (DOE, 2004). DOE has developed a series of reference building energy models to represent realistic building characteristics and construction practices for research purpose.

As a result, the residential building model together with a complete package of descriptions in dynamic simulation software was selected here as a starting point in the energetic performance evaluation for the STF building integrated application (NREL, 2011). All the dimensions and basic construction information of the reference building are given in Figure 7-3 and Table 7-2. And the basic settings and schedule

profiles in the overall building energy analysis are listed in Figure 7-5 and Table 7-3.
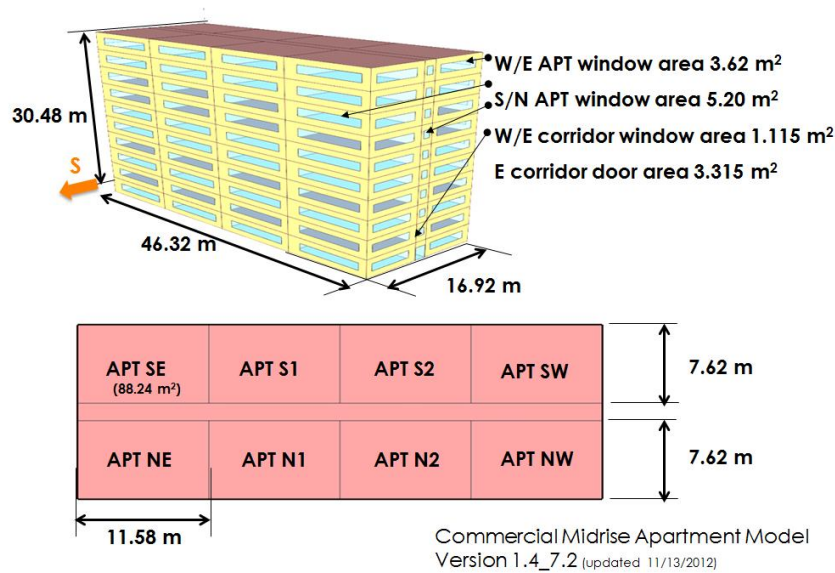
Figure 7-3 Dimension of the reference residential building (NREL, 2011)

7.5   Characterization of STF component in the model

The STF system was interacted physically within original building construction, and operated with HVAC system synergistically for a year. The detailed data flow and components connection in the proposed STF system is presented in Figure 7-4. It interprets how each component link to the others in both physical and information ways within the model.
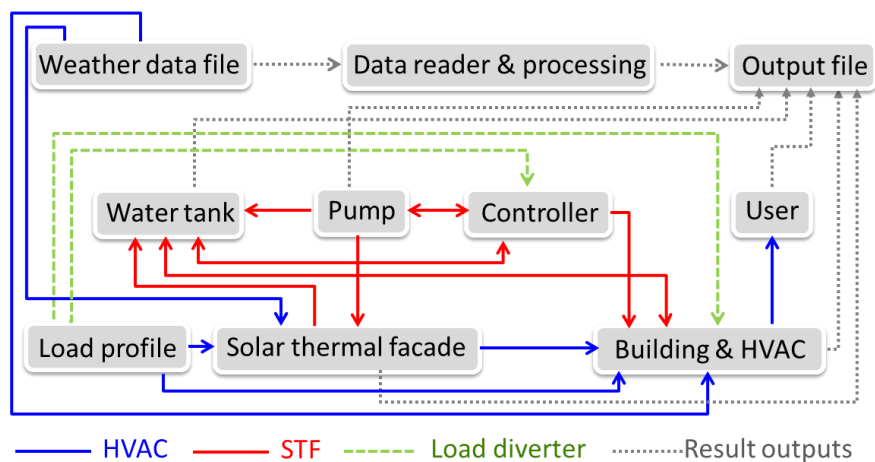
Figure 7-4 Schematic of system components connection for the proposed STF system in IES (VE) software
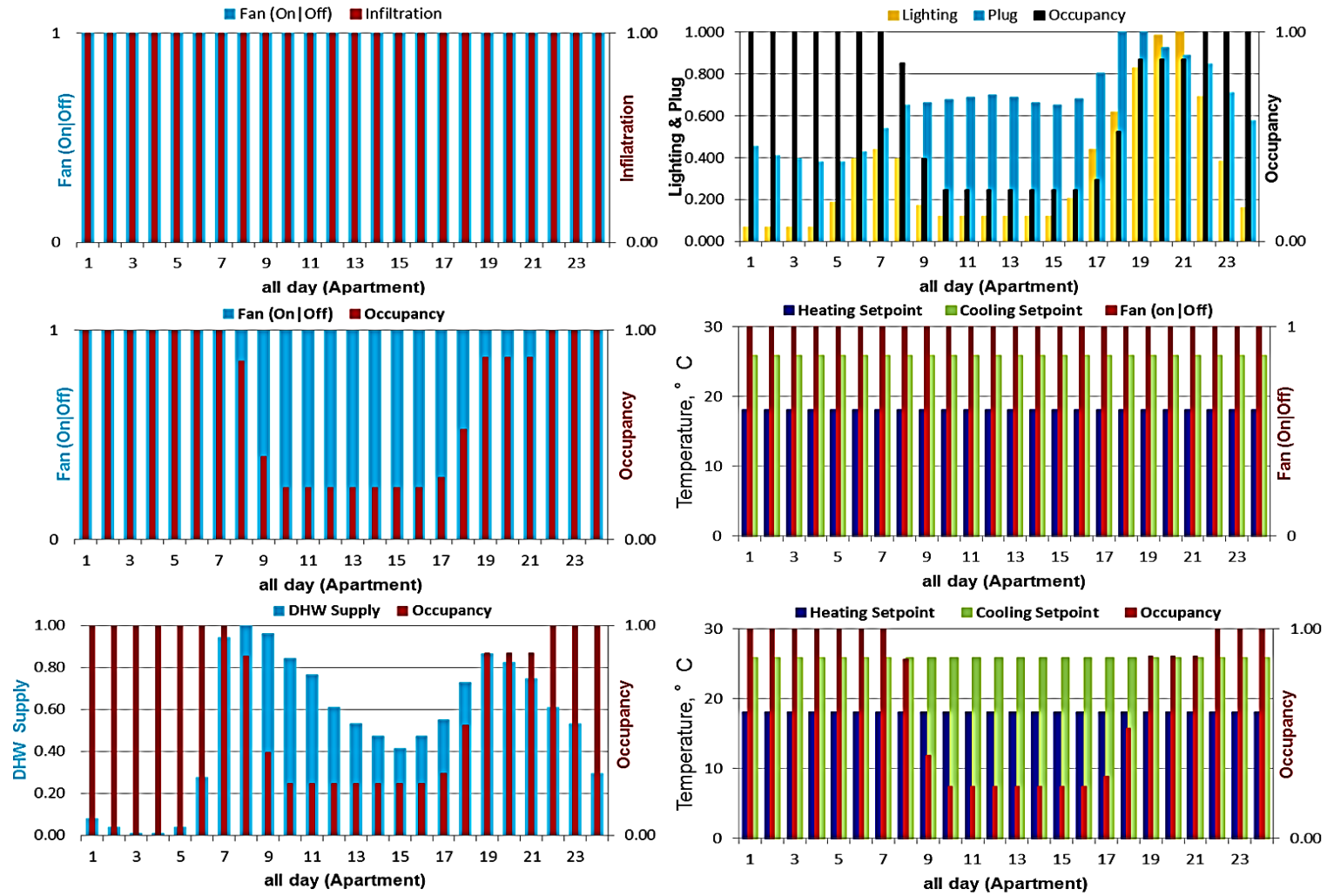
Figure 7-5 Schedule plots in the reference residential building model (NREL, 2011)

Table 7-2 Building summary of the simulated residential building model (NREL, 2011)

Item	Descriptions	Data Source
Form		
Total Floor Area	7,837 m^2	PNNL-16770: *Analysis of Energy Saving Impacts of ASHRAE 90.1-2004 for the State of New York*
Aspect Ratio	2.75	
Number of Floors	10	90.1 Envelope Subcommittee
Window-to-Wall Ratio	Average Total: 30%	Based on feedback from the National Multi-family Housing Council
Floor-floor height	3.05 m	
Sill height	1 m	
Architecture		
Exterior wall construction	U-value of 0.46 W/m^{2}K , 1cm plaster/60 cm XPS insulation/3 cm plaster/200cm concrete block/10cm plaster	
STF wall construction	U-value of 0.46 W/m^{2}K , 5 mm STF/60 cm XPS insulation/3 cm plaster/200cm concrete block/10cm plaster	
Roof construction	Built-up Roof: Roof membrane/Roof insulation/metal decking	PNNL-16770: Analysis of Energy Saving Impacts of ASHRAE 90.1-2004 for the State of New York. Base Assembly from 90.1 App. A.
Window dimensions	4.27m*1.69m/6.27m*1.69m	
Foundation Type	Slab-on-grade floors (unheated) with 8" concrete slab poured directly on to the earth	
Interior partitions construction	2 x 4 stud wall	
Internal Mass	8 lbs/ft^2 of floor area	Building America Research Benchmark
HVAC		
HVAC system	Heat Pump+ Water heater with storage tank (50°C as water temperature set point)	
Thermostat Setpoint	26°C Cooling/18°C Heating	
Fuel type	Electricity/Solar energy	PNNL 2014. Enhancements to ASHRAE Standard 90.1 Prototype Building Models
Thermal efficiency	ASHRAE 90.1 Requirements/ 68%	ASHRAE 90.1
Tank Volume	10,000 L (central)/100 l per APT	PNNL 2014. Enhancements to ASHRAE Standard 90.1 Prototype

Note: 1) This model is updated by Pacific Northwest National Laboratory on 03-21-2014
2) Briggs, R.S., R.G. Lucas, and Z.T. Taylor. 2003. Climate Classification for Building Energy Codes and Standards: Part 2—Zone Definitions, Maps, and Comparisons. ASHRAE Transactions 109(2).
3) Gowri K, MA Halverson, and EE Richman. 2007. Analysis of Energy Saving Impacts of ASHRAE 90.1-2004 for New York. PNNL-16770, Pacific Northwest National Laboratory, Richland, WA. http://www.pnl.gov/main/publications/external/technical_reports/PNNL-16770.pdf

4) Gowri K, DW Winiarski, and RE Jarnagin. 2009. Infiltration modeling guidelines for commercial building energy analysis . PNNL-18898, Pacific Northwest National Laboratory, Richland, WA. http://www.pnl.gov/main/publications/external/technical_reports/PNNL-18898.pdf
5) Building America Research Benchmark. http://www1.eere.energy.gov/buildings/building_america/index.html
6) DOE Commercial Reference Building Models of the National Building Stock: http://www.nrel.gov/docs/fy11osti/46861.pdf
7) RECS 2005. EIA's Residential Energy Consumption Survey. http://www.eia.doe.gov/emeu/recs/
8)PNNL. 2014. Enhancements to ASHRAE Standard 90.1 Prototype Building Models. Pacific Northwest National Laboratory, Richland, Washington. Available at
https://www.energycodes.gov/development/commercial/90.1_models.

Table 7-3 Assumptions of internal gains in the simulated residential building model (NREL, 2011)

Zone[1]	Area (m²)	Multipliers	People (m²/per)	Num. of People	Total ventilation (m³/h)[3]	Lighting (W/m²)[4]	Plug & Process (W/m²)[5]
G SW APT	88.26	1	35.33	2.5	94	3.78	6.67
G SE APT	88.26	1	35.33	2.5	94	3.78	6.67
G NW LOBBY	88.26	1	88.26	1.0	137	11.85	6.67
G NE/N1/N2/S1/S2 APTs	88.26	1	35.33	2.5	94	3.78	6.67
M SW/NW/SE/NE/N1/N2/S1/S2 APTs	88.26	8	35.33	2.5	94	3.78	6.67
T SW/NW/SE/NE/N1/N2/S1/S2 APT	88.26	1	35.33	2.5	94	3.78	6.67
T CORRI.[2]	77.67	1	--	--	85	5.94	264.37
G/M CORRIs.	77.67	1	--	--	85	5.94	--
TOTAL[3]	7,838	--	--	199	--	--	--
AREA WEIGHTED AVERAGE			32.42	--	--	4.08	8.63

Note: 1. Each APT zone contains one APT with two bedrooms, one living room and one bathroom;.
2. SW/NW/SE/NE/N1/N2/S1/S2 stand for rooms in Figure 7-3;;
3. Elevator load is added in the top floor corridor zone; And the minimum outdoor ventilation air requirements are from ASHARE 90.1-2010 (62.1-2007;)
4. Lighting Load Calculation Assumptions = (455 + 0.8 x Area)*0.8 *1000 / 365/Daily operation frequency from profile/ Area
 (Reference - Hendron R. 2008. Building America Research Benchmark Definition. TP-550-44816, National Renewable Energy Laboratory, Golden, Colorado))
5 Annual Appliance and Equipment Loads for Apartment (Source: Building America Research Benchmark) and Benchmark Annual Energy Consumption for Miscellaneous Electric and Gas Loads.

The proposed STF set was assumed with 4 stainless steel STF components for a household (0.6 m×1m×5mm for each one, illustrated in Figure 4-2 and Variant b in Figure 4-9). In practice, there exist heat transfer interactions between the STF module and the building envelope. For instance, part of the heat loss from the STF module will be transferred into the building envelope in summer increasing the cooling load accordingly. On the other hand, the STF will also reduce the heat loss from the building envelope in winter period and decrease the heating load as a result.

$$Q_{in\text{-}load} = k_{STF} \times A_{STF} \times (T_{STF} - T_{BE}) \qquad\qquad [7\text{-}1]$$

Equation [7-1] describes the basic interaction load $Q_{in\text{-}load}$ caused by heat transfer between the STF module and the building envelope using overall heat transfer coefficient k_{STF}, collecting area A_{STF} and temperature difference between the STF T_{STF} and building envelope T_{BE}. If the basic interaction load $Q_{in\text{-}load}$ is positive, it stands for the heat gain from the STF to the building envelop, whereas the heat loss from the STF to the building envelop. In the IES (VE) software, the basic interaction load represents as the external heat gain and temperature fluctuant feedbacks to the *Output File*. And the exchanged solar heat represents as heated water in the *Building and HVAC Output File*.

As a renewable system entity, the STF module is connected into the DHW system with circulation water pump, tee joint, valve, internal heat exchanger and water tank. The solar energy conversion and transfer with the STF module should involve these inter-linked processes, namely:

1) Absorbing the certain percentage of striking solar radiation;
2) Converting the absorbed energy into thermal heat;
3) Transporting thermal heat into the passing working fluid or transferring heat to/from the building envelope;
4) Exchanging the received heat in water tank.

7.6   Climate analysis of Shanghai China

The climate data applied in the model is derived from the standard FWT as the Example Weather Year file that contain individual weather years sourced from the Energy Plus website. The studied location is-Shanghai, China with the elevation of 7 m, the Latitude/Longitude of 31°11'N and 121°29'E.
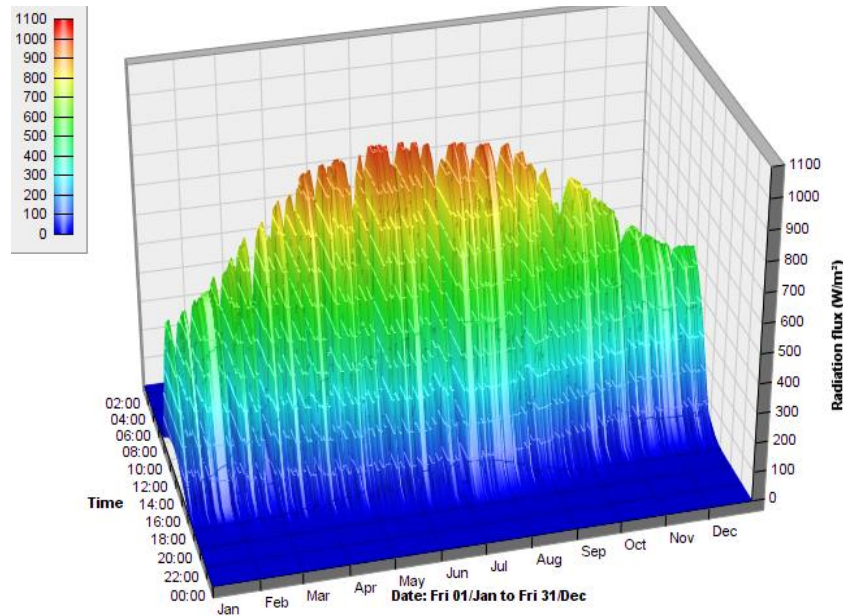
Figure 7-6 3D graph of global solar radiation flux in Shanghai

Figure 7-6 presents the global irradiance of Shanghai. The data are in great fluctuation, ranging from severely overcast conditions with about 100 W/m² to 1013 W/m² when the sky is clear. According this solar resource, Shanghai seems to be able to achieve the average annual global radiation of 1,237 kWh/(m²/p.a.). Continued with the solar shading analysis in *Suncase*, Figure 7-7 clearly illustrates the available solar resources around the reference residential building. It has been identified that the vertical wall has the radiation flux around 776 kWh/(m²/p.a.) with around 80% solar exposure time each year, showing a suitable solar radiation resource for STF application.
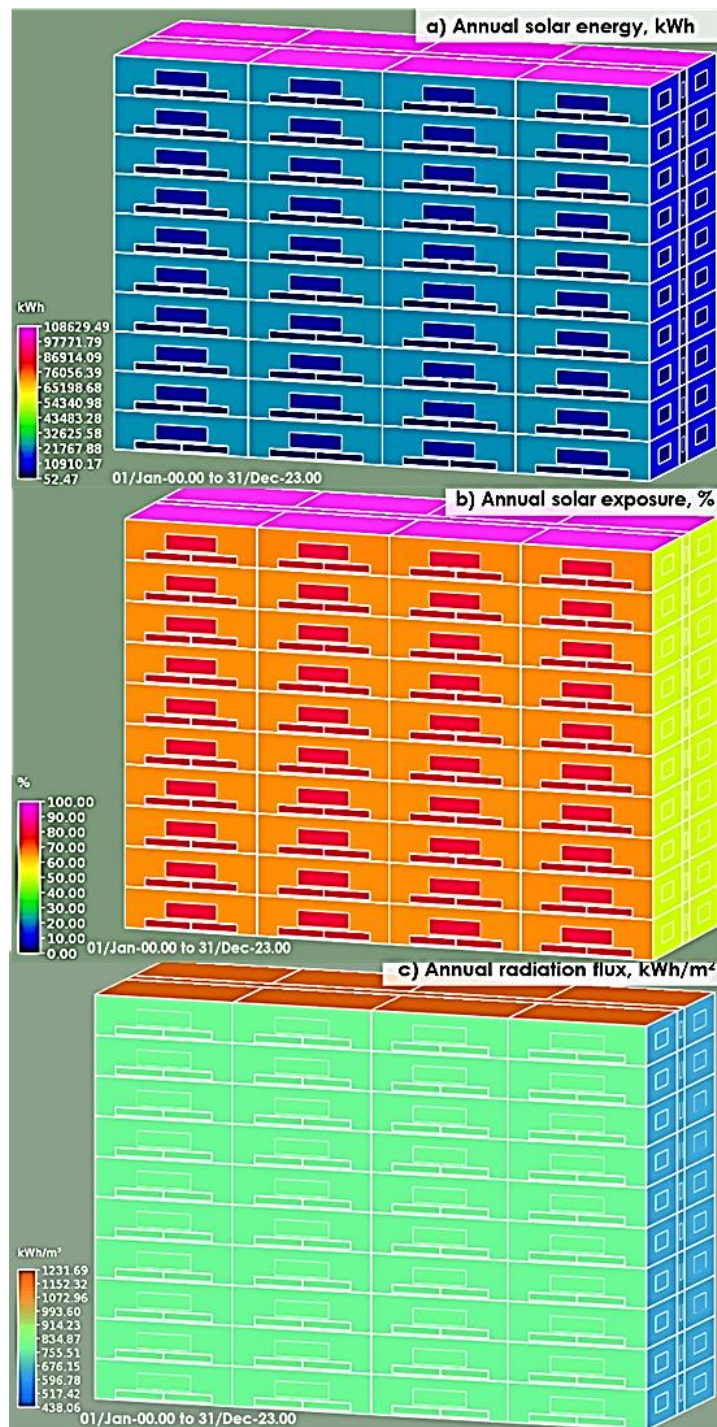
Figure 7-7 Colour gradient diagrams of reference residential building model from Suncast calculation

7.7   Characteristic annual operational performance parameters of the STF system

Given the good level of agreement achieved between the simulation

and the experimental test results, the previously established simulation

model is appropriate for characterizing the annual operational performance of the STF module via inputting monthly average weather data in dedicated Shanghai region (given in Table 7-4).

Table 7-4 Monthly average weather data in the Shanghai region (Zhang et al., 2014)

Month	Ground water temperature(°C)	Wind speed (m/s)	Air temperature (°C)	Solar radiation (W/m²)
Jan.	5.5	3.11	4.3	193.22
Feb.	7.5	3.05	5.5	235.54
Mar.	11.4	3.05	8.9	253.21
Apr.	15.2	3.97	14.6	317.44
May.	22.3	3.26	19.9	316.07
Jun.	26.0	2.57	24.0	293.90
Jul.	27.0	4.03	28.2	366.61
Aug.	25.1	2.62	27.7	387.83
Sep.	20.8	3.81	23.8	282.55
Oct.	15.3	2.7	18.2	301.80
Nov.	10.0	3.11	12.2	266.28
Dec.	6.4	2.65	7.1	230.08
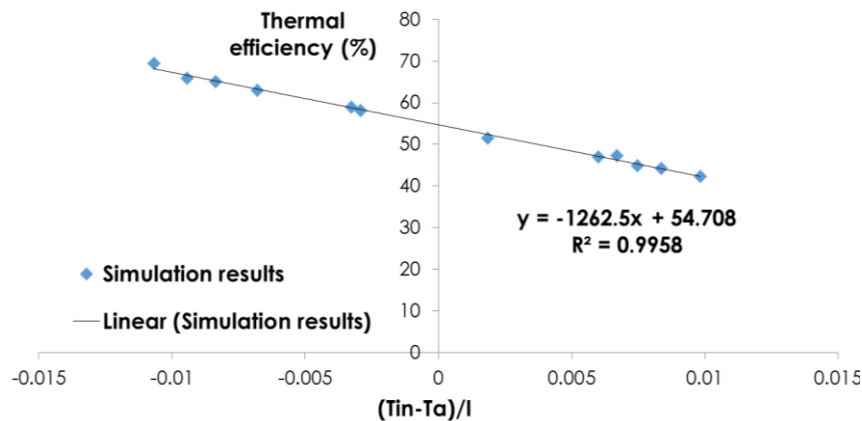
Figure 7-8 Best fit line for the simulation results of STF module thermal efficiency

According to the simulation results, the plotted η_{th} against the external weather and operational parameters $(T_{in} - T_a)/I$ can be determined by the linear fit method, as shown in Figure 7-8. The regression result is presented in the following expression with a correlation coefficient, R^2 of 0.9958:

$$\eta_{th} = -1262.5x + 54.708 \ (unit: \%) \tag{7-2}$$

It needs to be mentioned that there were some assumptions in order to simplify the simulation at the early design stage. Based on the

characteristic thermal performance and the preliminary estimation in the software, the basic settings of a typical STF component are:

1) U-value of 0.46 W/m^2k;

2) Emissivity and solar absorbance of 0.09 and 0.97 respectively;

3) Optical solar thermal efficiency of 54.708%;

4) First order heat loss correction value of 12.625 W/m^2k;

5) Assumed internal heat exchanger effectiveness of 84%;

6) Assumed decentralized DHW delivery efficiency of 90%.

7.8   Dynamic building environmental simulation results

Within this step, the characteristic performance of the STF was considered as principal technical parameters into the integrated building energy simulation model within the IES (VE) software. It is believed that the solar thermal efficiency may vary with lots of factors in practice and they are very hard (sometimes impossible) to consider during the integrated simulation of building energy performance. In this case, most of simulation models currently apply the normalization method to simplify the simulation algorithm and focus on the specific impacting factors during the quantitative and strategic analyses.

Based on this principle, this section takes the characteristic values of solar thermal efficiency and treats them as the annual mean energy performance of the STF system in broad terms during simulation. Such approach weakens/downplays the impact of system's variation but emphasizes the overall impact of the STF system to the building energy performance and the corresponding economic strategies to determine their effectiveness in achieving energy savings during the early design stage.

7.8.1   Annual temperature profile in the STF module

Figure 7-9 identifies that the humid subtropical climate of Shanghai has a clear seasonal change. In the simulation, the main heating period, defined as outdoor dry-bulb temperature below 18°C, (the period before the middle of April and after the middle of October), while the main cooling period, defined as outdoor dry-bulb temperature above 26°C(the period from the middle of June to the middle of September) in this model.

Moreover, Figure 7-9 further shows the annual mean temperature profile of the STF modules on the 5th floor as it was particularly selected as the target sample. Based on the maximum set-off temperature at 50 °C for the whole DHW system, it could be discovered that the mean module temperature similarly fluctuates along with the outdoor air temperature. Its vulnerability to environmental impact exactly fits the characteristic of the unglazed metal solar absorber. The STF sur-face temperature range varied from 5.12 °C to 37.01°C in a year which are above the corresponding air temperatures during different months. As a result, it stated that there is lower risk associated with freezing and stagnation problems, and the STF module can contribute energy to the DHW load yet it requires further heat upgrade as to achieve the required supply water temperature.

7.8.2   Water temperature profile in the system tank

Before the auxiliary heating system starts to operate, the water temperature in the tank would be heated up directly from the solar radiation source. As a result, it provides an intuitive way to assess the quality of useful solar resource from the STF modules. From Figure 7-10, it could be known that the temperature of water in the tank varied a lot in the early months, and most of them were below the set-off temperature of 50°C. This was sigficantly affected by the small

amount of vertical solar heat gain during early months. Especially in June, the available solar heat again on the vertical surface became the least, leading to the lowest water temperature profile in the tank in that month. Afterthen, the water temperature remained at higher level in consistency with the variation of solar heat gain.

In conclusion, it is obvious that the water temperature varied dependently with solar gain. The frequency in the water temperature variations above certain temperature levels can be summarised as:

1) Temperature above 50°C was about 2.1% period of a year;
2) Temperature between 45-50°C was nearly 32.2% period of a year;
3) Temperature between 40-45°C was around 23.2% period of a year;
4) Temperature between 35-40°C was about 21.3% period of a year;
5) Temperature between 30-35°C in about 15% period of a year;
6) Temperature between 25-30°C was around 6.1% period of a year;
7) Temperature below 25°C was only 0.1% period of a year;

7.8.3   Impacts of the STF system on energy load

Table 7-5 displays the breakdowns of heating and cooling loads, as well as solar heat input in the reference residential building model. The simulation results indicated that the total amount of contribution coming from the STF system was 9,368kWh for the heating and cooling loads with the average amount about 780.7kWh each month. Apart from the direct contribution to space conditiing load, more indirect impacts have been found. As a whole, the application of STF resulted in a general decrease in space conditiing load. But the impact on the heating load was relatively greater than the cooling load. In summary, the total heating load also decreased from 202.881MWh to 198.489 MWh, with an average decrease rate of 2.16%, while the total cooling load decreased from 207.501MWh to 206.209MWh with an average decrease rate of 0.62%.
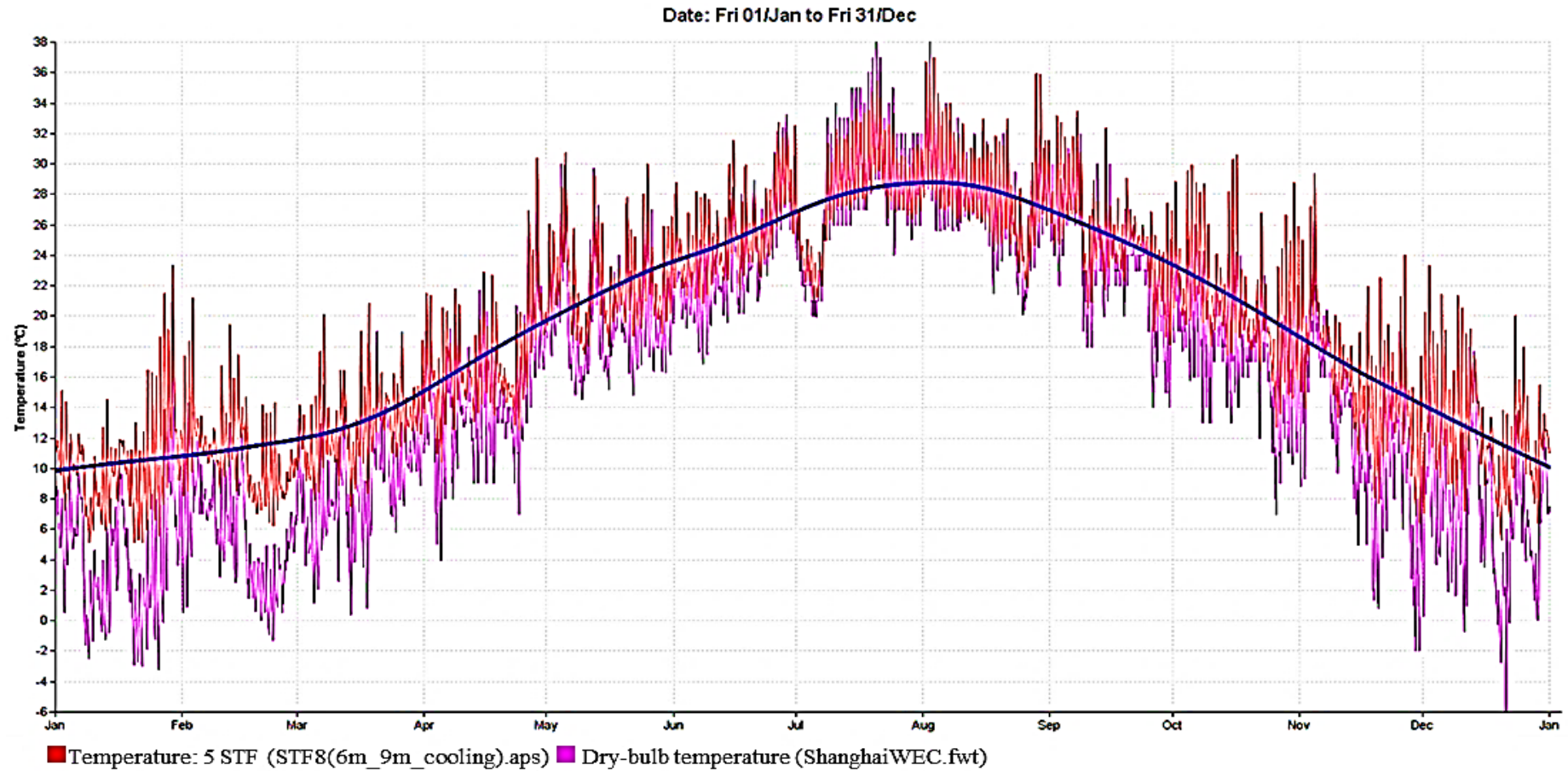
Figure 7-9 Annual mean temperature profile of the STF module on the 5th floor
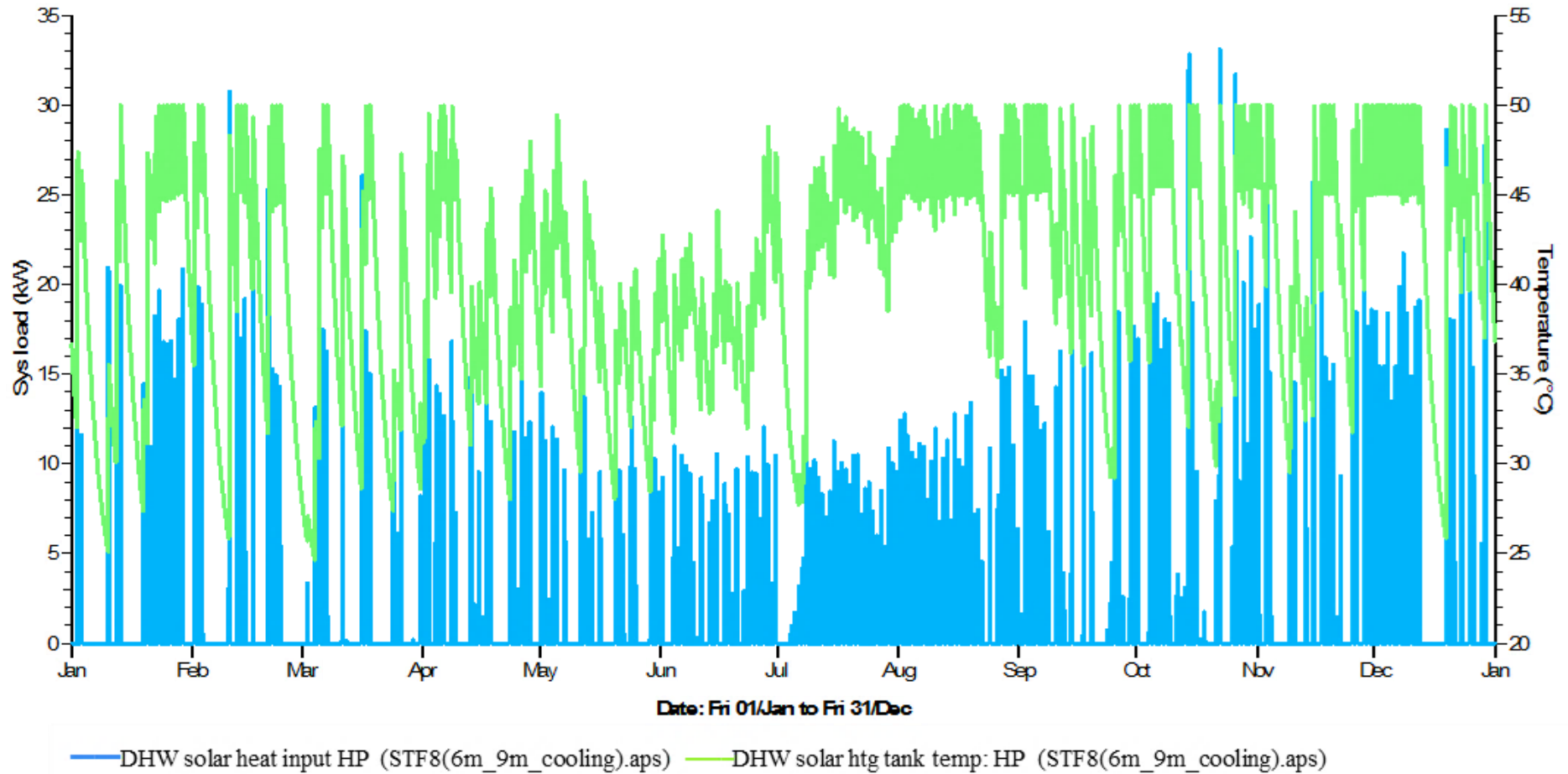
Figure 7-10 Annual variations in DHW solar water tank temperature against solar heating gain

The building integration with the STF affects the overall building energy performance through changes in the emissivity and the solar absorbance of the building envelope, and the corresponding temperature difference between the STF module and the original building envelope. By means of the dynamic building environmental simulation, Table 7-6 listed the external conduction gains in the typical floor, 5th floor, which specially demonstrated the different heat transfer amounts through between the envelopes coupled with STF and the conventional ones. In general, the total external conduction gain through the envelope coupled with STF was less than in the conventional ones, showing that the application of STF was useful to decrease negative external conduction.

As a result, the overall contribution of the STF application in such a case included both the direct solar heat gain (energy generation) and the decrease of indirect space conditiing load (demand reduction).

7.8.4   Energy saving, environmental revenue, and operation cost

On the basis of the caloric value, carbon emission factor and individual energy tariffs of Shanghai, the simualtion was performed to calculate the energy consumption, carbon emission and operational cost of the whole building presented in Table 7-7.

In terms of annual energy consumption, the dedicated building consumed total energy of 652,182kWh, showing substantial savings in total energy consumption with the specific solar thermal energy yield from the STF system around 45,727kWh. Although the additional system auxilary and pump energy consumption slightly added, the overall energy still has a net energy conservation amount of 85,270 kWh.

In terms of annual CO$_2$ emission reduction, the STF device contributed a total carbon emission reduction of 69,240 kgCO$_2$ on the condition that 1 kWh of the grid electricity emits 0.812 kg of CO$_2$ in the east region of China. When this energy saving amount is transferred into the standard coal amount for the Chinese energy efficiency subsidy application, the saved standard coal weight is estimated around 9.5ton.

While **in terms of annual operational cost**, the savings caused by STF application through modelling was about ¥93,799 per year on the condition that 1 kWh of the grid electricity costs ¥ 1.11 in Shanghai.

Meanwhile, the total investment was listed in Table 7-8 that comprises the cost of each component, sale profit (30% of the sub-total cost), Value Added Tax (VAT) (17% of profit) and installation cost (30% of the sub-total system cost). The total initial investment of the STF upgrade (total 80 sets) for the whole building was therefore estimated around ¥423,800. From an engineering perspective, it is usual to access the annual operational savings to appraise the cost effectiveness of an emerging technology. The result of annual operating savings shows that the Static Payback Period (SPP) of the STF investment is around 4.5 years. Through the quick and approximate assessment, the STF upgrade could be hereby regarded as an acceptable investment option. However, the SPP overlooked basic finanical related elements, such as cost of capital, cash in-/outflow, depreciation cost and installment etc. Meanwhile various payments/revenues and energy conservation measures envoled are unneglectable. Therefore, it is worthy to study the economic outputs with a detailed busniess model to evaluate the STF implemention using a dynamic economic and financial analysis that addresed in follwing section.

7.9   Economic feasibility analysis

A dedicated business model is specially set up to appraise the proposed STF system in term of monetary form. Compared to the static method, the adapted dynamic approach takes consideration of the value of monetary flows depending on the time at which the transaction takes place.

7.9.1   Key parameters

In reality, there are a variety of fundamental criteria for the uncertainty assessment in each investment project (Kuchta, 2000). The most popular parameters are:

1) **Net Present Value (NPV)** takes uncertainty into consideration;

2) **Internal Rate of Return (IRR)** makes the profitability of investments measuable to compare its anti-risk capability;

3) **Dynamic Payback Period (DPP)** presents the direct return time of investment.

They are general approaches in determining acceptance or rejection decision for a project that treats the cash flows as known with certainty using spreadsheets in Excel (Bas, 2013).

To compare different investment schemes on a common basis, each year's cash net flow needs to be multiplied by a discount factor so that all inflows and outflows linked to a given investment can be compared on a 'present' day level. When comparing several investments, the project with the highest positive *NPV* is usually the most attractive (Kuchta, 2000).

$$NPV = CF_0 + \sum_{i=1}^{n} \frac{CF_i}{(1+r)^i} \qquad [7\text{-}3]$$

Another economic appraisal factor, IRR is calculated from the NPV equation on condition that there is such a cut-off rate for which the *NPV* is equal to zero (Walker C., 2013). The *IRR* rule states that if the *IRR*

of an investment is greater than a pre-defined cut-off discount rate (typically, sum of the cost rate of capital and the inflation rate), then a given investment project will be viewed favorably. The *IRR* balance equation is accordingly given as (Kuchta, 2000):

$$CF_0 + \sum_{i=1}^{n} \frac{CF_i}{(1+IRR)^i} = 0 \qquad\qquad [7\text{-}4]$$

The *DPP* is calculated by the means of simply written in the following Equation [7-5]. It is obvious that the smaller value, the quicker the payback time.

$$DPP = n_k + \frac{\sum_{i=0}^{k} CF_i}{CF_{k+1}} \qquad\qquad [7\text{-}5]$$

In above equations, the related parameters are addressed as followings:

1) *n* (an integer) is the project duration in the assumed time years;

2) *r* is the discount rate in NPV calculation;

3) C_OF_i (a non-negative number) is the cash outflow at the end of the ith year (i = 0; 1......n) and C_lF_i (a non-negative number) is the cash inflow at the end of the ith year (i = 1......n). Both yearly cash flows will be often summarised as a single cashflow CF_i, occurring at the end of the ith year (i = 0; 1......n), where $CF_0 = -C_OF_0$; $CF_i = C_lF_i - C_OF_i$ (i = 1......n);

4) k is the last period with a negative cumulative cash flow, and CF_{k+1} is the total cash flow during the period after year k.

Table 7-5 Monthly breakdowns of heating/cooling loads

Month	Baseline (MWh)		STF coupled envelope (MWh)			Space cond'g load decrease rate (%)
	Sys cooling cond'g load	Sys boilers space cond'g load	Sys cooling cond'g load	Sys boilers space cond'g load	Solar heat input	
Jan.	0	66.018	0	64.770	0.733	1.89
Feb.	0	49.673	0	48.648	0.650	2.06
Mar.	0	28.371	0	27.612	0.655	2.68
Apr.	0	3.460	0	3.375	0.754	2.45
May.	0	0	0	0	0.689	0.00
Jun.	29.433	0	29.350	0	0.723	0.28
Jul.	76.509	0	75.998	0	0.848	0.67
Aug.	75.514	0	74.947	0	0.991	0.75
Sep.	26.045	0	25.914	0	0.836	0.50
Oct.	0	0.525	0	0.514	0.861	2.10
Nov.	0	12.704	0	12.347	0.800	2.81
Dec.	0	42.130	0	41.223	0.828	2.15
Summed total	207.501	202.881	206.209	198.489	9.368	2.16

Note: "cond'g" stands for "conditioning".

Table 7-6 External conduction gain comparison of the typical floor apartments

Month	Baseline (MWh)	STF coupled envelopes(MWh)
Jan.	-3.785	-3.631
Feb.	-3.111	-2.984
Mar.	-2.566	-2.462
Apr.	-1.624	-1.578
May.	-1.745	-1.694
Jun.	-0.740	-0.722

Jul.	+0.831	+0.788
Aug.	+0.861	+0.810
Sep.	-0.854	-0.834
Oct.	-1.989	-1.940
Nov.	-2.292	-2.221
Dec.	-3.069	-2.955
Summed total	-20.083	-19.423

Table 7-7 Annual energy consumption, carbon emission and operational cost

Date	Total energy (MWh)		Total system CE (kgCO$_2$)		Total energy bills (¥)	
	Baseline	STF upgrade	Baseline	STF upgrade	Baseline	STF upgrade
Jan.	80.523	66.585	65,384.68	54,067.02	88,575.30	73,243.50
Feb.	67.401	56.250	54,729.61	45,675.00	74,141.10	61,875.00
Mar.	60.347	51.967	49,001.76	42,197.20	66,381.70	57,163.70
Apr.	45.521	41.186	36,963.05	33,443.03	50,073.10	45,304.60
May.	45.098	41.168	36,619.58	33,428.42	49,607.80	45,284.80
Jun.	57.483	51.886	46,676.20	42,131.43	63,231.30	57,074.60
Jul.	81.031	75.092	65,797.17	60,974.70	89,134.10	82,601.20
Aug.	80.564	74.570	65,417.97	60,550.84	88,620.40	82,027.00
Sep.	55.893	50.127	45,385.12	40,703.12	61,482.30	55,139.70
Oct.	45.380	41.329	36,848.56	33,559.15	49,918.00	45,461.90
Nov.	50.482	44.668	40,991.38	36,270.42	55,530.20	49,134.80
Dec.	67.730	57.353	54,996.76	46,570.64	74,503.00	63,088.30
Summed total	737.452	652.182	598,811.84	529,570.97	811,198.30	717,399.10

Table 7-8 Capital cost calculation sheet of one set of STF system

System components	Unit cost (¥)	Quantity	Cost (¥)
Absorber module(0.6m*1m)	500.0	2.4	1200.0
Electrical water pump	200.0	1	200.0
PPR pipe fittings	200.0	1	200.0
Control system	1500.0	1	1500.0
Insulation backboard (m²)	5.2	2.4	12.5
		Subtotal cost	3112.5
	Installation cost (30% of sub-total cost)		933.7
	Pre-tax profit (30% of sub-total cost)		933.7
	VAT (standard 17% of profit)		317.5
	Capital cost of each compact unglazed STF system		5297.5

Note: the standard Value Added Tax in China is 17%; the CPI in Shanghai is 61.26 (09.2015)

Table 7-9 Basic parameter inputs in the business model

	Items	Value	Note
STF data	Investment costs	423,798	¥
	Total lifetime	25	yrs
	Depreciation Straight line rate	0.04	yr
	Annual maintenance deduction	0.02	Caused by STF
Building characteristics	Rent current state[1]	72,000	¥/(apt-yr)
	Fixed plug electricity fee[2]	6,129	¥/(apt-yr)
	O&M charge (Tenant)	100	¥/(m²-yr)
	HVAC+DHW charge (Tenant)[3]	47	¥/m²
	Overhead multiple	20%	
Energy cost	Electricity tariff[4]	1.10	¥/kWh
	Heat capacity per unit of electricity[4]	860	kcal/kWh
	CO_2 emission per unit of electricity[4]	0.812	kg CO_2/kWh
Economic data	Amortization period	15	yrs
	Inflation rate (10-yrs mean CPI)[1]	0.029	yr
	Energy growth rate (incl. inflation)	0.079	yr
	Discount rate[5]	0.1	yr
	Interest rate of private equity[1]	0.029	yr
	Commercial interest rate[1]	0.072	yr
ESCO fiscal benefits	Business Tax Rate[6]	0.05	yr
	Corporate Tax Rate[6]	0.25	yr
	Business tax deduction rate[7]	0.030	yr
	Corporate income tax rate	0	1-3yrs
		0.125	4-6yrs
		0.250	after 7yrs
	Energy efficiency subsidy	600	¥/ton standard coal

Note: 1) data from Numbeo worldwide living database, http://www.numbeo.com/cost-of-living/city_result.jsp?country=China&city=Shanghai;

2) It covers appliance & equipment loads and lighting load. Calculation assumptions are referenced from Hendron R. 2008. Building America Research Benchmark Definition. National Renewable Energy Laboratory, Golden, Colorado);

3) DHW consumption is referenced from 2

4) Data are checked from local utility suppliers (09 Sep 2015), and the solar heated water tariff was assumed based on 50% of electrical water heating cost (90% in efficiency);

5) Financial figure, set 10% for building service appliance;

6) Financial figures from Shanghai local government in 2015

7) Fiscal benefits are referenced from http://news.ces.cn/fuwu/fuwuzhengce/2015/09/25/75688_1.shtml.

7.9.2   Background financial parameters

DPP, NPV and *IRR* were selected to evaluate the investment feasibility of the proposed STF system applied in a reference building. As mentioned in Equations form [7-3] to [7-5], the calculation of the key parameters contains background parameters, such as initial system investment, inflation rate and local annual capital cost, etc. The initial investment of the compact unglazed STF system was provided from the prototype manufacturer. And Table 7-9 listed all the required basic statistics data for the financial calculation.

Via referencing the statistical data from the Chinese domestic sector, the mean annual rate of *Consumer Price* Index (CPI) (2.92% from 2005 to 2014) and the average one-year interest rate of saving account (2.90% from 2005 to 2014) were deemed suitable for representing inflation rate and interest rate of private equity respectively (Chang et al., 2015). Besides, operational and maintenance (O&M) costs and rental were assumed here (Koene, 2012).

7.9.3   Setting up business model of the STF

The buisness model has taken four states into consideration, as
   1) *0. Current state*;
   2) *A. Private equity*;
   3) *B. Loan from bank to owner*;
   4) *C. Operate leasing*.

And the four states invovled with three main investment schemes:
   1) *Buying Outright* **(BO)**;
   2) *Buying by Installment* **(BI)**;
   3) *Power Purchase Agreement* **(PPA)**.

These different schemes are the prevalent finance methods for renewable technology investment on the market, and can basically cater for different circumstances with individual key benefits. **BO** and **BI** are common purchase schemes for the building owner. Unfortu-

nately, the renewable subsidy program is only accessible to the public party or *Energy Service Company* (ESCO) at the moment in China. Therefore, **PPA** is the other popular purchase scheme in China. There are a number of reasons to involve an ESCO in a renewable technology investment. Firstly, it prevents a financial risk in making the upfront investment. Secondly, the whole investment can be paid back in the user phase by energy savings. Thirdly, an ESCO is able to enjoy plentiful fiscal or other benefits currently in China when carrying out an energy conservation investment. What is more, an ESCO is a pofessional party to provide outsource services of new technology upgrade, building energy management and O&M. In this case, it is assumed that:

In the **0.state**, the tenant pays a fixed fee (including rent, fixed energy service fee covering fixed amount of both electricity and HVAC consumption, and routine O&M service) to the building owner, and the latter takes care of public service, supplements of the fixed amount electricity, HVAC (heating,cooling and DHW) and routine O&M service.

In the **A. state** and **B. state**, the tenant still pays the same rent for the upgraded mordern building outlooking and the improved indoor comfort, and keeping the same amount payment of electricity, HVAC, and routine O&M service to the building owner. However, the building owner benifits from savings on energy consumption and additional 2% of O&M expense deduction cased by STF upgrade compared to the DHW operation under **0. state**. The only difference between **BO** and **BI** lies in the finance method. **BO** invested the project through private equity, meanwhile **BI** invested through commercial loan from bank.

The scenario is a little different in the **C. state**. In the **PPA** scheme, the tenant still pays the same amount of rent and the fixed amount of

electricity, HVAC, and O&M expense to the building owner, while the building owner authorizes an ESCO to run operate leasing of the STF system. As mentioned previously, given that STF system invested by ESCO can reduced the total energy for the building owner, the energy savings should be shared between the ESCO and the building owner with the assumed ratio of 9:1. But in the end of the amortization period (the 15th year), the building owner will have the ownership of the entire STF system (worthy of ¥10,467's at that time). Moreover, because an ESCO is a kind of orgnization that provides practical technical assistances and services to promote energy conservation activities to the society, Chinese government has released a series of fisical benifits to foster its rapid growth. Currently, an ESCO can benifit from a business tax deduction (with the rate of 5%), a portfolio of corporate income tax rate (0% during 1st-3nd yr, 12.5% during 4th-6th yrs and 25% after the 7th yr), an Energy Efficiency Funding (with green credit interest rate of 6.2%) and one-off energy efficiency subsidy (¥600/ton of stand coal equivalent in Shanghai district in 2015).

7.9.4   Conclusions from the financial outputs

On the basis of basic fundamental parameters from Table 7-9, key parameters from three STF investment schemes can be summarized in Table 7-10.

Table 7-10 Financial outputs from different STF investment schemes

Options	Total invest-ment amount	NPV (15 yrs)	IRR	DPP
BO scheme (Option A-Current 0)	¥423,798	¥594,674	27.4%	5yrs 2mths
BI scheme (Option B-Current 0)	¥706,803	¥700,435	126.9%	1yr 11mths
PPA Owner (Option A-Current 0)	¥663,111	¥499,527	--	--
ESCO		¥332,398	54.4%	3 yrs 8mths

The STF investments in the reference residential building in Shanghai seemed to be all profitable with positive *NPVs* within 15 years and greater *IRRs* than the pre-defined cut-off discount. In terms of *DPP*, it was found that all the *DPPs* were within 6 years, which is cost effective for a kind of building service application and matches the initial design objectives of lower cost and fine operating performance.

When looking into each scheme, each one has quite different outputs:

Firstly, the popular *BO* scheme actually has a gentle outcome for an investment decision. Because of the feature in buying outright, the inflexible payment method has the lowest acquisition outlay and avoidance of annuities in the coming years. However, the *NPV* over 15 years was the least. In another word, it can be regarded as the saftest investment method with the lowest financial risk and the longest *DPP*.

Similar to *BO*, *BI* is another self investment option yet with a more flexible payment method using installment. With the assumed 7.2% commercial interest rate fixed within 15 years, all the financial outputs presented with an attractive financial outcome. Although the overall investment cost is much higher than *BO*, *BI* yet had the optium performance with highest *IRR* and the shortest *DPP*. Looking into the financial calculation process, it could be found that positive contributions coming from: 1) amortisation payment made the time value of money to be an additional profit for the building owner; 2) the annual installment amount was considered as "tax deductible" item in the corporate income tax calculation. But this purchase scheme still has to face potential risk in fluctuating commercial interest rate.

As compared to both *BO* and *BI*, *PPA* is an evolutionary option by the third party ESCO and available for all businesses, aiming in helping

customers for energy conservation whilst budgeting through affordable payments. Ideally, the savings in energy consumption and fiscal benefits render the STF upgrade beneficial to both the building owner and the ESCO itself. Benifit from both energy savings and lower green credit interest rate of 6%, the financial outputs seemed to be most acceptable in terms of **NPV**, **IRR**, and **DPP**. When combining the **NPVs** from both the owner and the involved stakeholders, it had the maximum **NPVs**.

In the perspective of the ESCO, it has got a much higher **IRR** of 54.4% to overcome common finiancal risks, and could reclaim all the investment with a rapid **DPP** with 3 years and 8 months.

In the perspective of the building owner, although the profit had been shared with a third party, it would actually take advantages of 1) flexibility in budgeting to conserve existing working capital; 2) energy savings from solar thermal technology application; 3) upgrades in both the property value and the built environment; 4) the pofessional O&M service of the STF system for 15 years without any upfront cost; and 5) the free ownership of the STF system for the remaining 10 years.

Overall, this comprehensive business model assists in elaborating a suitable investing way of the proposed system deployment for the building owner. In view of the shortest **DPP**, the investment scheme of **BI** is recommended with both the highest **NPV** and the highest **IRR**. In view of the upfront investment and innovative technology application, the investment scheme of **PPA** is recommedned with no capital investment threshold and professional O&M, as well as acceptable *NPV* and *DPP*. Therefore, it is recommend for engineering application.

7.10   Chapter executive summary

This chapter presented a multidisciplinary research method that would be beneficial for strategic decision and offer a different angle to assess both feasibility exploration and economic performance for the proposed STF integration design at early design stage in Shanghai, China. The whole study are composed with a dynamic building environmental simulation of a reference DOE residential building model in IES (VE) sotfware and a dynamic business model consisting of several critical financial indexes with results listed in Table 7-11.

Table 7-11 Results summary of feasibility exploration and economical analysis

Dynamic Building Environmental Simulation Results	Dynamic Economic Analysis Results
• Annual southern vertical wall has the radiation flux up to 776 Wh/m^2 with around 80% exposure time in a year;	The popular **Buying Outright** scheme needs total investment of ¥423,798. It actually has a gentle performance with the **NPV** of ¥ 594,674 over 15 years and the **DPP** of 5 years and 2 months.
• The mean STF module temperature fluctuated similarly with the outdoor dry-bulb temperature, exhibiting less risk in freezing and stagnation;	It can be regarded as the saftest investment method but lowest risk along with disadvantages of the longest payback period and inflexible payment method.
• Annually direct contribution of solar thermal energy yield is 45,727 kWh (energy genera-tion);	**Buying by Installment** scheme needs total investment of ¥706,803. It has the **NPV** of ¥ 700,435 over 15 years and the **DDP** of 1 years and 11 months.
• Annually indirect loads reduc-tions of space conditioning load are 5,684 kWh (demand reduction);	With the assumed 7.2% commercial interest rate fixed within 15 years, all the financial outputs presented with the highest values of **NPV** and **IRR**, as well as the shortest payback period.
• STF coupled building has substantial annual savings of 85,270 kWh in total energy consumption, being equivelent to 69,240 KgCO$_2$ redection and ¥93,799 operation cost reduction.	**Power Purchase Agreement** scheme needs the total investment of ¥663,111. It can benifit the building ower directly from an innovative technology and the pofessional building energy management service for 15 years without any upfront cost. And from the view of the ESCO, the investment of STF system can have the **NPV** of ¥ 332,398 over 15 years with a rapid **DDP** of 3 years and 8 months.

DESIGN STRATEGY FOR HIGH-PERFORMANCE STF BUILDING INTEGRATION 8

8.1 Chapter abstract

This chapter discusses the specific design strategy of the STF for building performance research in architectural practice. It has following tasks as below:

1) Identify the role of STF in the building design and the building performance analysis;

2) Demonstrate the importance of building performance simulation and analysis;

3) Develop dedicated design strategy based on the BIM concept for application of the proposed STF.

This part of research work clarifies the design methods for the proposed STF, and the necessary steps in ensuring that environmental/economic factors and energy-efficiency strategies are integrated with the building design and analysis process at the early stage.

8.2 STF's role for high-performance building design

Generally, there are three main methods for the high-performance building design, as the passive design strategies, the employment of advanced building technologies and the application of renewable energy systems (Aksamija, 2013).

Passive design strategies include factors of shading, response to building orientation, solar heat gain, natural ventilation, and daylight effect etc. Active design approaches include the use of energy-efficient building systems and advanced building technologies where appropriate, such as mixed-mode ventilation, heating and cooling systems, hot water supply, and power systems. Renewable energy systems

should be used to supplement energy demand with clean energy. As a multi-function technology, STF can be employed as shading or rain screen as a passive design strategy, an advanced building envelope to buffer overall building energy load as an active building technology, and solar thermal delivery as a renewable energy system. As a result, these characteristics endow the STF technology as a subset of the three main methods that provides one of the most appropriate solutions for the high-performance building design as shown in Figure 8-1.
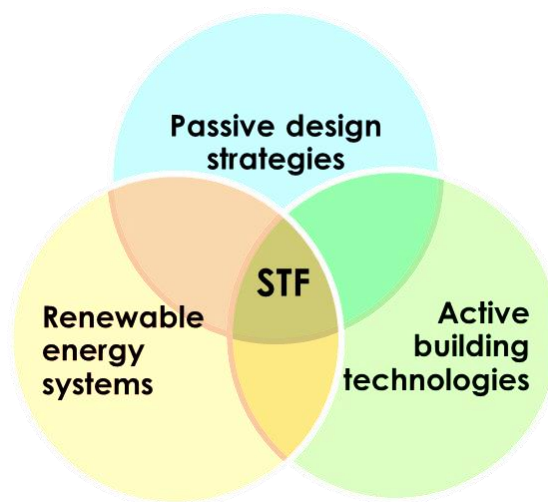
Figure 8-1 STF's role in high-performance building design

8.3 Importance of building performance simulation and analysis

Because there are growing number of strategies/technologies gathered in a single building project, building performance simulation is considered more indispensable for temporary design process in contrary to the conventional design process. Building performance simulation as an integral part of design process can help in:

1) Understanding and investigating different options;
2) Establishing metrics to measure improvements associated among different strategies/technologies;
3) Maximizing real contribution;

4) Making design decision in achieving low and zero energy build-
   ings, i.e. different passive/active design options or renewable
   energy systems.

As for the STF technology application, it requires solar exposed orien-
tation, wind shielding direction, collecting area, solar thermal de-
mand and system size etc. Therefore it is more significant to carry out
solar resources prediction, optimal design option and further im-
provement using modelling techniques. However, a disconnection
between architecture design and environmental thinking normally ex-
ists, where green components like STF can be included as part of a
design strategy for the high-performance building, but such informa-
tive knowledge is hard to be shared through the whole process. Tradi-
tional design process is used to start from architects to engineers simp-
ly in one-way direction within knowledge silos, leading to high level of
congenital design strategies, i.e. conventional air conditioning, dou-
ble skin facades, extra thermal insulation layer or complex motorized
shading systems etc. These design strategies often mask an underlying
lack of basic environmental thinking and impede the widespread de-
ployment of promising technology.

In order to better understand the dedicated effects of STF on building
performance, and enable the parallel architecture design proceed-
ing, different cycles of building performance simulation and analysis
should be involved as part of an integrated design process on the ba-
sis of current available simulation tools or platforms.

8.4 Design strategy of STF based on BIM concept (STF-BIM)

One of best methods for integrating performance simulations of STF
with the building design is BIM concept (see Figure 8-2). BIM is a holis-
tic information sharing approach that enabled by the information
mobility across engineering disciplines and building lifecycle. It drivers

better use of both 2D and 3D data held in documents, spreadsheets and other databases to create simple, effective cooperation among design, construction and operations aspects of the building lifecycle. It contributes to overcome traditional silos, reduce duplication, mini-mise errors streamline processes and facilitate collaboration. The discussion below primarily presents the design strategy of the proposed STF depending on BIM concept (entitled as STF-BIM).
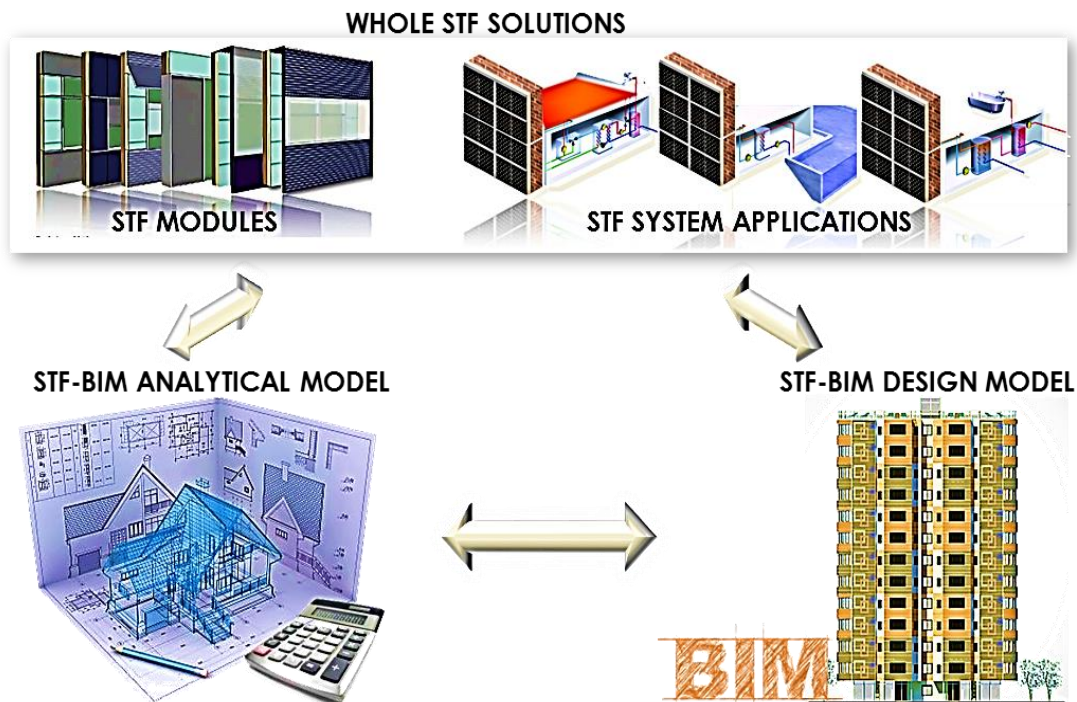
Figure 8-2 Design strategy circle of the STF-BIM proposal

8.4.1 Advantages of the STF-BIM design strategy

Typically, a traditional design method for STF usually simplifies the design by assumptions from the rules-of-thumb, which could be inaccurate sometimes. It often cares more in aesthetic feature without considering performance impacts or without possibility in offering performance measurement and evaluation of a STF solution especially at early design stages. These are mainly because of the limitations in conventional design and simulation tools that are not compatible with working methods and the needs of architects and designers, or

the tools judged as complex and cumbersome (Gratia et al., 2002; Punjabi & Miranda, 2005).

With the widespread of building information modelling, STF-BIM is proposed as one of promise methods for integrating performance simulations of STF within building design. BIM is the holistic approach of information sharing enabled by information mobility (across engineering disciplines and the building lifecycle). It provides designers, engineers, contractors and owner operators with access to key design data that can be used to transform effectiveness throughout the construction and operations processes. Compared to tradition design method, it drives better use of 3D across the industry, but not only 3D. 2D data remains important, as does information held in documents, spreadsheets, and other databases (Glanville, 2014).

The STF-BIM design strategy has an ability to estimate the impact of a STF decision across the whole process. The performance is simulated, analyzed, and predicted with reliable quantitative data through sufficient building and STF models, rather than simple assumptions from design experience. For example, analytic data from the STF-BIM analytical model could be a driver to parametrically control the geometry of STF elements in the design model, such as sun shades, orientation, or inclination angles etc. Such feature enables the high possibility for design professionals to produce the evaluation of multiple STF alternatives against different design priorities, like time, resources, energy, investment, and other valuable information, thus helping in the decision-making process towards sustainable design.

8.4.2 STF-BIM design procedures

Figure 8-3 shows the impact of STF design decisions on building performance at different project stages based on the work stages of the Royal Institute of British Architects (RIBA).
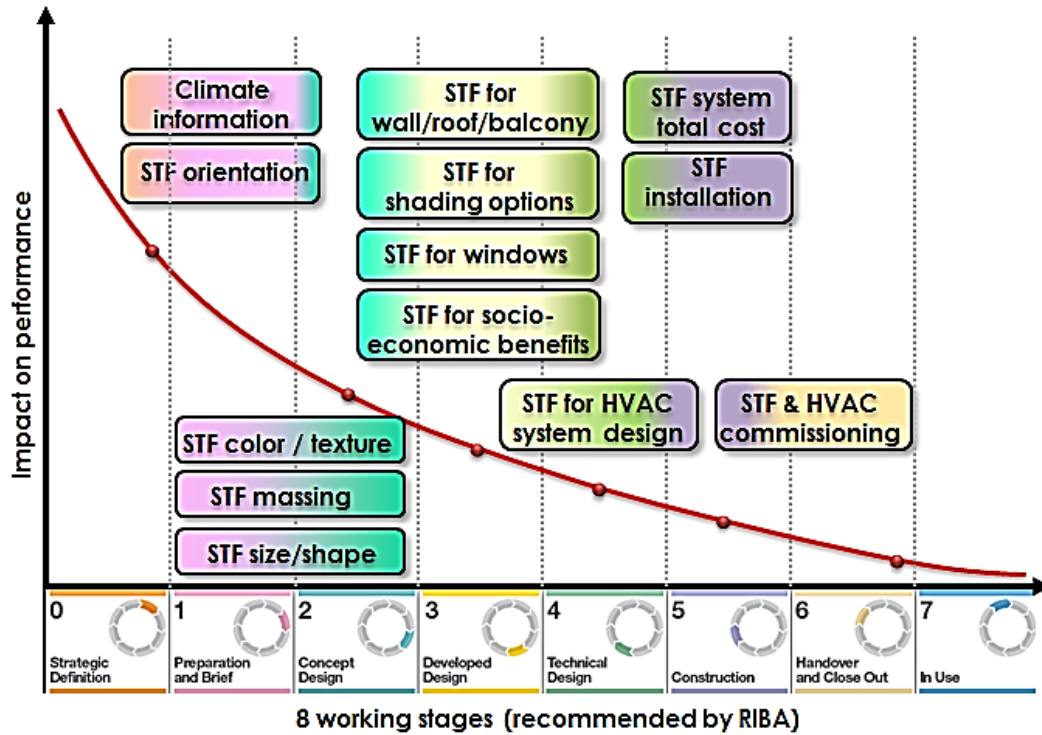
Figure 8-3 STF design tasks bars and impact performance curve along with RIBA working stages

As can be seen, as early as programming and conceptual stages the analysis may focus on the contextual aspects, such as climate information, STF orientation, STF colour/texture, STF size/shape and STF massing. Then at conceptual and schematic phases, the analysis observes the whole impact of STF to the building when it serves as different envelope components. In addition, an iterative cycle of different design options should be analysed in terms of sun shading, overshadowing of surrounding buildings, thermal comfort, and daylighting etc. The decisions at these stages are of high impact on the design because they influence the exterior design character of the project, potential energy use reduction, and the comfort levels inside the spaces as well as the environmental and economic benefits. Finally, the STF

array connection and the associated HVAC system together with the related cost should be highlighted mostly at design development and construction documentation phases. It is usually more important for designers to evaluate STF and building energy performance at the early project phases (programming, conceptual, schematic and de-sign development), which prevents the project from drastic changes due to unsuitable energy and cost goals.
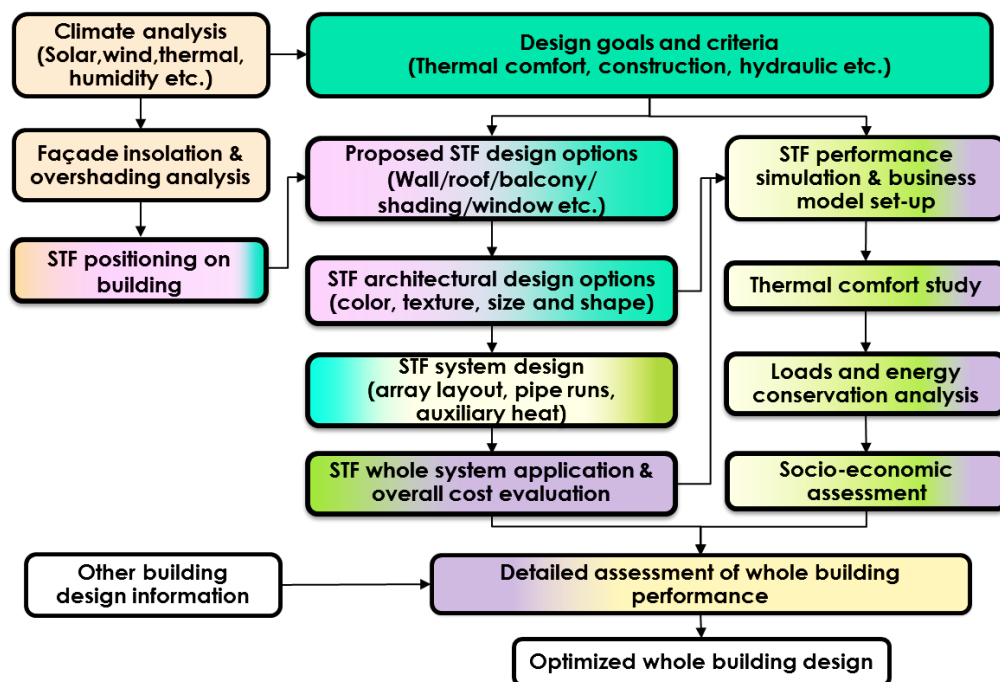
Figure 8-4 Frameworks of incorporating building performance analysis procedures with STF design

Figure 8-4 presents the basic framework for incorporating building per-formance analysis procedures with STF design. By initially defining en-ergy target goals and setting up design criteria, the early design characteristics and decision could be explored, such as site, climate information, building orientation, shadow ranges, solar exposure, and daylighting etc. After then, the design solutions and optimizations are proposed and tested using more detailed three-dimensional building model for analysis of STF including aesthetical matching, components adaptability, and the associated solar exposure etc. Finally, the com-prehensive energy and socio-economic simulation are conducted for

the performance analysis of the STF incorporated three-dimensional building model, aiming to figure out the optimum design of the STF as well as the whole building energy systems.

However, BIM design authoring software programs and analysis applications are currently distinct, and require the exchanges of data and building information (Aksamija, 2013). To successfully employ STF-BIM models (contains both design and analytical models) for energy performance and socio-economic analysis of building, it is important to consider the Level of Development/Detail (LOD) of STF-BIM design models, which indicates the necessary information from STF-BIM design models to develop STF-BIM analytical models, data exchange mechanisms and workflow between different software programs. LOD refers to the amount of information embedded in BIM design models, and is widely accepted by American Institute of Architects (AIA) document E20212 (Aksamija, 2013). Figure 8-5 illustrates the relations of STF-BIM design process and analysis documentation, which recommends the LOD in STF-BIM design models corresponding to each simulation analysis at different design stages.

STF-BIM analysis documentation

PROGRAMMING	CONCEPT DESIGN	DEVELOPED DESIGN	TECHNICAL DESIGN	CONSTRUCTION
Climate (LOD 0) / Passive strategies and massing (LOD 0/100)	Shading (LOD 100) / Solar access (LOD 100) / Building envelope (LOD 100)	Shading devices (LOD 200/300) / Daylighting (LOD 200/300) / Energy (LOD 200 or 300) / Thermal analysis (LOD 200/300) / Socio-economic assessment (LOD 200/300) / Optimization (LOD 200/300)	Impact on building performance is too small to justify analysis at these design stages (LOD 350)	Impact on building performance is too small to justify analysis at these design stages V (LOD 400)

STF integrated building design process (STF-BIM design process)

Figure 8-5 Relations of STF-BIM design process and analysis documentation

In Figure 8.5, LOD 100 should include overall building massing, area, height, and volume. It can be applied to analyse building orientation, solar exposure and some passive initiatives. LOD 200 contains model elements as generalized systems or assemblies, and may include non-geometric information, such as material properties, cost etc., which can be used for performance analysis of shading devices, daylight analysis, basic energy analysis, thermal evaluation, and socio-economic assessment. LOD 300 consists of model elements that are more accurate in terms of quantity, colour, texture, size, shape, location, and orientation etc. It is considered for more detailed analysis done at LOD 200 in additional to the optimization of STF and its associated systems. It is important to note that these types of studies have the greatest impact on the building performance if they are conducted early in the design process (Aksamija, 2013).

8.4.3 Methods for information exchange

Typical workflow and data exchange between STF-BIM design model and environmental analysis applications require the export of model information depending on the analysis objectives and the necessary information or LOD. For example, in order to determine the STF orientation that maximizes solar exposure on the facade, data exchange of basic LOD 100 through DXF file format is adequate for analysis. In terms of higher LOD 200 or LOD 300, data exchange can be performed through Green Building XML (gbXML) schema, a computer language specifically developed to facilitate transfer of building properties stored in BIM to analysis tools. In some cases, necessary modification of translated geometry or element properties may be required in the analysis software application.

However, importing the analysis results back into the STF-BIM design model and controlling the related geometric elements are still chal-

lenging. A custom-built plug-in for a typical BIM software - Revit platform has been recently developed that allows the import of analytical results, such as solar radiation into BIM design model (Aksamija et al., 2011). It enables importing of data through Excel spreadsheets and parametric control of Revit families based on the numeric values contained in the imported data, as indicated in Figure 8-6.
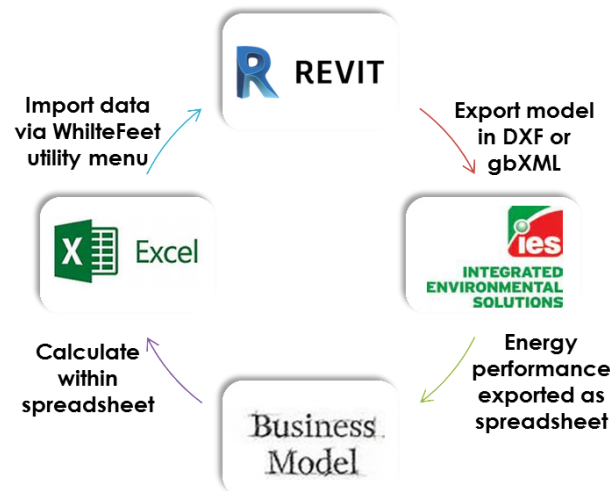
Figure 8-6 Data exchange between design and analytical applications

8.4.4   Case study of a STF-BIM design project

In order to strategically verify the effectiveness of STF-BIM design method, a case study of the proposed STF integration with a high-rise building was conducted at the very early design stage.

The plan for a typical STF integrated high-rise residential building is illustrated from Figure 8-7 to Figure 8-9, indicating the proposed STF combination with balcony, south wall and punched window. Three different STF types are used along the east-south-west orientation, including **Type 1** curved STF for balcony, **Type 2** STF with various textures for south wall, and **Type 3** STF with different colours of light dark and light orange for punched window. Figure 8-10 and Figure 8-11 display the schematic connections with DHW service system from different angles of view. All these designs are accomplished within the Revit software.

Front view

Three dimensional view
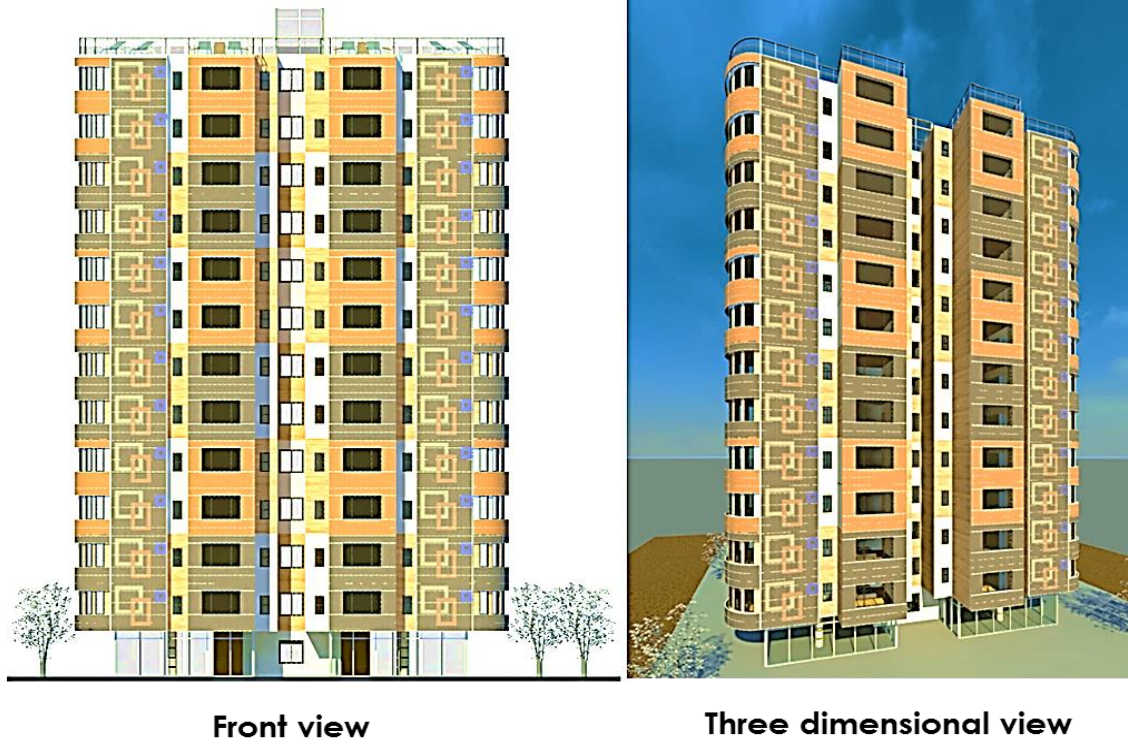
Figure 8-7 Overall view of the STF integrated high-rise residential building

Type 1 STF

Type 2 STF

Type 3 STF
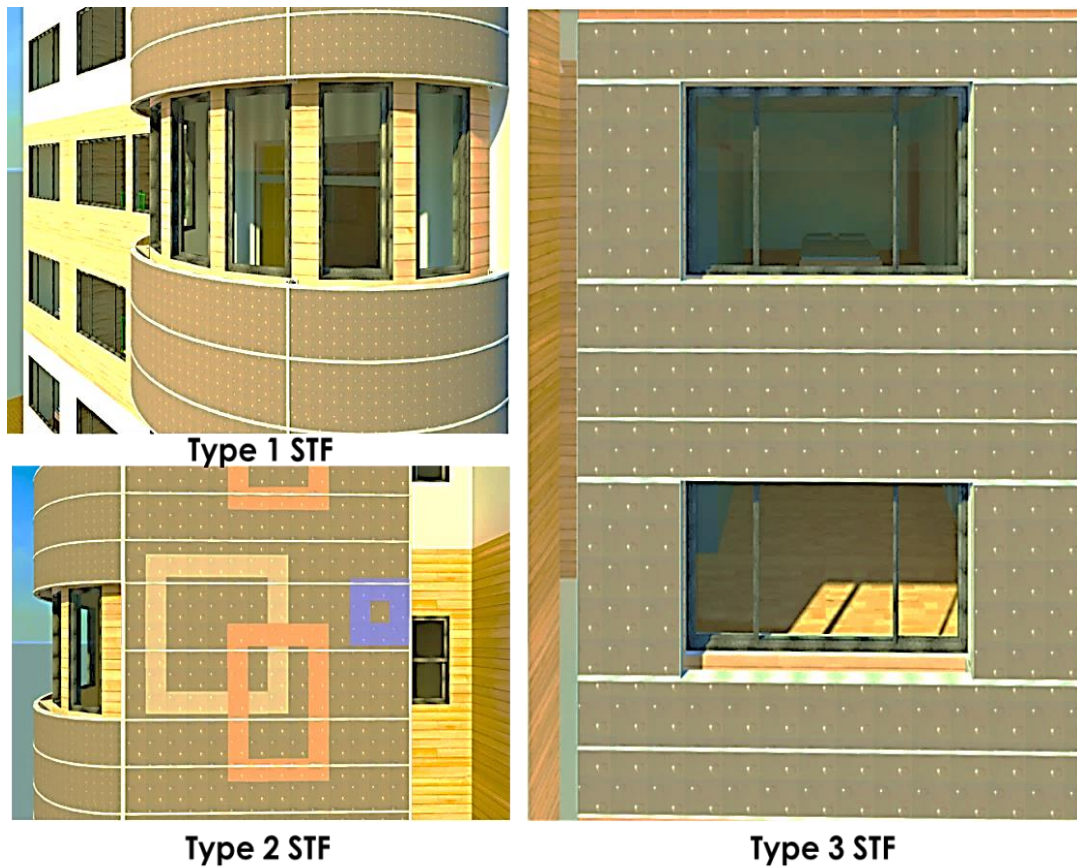
Figure 8-8 Three different STF types for building integration

Figure 8-9 Three different STF types integrated with the high-rise residential building
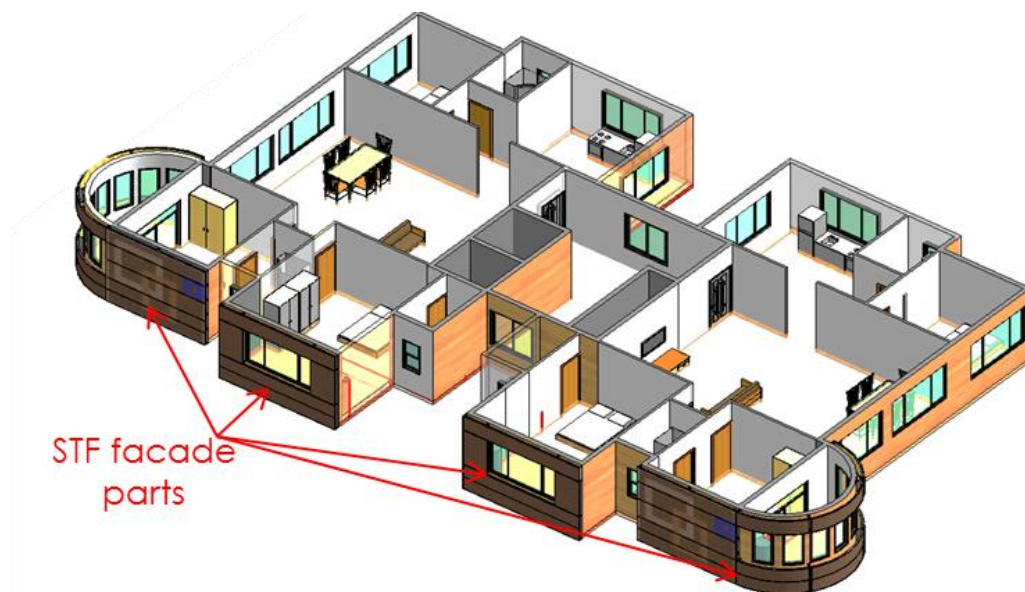
Figure 8-10 STF connection with HVAC system: architectural section view
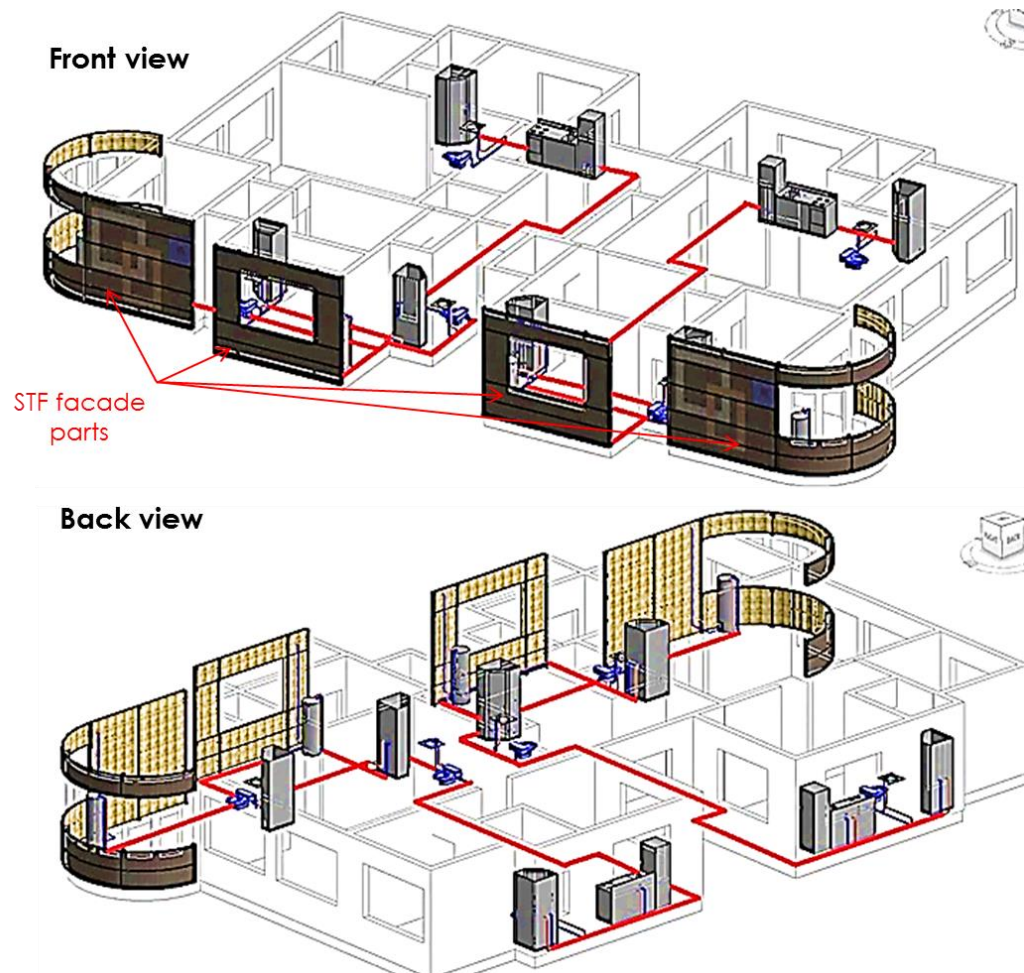
Figure 8-11 STF connection with DHW service system: front and back views
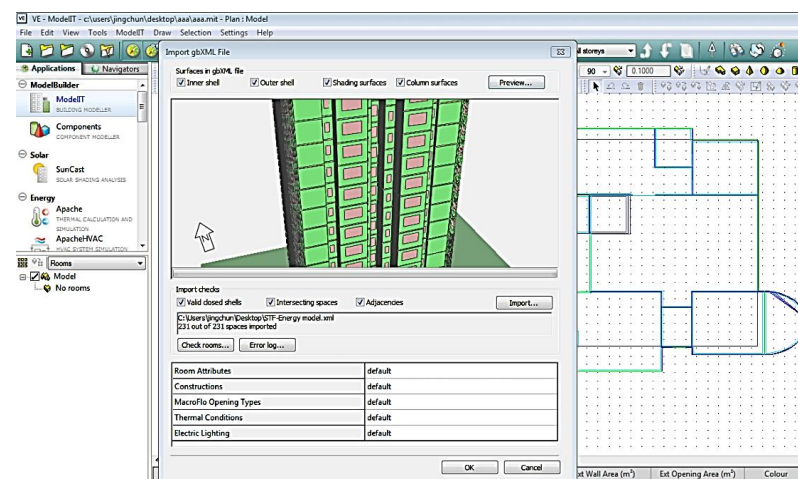
Figure 8-12 Example of STF gbXML inputting from Revit into IES (VE) for further para-metrical optimization

The example case was tested in relation to building envelope design with special focus on various types of cladding devices along with

complex solar exposures on respective surfaces obtained from IES (VE) software as:

1) In order to align the IES (VE) data with the individual instances of Revit panel families, several instance parameters were created within the family according to the STF performance addressed in previous chapters. This allows the subdivision of families to be logically ordered for alignment with IES (VE) principle.

2) After creating the physical model in the Revit, different divisions were subdivided into a desired number, which were then exported as a gbXML file and further imported into IES (VE) to analyse incident solar radiation, as shown in Figure 8-12, and obtain solar radiation values depending on different climate regions and specific orientation of the STF.

3) These values were subsequently exported from IES (VE) into an Excel spreadsheet. The obtained solar radiation data in Excel spreadsheet must be normalized based on minimum and maximum solar radiation values from 0 to 1, which was then imported into Revit using WhiteFeet utility menu, and used to control the geometry of Revit panel families (Aksamija, 2013). This was achieved by matching the normalized values from 0 to 1 to control the position and geometry of the solar radiation gain relative to the centre-point of each STF. As a result, the preliminary optimization of different STF's solar exposure and position in various climate regions could be achieved based on the developed STF-BIM design strategy.

4) Furthermore, complex analysis and optimization of such STF system could be therefore conducted accordingly based on different design scenarios and criteria.

8.5 Chapter executive summary

Rather than simple assumptions from design experience, the proposed STF-BIM design strategy for building performance research in this chapter has an ability to estimate the impact of a STF decision across the whole process. Its associated feature enables the high possibility for design professionals to produce the evaluation of multiple

STF alternatives against different design priorities, like time, resources, energy, investment, and other valuable information, thus helping in the decision-making process towards sustainable design.

The part also presented 4 diagrams relevant to the STF-BIM design strategy as:

1) Impact of STF design decisions on building performance at different project stages based on the work plan of the Royal Institute of British Architects;

2) Basic framework for incorporating building performance analysis procedures with STF design;

3) Relations of STF-BIM design process and analysis documentation with the recommendations of LOD in STF-BIM design models, corresponding to each simulation analysis at different design stages;

4) Data exchange between STF-BIM design model and the dedicated analysis applications.

Finally, the preliminary optimization of different STF's solar exposure and position in various climate regions at early design stage was accomplished by means of a typical BIM tool (Revit) and a building performance analytical application IES (VE). It showed a strategical verification of the effectiveness of STF-BIM design method at the very early design stage. In line with the proposed STF-BIM design strategy, complex analysis and optimization of such STF could be conducted based on different design scenarios and criteria, while the environmental/economic factors and energy-efficiency strategies could be integrated with the building design and analysis process at early stage as well.

9 CONCLUSIONS AND FURTHER WORK

9.1 Conclusions

In spite of the solar thermal technology is mature with competitive operational performance and technical advances, it is nearly playing pivotal role as it deserves in the expectation of energy conservation in the building sector. Apart from affordable price and technical advances, the architectural quality and the economic feasibility are regarded as 2 main reasons for its partial development. This research therefore presented an in-depth investigation into a novel compact unglazed STF system.

The overall achievements in this thesis are:

1)   A comprehensive literature review were completed into the solar thermal facade (STF) from:
- Concept;
- Classification;
- Structural;
- Configuration;
- Indicative performance;
- Economic and environmental evaluation;
- Current research and development progress;
- Theoretical analysis;
- Economic and environmental performance assessment;
- Overview of the STF design criteria ;
- Overview of available commercial products,
- Summary of STF application cases highlighted the integrity realized in the existing STF applications.

2)   The novel compact unglazed STF system was proposed along with alternative designs in terms of:
- Material;
- Colour;
- Texture;,
- Shape;

- Geometric size;
- Architectural design;
- Installation method;
- Array connection;
- Hypothetical system application;
- Solar coverage.

3)   The analytical simulation for STF's thermal performance optimization was established on the basis of mathematical thermal-fluid analysis that includes both energy balance and heat transfer process. In this part, 7 impact factors were conducted for the STF optimization, including:

- Fabrication materials;
- Colourful paints;
- Pin-fin diameter;
- Pin-fin length;
- Number of pin-fin rows;
- Longitudinal and transverse distance between fin rows;

4)   The fabrication of both the STF prototype and testing rig were achieved. The parallel comparison of modelling and test results indicated that the established simulation model was at a reasonable accuracy to predict the STF's thermal performance;

5)   The dynamic performance simulation model was set up in IES (VE) software to provide whole building performance evaluation for the proposed STF integrated in the reference residential building in Shanghai, China. And the dedicate business model consisting of several critical financial indexes was set up for the feasibility analysis;

6)   The design strategy of the proposed STF based on BIM concept was proposed for building performance simulation and analysis.

The conclusions derived from previous chapters are given in the followings.

9.1.1   Concept summary

The compact unglazed STF concept is defined as the "multifunctional energy facade" that differs from the conventional solar module. It offers a wide range of solutions in architectural design features (i.e.,

colour, texture, and shape), exceptional applicability, safety in construction, as well as additional energy production.

From the context, the proposed STF concept is shown advantages in simple structure, economical cost, and aesthetically appealing with easy installation (plug & play). In practice, it can be applied as either wall/roof or balcony external cover/claddings with alternative designs. Through using the cladding design variant and the prefabricated wall design variant, the proposed STF can be applied in both the new building implementation and the existing building renovation.

Moreover, it has feasible functions in heating/cooling, domestic hot water generation, insulation enhancement and overall building appearance update. And the decentralized connection was recommended for a high-rise building due to the higher the solar coverage (scalability) means the lower the specific yield (efficiency).

9.1.2 Technical summary

1) Parametric analysis of STF module

In the established analytical model, seven impact factors were considered in the parametric studies, including fabrication materials, colourful paints, pin-fin diameter, pin-fin length, number of pin-fin rows, longitudinal and transverse distance between fin rows. To achieve a high thermal performance of STF, the recommendations from the simulation results were concluded in Table 5-2.

2) Characterise study of STF hot water system rig

The characteristic studies of the operating performance exploration of the proposed STF were conducted under different operational conditions by virtue of both the established computation model and the experimental testing.

Given the baseline testing condition defined in Table 6-2, the physical parameters were listed in Table 6-3, demonstrating that such a STF could achieve an equivalent or even better thermal performance while comparing to recent reported bionic STF (F'=0.963) or the conventional ones.

And the characteristics of operating performance are given in Table 6-4 according to parallel comparison between the STF's thermal efficiency and operational conditions.

In addition, the maximum theoretical possible useful heat gain capacity (intercept $F_R a_p$) of such STF at the given operating conditions was about 96.20%. And the mean slope ($F_R U_L$) was as much as about -13.06, representing a sharp decreasing trend of this SFT's thermal efficiency against the $(T_{in}\text{-}T_a)/I$ as there was no glazing cover attached in the front. So in case of current design, such STF could match the applications in pool heating, domestic hot water and radiant space preheating in those regions with warm surrounding temperature and sufficient solar radiation.

9.1.3   Socio-economic summary

In order to figure out the cost effectiveness of the STF proposal, the feasibility study of STF building integration concept in a reference residential building covered both the feasibility exploration and the economic performance at early design stage in Shanghai, China. The whole study were composed with a dynamic building environmental simulation of a reference DOE residential building model in IES (VE) sotfware and a dynamic business model consisting of several critical financial indexes. Both the dynamic building environmental simulation results and the dynamic economic analysis results are listed in Table 7-11.

9.1.4   Design strategy summary

Rather than simple assumptions from design experience, the STF-BIM design strategy was suggested to estimate the impacts of a STF decision across the whole process. Its associated features enable the high possibility for design professionals to produce the evaluation of multiple STF alternatives against different design priorities, like time, resources, energy, investment, and other valuable information, thus helping in the decision-making process towards sustainable design.

In addition to detail the STF-BIM design strategy, 4 diagrams have been illustrated in accordance with:

1) Impact of STF design decisions on building performance at different project stages based on the work plan of the Royal Institute of British Architects;

2) Basic framework for incorporating building performance analysis procedures with STF design;

3) Relations of STF-BIM design process and analysis documentation with the recommendations of LOD in STF-BIM design models, corresponding to each simulation analysis at different design stages;

4) Data exchange between STF-BIM design model and the dedicated analysis applications.

Furthermore, an example case was given in relation to building envelope design with special focus on various types of cladding devices along with complex solar exposures on respective surfaces obtained by means of a typical BIM tool (Revit) and a building performance analytical application IES (VE). It aimed to present a strategical verification of the effectiveness of STF-BIM design method at the very early design stage.

9.2 Future opportunities and challenges

9.2.1 Technical improvements in STF system

1) Outdoor performance evaluation

Given with the limited experimental condition, a short time outdoor experimental measurement of the proposed STF prototype system had been carried out. The whole field-testing in a summer week demonstrated the performance reliability to some extent, and the associated preliminary description can be found in Appendix A.

However, a dynamic outdoor experiment in a long-term (seasonal or annual) scheme is still compulsory in the future to investigate the long period working performance and to resolve different uncertainties in practice, especially integrating whole STF system into building.

2) System control strategy study

Apart from the optimized design in absorber, more attentions should be paid to controlling as it has greatly indirect impacts on safety processing and cost effective operation.

Table 9-1 displays the potential controlling strategy of the STF hot water system. The future investigation associates with climate conditions and temperature difference in the tee-joint between STF surface and water tank. Such a set of controlling strategy will be conducive to:

1) Prevent freezing in winter operation;
2) Increase heat transfer efficiency through solar thermal accumulation within a certain threshold;
3) Avoid overheating for summer operation;
4) Meanwhile if the set temperature of water tank is insufficient, the auxiliary heater would be controlled to heat up as much as to achieve a set exit temperature, for instance, 50℃.

9.2.2 Demonstrative project with STF

Apart from the prototype fabrication and testing, a pilot-scale building application is strongly suggested in the future work. Currently, China' is under transformation in both economic development and structural adjustment in the coming 5 years. And the thirteenth "Five-year Plan" focuses on: 1) adjusting national energy structure, being independent on high-emission energy in the intensive building consumption; and 2) promoting industry upgrading and renewable energy implementation.

Such a policy directs a prospective opportunity for the STF building application. Therefore the establishment of pilot-scale STF building integration with the building contactor or the professional event/exhibition holder, such as *Solar Decathlon China* is expected to raise the public's attention. The expected cooperation between industries will:

1) Configure a technical breakthrough in the subject for the widespread market penetration of the STF technology;

2) Seek a feasible solution for solar thermal technology in future building application;

3) Accelerate more advanced multifunctional STF development.

9.2.3 Industrialization in STF implementation

For achieving sustainable development in China, industrialization has been recently assumed as a fundamental solution to accomplish the transformation of construction industry. It is worthy of investing on account of the increases in both productivity and cost effectiveness, and the reductions in both the consumed energy and the on-site construction pollution.

1) In terms of STF manufacturing, industrial robot manufacturing will come to stage soon, especially for the prefabricated STF

component, in the fourth revolution of science and technology. Both production cycle and cost can be benefited from not only quality control procedures but also the advanced flow line production;

2) In terms of STF application, industrializing construction can facilitate product's quality improvement, accurate on-site installation. Moreover, due to both quality control procedures and the advanced flow line production, the on-site construction resource can be utilized more efficiently with less pollution.

Via means of the mature production process of solar thermal technology, the relevant manufacturers can realize updates in new products development, the segment market penetration as well as production techniques.

9.2.4   Further STF promotion with financial supportive analysis

Different from "business as usual" product, the investment of STF implementation in a larger scale still faces uncertainty on condition that all future values of variables are not assured at present. Typical examples of such data are: service life of a given investment project, investment costs, energy cost savings potential in relation to the utilization/load factor escalation of energy prices, and interest and discount rates. Therefore, it is essential to carry out a sensitivity analysis to assess the sensitivity with the variations in a number of input parameters.

The potential research method can be the computational algorithm that relies on the repeated random sampling between a minimum and a maximum to obtain numerical results of the economic consequences of crucial input parameters. Other than a single parameter calculation, (while keeping the others constant), the advantages of computational algorithm are the sensitivity for all parameters over the full range of all parameters in assessed.

On the other hand, the green finance scheme is another prospective aspect to be focused on, so as to boost the wide spread of the innovative renewable technology application, such as the proposed STF in the building sector, as well as promote sustainable development for the society. And the financial support scheme of the innovative renewable technology is suggested to set up from 3 perspectives of inclining financial policies, multidimensional financial suppliers and diversified financing channels.

9.2.5 Further application with STF-BIM design approach

Based on the mentioned BIM-STF design proposal, a variety of building typologies and application fields can be explored and optimized:

1) Coordination with other software to carry out the integrated quantifications and the detailed impacts investigations, like shading, thermal behaviour, energy potentiality, socio-economic benefits (at early design stage of the STF implementation);

2) Aggregation of model file and construction data with the objectives of: photorealistic model rendering, object animation, reality capture enhancement, real time navigation, clash detection, and interference checking (at construction and commission stage of the STF implementation);

3) Streamlining collaboration with interoperability enhancements and providing further information application with human behaviour data analysis for the future smart home control and related policy making (at daily operation stage of the STF implementation).

Table 9-1 Control strategy of the STF DHW system throughout a whole year

No.	Variation range			Control[3]		Operation status
	I (W/m²)	T_a (℃)[1]	ΔT(℃)[2]	P_1	P_2	
1	$I \leq 100$	$T_a < 0$	--	On		Anti-freezing protection with auxiliary heater at a lower flowrate;
2		$0 \leq T_a < T_{set1}$	--	Off		Heat accumulation;
3		$T_a \geq T_{set1}$	$\Delta T \leq 0$	Off/On		Heat accumulation or heat dissipation judged by DHW consumption status;
4			$\Delta T > 0$	On	Off	Heat dissipation for facade during summer night time;
5	$100 < I \leq 500$	$T_a < 0$ & $T_{set1} < T_a \leq 0$	$\Delta T \leq 0$	Off		Cut-off STF operation;
6			$T_{set2} > \Delta T > 0$	On	Off	Heat accumulation for facade at a lower flowrate;
7			$T_{set3} > \Delta T \geq T_{set2}$		On	Normal operation;
8		$T_a \geq T_{set1}$	$\Delta T \leq 0$	Off		Cut-off STF operation;
9			$T_{set2} > \Delta T > 0$	On	Off	Heat accumulation at a lower flowrate;
10			$T_{set3} > \Delta T \geq T_{set2}$		On	Normal operation;
11			$\Delta T \geq T_{set3}$			Enhanced operation at a greater flowrate;
12	$I > 500$	$T_a < 0$	$\Delta T \leq 0$	Off		Cut-off STF operation;
13			$T_{set2} > \Delta T > 0$	On	Off	Heat accumulation for facade at a lower flowrate;
14			$T_{set3} > \Delta T \geq T_{set2}$		On	Normal operation;
15		$0 \leq T_a < T_{set1}$	$\Delta T \leq 0$	Off		Cut-off STF operation;
16			$T_{set2} > \Delta T > 0$	On	Off	Heat accumulation for facade at a lower flowrate;
17			$T_{set3} > \Delta T \geq T_{set2}$	On	On	Normal operation;
18			$\Delta T \geq T_{set3}$			Enhanced operation at a greater flowrate;
19		$T_a \geq T_{set1}$	$\Delta T \leq 0$	Off	Off	Cut-off STF operation;
20			$T_{set2} > \Delta T > 0$			Heat dissipation for facade at a lower flowrate;
21			$T_{set3} > \Delta T \geq T_{set2}$	On	On	Normal operation;
22			$\Delta T \geq T_{set3}$			Heat dissipation at a greater flowrate to prevent overheating without DHW demand

Note:1)The value range of T_{set1} would be defined between 20 and 30 ℃ for efficient operation results;

2)ΔT is temperature difference between STF surface and water tank; T_{set2} is less than T_{set3};

3) P_1 is defined as the position of the water pump in the system, while P_2 is defined as the position of the internal heat exchanger in water tank;

APPENDIX A

A.1 Outdoor experimental set up

The outdoor experimental rig for the proposed STF system was continuously operated and recorded in the overcast and cloudy weather conditions from 14th to 21st July 2015 in Shanghai, China.
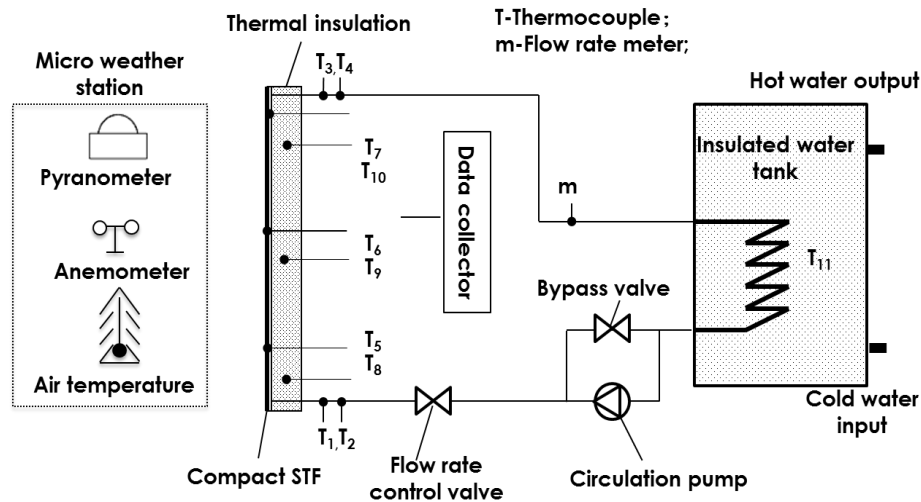
Figure A-1 Schematic design of the outdoor STF testing rig

Different from the laboratory controlled indoor measurement, the outdoor testing was fully operated for about eight hours daily. And all the measurement instruments were shown in Table 6-1. Figure A-1and Figure A-2 provide a schematic and photographic illustration of the experimental rig respectively. As for the number of T-type thermocouples, No. 1/2/3/4 and No.11 were respectively placed in the inlet/outlet of the water loop and the middle of water tank, while No.5/6/7/8/9/10 were equidistantly attached along the external surface of STF absorber from top to bottom. All these thermal couples were linked to the Agilent 34970A data logger associated with a computer for data recording. Moreover the ultrasonic thermal flow meter was connected into the pipe to measure the instantaneous flow rate. The micro weather station was applied to record the surrounding climate statuses, such as solar radiation, dry bulb outdoor temperature, humidity, wind speed/direction, barometric pressure,

precipitation and solar irradiation. All the testing results were recorded at one-hour interval.
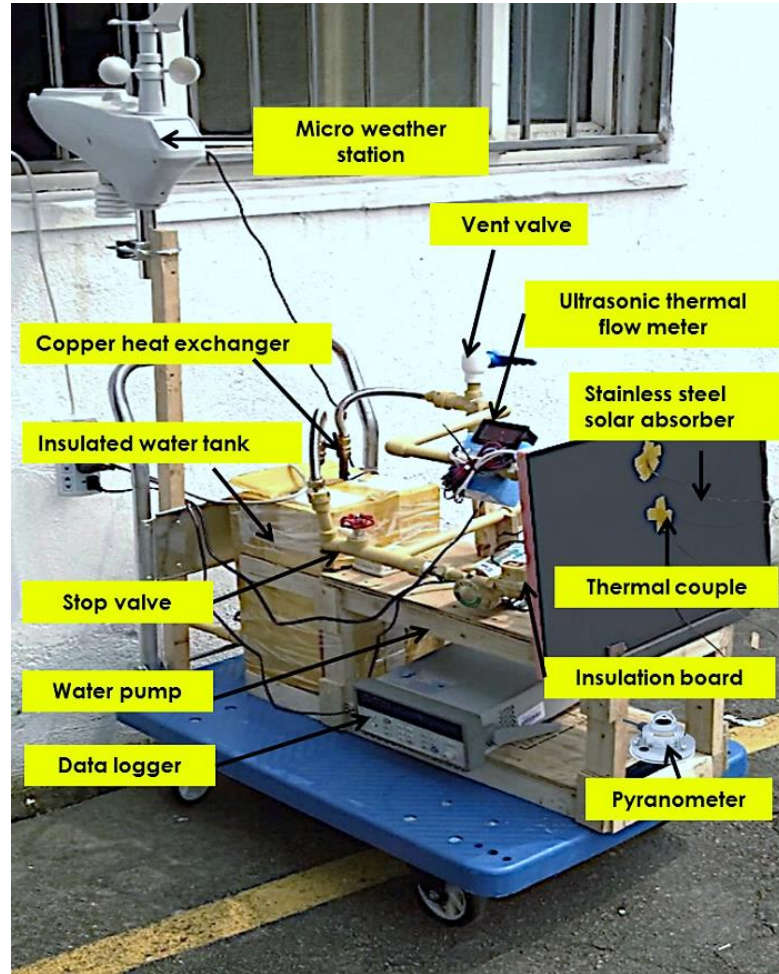
Figure A-2 Images of the outdoor STF testing rig

A.2 Definition of performance metrics

During the experiment, the useful heat gain of the STF Q_U is expressed as

$$Q_U = m_w C_P (T_o - T_{in}) \qquad \text{[A-1]}$$

And the STF thermal efficiency is then

$$\eta_{th} = F_R [\alpha_P - \frac{U_L(T_{in} - T_a)}{I}] \qquad \text{[A-2]}$$

While the definition of thermal efficiency of a STF module is the ratio of useful thermal energy Q_U to incident irradiation I striking on the collecting area of STF plate A_P.

$$\eta_{th} = \frac{Q_U}{IA_p} \tag{A-3}$$

As a type of solar thermal system, the module thermal efficiency can be alternatively derived from the following semi-empirical efficiency model to correlate with external weather and operational conditions. Hereby, the useful heat gain can be rewritten by F_R and the inlet water temperature, T_{in} (Kalogirou, 2009):

$$Q_U = A_p F_R [I\alpha_P - U_L(T_{in} - T_a)] \tag{A-4}$$

A.3 Operational performance results

A.3.1 Daily performance

The daily testing results of the testing rig are given in Table A-1. The temperature of absorber varied from 26.2 °C to 42.8 °C along with the water temperature variation in water tank from 25.5 °C to 40.1°C accordingly. In general, the daily average solar thermal efficiency of the STF fluctuated from 40% to 45.5%, with an average of 43.3%. Based on Equation [A-4], the semi-empirical thermal efficiency can also be expressed with the correlations of both external weather and operational conditions:

$$\eta_{th} = \eta^*_{th} - \frac{U_L(T_{in} - T_a)}{I} \tag{A-5}$$

where, η^*_{th} is the characteristic module thermal efficiency, and can be interpreted when the temperature of the inlet working fluid T_{in} equals to the mean ambient air temperature T_a; U_L is the heat loss coefficient mentioned from Equation [5-2] to [5-5]. With the measured weather and operational conditions, the values of η^*_{th} and U_L/I for this STF module can be determined by the linear regression analysis.

From Figure A-3, it could be found that both the linear coefficient and the intercept in Equation [A-6] were relatively low under this summer

operation. According to the definition from Equation [5-2] to [5-5], it then could be identified that the linear coefficient relevant to heat loss coefficient was beneficial from the warmer outdoor temperature range (29.9℃ to 32.5℃ in average) and the median wind speed range (0.17 m/s to 1.22 m/s in average), while the intercept relevant to the characteristic module thermal efficiency were attributed to cloudy or overcast weather conditions (166.4 W/m^2 to 325.8 W/m^2 in average). However, the linear coefficient would increase significantly along with the extreme weather conditions with lower surrounding air temperature or/and higher wind speed.

$$\eta_{th}=-2.9471(T_{in}-T_a)/I+0.5381 \hspace{4cm} [A-6]$$
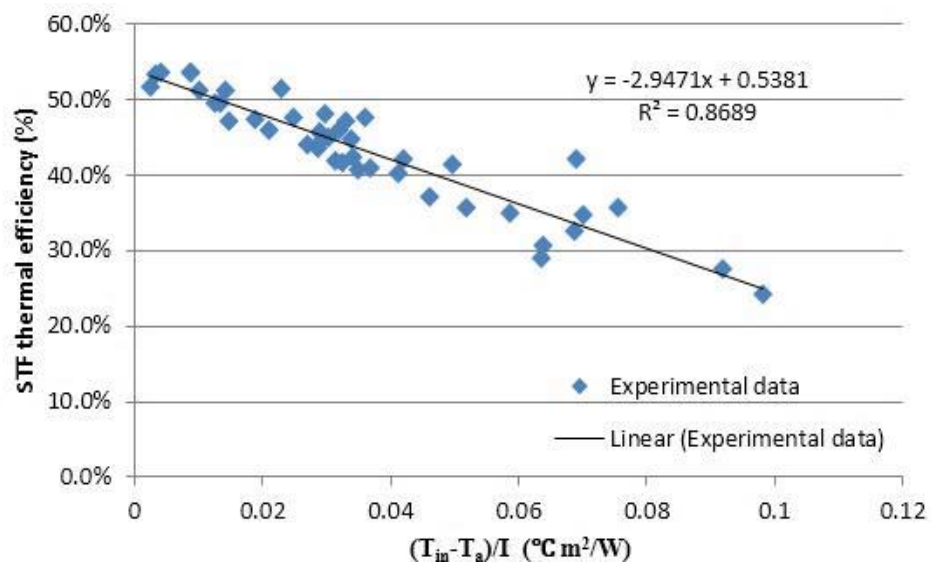
Figure A-3 Linear regression graph of the proposed STF's thermal efficiency

A.3.2 Instantaneous Performance

Figure A-4 depicted the instantaneous temperature distributions of different system components and the surrounding air in the testing day of 16th July 2015.

It was found that all temperature values present similar variations along with the ambient temperature, being up-rising in the morning and down falling in the afternoon. The temperature of the tank water

grew continuously from 25.5℃ at the beginning to the highest of 37.4℃ around the early afternoon, but finally fell down to 35.℃ at the end of day. This was because higher-temperature working fluid circulated in the loop led to a higher heat loss to surroundings especially after the peak time point of both solar radiation and air temperature, and consequently slightly decreased the water temperature in the water tank.
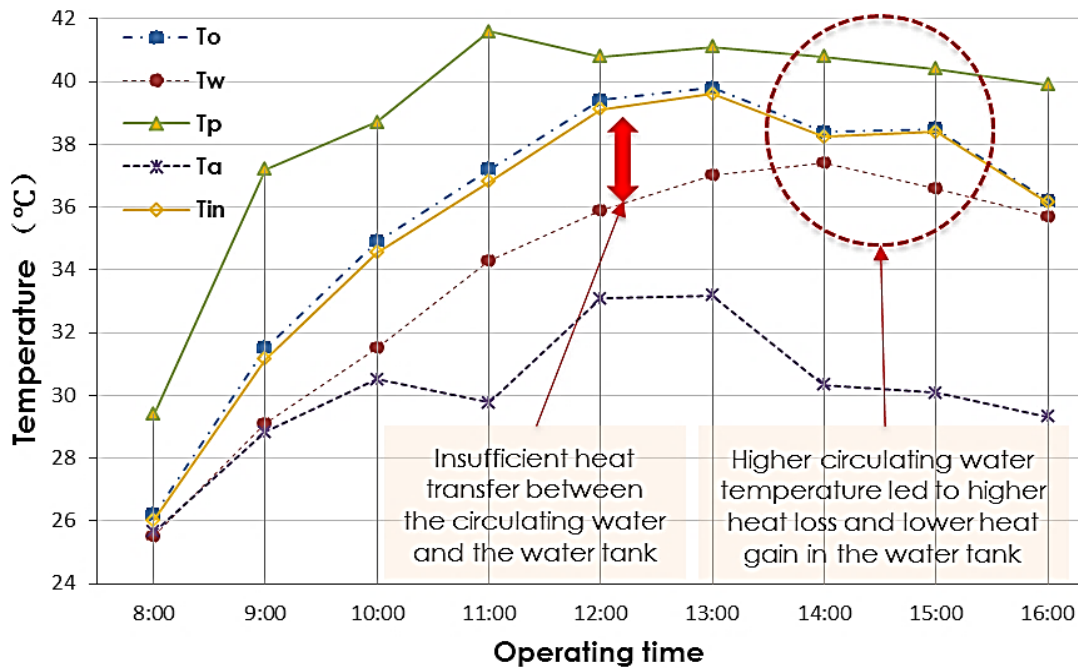
Figure A-4 Temperature variation in different STF components over testing duration

On the other hand, the stainless steel material also contributed partially to the quick response of both heat gain and heat loss for the STF module. This could be mitigated through accurate system control, such as regulating circulation flow rate, or bypassing solar circuit to the water tank. In addition, there was an obvious temperature gap between the water tank and the inlet of absorber. It could attribute to the insufficient heat transfer in the internal heat exchanger caused by the implementation of a simple U-shape pipe as the internal heat exchanger. In terms of temperature distribution in STF absorber, it varied in the range between 29.4℃ to 41.6℃ with a mean value of 38.9℃. The temperature gap between STF surface and the outlet of absorber were about 1.3℃ to 5.7℃. And the greatest and smallest gaps oc-

curred in the beginning and the middle day respectively due to the variations in solar radiation, incidence angle of solar beams and surrounding temperature.
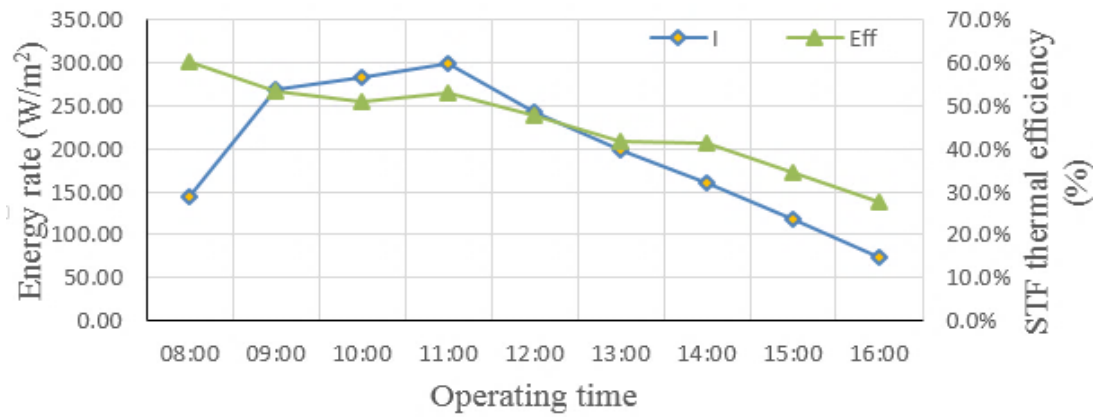
Figure A-5 Variation of solar radiation, STF thermal efficiency over testing duration

Finally, Figure A-5 illustrated the variation of solar radiation and its corresponding thermal efficiency changes over the testing duration. The variation of the STF's thermal output was similar to the variation of the solar radiation, presenting a sharp increasing trend in the morning, and a decreasing trend in the later afternoon. The possible reason was that solar incidence angle, air temperature, and wind speed primarily affect the solar thermal efficiency. Since the change magnitudes of wind speed and air temperature were evenly distributed around 30.1℃ and 1.2m/s respectively. Solar incidence angle was concluded as the dominating factor in this case, leading to sharp changes in both the solar thermal efficiency and the STF's thermal output. In the remaining operational periods, the above parameters counteracted each other equivalently and enabled a relatively steady thermal efficiency and thermal output.

Table A-1 Testing results over a consecutive period under real climate conditions

Day	Time	8:00	9:00	10:00	11:00	12:00	13:00	14:00	15:00	16:00	Mean
14 July 2015	T_a (°C)	28.6	32.0	33.0	33.9	34.2	34.0	32.3	32.6	32.1	32.5
	I (W/m²)	339.7	308.3	402.9	410.0	246.0	205.0	137.1	115.3	85.0	249.9
	T_{in} (°C)	30.2	33.0	34.6	39.9	42.0	42.6	41.8	41.3	40.5	38.4
	T_o (°C)	30.6	33.4	35.1	40.4	42.2	42.8	41.9	41.4	40.5	38.7
	η	52.1%	53.4%	53.6%	47.2%	41.8%	42.2%	42.0%	35.7%	24.2%	43.6%
	$V_{a,ave}$ (m/s)					0.58					
	$T_{w,min}$ (°C)					27.5					
	$T_{w,max}$ (°C)					40.1					
15 July 2015	T_a (°C)	27.4	29.9	31.0	30.7	30.6	30.6	30.3	29.5	29.1	29.9
	I (W/m²)	310.0	426.8	528.5	478.7	368.9	266.3	282.6	171.2	99.1	325.8
	T_{in} (°C)	30.1	34.3	37.7	39.6	41.2	40.2	37.9	36.5	35.9	37.0
	T_o (°C)	30.5	34.8	38.3	40.2	41.6	40.5	38.2	36.7	36.0	37.4
	η	53.5%	51.1%	49.5%	47.3%	43.4%	47.6%	44.1%	40.3%	32.6%	45.5%
	$V_{a,ave}$ (m/s)					0.97					
	$T_{w,min}$ (°C)					25.7					
	$T_{w,max}$ (°C)					39.7					
16 July 2015	T_a (°C)	25.7	28.8	30.5	29.8	33.1	33.2	30.3	30.1	29.3	30.1
	I (W/m²)	143.5	269.0	282.2	298.65	242.0	197.8	159.5	118.8	74.4	198.4
	T_{in} (°C)	26.0	31.2	34.5	36.8	39.1	39.6	38.2	38.4	36.2	35.6
	T_o (°C)	26.2	31.5	34.9	37.2	39.4	39.8	38.4	38.5	36.2	35.8
	η	60.3%	53.6%	51.1%	45.5%	47.6%	41.6%	41.3%	34.7%	27.7%	44.8%
	$V_{a,ave}$ (m/s)					1.22					
	$T_{w,min}$ (°C)					25.5					
	$T_{w,max}$ (°C)					37.7					

17 July 2015	T_a (°C)	26.9	28.2	29.3	29.7	30.9	31.4	31.1	30.8	30.6	29.9
	I (W/m^2)	131.2	170.1	198.6	212.7	279.1	149.6	140.7	114.5	101.3	166.4
	T_{in} (°C)	29.7	33.1	35.0	36.5	39.2	40.2	38.4	38.1	37.0	36.3
	T_o (°C)	29.8	33.3	35.2	36.7	39.5	40.3	38.5	38.2	37.1	36.5
	η	45.9%	45.7%	43.9%	45.9%	48.0%	35.1%	35.7%	30.6%	29.0%	40.0%
	$V_{a,ave}$ (m/s)						0.75				
	$T_{w,min}$ (°C)						25.9				
	$T_{w,max}$ (°C)						38.7				
18 July 2015	T_a (°C)	28.6	30.1	31.2	31.5	33.7	34.1	32.4	31.9	31.8	31.7
	I (W/m^2)	81.7	92.0	114.1	145.2	153.7	197.0	178.3	138.7	94.6	132.8
	T_{in} (°C)	29.7	33.2	35.1	36.6	39.3	40.1	38.3	38.3	37.6	36.5
	T_o (°C)	29.8	33.3	35.2	36.7	39.5	40.3	38.5	38.4	37.6	36.6
	η	49.6%	44.8%	42.4%	40.8%	40.8%	44.9%	47.2%	37.2%	39.2%	43.0%
	$V_{a,ave}$ (m/s)						0.17				
	$T_{w,min}$ (°C)						26.4				
	$T_{w,max}$ (°C)						37.1				

REFERENCES

Ackermann, J.A., Ong, L.-E. & Lau, S.C., 1995. Conjugate heat transfer in solar collector panels with internal longitudinal corrugated fins—Part I: Overall results. Forschung im Ingenieurwesen, 61(4), pp.84–92.

Akhtar, N. & Mullick, S.C., 2012. Effect of absorption of solar radiation in glass-cover(s) on heat transfer coefficients in upward heat flow in single and double glazed flat-plate collectors. International Journal of Heat and Mass Transfer, 55(1-3), pp.125–132.

Aksamija, A. et al., 2011. Parametric Control of BIM Ele-ments for Sustainable Design in Revit: Linking Design and Analytical Software Applications through Cus-tom-ization, Perkins+Will Research Journal, Vol. 3, No. 1, pp. 32-45.

Aksamija, A., 2013. Building simulations and high-performance buildings research: use of Building Information Modeling (BIM) for Integrated Design and Analysis, Perkins+Will Research Journal, Vol. 5, No. 1, pp. 19-37.

Anderson, T. N. et al. ,2010. The effect of colour on the thermal performance of building integrated solar collectors. Solar Energy Materials and Solar Cells. 94 ,2., 350–354.

Aste, N. et al., 2015. Effectiveness and weaknesses of supporting policies for solar thermal systems—A case-study. Sustainable Cities and Society. 14146–153.

Badescu, V., 2007. Optimal control of flow in solar collectors for maximum exergy extraction. International Journal of Heat and Mass Transfer, 50(21-22), pp.4311–4322.

Barshilia H., 2014. Characterization and performance evaluation of Ti/AlTiN/AlTiON/AlTiO high temperature spectrally selective coatings for solar thermal power applications. Solar Energy Material and Solar Cells, 130 (2014), pp. 322–330

Bas, E., 2013. A robust approach to the decision rules of NPV and IRR for simple projects. Applied Mathematics and Computation, 219(11), pp.5901–5908.

Bergman, T.L. et al., 2011. Fundamentals of Heat and Mass Transfer. 7 edition. John Wiley & Sons.

Blickensderfer R. et al., 1977. Spectral reflectance of TiNx and ZrNx films as selective solar absorbers, Solar Energy, 19 (1977), pp. 429–432

Bobes-Jesus,V. et al.,2013. Asphalt solar collectors: a literature review. Applied Energy, 102, pp. 962–970

Bonhôte, P., et al., 2009. Unglazed coloured solar absorbers on façade: Modelling and performance evaluation. Solar Energy, 83(6), pp.799–811.

Bosanac, M. et al., 2003. Photovoltaic/ thermal solar collectors and their potential in Denmark,

Buker, M. S. & Riffat, S. B., 2015. Building integrated solar thermal collectors – A review. Renewable and Sustainable Energy Reviews. 51327–346.

Buker, M.S. et al., 2014. Performance evaluation and techno-economic analysis of a novel building integrated PV/T roof collector: An experimental validation. Energy and Buildings, 76, pp.164–175.

Burnett, D. et al., 2014. The UK solar energy resource and the impact of climate change. Renewable Energy, 71, pp.333–343.

Cappel et al., 2014. Barriers to the market penetration of façade-integrated solar thermal systems. Energy Procedia. Proceedings of the 2nd International Conference on Solar Heating and Cooling for Buildings and Industry (SHC 2013), vol. 48 (2014), pp. 1336–1344

Cengel, Y. & Ghajar, A., 2014. Heat and Mass Transfer: Fundamentals and Applications. 5 edition. McGraw-Hill Education.

Chan, H.-Y. et al., 2010. Renewable and Sustainable Energy Reviews - Review of passive solar heating and cooling technologies. Renewable and Sustainable Energy Reviews, 14(2), pp.781–789.

Chang et al., 2015, Theoretical and Experimental Research on Thermal Performance of Solar Air Collector with Finned Absorber, Energy Procedia 70: 13–22

Chen, K. et al., 2010. Fabrication and testing of a non-glass vacuum-tube collector for solar energy utilization. Energy, 35(6), pp.2674–2680.

Chow, T.T., 2010. A review on photovoltaic/thermal hybrid solar technology. Applied Energy, 87(2), pp.365–379.

Colombo et al., 2014, An Approximate Analytical Approach to Steady State Simulation of Unglazed Solar Collectors, Energy Procedia 48: 28–36

Compagno, A. ,2002. Intelligent Glass Facades. Princeton Architectural Press.

D'Antoni, M. & Saro, O., 2012. Massive Solar-Thermal Collectors: A critical literature review. Renewable and Sustainable Energy Reviews, 16(6), pp.3666–3679.

Delgado, M. et al., 2012. Experimental analysis of a microencapsulated PCM slurry as thermal storage system and as heat transfer fluid in laminar flow. Applied Thermal Engineering, 36, pp.370–377.

Deng, Y. et al., 2013. Experimental investigation of performance for the novel flat plate solar collector with micro-channel heat pipe array (MHPA-FPC). Applied Thermal Engineering, 54(2), pp.440–449.

Department of Engergy & Climate Change, DECC, 2012. The future of heating: a strategic framework for low carbon heat, Department of Energy & Climate Change.

Department of Energy and Climate Change, DECC ,2014. Renewable sources of energy: chapter 6, Digest of United Kingdom energy statistics. gov.uk

Department of Energy Centre, DOEC, 2013. The future of heating: meeting the challenge – Publications. Available from: https://www.gov.uk/government/publications/the-future-of-heating-meeting-the-challenge ,Accessed 19 May 2015.

Du X. et al., 2008. Microstructure and spectral selectivity of Mo–Al2O3 solar selective absorbing coatings after annealing,Thin Solid Films, 516 (2008), pp. 3971–3977

Dubois, M.-C. & Horvat, M. eds., 2010. State-of-the-Art of Digital Tools Used by Architects for Solar Design, IEA SHC.

Duerr, U., 2006. Welding thermal solar absorbers - Industrial Laser Solutions. industrial-lasers.com. Available at: http://www.industrial-lasers.com/articles/2006/09/welding-thermal-solar-absorbers.html [Accessed June 16, 2013].

Duffie, J.A. & Beckman, W.A. (2006) Solar Engineering of Thermal Processes. John Wiley & Sons.

Dymond C., & Kutscher C., 1997. Development of a flow distribution and design model for transpired solar collectors. Solar energy, 60(5) pp.291-300

Ehab AlShamaileh, 2010.Testing of a new solar coating for solar water heating applications.Solar energy, 84(9) pp.1637-1643

Emmer Pfenninger Partner AG, 2012, D4.1.2 Integrated Concepts - Construction Aspects. European community seventh framework programme. Seventh framework programme cooperation – Theme 4

European solar thermal industry federation, ESTIF, 2012. Guide on Standardisation and Quality Assurance for Solar Thermal. solarthermalworld.org. Available at: http://solarthermalworld.org/sites/gstec/files/standardisation.pdf [Accessed May 10, 2013].

European Solar Thermal Technology Platform, ESTTP ,2009. Solar Heating and Cooling for a Sustainable Energy Future in Europe, European Solar Thermal Technology Platform.

Faninger, G. ,2010. The Potential of Solar Thermal Technologies in a Sustainable Energy Future. IEA Solar Heating & Cooling Programme

Farahat, S.et al., 2009. Exergetic optimization of flat plate solar collectors. Renewable Energy, 34(4), pp.1169–1174.

Fleck, B.A. et al., 2002. A field study of the wind effects on the performance of an unglazed transpired solar collector. Solar Energy, 73(3), pp.209–216

Fraunhofer ISE, 2009. Bionicol - development of a bionic solar collector with aluminium roll-bond absorber. 7th framwork programme— Website of the BIONICOL project. Available from: http://www.bionicol.eu/ ,Accessed 5 June 2015.

Fudholi, A. et al., 2015. Techno-economic of solar drying systems with water based solar collectors in Malaysia: A review. Renewable and Sustainable Energy Reviews, 51, pp.809–820.

Glanville N., 2014. BIM must be embraced as a business process not a design technology, Infrastructure Intelligence, 2014 May 08 . Available from: http://www.infrastructure-intelligence.com/article/may-2014/bim-must-be-embraced-business-process-not-design-technology Accessed 5 June 2015.

German Solar Energy Society, GSES, 2010. Planning and Installing Solar Thermal Systems. 2nd edition. Earthscan Ltd.

Giovanardi, A. ,2012. Integrated solar thermal facade component for building energy retrofit. PhD thesis of Doctoral School in Environmental Engineering, Università degli studi di trento in collaboration with Eurac research.

Giovanardi, A. et al., 2015., Integrated solar thermal façade system for building retrofit. Solar Energy, 122, pp.1100–1116.

Golić, K. et al., 2011. General model of solar water heating system integration in residential building refurbishment—potential energy savings and environmental impact. Renewable and Sustainable Energy Reviews, 15(3), pp.1533–1544.

Gratia, E. & De Herde, A., 2002. A Simple De-sign Tool for the Thermal Study of an Office Building, Energy and Buildings, Vol. 34, pp. 279-289.

Griffith, B.T. & Ellis, P.G., 2004. Photovoltaic and Solar Thermal Modeling with the EnergyPlus Calculation Engine. In the World Renewable Energy Congress VIII and Expo.

GSWH ,2012. Guide on Standardisation and Quality Assurance for Solar Thermal. . 10 May 2012. solarthermalworld.org. Available from: http://solarthermalworld.org/ sites/gstec/files/standardisation.pdf [Accessed: 10 May 2013].

GUM,1995, Evaluation of measurement data-Guide to the expression of uncertainty in measurement JCGM 100:2008. Joint Committee for Guides in Metrology. Available at: http://www.iso.org/sites/JCGM/GUM-introduction.htm [Accessed December 7, 2015].

Gunnewiek et al., 2002. Effect of wind on flow distribution in unglazed transpired-plate collectors. Solar Energy, 72(4), pp.317–325.

Haillot, D. et al., 2012. Optimization of solar DHW system including PCM media. Applied Energy.

Harrison, S. & Cruickshank, C.A., 2012. A review of strategies for the control of high temperature stagnation in solar collectors and systems. Energy Procedia, 30, pp.793–804.

He, W. et al., 2015. Operational performance of a novel heat pump assisted solar façade loop-heat-pipe water heating system. Applied Energy, 146, pp.371–382.

Hellstrom, B. et al., 2003. The impact of optical and thermal properties on the performance of flat plate solar collectors. Renewable Energy, 28(3), pp.331–344.

Hendriksen, O. J. et al. ,2000. Double skin facades—fashion or a step towards sustainable buildings . Available from: http://www.google.com/search?client=safari&rls= en&q=Double+skin+facades%E2%80%94fashion+or+a+step+towards+sustainable+b uildings&ie=UTF-8&oe=UTF-8 ,Accessed 9 April 2013.

Hermann, M., 2012, Development of a Bionic solar collector with aluminium roll-bond absorber. 7th framework programme Theme 5 (Energy). Available at:

http://www.bionicol.eu/Final_Report_BIONICOL.pdf/view [Accessed August 31, 2015].

Ho, C. D. et al. ,2005. Heat-transfer enhancement in double-pass flat-plate solar air heaters with recycle. Journal of the Taiwan Institute of Chemical Engineers, Volume 42, Issue 5, September 2011, Pages 793–800

Ho, C. D. et al. ,2011. Collector efficiency of upward-type double-pass solar air heaters with fins attached. International Communications in Heat and Mass Transfer. . 38 ,1., 49–56.

Jaehnig, D. & Isaksson, C. ,2006. Solar integration, five easy ways to incorporate solar thermal into conventional heating systems . Available from: http://www.solaripedia.com/files/367 ,Accessed 13 August 2015.

Jafarkazemi, F. & Ahmadifard, E., 2013. Energetic and exergetic evaluation of flat plate solar collectors. Renewable Energy, 56, pp.55–63.

JCGM, 2008. BIPM - Guide to the Expression of Uncertainty in Measurement (GUM), Bureau international des poids et measures.me

Ji, J. et al. ,2011. Thermal characteristics of a building-integrated dual-function solar collector in water heating mode with natural circulation. Energy. . 36 ,1., 566–574.

Kalogirou, S.A. ,2004. Solar thermal collectors and applications. Progress in Energy and Combustion Science. . 30 ,3., 231–295. Available from: doi:10.1016/j.pecs.2004.02.001.

Kalogirou, S.A. et al., 2005. Performance of solar systems employing collectors with colored absorber. Energy and Buildings, 37(8), pp.824–835.

Kalogirou, S.A. ,2009. Solar Energy Engineering. Academic Presses: Elsevier.

Karlessi, T., 2012. A DST tool including case studies with examples and pictures of virtual and real buildings. Support for planners and how to integrate the new concept in BMS. Best practice catalogues, examples of business models, test results for components. Support for design and commissioning of BMS, Cost Effective Project

Khoukhi, M. & Maruyama, S., 2005. Theoretical approach of a flat plate solar collector with clear and low-iron glass covers taking into account the spectral absorption and emission within glass covers layer. Renewable Energy, 30(8), pp.1177–1194.

Khoukhi, M. et al., 2007. Non-grey calculation of plate solar collector with low iron glazing taking into account the absorption and emission with a glass cover. Desalination, 209(1-3), pp.156–162.

Koene, F., 2010. Report on unambiguous technical/physical specifications for the building elements, components and constructions described in D2.1.3, Seventh Framework Programme Cooperation - Theme 4.

Koene, F. ,2012. Report on the developed techno-economic integrated concepts. European Community Seventh Framework Programme.

Kollektorfabrik GmbH & Co. , 2011. D3.2.2 Prototype of an air heating vacuum tube collector for façade integration. European Community Seventh Framework Programme. Seventh framework programme cooperation - theme 4.

Kuchta, D., 2000. Fuzzy capital budgeting. Fuzzy Sets and Systems, 111(3), pp.367–385.

Kumar, R. & Rosen, M.A., 2011. A critical review of photovoltaic–thermal solar collectors for air heating. Applied Energy, 88(11), pp.3603–3614.

Kurzböck, M. et al., 2012. Black pigmented polypropylene materials for solar absorbers. Energy Procedia, 30, pp.438–445.

Lambert, A. A. et al. ,2006. Enhanced heat transfer using oscillatory flows in solar collectors. Solar Energy. . 80 ,10., 1296–1302.

Lamnatou, C. et al., 2015. Life cycle energy analysis and embodied carbon of a linear dielectric-based concentrating photovoltaic appropriate for building-integrated applications. Energy and Buildings.V107, 366-375

Lamnatou,C. et al., 2016. Building-integrated solar thermal systems based on vacuum-tube technology: Critical factors focusing on life-cycle environmental profile, Renewable and Sustainable Energy Reviews, Volume 65, November 2016, Pages 1199-1215, ISSN 1364-0321,

Leon, M.A. & Kumar, S., 2007. Mathematical modeling and thermal performance analysis of unglazed transpired solar collectors. Solar Energy, 81(1), pp.62–75.

Lewis M. F. et al., 2010. Solar Cells and Their Applications,2nd edition, John Wiley & Sons, Inc. pp. 171–206.

Liu Y. et al., 2012. The spectral properties and thermal stability of NbTiON solar selective absorbing coating,Solar Energy Material and Solar Cells, 96 (2012), pp. 131–136

Lobaccaro, G. et al., 2012. District Geometry Simulation: A Study for the Optimization of Solar Façades in Urban Canopy Layers. Energy Procedia, 30, pp.1163–1172.

Löwe, K. et al., 2011. Determining the environmental influence of energy generating components for façade integration within existing high-rise buildings by means of LCA. 5th LCM 2011 conference on Life Cycle Management. Available at: http://www.cost-effective-renewables.eu/ includes/images/Publications/Files/07dc7be2a4ce67049374c93afc5e7c79.pdf[Accessed May 21, 2013].

Lundh M. et al., 2010. Antireflection treatment of Thickness Sensitive Spectrally Selective (TSSS) paints for thermal solar absorbers. Solar Energy, 84(1), pp.124–129.

MacLeay, I. et al.,2012. The Digest of UK Energy Statistics 2012. A National Statistics publication

Mahdjuri, F., 1999. Solar collector with temperature limitation using shape memory metal. Renewable Energy, 16(1-4), pp.611–617.

Martinopoulos, G. et al.,2010. CFD modeling of a polymer solar collector. Renewable Energy. . 35 ,7., 1499–1508.

Matuska, T. & Sourek, B., 2006. Façade solar collectors. Solar Energy, 80(11), pp.1443–1452.

Maurer, C. & Kuhn, T.E., 2012. Variable g value of transparent façade collectors. Energy and Buildings, 51, pp.177–184.

Maurer, C. et al.,2012. Solar Heating and Cooling with Transparent Façade Collectors in a Demonstration Building . Available from: http://www.sciencedirect.com/science/article/pii/S1876610212016323 ,Accessed 15 April 2013.

Mauthner et al., Solar heat worldwide. IEA Solar Heating & Cooling Programme. Available at: http://www.iea-shc.org/data/sites/1/publications/Solar-Heat-Worldwide-2015.pdf [Accessed August 7, 2015].

Meaburn, A. & Hughes, F.M., 1996. A simple predictive controller for use on large scale arrays of parabolic trough collectors. Solar Energy, 56(6), pp.583–595.

Medved, S. et al., 2003. A large-panel unglazed roof-integrated liquid solar collector—energy and economic evaluation. Solar Energy, 75(6), pp.455–467.

Mertin, S. et al., 2013. Reactively sputtered coatings on architectural glazing for coloured active solar thermal façades. Energy and Buildings.

Mintsa Do Ango, A. C. et al.,2013. Optimization of the design of a polymer flat plate solar collector. Solar Energy. . 8764–75.

Motte, F. et al.,2013a. Design and modelling of a new patented thermal solar collector with high building integration. Applied Energy. . 102631–639.

Motte, F. et al.,2013b. A building integrated solar collector: Performances characterization and first stage of numerical calculation. World Renewable Energy Congress - XI, 49, pp.1–5.

Musall, I. et al.,2013. Net Zero Energy Solar Buildings: An Overview and Analysis on Worldwide Building Projects, solar heating & cooling programme international energy agency Task 49: Solar heat integration in industrial process.

Nasrin, R., Alim, M.A. & Chamkha, A.J., 2012. Effects of physical parameters on natural convection in a solar collector filled with nanofluid. Heat Transfer?Asian Research, 42(1), pp.73–88.

National Renewable Energy Laboratory, NREL, 2011, U.S. Department of Energy Commercial Reference Building Models of the National Building Stock. Technical Report NREL/TP-5500-46861. Avaiable from:
http://www.nrel.gov/docs/fy11osti/46861.pdf

Nuru Z. et al., 2012. Pt–Al2O3 nano coatings for high temperature concentrated solar thermal power applications, Physica B: Condensed Matter, Volume 407, Issue 10, 15 May 2012, Pages 1634-1637

Nuru Z. et al., 2016. Optimization and preparation of Pt–Al2O3 double cermet as selective solar absorber coatings, Journal of Alloys and Compounds, Volume 664, 15 April 2016, Pages 161-168.

Oelhafen P., et al., 2005.Nanostructured materials for solar energy conversion, Solar Energy, 79 (2005), pp. 110–121

O'Hegarty et al.,Review and analysis of solar thermal facades, Solar Energy, Volume 135, October 2016, Pages 408-422, ISSN 0038-092X,

Orel, B. et al., 2007a. Silicone-based thickness insensitive spectrally selective (TISS) paints as selective paint coatings for coloured solar absorbers (Part I). Solar Energy Materials and Solar Cells, 91(2-3), pp.93–107.

Orel, B. et al., 2007b. Selective paint coatings for coloured solar absorbers: Polyurethane thickness insensitive spectrally selective (TISS) paints (Part II). Solar Energy Materials and Solar Cells, 91(2-3), pp.108–119.

Permasteelisa group, PG, 2011. Prototype for transparent thermal collector for window integration, 7th Frame work programme cooperation-Theme .

Pinel, P. et al. ,2011. A review of available methods for seasonal storage of solar thermal energy in residential applications. Renewable and Sustainable Energy Reviews. . 15 ,7., 3341–3359.

Probst, M. & Roecker, C. ,2007. Towards an improved architectural quality of building integrated solar thermal systems ,BIST. Solar Energy. . 81 ,9., 1104–1116.

Probst, M. C. M. ,2008. Architectural integration and design of solar thermal systems. PhD thesis of École Polytechnique Fédérale De Lausanne.

Probst, M.C.M. & Roecker, C. eds., 2012. Solar energy systems in architecture. T.41.A.2 I Task 41 - Solar energy & Architecture

Punjabi, S., and Miranda, V., 2005. Development of an Integrated Building Design Information Interface, Proceedings of IBPSA '05 Buildings Simulation Conference, Montreal, pp. 969-976.

Rassamakin B. et al., 2013. Aluminum heat pipes applied in solar collectors. Solar Energy, 94,pp.145-154

Rebouta L. et al., 2012. Optical characterization of TiAlN/TiAlON/SiO2 absorber for solar selective applications, Surface Coating Technology, 211 (2012), pp. 41–44

Reijenga T., 2012. Integrated concepts – catalogue of technical composition. European community seventh framework programme. Seventh framework programme cooperation – Theme 4; 2012 October. Report no.: D4.1.4.

Ridal, J., Garvin, S., Chambers, F. & Travers, J. ,2010. Risk assessment of structural impacts on buildings of solar hot water collectors and photovoltaic tiles and panels – final report. . 12 March 2010. solarthermalworld.org. Available from:http://solarthermalworld.org/sites/gstec/files/solar_thermal_collector_building_loads.pdf [Accessed: 12 April 2013].

Rodriguez-Ubinas, E. et al., 2012. Applications of Phase Change Material in highly energy-efficient houses. Energy and Buildings, 50, pp.49–62.

Roecker, C. et al., 2009. Facade Integration of Solar Thermal Collectors: A Breakthrough. In Berlin, Heidelberg: Springer Berlin Heidelberg, pp. 337–341

Rogers, J.G., McManus, M.C. & Cooper, S.J.G., 2013. Potential for reliance on solar water heating throughout the summer in northern cloudy climates. Energy and Buildings, 66, pp.128–135.

Romdhane, B.S., 2007. The air solar collectors: Comparative study, introduction of baffles to favor the heat transfer. Solar Energy, 81(1), pp.139–149.

Saha, S.K. & Mahanta, D.K., 2001. Thermodynamic optimization of solar flat-plate collector. Renewable Energy, 23(2), pp.181–193.

Sayigh A.A.M., 2000. Renewables: The Energy for the 21st Century World Renewable Energy Congress VI 1–7 July 2000 Brighton, UK. pp. 1036–1040.

Schimpf, S. & Span, R., 2015. Techno-economic evaluation of a solar assisted combined heat pump – Organic Rankine Cycle system. Energy Conversion and Management, 94, pp.430–437.

Schüler et al., 2000. Application of titanium containing amorphous hydrogenated carbon films (a-C:H/Ti) as optical selective solar absorber coatings, Solar Energy Ma-terials and Solar Cells, Volume 60, Issue 3, 31 January 2000, Pages 295-307, ISSN 0927-0248,

Selvakumar, N. & Barshilia, H.C., 2012. Review of physical vapor deposited (PVD) spectrally selective coatings for mid- and high-temperature solar thermal applications. Solar Energy Materials and Solar Cells, 98, pp.1–23.

Serra, V., Zanghirella, F. & Perino, M. ,2010. Experimental evaluation of a climate façade: Energy efficiency and thermal comfort performance. Energy and Buildings. 42 ,1., 50–62.

Shimizu M. et al., 2014. High-temperature Photonics Using Self-organization of Superalloys for Solar Selective Absorbers, Energy Procedia, Volume 57, 2014, Pages 411-417

Shukla, A. et al., 2012. A state of art review on the performance of transpired solar collector. Renewable and Sustainable Energy Reviews, 16(6), pp.3975–3985.

Shukla, R. et al., 2013. Recent advances in the solar water heating systems: A review. Renewable and Sustainable Energy Reviews, 19, pp.173–190.

Slaman, M. & Griessen, R., 2009. Solar collector overheating protection. Solar Energy, 83(7), pp.982–987.

Smyth, M., Eames, P.C. & Norton, B., 2000. Life Cycle Assessment of a Heat Retaining Integrated Collector/Storage Solar Water Heater (ICSSWH) - World Renewable Energy Congress VI - Chapter 210. In World Renewable Energy Congress VI

Sonnenenergie, D.G.F., 2010. Planning and installing solar thermal system. 2nd ed., Earthscan Ltd.

Sopian, K. et al., 2009. Evaluation of thermal efficiency of double-pass solar collector with porous–nonporous media. Renewable Energy, 34(3), pp.640–645.

Spur, R. et al., 2006. Performances of modern domestic hot-water stores. Applied Energy, 83, pp.893–910.

Stephens, B. R. ,1981a. Temperature responsive optical switch, US patent 4261331 . Available from: http://www.google.com/patents/US4261331 ,Accessed 31 May 2013.

Stephens, R. B. ,1981b. Fluid optical switch for a solar collector . Available from: http://www.google.co.uk/patents/US4270517 ,Accessed 31 May 2013.

Stojanović B, et al., 2010, A steady state thermal duct model derived by fin-theory approach and applied on an unglazed solar collector, Solar Energy 84 (10): 1838–1851

Szokolay, S.V., 2008. Introduction to architectural science, 2nd edition, Elsevier Ltd.

Tang, R., Yang, Y. & Gao, W., 2011. Comparative studies on thermal performance of water-in-glass evacuated tube solar water heaters with different collector tilt-angles. Solar Energy, 85(7), pp.1381–1389.

Tesfamichael, T. et al., 2001. Optical characterization and modeling of black pigments used in thickness-sensitive solar-selective absorbing paints. Solar Energy, 69, pp.35–43.

Tian, Y. & Zhao, C.Y., 2011. A numerical investigation of heat transfer in phase change materials (PCMs) embedded in porous metals. Energy, 36(9), pp.5539–5546.

Tian, Y. & Zhao, C.Y., 2013. A review of solar collectors and thermal energy storage in solar thermal applications. Applied Energy, 104, pp.538–553.

Tripanagnostopoulos, Y. et al., 2002. Hybrid photovoltaic/thermal solar systems. Solar Energy, 72(3), pp.217–234.

Tripanagnostopoulos, Y., 2007. Aspects and improvements of hybrid photovoltaic/thermal solar energy systems. Solar Energy, 81(9), pp.1117–1131.

Tyagi, V.V. & Buddhi, D., 2007. PCM thermal storage in buildings: A state of art. Renewable and Sustainable Energy Reviews, 11(6), pp.1146–1166.

Ucar, A. & Inallı, M., 2006. Thermal and exergy analysis of solar air collectors with passive augmentation techniques. International Communications in Heat and Mass Transfer, 33(10), pp.1281–1290.

Wall, M. et al. ,2012. Achieving Solar Energy in Architecture-IEA SHC Task 41. Energy Procedia. . 301250–1260.

Walker C. |., 2013. ROI, NPV and IRR. agilebok.org. Available at: http://www.agilebok.org/index.php?title=ROI,_NPV_and_IRR [Accessed November 4, 2015].

Wallner, G. M. et al. ,2008. Property and performance requirements for thermotropic layers to prevent overheating in an all polymeric flat-plate collector. Solar Energy Materials and Solar Cells. . 92 ,6., 614–620.

Wang, Z. et al., 2012. Dynamic performance of a facade-based solar loop heat pipe water heating system. Solar Energy, 86(5), pp.1632–1647. Available at: http://linkinghub.elsevier.com/retrieve/pii/S0038092X12000965.

Weber, A. & Resch, K. ,2012. Thermotropic glazings for overheating protection. Energy Procedia. . 30471–477.

Weiss, W., 2003. Solar Heating Systems for Houses W. Weiss, ed., James & James.

Werke, V., 2015, Technical guide: Solar thermal systems, www.viessmann.com, assessed on 21 December 2015.

"Wijewardane & Goswami, 2012.A review on surface control of thermal radiation by paints and coatings for new energy applications. Renewable and Sustainable Energy Reviews, 16(4), pp 1863-1873

Wijewardane, S. & Goswami, D.Y., 2012. A review on surface control of thermal radiation by paints and coatings for new energy applications. Renewable and Sustainable Energy Reviews, 16(4), pp.1863–1873.

Witzig, A. et al., 2009. Simulation tool for architects optimization of active and passive solar use. the international conference CISBAT. Available at: http://www.velasolaris.com/vs2/files/2009-09-cisbat-polysuninside.pdf [Accessed June 3, 2013].

Yadav, A.K. & Chandel, S.S., 2013. Tilt angle optimization to maximize incident solar radiation: A review. Renewable and Sustainable Energy Reviews, 23, pp.503–513.

Yang, Y. et al., 2013. A building integrated solar collector: All-ceramic solar collector. Energy and Buildings, 62, pp.15–17.

Youssef, Z. et al., 2013. State of the art on phase change material slurries. Energy Conversion and Management, 65, pp.120–132.

Zhai et al. ,2008. Experience on integration of solar thermal technologies with green buildings. Renewable Energy. . 33 ,8., 7–7.

Zhan, C. et al., 2011. Comparative study of the performance of the M-cycle counter-flow and cross-flow heat exchangers for indirect evaporative cooling – Paving the path toward sustainable cooling of buildings. Energy, 36(12), pp.6790–6805.

Zhang K. et al., 2017. A review on thermal stability and high temperature induced ageing mechanisms of solar absorber coatings, Renewable and Sustainable Energy Reviews, Volume 67, January 2017, Pages 1282-1299, ISSN 1364-0321,

Zhang Q. et al., 1996. High efficiency Mo-Al2O3 cermet selective surfaces for high-temperature application, Solar Energy Mater Sol Cells, 40 (1996), pp. 43–53

Zhang Q. et al., 2001. Optimizing analysis of W-AlN cermet solar absorbing coatings, Journal of Physics D: Applied Physics, 34 (2001), p. 3113

Zhang X., et al., 2014. Photovoltaic/loop-heat-pipe heat pump techno for low carbon buildings-Energy efficient technique for building services. LAP LAMBERT academic publishing

Zhang, X. et al. ,2015a. Active Solar Thermal Facades ,ASTFs.: From concept, application to research questions. Renewable and Sustainable Energy Reviews. . 5032–63.

Zhang, X. et al., 2015b. The early design stage for building renovation with a novel loop-heat-pipe based solar thermal facade (LHP-STF) heat pump water heating system: Techno-economic analysis in three European climates, Energy Conversion and Management, 106, pp.964-986.

Zhang, Y.L., Qin, B.Q. & Chen, W.M., 2004. Analysis of 40 year records of solar radiation data in Shanghai, Nanjing and Hangzhou in Eastern China. Theoretical and applied climatology, ,78., pp.217–227.

Zhao, C.Y., Lu, W. & Tian, Y., 2010. Heat transfer enhancement for thermal energy storage using metal foams embedded within phase change materials (PCMs). Solar Energy, 84(8), pp.1402–1412.